

MICRO-FADING SPECTROMETRY: AN  
INVESTIGATION INTO THE DISPLAY OF  
TRADITIONAL WATERCOLOUR PIGMENTS IN  
ANOXIA

ANDREW J LERWILL

A thesis submitted in partial fulfilment of the requirements  
of Nottingham Trent University for the degree of Doctor of Philosophy

September 2011

This work is the intellectual property of the author, and may also be owned by the research sponsor(s) and/or Nottingham Trent University. You may copy up to 5% of this work for private study, or personal, non-commercial research. Any re-use of the information contained within this document should be fully referenced, quoting the author, title, university, degree level and pagination. Queries or requests for any other use, or if a more substantial copy is required, should be directed in the first instance to the author.



## **Acknowledgments**

Thanks go to Dr Joyce Townsend and Stephen Hackney at Tate and Dr Haida Liang, Dr Gareth Cave and Dr Mike Newton of Nottingham Trent University for supervision of the project.

Thanks and appreciation also goes to all at the Tate Conservation Department for support of the project, to Jacob Thomas, Anna Brookes, Charlotte Caspers, Monserrat Pis Marcos and Sarah Styler and everyone at Nottingham Trent University School of Science and Technology.

Samples tested in this thesis were collected from a variety of generous sources. I would like to express my gratitude to: Martin Bijl, Margriet van Eikema Hommes, Renate Woudhuysen-Keller, Jeff Parkes, The Hamilton Kerr Institute, The Instituut Collectie Nederland, The Museum of London, The National Gallery, London, Old Holland and The Teylers Museum.

This research was funded by the Public Sector Research Exploitation Fund (PSRE) which sponsors the project at Tate.

## Abstract

In this work a novel micro-fading instrument has been developed that has increased structural stability, hence increasing the portability over previously reported instruments of this type. Using this instrument several new experimental methods have been developed and applied for the investigation of the photosensitivity of painted samples and coloured works of art (with particular focus on the effects of anoxic housing).

The colour fading and reversion behaviour of a traditional Prussian blue pigment ground in gum Arabic was investigated for the first time in 0%, 2%, 3.5%, 5%, 10% or 21% oxygen concentrations. Results from this investigation indicated that the previously reported deleterious effects of reduced oxygen concentrations (hypoxia) for Prussian blue may only become relevant at oxygen lower levels (beginning at an hypoxic oxygen level above 2% and below 3.5%). An extension of the investigation to a large sample set of Prussian blues indicated that relatively low concentrations of oxygen (around 5%) may be tolerated by Prussian-blue containing works of art.

The novel investigation of the effect of reduced oxygen housing using the microfading technique was extended to a very large varied sample set of traditional watercolour pigments ground in gum Arabic. This new avenue of investigation for the conservation of art work produced encouraging results to overcoming some of the problems of anoxic storage for a wider variety of watercolour pigments. This broad investigation also led to a better understanding of how much light exposure, in and out anoxia, is permissible for different types of watercolour pigments.

Incorporating a linear variable filter into the design enabled the investigation of the wavelength dependence of fading of many samples to a greater degree of resolution than had previously been attempted. The wavelength dependence of fading for the samples tested was found to correlate well with the absorption spectra although an exception was found when testing a sample of Prussian blue pigment, where the degree of fading decreased with the wavelength of incident radiation.

# Table of Contents

1.	<b>Introduction</b>	5
1.1	<b>Background</b>	5
1.2	<b>Accelerated aging</b>	6
1.3	<b>Range and class of stability of samples</b>	7
1.4	<b>Theoretical aspects of photochemical deterioration</b>	8
1.4.1	Photochemical degradation	8
1.4.2	Principles of photochemical degradation	9
1.4.3	The influence of wavelength	12
1.4.4	The influence of oxygen concentration on degradation	12
1.5	<b>Quantifying colour change</b>	13
1.5.1	Commission Internationale d'Eclairage colour matching functions	14
1.5.2	Calculating chromacity coordinates	14
1.5.3	CIE 1976 L* a* b*	16
1.5.4	CIEDE2000	16
1.6	<b>Photometric and radiometric units</b>	17
1.7	<b>Pigment samples tested and their provenance</b>	19
1.8	<b>Thesis layout</b>	20
2	<b>Micro-fading spectroscopy</b>	22
2.1	<b>The Micro-fading technique</b>	22
2.2	<b>Instrument characterisation and analysis</b>	23
2.2.1	Instrument design	23
2.2.2	Colour measurement	25
2.2.3	Probe alignment	26
2.2.4	Light source behaviour	27

2.2.5	Probe position sensitivity _____	30
2.2.6	Sample visibility and size _____	33
2.3	<b>Results and discussion</b> _____	36
2.3.1	The rate of fading _____	36
2.3.2	Temperature increase _____	37
2.3.3	Repeatability of results _____	38
2.3.4	Propagation of error _____	41
3.0	<b>The wavelength dependence of fading</b> _____	44
3.1	<b>Introduction</b> _____	44
3.2	<b>Technique introduction</b> _____	45
3.2.1	Experimental arrangement _____	45
3.2.2	Experimental method _____	47
3.3	<b>Sample sets</b> _____	47
3.3.1	Artists' pigments _____	47
3.3.2	Light dosimeters and standards _____	49
3.4	<b>Light exposure</b> _____	50
3.5	<b>Results</b> _____	51
3.5.1	Appraisal of the technique _____	51
3.5.2	Comparison of results with reflection spectra _____	55
3.6	<b>Discussion</b> _____	61
4	<b>Investigation of Prussian blue</b> _____	64
4.1	<b>Introduction</b> _____	64
4.1.1	The prevalence of the pigment _____	64

4.1.2	Fading and reversion characteristics _____	65
4.1.3	Prussian blue manufacture and chemical structure _____	65
4.1.4	The fading and reversion mechanisms _____	66
4.2	<b>Experimental method</b> _____	67
4.2.1	The micro-fadometer arrangement _____	67
4.2.2	Error connected with the method _____	69
4.2.3	Results _____	69
4.2.4	Reversion behaviour _____	69
4.2.5	Modelling reversion behaviour _____	71
4.2.6	Effect of oxygen concentration on behaviour _____	72
4.2.7	Influence of fade duration upon $\Delta E_f$ , $\Delta E_0$ , and $\beta$ _____	74
4.2.8	Influence of O <sub>2</sub> concentration upon $\Delta E_f$ , $\beta$ . _____	75
4.3	<b>Experimental extension to other Prussian blue samples</b> _____	77
4.3.1	Experimental technique _____	77
4.3.2	Results _____	79
4.3.2.1	Fading and reversion in air _____	80
4.3.2.2	Fading and storage in anoxia and reversion in air _____	82
4.3.2.3	Fading and storage in hypoxia and reversion air _____	84
4.3.2.4	Comparison of the 3 environments for fading and storage _____	86
4.3.2.5	Comparison of the degree of fading _____	86
4.3.2.6	Reversion within modified environments _____	87
4.3.2.7	Reversion after exposure to air _____	88
4.4	<b>Discussion</b> _____	90
5	<b>Reduced oxygen for other watercolour pigments</b> _____	92
5.1	<b>Introduction</b> _____	92
5.2	<b>The pigments selected for study</b> _____	93
5.3	<b>The experimental method</b> _____	95

5.4	<b>Results</b>	96
5.4.1	Fugitive characterised pigment groups	96
5.4.2	Light stable characterised pigment groups	138
5.4.3	Poorly identified pigments	142
5.4.4	Uncharacterised stable pigments	150
5.5	<b>Discussion</b>	153
6.	<b>Conclusions</b>	155
7.	<b>References</b>	158

## Appendix

A.	Parts List	173
B.	Accuracy measurements	174
C.	Modeling of the fading of Prussian blue	178
D.	Reversion plots of Prussian blue sample	179
E.	Pigment samples: sources and suppliers	182
F.	List of publications arising from this research	194

# 1. Introduction

## 1.1 Background

Those within museums responsible for the world's cultural treasures have a duty to ensure preservation of these works whilst allowing public access. Often these two duties result in museum policy being driven in opposing directions. As a result many art galleries and museums are under considerable pressure with regards to this area of policy. There is a need to attract the public, while a restriction is placed on lighting for the wholly necessary cause of conservation of works (despite lighting limits reducing the duration and appeal of display). An approach to addressing this problem has been to darken the general environment of the gallery to such a degree that the illuminated objects appear bright enough to attract attention, while allowing visual adaption to take place, by means of visitor control measures. This can be considered far from a perfect solution.

At present nearly all works of art on paper are regarded as equally sensitive to light (see Ashley-Smith *et al.* 2002). This is due to lack of detailed knowledge. There is therefore a need for a portable, well characterised research tool capable of directly and rapidly discriminating the degree of photosensitivity or lightfastness of objects. This information can then enable informed decisions to be made which will lead to safe increases in intensity of illumination and duration of display.

The need to illuminate (for display) photo-sensitive works of art on paper is an example of an impasse that justifies the application of research and technology. An attempt to solve this problem could be via the construction and application of oxygen free (anoxic) environments. The potential for such a system has massive scope for employment as it may make both longer display times and a reduction in the rate of degradation possible. It was hoped this research would lead to a better understanding of how much light exposure, in and out of anoxia, is safe for different types of traditional watercolour materials. It is also necessary to highlight those materials that perform poorly under anoxic conditions and if possible provide solutions to the obstacles those materials pose when they are contained within art works that would otherwise potentially benefit from anoxia.

The necessity of this research can be neatly illustrated by figure 1.1. These works already display considerable colour changes due to light exposure: they were once covered by a

'close frame' or mount that has over many years shielded the edges of the works. This has meant that the colour is less faded in that region. Those areas that were beneath the frame were largely protected from photochemical degradation.



*Figure 1.1. J.M.W. Turner, Loch Fyne with Inveraray Castle (D03635) (left) and Fisherman on a Loch (D03636) (right). Light exposure has caused severe fading of blue pigment(s) and considerable yellowing of the paper support. © Tate 2010*

It is hoped this work will contribute to making it possible for safer display of collections – and perhaps also lead to longer or more frequent display of iconic but delicate artworks.

## 1.2 Accelerated aging

Photochemical deterioration is induced by exposure to visible and near-ultraviolet radiation. Accelerated aging aims to selectively increase the underlying chemical processes of this deterioration, without introducing or over-emphasising other processes that would not take place under natural ageing conditions. When it is successful it provides a useful indication of 'life expectancy' under certain conditions.

This can be done via increasing light intensity in order to simulate a larger number of hours of exposure of the sample under test, or via an acceleration of thermally initiated deterioration via prolonged temperature increase of the sample (though the latter was not used in this research). Typically the time scale and intensity of fading illumination in any set of accelerated-aging tests is related to years of display at recommended illuminance, which for watercolours is 50-80 lux for long-term display (Feller 1994). Note that for the unfamiliar a discussion of radiometric and photometric units can be found in section 1.6.

The American Society for Testing Materials introduced a procedure for classifying lightfastness of pigments over 20 to 100 years (ASTM 2006). Accelerated-aging tests are typically considered to be conducted for three major purposes. The most fundamental and easiest to achieve is to establish the relative degree to which the materials under test are fugitive or prone to degradation.

A second and more ambitious goal could be to predict the long-term behaviour of the material under test.

A third goal is to shed light on the degradation pathway or the mechanism that is increased via the experiment.

There are limitations to the technique and differences between facilities that make interlaboratory comparison difficult. When 9 types of accelerated light aging regimes at 5 institutions were compared, no strong similarity in the results for the same set of samples (including lake pigments on paper) and exposure was found (for a description of lake pigments see section 5.2). This was thought to be due to variation in the spectral power distribution of the illuminant used and also the differing temperatures at which they were faded (Saunders and Kirby 2001). This is a concern for repeatability and therefore in this work whenever possible samples were compared with others that were faded in similar conditions to make relative statements about light sensitivity.

Due to the very large number and variety of the samples studied in this work, it was necessary to place limitations on the objectives and depth of study of the accelerated aging tests conducted, therefore this work should not be considered a photochemical study. Any insight into the mechanism of fading is limited and the research herein is largely connected with the first two objectives of accelerated aging previously stated.

### **1.3 Range and class of stability of samples.**

Feller (1975) suggested 4 classes of photochemical stability. The 4 Classifications (A, B, C & T) were equivalent to an intended useful lifetime of the sample. According to Tate lighting policy objects are grouped into similar categories according to photosensitivity.

High photo-sensitivity. Suitable for illumination at either 50 or 80 lux.

This includes works of art with paper supports, paintings with exposed canvas, textiles, objects with colorants of known poor lightfastness, and works with evidence of previous light damage.

Medium sensitivity; suitable for illumination at 100 lux.

Contemporary photographs, works on good quality paper.

Low sensitivity; suitable for illumination at 200 lux.

This includes oil paintings, painted sculpture, exposed wood, Perma-prints.

Not photo-sensitive; suitable for illumination greater than 200 lux, in practice up to 1500 lux. This includes metal, stone, plaster sculpture without colorants.

Within a 4 year period, the maximum accumulated duration of display of a high or medium photosensitive work of art at its recommended lux level is 2 years.

A typical museum environment was defined by Thomson (1967). The average annual exposure of the National Gallery, London was estimated. A figure of 1.5 Mlxh (million lux hours) was given (average intensity of 320 lux).

## **1.4 Theoretical aspects of photochemical deterioration**

### **1.4.1 Photochemical degradation**

Damage to pigments by light is the result of numerous degradation pathways (due to their complexity few are fully understood). The pathways consist of a series of complex photochemical processes (Thomson 1964). For the absorbed photon to initiate chemical change, threshold energy of the receiving molecule must be exceeded. This threshold energy is known as the activation energy.

When a photon of sufficient energy is absorbed an electron exits the ground state and enters the excited state. The excited molecule may then lose the absorbed energy (relaxation) via the photophysical processes of heat dissipation, by the emission of radiant energy in the form of fluorescence or phosphorescence, or by the photochemical processes of undergoing a chemical change within the molecule (Geuskens 1975).

Many materials found in art museum collections are cellulosic or proteinaceous materials (for example support materials for paintings, paint media and traditional and synthetic varnishes). During light aging they undergo a number of reactions indicative of oxidation. The first 3 stages of degradation follow a common pathway; absorption of a photon, the formation of a free radical and then combination of the free radical with an oxygen molecule (Thomson 1978). Photochemical reactions which lead to colour change are discussed in more detail by Schaeffer (2001).

The effects of pigment particle size, substrate medium and mordant (a chemical that fixes a dye) have been shown to be considerable factors in the rate of degradation of pigment samples (Michalski 1987).

Generally degradation will be increased by the presence of moisture. It is therefore necessary to control relative humidity in any accelerated aging experiment. Water can participate in the processes of deterioration in a number of ways. In a few cases, moisture has little effect and often the role of water remains far from being understood at the molecular level (Feller 1994).

#### **1.4.2 Principles of photochemical degradation**

A key principle of photochemical degradation is the Grotthus-Draper law: only that radiation which is absorbed by a substance may cause a chemical reaction (Watkins 1978). It is therefore logical to state that wavelengths of radiation absorbed by the sample undergoing fading provide the largest contribution to the degradation observed. This is however not always correct as fading can also be caused by the absorption of radiation by some other substance, which then passes the absorbed energy on. This is known as photosensitized fading and under these circumstances, an absorption curve of the colorant, would not correspond to those wavelengths that initiated the process of colour change (Feller 1994).

Photochemical damage is largely a surface phenomenon taking place only in the top 4 - 40µm of the material (Johnston and Feller 1986). Beer-Lamberts Laws holds with respect to penetration of the surface:

$$I_x = I_o \exp^{-\alpha x}$$

$I_o$  is the incident intensity

$I_x$  is the intensity at a depth  $x$

$x$  is depth of light penetration

$\alpha$  is the absorption coefficient sample.

Experimentally to differing levels of approximation a large number of reaction rates vary with temperature according to the Arrhenius equation which can be summarised as

$$k_{(T)} \propto \exp\left(\frac{-E_a}{RT}\right)$$

Where

$k_{(T)}$  is the reaction rate

$E_a$  is the activation energy (J/mol)

$T$  is the temperature (K)

$R$  is the gas constant (Laidler 1984).

Simulating the aging of an object by increasing its temperature and therefore increasing the rate the chemical reaction causing degradation occurs is not without critics. Degradation pathways of objects are often complex and therefore the Arrhenius equation can only be applied to first-order reaction elementary kinetics in this instance. It can also be argued that at higher temperatures different reactions are possible compared to those in natural aging for the same material (Bansa 2002) (Porck 2000). The degree to which a chemical reaction is accelerated by increasing the temperature also varies and the “rule of thumb” that a doubling of the reaction rate occurs per increase of 10°C does not apply when discussing typical museum objects. A doubling per 10°C applies to materials with activation energies of around 50kJ/mol where typical activation energies within museums can be considered as 100-125 kJ/mol for paper and wood with a doubling of the rate per 5°C for cellulosic materials (Thomson 1976).

A central principle necessary to achieve meaningful results in accelerated aging experiments is the reciprocity principle or the Bunsen-Roscoe law (Cuttle 1988).

This law states total damage equates to the incident irradiance which can be defined as;

$$H_D = \int_t E_D dt$$

$H_D$  is the Damage exposure (lx h)

$E_D$  is the Damage irradiance (lx)

This implies that the total amount of photochemical damage is not dependent on the rate of irradiance but directly related to exposure.

This is represented by the product of the intensity of the irradiance (the luminous flux, if irradiation is limited to the visible spectrum) multiplied by the duration of fade. In other words, 100 mW of intensity for 1 hour is considered to produce as much damage as 1 mW of the same radiation for 100 hours.

Experimentally there are potential reasons that can cause reciprocity failure. These are that high intensities of illumination employed in accelerated aging tests raise the temperature of the samples and alter the rate of chemical reaction. High temperatures can also lower a samples moisture level (Wilhelm 1993). Discontinuity of exposure can also create differences from a continuity of illumination over the experimental period and potentially post-irradiation changes in the absence of illumination can also occur. Theoretically there are also certain photochemical reactions that do not follow the reciprocity principle, and are proportional to the square root of the intensity (Kollmann and Wood 1980). Reciprocity may also fail when one of the accelerated chain reactions that leads to degradation of a pigment reaches a bottle neck. Due to this upper limit the reaction cannot proceed sufficiently to maintain the rate of change (Saunders and Kirby 1996).

Light aging experiments on a variety of colourants arranged to investigate the phenomena have produced no evidence of breakdown at reasonable light levels (Saunders and Kirby 1996). Reciprocity breakdown has been reported in the case of Prussian blue by Ware (1999a). It has also been found that Alizarin Crimson and some other colourants are affected differently when exposed to a light/dark cycle rather than to continuous exposure (ASTM 2006). Caution should be employed due to potential breakdown but despite these issues (and perhaps for want of a better technique), accelerated aging has been fruitfully employed to guide the care of museum materials for a considerable time.

### **1.4.3 The influence of wavelength**

Studies of the relationship between wavelength and light damage has resulted in the following terminology; an action spectrum can be considered as the accumulated effects of wavelength on degradation, where as the wavelength specificity has been defined as the influence of wavelength on the mechanism and type of degradation (Feller 1994). An important clarification is that the activation spectrum (rather than the previously mentioned action spectrum) refers to data that has not involved any correction for the variation of spectral power distribution. Activation spectra are therefore dependent on the spectrum of the illuminating light source causing damage.

According to the Grothus-Draper Law or principle of photochemical activation, only radiation which is absorbed by the reacting system is effective in producing photochemical degradation (Watkins 1978). In addition, the Damage Function, based on data from the National Bureau of Standards (NBS) illustrates how shorter wavelengths are responsible for greater damage (Harrison 1953). Via the NBS damage function each wavelength is specified a value based on its influence on photochemical degradation. Thirty years later Aydinli *et al.* (1983) produced a new damage function which gave a higher weighting to the damage caused by visible wavelengths. The Krochmann damage weighting function was incorporated into ISO/CIE publication 89/3 “On the deterioration of exhibited museum objects by optical radiation” (Aydinli *et al.* 1990).

It remains that insufficient data on the wavelength specificity of fading is available for historical pigments (Michalski 1987) and highly sensitive materials (Cuttle 1988). Therefore more research is required in this area.

### **1.4.4 The influence of oxygen concentration on degradation**

Anoxia retards the oxidative degradation pathway (Russell and Abney 1888) and this pathway is often associated with light exposure. Organic dyes, lakes and pigments should benefit from anoxia as most undergo oxidative fading. The majority of inorganic pigments should not be negatively affected by storage in anoxia, though some can undergo reductive colour change (Hackney 2006).

At low oxygen levels Thomson (1965) argued that the degree of oxidative degradation of most organic pigments would show little or no decrease in the rate of degradation until an oxygen level of parts per million was achieved. It was cited that degradation obeys a non linear relationship where the positive effect of anoxia is rapidly negated by small quantities of oxygen, which might be desorbed from other components of an artwork, for example the paper substrate. This conclusion is backed by artificial aging experiments conducted by Leene *et al.* (1975). Alternatively Giles *et al.* (1956) argued that the rate for most organic colourants decreases linearly with oxygen concentration, a claim which was backed empirically by Lasareff (1912) via an investigation of 2 cyanine dyes.

Arney *et al.* (1979) addressed this issue of contradicting arguments and conclusions by testing a number of pigments at various increments of oxygen concentration from 0% to 1% in order to clarify the matter. The results of the investigation indicated the relationship was dependent upon the sample under test and therefore both relationships applied over the oxygen concentration tested. Therefore the degradation of some pigments will be greater in reduced oxygen concentrations that are greater than an oxygen level of parts per million. Others would require oxygen levels less than parts per million to see a reduction in the degree of oxidative degradation.

## **1.5 Quantifying colour change**

Rather than being viewed as an intrinsic property of an object, colour can be viewed as the human sensation created by the combination of a particular spectral power distribution of light and the reflective nature of the object. For example a white object viewed under red illumination will appear red or a red object viewed in a blue light will appear black.

The sensation of colour is made possible by the human eye. The retina clads the inside of the eyeball and is the light sensitive part of the eyes structure. The cell structure of the retina contains light-sensitive rod cells and cone cells. Rod cells (which are sensitive over the entire visible spectrum) are more prevalent and have a higher light sensitivity than cone cells. Three variants of the cone cell exist, which are sensitive in the red, green, and blue spectral ranges with peak sensitivity at the long (558nm), middle (531nm) and short (419nm) wavelengths of the visible range (Dowling 1987).

Resulting from this variety of sensors three different regimes of human vision are found, each with differing use of the available receptors. Photopic vision functions within daylight and uses the 3 variants of cone cells affording colour vision. Scotopic vision uses rods which do not enable colour perception and function at low light levels (at night.) Mesopic vision relates to light levels between the 2 regimes and employs both rods and cones (Wyszecki and Stiles 2000). Attached to the retina are nerve fibers that carry information to the brain via the optic nerve.

As an aside Ganglion cells also exist within the retina and do possess some optical sensitivity peaking in the blue region with impact on human circadian rhythm (Berson *et al.* 2002) (Hattar *et al.* 2002).

### 1.5.1 Commission Internationale d'Eclairage colour matching functions

The International Commission on Illumination (*Commission Internationale d'Eclairage or CIE*) colour matching functions are  $\bar{x}$   $\bar{y}$  and  $\bar{z}$  (ISO CIE 10527 1991). These empirically determined functions are used to quantify the chromatic response of a standard observer over a 2° field of view.  $\bar{x}$   $\bar{y}$  and  $\bar{z}$  peak in the red, green and blue or long, middle and short wavelength ranges respectively see figure 1.2. (Shaw and Fairchild 2002).

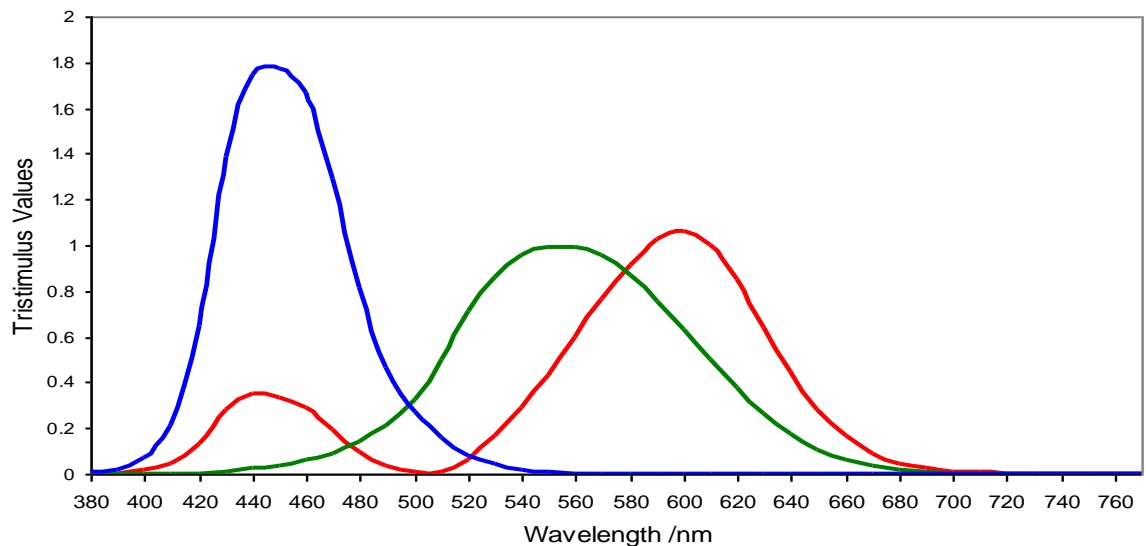


Figure 1.2. The colour matching functions for the CIE 1931 2° standard observer.  $\bar{x}$   $\bar{y}$   $\bar{z}$  are the red green and blue curves respectively.

### 1.5.2 Calculating chromacity coordinates.

The tristimulus values XYZ for a colour with a reflectance  $R(\lambda)$  view under an illuminant with a spectral power distribution  $I(\lambda)$  are given in terms of the standard observer by:

$$X = \int_0^{\infty} I(\lambda) \bar{x}(\lambda) \delta\lambda$$

$$Y = \int_0^{\infty} I(\lambda) \bar{y}(\lambda) \delta\lambda$$

$$Z = \int_0^{\infty} I(\lambda) \bar{z}(\lambda) \delta\lambda$$

As a colour is defined by the relative stimulus of the eye's three sensors, it makes sense therefore to instead define a colour by a xyz triplet of chromaticity coordinates which are normalised versions of XYZ (CIE 1986).

$$y = \frac{Y}{X + Y + Z}$$

$$z = \frac{Z}{X + Y + Z}$$

By definition now,

$$\mathbf{1} = \mathbf{x} + \mathbf{y} + \mathbf{z}$$

### 1.5.3 CIE 1976 L\* a\* b\*

It is possible to define colours by their  $x$  and  $y$  chromaticity coordinates (defined previously) it is possible to plot the gamut of human colour perception via the Commission Internationale d'Eclairage 1931 XYZ colour space.

The conversion to the CIE 1976 L\* a\* b\* colour space can be achieved using the method as defined by CIE (1986).

The CIE 1976 L\* a\* b\* colour space has chromaticity coordinates of L\*, a\* and b\*. The L\* value represents luminance and values range from 0 for black to 100 for white. The a\* and b\* values represent coordinates on the axis moving from red to green (+a\* to - a\* respectively) and yellow to blue (+ b\* to - b\* respectively).

The resulting unit of colour difference is represented by the symbol  $\Delta E_{ab}^*$  which can be simply calculated as the Euclidian distance between 2 locations in the CIE 1976 L\* a\* b\* colour space.

### 1.5.4 CIEDE2000

An issue with CIE 1976 L\* a\* b\* colour space is that the eye is most sensitive to hue differences, then chroma and finally lightness and also weaknesses exist with respect to the neutral and blue regions.  $\Delta E_{ab}^*$  does not take this into account.

There are several other methods by which to calculate colour difference units including  $\Delta E_{CMC}$  (BSI 1988) and  $\Delta E_{1994}$  (CIE 1995) which included correction factors for the problems associated with chroma and hue and  $\Delta E_{2000}$  (also written as CIEDE2000) (CIE 2001). CIEDE2000 attempted to correct for neutral and blue region weaknesses (Luo *et al.* 2001). Each increases the uniformity of the CIE 1976 L\* a\* b\* colour space. When colour difference is expressed using CIEDE2000 the corresponding colour difference unit is represented by the symbol  $\Delta E_{00}$ .

A rough rule of thumb is that if more than 1  $\Delta E_{ab}^*$  separates two colours, the difference would be just distinguishable to the observer if they were side-by-side for comparison (BSI 1978) and fading to a just noticeable degree is usually taken as 2 colour difference units (Michalski 1997). Experimentally a likelihood of distinguishing 2 colours under ideal viewing conditions was determined to be 50% for a colour difference of 1.5  $\Delta E_{00}$  (Pretzel 2000).

There have been attempts since the 1930s to accurately define and quantify colour measurement in terms that can be related directly to human vision. The process is empirical, and resulted in greater perceptually uniformity for each newly-defined colour difference unit. Two colour space models have become widely used in this field; CIE 1976 L\* a\* b\* and CIEDE2000 and these have been used in this research.

In this thesis the colour space chosen was the same as previous published research conducted in the particular area of investigation. This was done in order to cross compare data with previous publications with greater ease. Exceptions to this were made when it was thought this would lead to misleading conclusions.

The colour difference units used within this work therefore vary between CIE 1976 L\* a\* b\* and CIEDE2000 depending upon the investigation.

## 1.6 Photometric and radiometric units

Photometric and radiometric units are both used to quantify illumination. In the case of radiometric units, all wavelengths are equally weighted, where as photometric units are weighted to the human eye's visual system. This weighting factor varies with wavelength and is known as the luminosity function (see figure 1.3). The function peaks at 555nm in the green and falls to zero outside the visible range (CIE 1931).

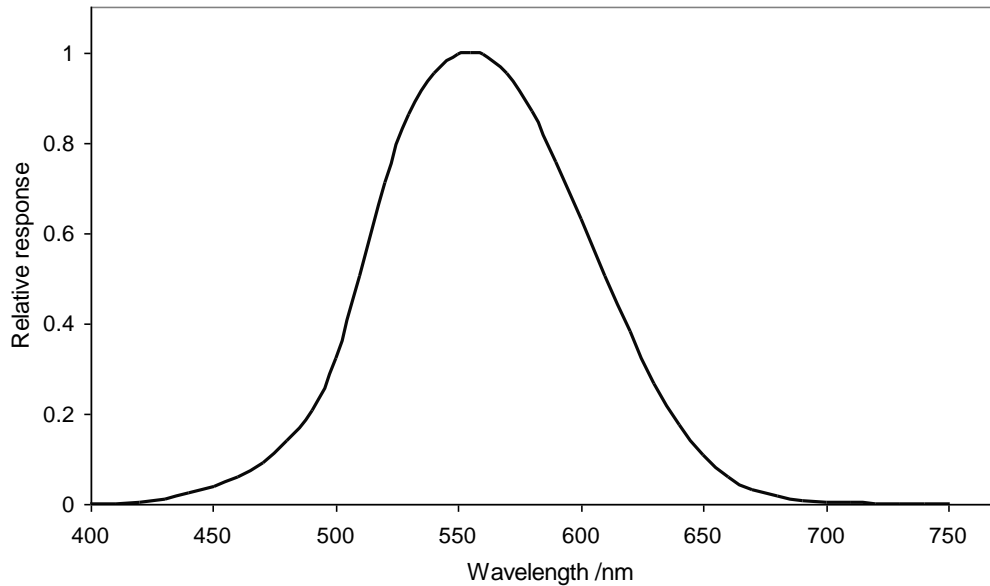


Figure 1.3. The luminosity function or photopic response curve. The function peaks at 555nm in the green and falls to zero outside the visible range.

The radiometric unit of flux is the watt (W). The corresponding photometric unit is the lumen (lm). The unit of lux is one lumen/metre<sup>2</sup> (lm/m<sup>2</sup>) the corresponding radiometric unit of irradiance is watt/metre<sup>2</sup> (W/m<sup>2</sup>) (see table 1.1).

Practically it is not possible to convert simply between lux and watt/metre<sup>2</sup> as there is a wavelength dependency. To make a conversion it is necessary to know the spectral power distribution of the light source and use the luminosity function.

Physical Quantity	Description	Radiometric Units	Photometric Units
Flux	Total power (energy/second) emitted by source	watts (W)	lumens (lm)
Irradiance	Rate that light energy is incident on a surface	irradiance (W/m <sup>2</sup> )	lux (lm/m <sup>2</sup> )

Table 1.1. The SI units used to characterise the light source in this project physically and perceptually. Each radiometric unit is shown with it corresponding photometric unit.

## 1.7 Pigment samples tested and their provenance

Research was largely conducted on historically accurate reproductions of 19<sup>th</sup> century traditional watercolour materials. In choosing to follow this route the effect of pigment size and lake pigment substrate were considered outside the scope of the research, though they have been shown to be considerable factors in the rate of degradation (Feller and Johnston-Feller 1997).

It was imperative to conduct research on genuine 19<sup>th</sup>-century pigments of known provenance dated with reasonable security. Therefore the particle size was not amenable to control. In order to do this historic collections and private collectors in the Netherlands, the United Kingdom and Germany were approached for material by Drs Charlotte Caspers, whose practical research for a masters degree in materials history was carried out in parallel with the research reported here (Caspers 2008).

Dating historic pigments and watercolour cakes is difficult. This is still the case when samples are gained from renowned institutions and collections. There is always a possibility that a jar of named pigment has been substituted or never had the expected contents. A detailed description of the sample set and analytical results used to support the identification of each pigment can be found in appendix E.

These collections contained historic watercolour pigments that could be mixed with water and gum Arabic and painted onto the chosen substrate, which unless otherwise stated (for example when samples were received already painted onto a substrate) the paper used was gelatine sized and glazed paper from Ruscombe Mill, 33460 Margaux, France, specified and created for related research (Thomas 2011). The paper contained approximately 60% lincell (cellulose from flax) and 40% long cotton linter (Townsend 2009).

Modern 20<sup>th</sup> century pigments were used only when samples could not be obtained from a historical collection.

## 1.8 Thesis layout

Chapter 2 describes a novel micro-fading spectrometer which was designed and constructed. The mode of operation was characterised and appraised to a greater degree than previously published.

It was thought that areas of the previous instrument could be improved and developed (see Whitmore *et al.* 1999, Whitmore *et al.* 2001 and Whitmore 2002). The basis of what was necessary was set out by Neeval (2007) in his appraisal of the instrument and these were addressed.

An automated high throughput system was also created using the instrument which gained data on a larger number of samples than had previously been attempted in accelerated aging experiments.

In chapter 3 in order to address the shortage of data in the field of the wavelength specificity of fading, traditional watercolour pigments and dosimeters were investigated. By altering the micro-fading technique and the introduction and appraisal of a new method it is possible to gain further knowledge in this field more rapidly.

Chapter 4 involves a study of Prussian blue. Many reports suggest that Prussian blue is unstable in anoxia (Kirby, and Saunders 2004). This would be a major obstacle to the application of anoxia for preservation of traditional watercolours. Prussian blue is also found widely in a variety of objects (Townsend *et al.* 2008). Using a modified micro-fading technique a Prussian blue pigment from the studio of J.M.W. Turner (1775-1851) was investigated.

An analysis of the behaviour when faded in different oxygen concentrations indicated a 5% oxygen level was not harmful to Prussian blue. In a separate investigation this 5% hypoxic state was then applied to a larger number of historic and a smaller number of modern Prussian blues resulting in the same conclusion.

Chapter 5 investigates the harmful effects of anoxia on traditional watercolour pigments. Giles and McKay (1963) and Arney *et al.* (1979) concluded insufficient knowledge of the more sensitive materials under anoxic conditions is available to justify using long term anoxic storage and further investigation into these pigments was required. Typically a

single example of each pigment type was previously tested in any investigation regarding the effects of anoxia.

The provenance and independent identification of the pigments were often not discussed in detail, and/or the degree of exposure to anoxia the samples received was often ambiguous. This issue is addressed in this chapter by testing a greater number of pigments, in particular all the pigments that were reported to suffer greater colour change in anoxia than in air.

Using automated micro-fading an investigation into a large number of pigments in anoxia was conducted. The 5% oxygen hypoxic state found suitable for Prussian blue in chapter 4 was also investigated by extending the investigation of the sample set used in this chapter to this hypoxic state.

## 2. Micro-fading spectroscopy

### 2.1 The micro-fading technique

A novel micro-fading spectrometer has been designed and constructed taking inspiration from the Whitmore design (Whitmore *et al.* 1999, Whitmore *et al.* 2001, Whitmore 2002) and its application (Bowen *et al.* 2002, Connors *et al.* 2005, Lavédrine *et al.* 2006).

An instrument was constructed that was capable of identifying materials more light sensitive than Blue Wool Standard #2 (see British Standard 1006:1978) through direct fading in artworks on a sub-millimeter diameter spot such that the faded spot is not discernable by the viewer. Fading and colour measurement are carried out simultaneously.

Areas where the previous instrument required improvement were set out by Neeval (2007) and were addressed by this research. Those limitations and problems as set out by the previous design were summarised as,

- Precise positioning of the probe heads was problematic.
- Difficulty in alignment of the illuminating and receiving probe.
- Inhomogeneous illumination in the fading area sampled.
- Uncontrolled intensity at the illuminated surface.
- Heating of the sample to unacceptably high temperatures.
- Colour measurement inaccuracy.
- No portability and therefore the need for object transportation
- Documentation of exact location of fading not possible.
- Where to fade to get representative data of the artwork under test.

With the exception of the last of these issues all were addressed by this new instrument which was novel in design and independently constructed.

Tests are carried out on sub-millimetre diameter spot size while at the same time monitoring change in the reflectance of the sampled region. To do this the monitored spectrum is converted using CIE 1976 L\* a\* b\* colour measurements calculated for the 2° standard observer under standard illuminant D65. Via this method an automated calculation of colour difference of the fading spot is monitored in real time in  $\Delta E_{ab}^*$  units.

Additionally by automated recording of the changing  $L^*$   $a^*$   $b^*$  data during the fading process it is possible to calculate offline the colour change in terms of CIEDE2000 ( $\Delta E_{00}$ ) units for the same fade. Altering the standard spectrometer software to make this calculation an online method was not permitted by the manufacturer.

## 2.2 Instrument characterisation and analysis

### 2.2.1 Instrument design

The instrument developed is approximately half the cost of the previous published design (a parts list and cost in 2007 can be found in appendix A). No new computer programming was necessary to build and use the instrument. It is a flexible, compact, lightweight and mobile instrument which removes the need for transportation of art work and unnecessary art handling (see figures 2.1, 2.2 and 2.3). It has been used in many modes of operation in the course of this research; however this chapter discusses its use as a transportable compact micro-fading spectrometer capable of identifying the sensitivity of artifacts to visible light exposure. Other applications to gain other information are discussed as necessary elsewhere.

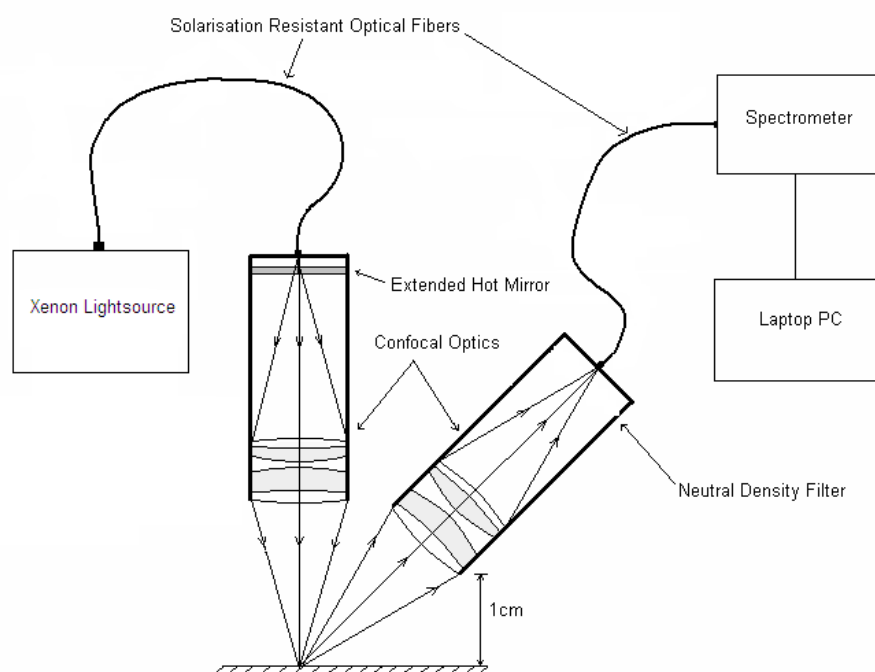
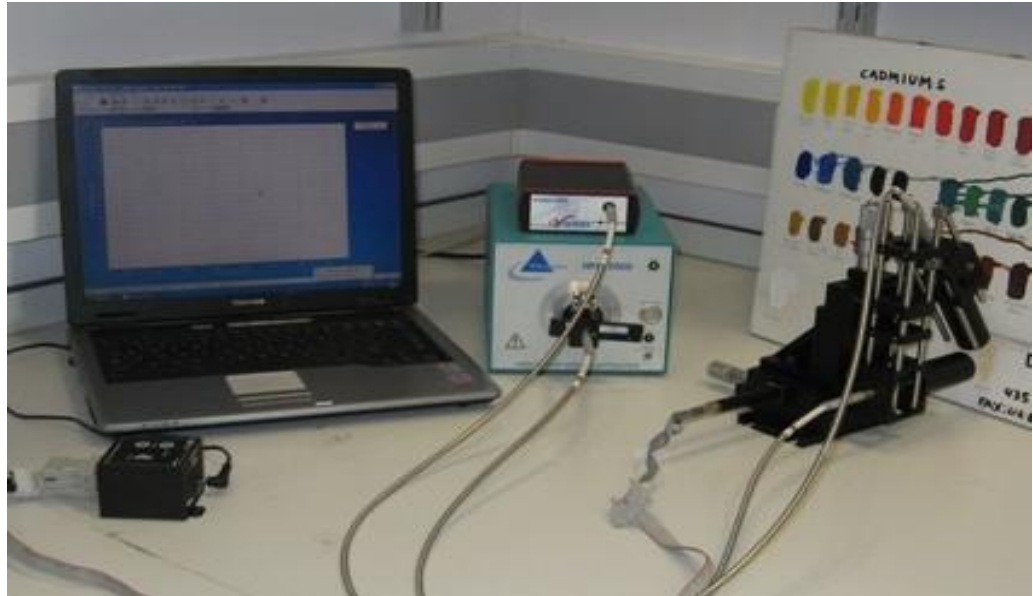
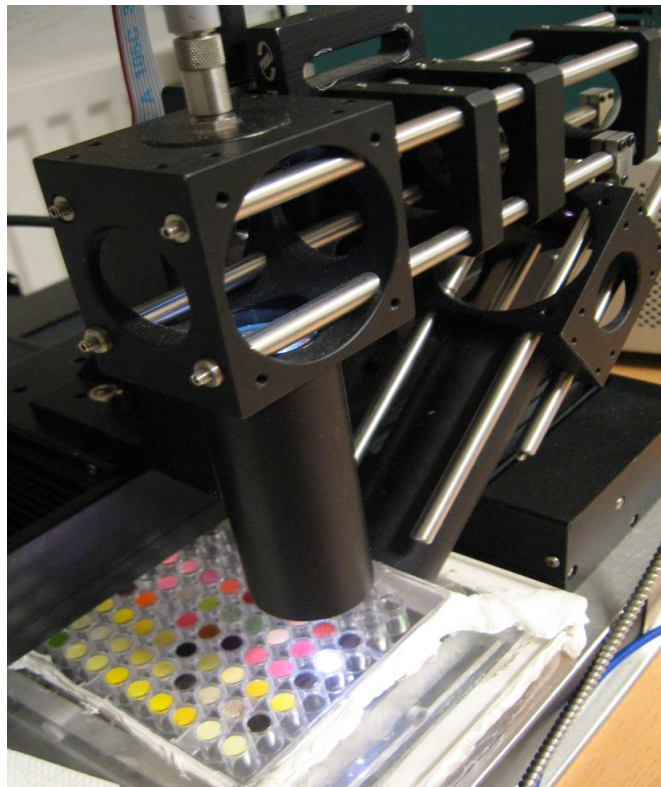


Figure 2.1. A schematic representation of the micro-fadometer.



*Figure 2.2. The instrument fading a sample in portable mode.*



*Figure 2.3. The instrument probe head fading a matrix of samples housed in a 96 well plate, in automated mode.*

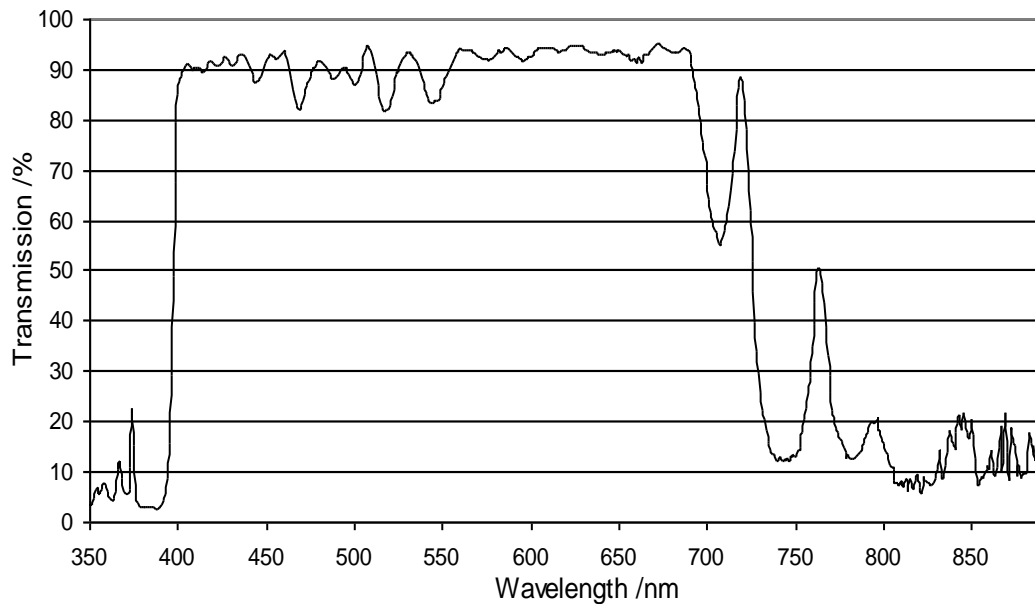


Figure 2.4. The measured transmission of the extended hot mirror used to filter the incident radiation of the instrument.

For use as a micro-fadometer, a high-powered continuous-wave xenon light source (Ocean Optics HPX2000) is connected directly to a solarisation resistant optical fiber with a 600 micron fiber core. The end of this fiber is connected to a confocal probe designed for this task, containing two lenses (matched achromatic pairs optimized for the visible region). Light passes through an extended hot mirror utilized to remove the infrared in order to reduce temperature and the ultraviolet to better simulate the museum environment (see figure 2.4). The filtered light is focused to a 0.25mm spot.

### 2.2.2 Colour measurement

In order to monitor colour change, scattered light from the small sample area is coupled back into the optical system via another optical probe of the same design at 45 degrees to the normal. This design follows ASTM (1993a) (1993b) as a standard test method for colour (CIE 1986). Sampled radiation then passes through a neutral density filter to avoid saturation of the fiber optic spectrometer. The spectrometer (Avantes Avaspec 2048) receives this signal via an optical fiber, and the software (AvaSoft 7.0) analyzes change in the spectrum and the rate of fading.

The probe can be mounted on an XYZ stage capable of sub-micron scale movements. All axis of the stage are motorized. It is therefore possible to achieve fine alignment of the

probe with the surface remotely rather than leaning over the artwork. This in turn enables adjustment when the probe is beyond arms-reach, e.g. over an art work when the probe is mounted on a gantry to enable movement over the surface of an artwork that is laid flat. This is also an important aspect of the design, as it becomes possible to achieve best focus remotely.

To achieve best focus the software calculates the integrated reflection spectrum over the visible range and so small improvements which would otherwise be undetectable when solely aligning by eye are possible. By making small incremental adjustments in position that would not be possible using a manual micrometer screw it is possible to define best focus to a greater accuracy.

### 2.2.3 Probe alignment

To ensure confocality, both probes were illuminated with low intensity radiation, and focused onto a CCD chip (see figure 2.5). For easier analysis in figure 2.5c the red area indicates the sampling area of the receiving probe and green the illuminating area (this creates a yellow overlap). The yellow region indicates where both fading and colour monitoring takes place. The sampling region was larger elliptical and not all in focus as it was incident at an angle to the surface. Although the sampling area was greater than the illuminated area, light interference from outside the sampling area was undetectable.

When correctly aligned, it was shown that best focus of the probe provides the maximum signal to the spectrometer, and ensures reproducible spot size. Failure to align correctly led to the probe focusing incorrectly, which can lead to a large variation in the calculated fading rate.

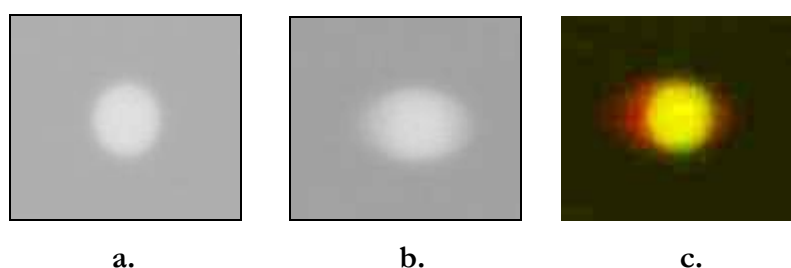


*Figure 2.5. Images produced in focusing the instrument probes onto a CCD chip (a) illuminating probe, (b) sampling probe, (c) illuminating and sampling probe (a and b) combined in alignment*

To fade a sample, the instrument operates as a reflectance spectrometer with a high powered light source. To make reflection measurements, a dark spectrum and reference spectrum are acquired. The reference spectrum is recorded on a polished barium sulphate sample which acts as a 'standard white'.

A neutral density filter is used to reduce the beam to a level where best focus can be obtained without a significant level of radiation being incident on the sample. The probe is adjusted on the sample in order to come to best focus and acquire maximum reflected intensity on the object in the desired location. The shutter of the lamp is then used to stop illumination. The instrument is set up while the shutter is closed.

Colour differences are monitored in real time using the spectrometer software in order to prevent fading beyond acceptable levels which have been independently determined in the development process. Should alternative methods of monitoring change have been employed (e.g. optical density changes in the material or spectroscopic changes), real time colour change would not have been easily interpretable for the user. This is especially the case when considering the very small colour differences concerned. Therefore a more rapid and easily interpretable method was thought to pose less risk when the method was applied to real objects.

#### **2.2.4 Light source behaviour**

The instrument produces 2.59mW or 0.82 lumens ( $1.7 \times 10^7$  lux for a 0.25mm focused spot). The relative power spectrum of light incident on the sample measured using a calibrated spectrometer is shown in figure 2.6. The bulb lifetime and therefore stability was guaranteed for 1000 hours with a typical bulb lifetime of 2000 hours. Refitting and calibration of the bulb output was conducted by the manufacturer. Monitoring was typically weekly and remained constant during all experiments within this work.

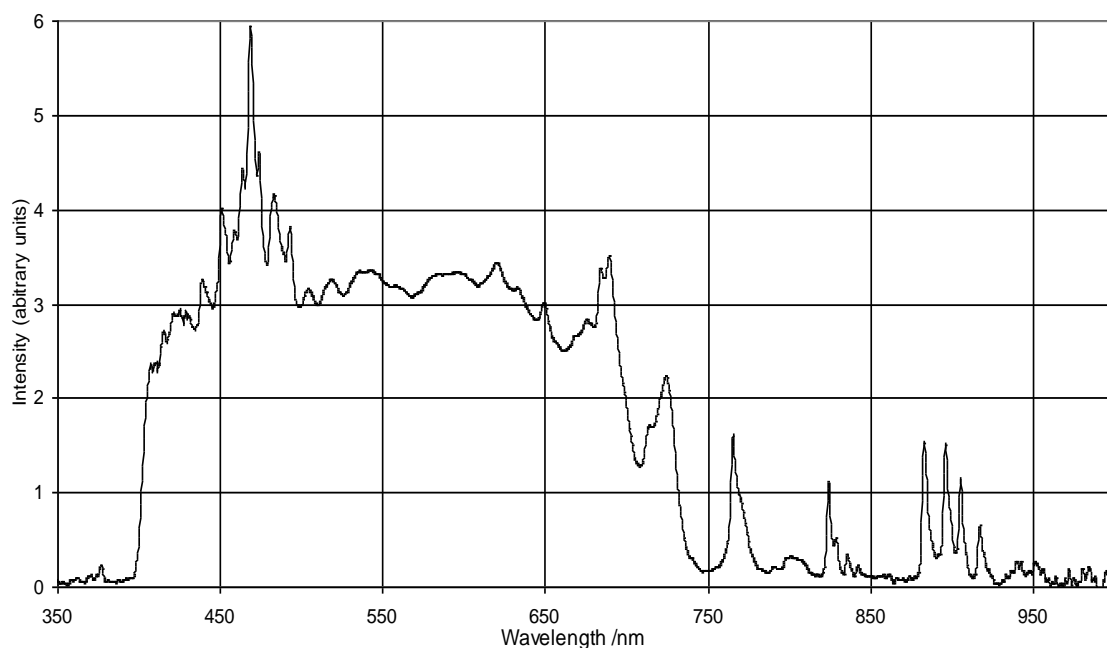


Figure 2.6. The relative power spectrum of incident radiation used in broad spectrum fading tests.

Illumination from the light source is by necessity relatively high. Schaeffer (2001) discusses the likelihood of 2 photon processes taking place as a result of flash photography. A calculation found the likelihood in the region of one in one billion. This is done via a calculation of the likelihood of a photon hitting an already activated molecule. The likelihood of a second photon process taking place was found to be considerably higher in the case micro-fading when using the same calculation and assumptions. Taking the average wavelength of incident photons to be 550nm for a 2.50mW illumination an estimated  $6.9 \times 10^{15}$  photons were incident on the sample every second. Then further in applying an example excitation time of  $10^{-5}$  seconds as applied previously, the number of photons incident during this period of activated molecules was calculated as  $6.9 \times 10^{10}$  photons. For the illuminated  $1.97 \times 10^{-7} \text{ m}^2$  area provided by the 0.25mm spot an estimated  $3.5 \times 10^{17}$  photons were incident per unit area. Further applying the estimates used by Schaeffer of  $10^{18}$  molecules being present per unit area the likelihood of a molecule being activated in this time period can be calculated as approximately 1 in 3. For a photon event to happen to the same molecule twice in this period and therefore for a molecule to undergo a biphotonic process a significant 1 in 10 possibility is present. A more typical excitation time of  $10^7$  seconds leads to a likelihood of a biphotonic event as approximately 1 in 81000. These results indicate a significant number of biphotonic events over any period of fading. However far from every incident photon would be absorbed or result in an excitation. This is an important point which reduces the likelihood as calculated.

Assuming the reciprocity principle holds for light-sensitive materials and a display is set at 50 lux for 8 hours per day 7 days per week, the fading rate of the instrument can be considered as approximately 2 years in a gallery setting per minute. Some limitations of the technique which prevent more certain statements being made do need to be considered; differences in the spectral power distribution between gallery lighting and the xenon lamp of the instrument, sample colour reversion post-fading and the angle of illumination of the object by the instrument which differs from the gallery environment (Whitmore *et al.* 2001).

Stability analysis of the illuminant took place over 400 minutes using a polished barium sulphate standard as a non-fugitive reference. Above 400nm to 780 nm variation was within 1.5% (peak to peak) with the average less than 1%. From 380nm to 400nm illumination was significantly reduced resulting in a different signal to noise ratio. Percentage variation increased to up to a maximum of 5% with an average value of 1% in the wavelength region.

Total counts of the spectrometer integrated over all wavelengths (380 to 780nm) increased 1% over the period (see figure 2.7). The dark current over 7 hours was constantly monitored and subtracted by the spectrometer software via the inbuilt electronic dark correction facility.

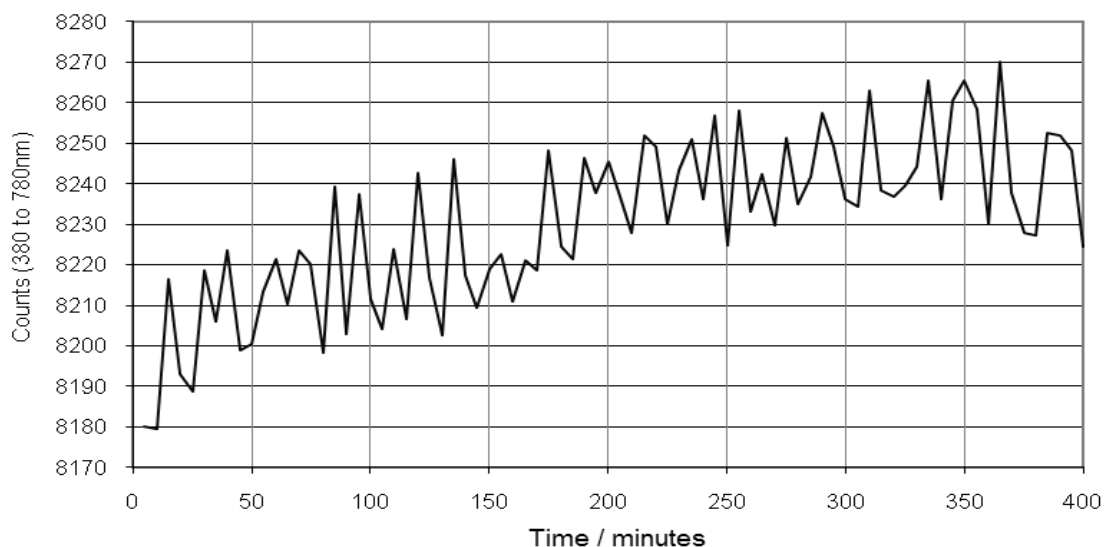


Figure 2.7. The total counts of the spectrometer from 380nm to 780nm over 400 minutes.

## 2.2.5 Probe position sensitivity

In order to determine empirically the diameter of the area that would be faded, the focused spot of the probe was analyzed through focus using a CCD camera. Full width half maximum (FWHM) values were measured when varying the working distance of the probe to the CCD (see figure 2.8 and 2.9).

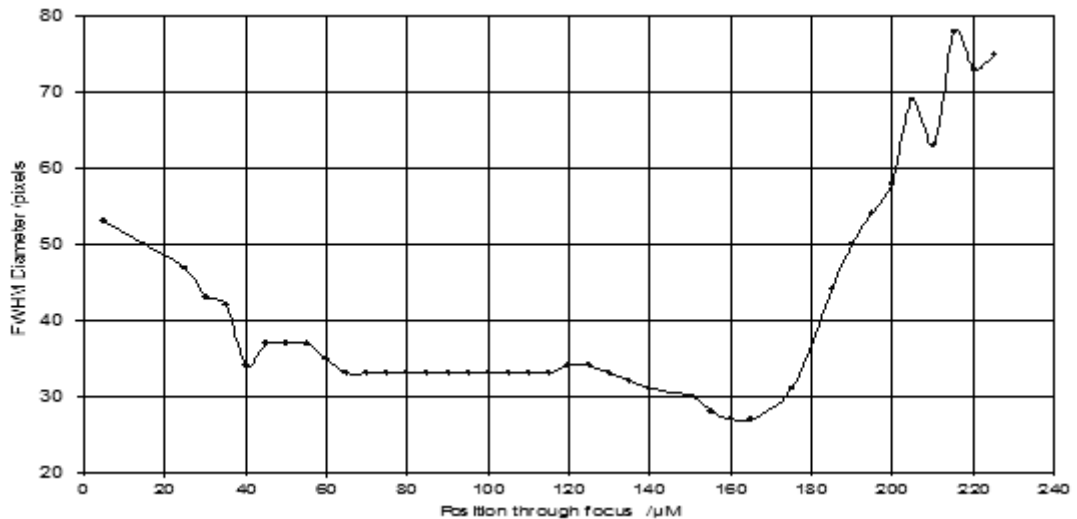


Figure 2.8. The FWHM of the spot profile through focus in 5 micrometer increments.

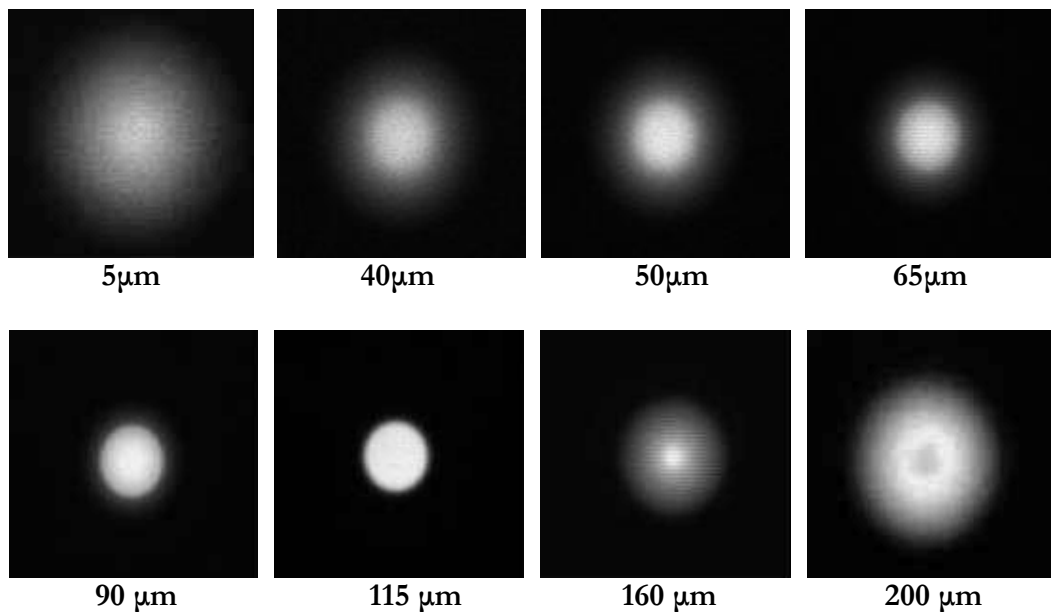


Figure 2.9. The intensity profile of the fading optical arrangement at different key locations 195  $\mu\text{m}$  through focus. Values given in micrometers correspond with data points given in figure 2.8.

This analytical method led to the realization that the FWHM of the recorded spot size on the CCD chip is 33 pixels or 0.25 mm and the area did not alter for 50 $\mu$ m through focus any more than 6% (which was the limitation of the measurement technique).

The effect that small errors in focusing have on received signal and colour measurement was also investigated. To do this the sensitivity in positioning of the probe relative to a white tile was determined. This was done by calculating relative  $\Delta E^*_{ab}$  values at various locations through focus, compared to values  $L^*=100$   $a^*=0$   $b^*=0$ . This provided an illustration of how a small change in probe position, (for example relaxation of the probe holder, or altering of the sample/probe geometry in repositioning the probe from the white target to sample) can create error in measured colour (see figure 2.10).

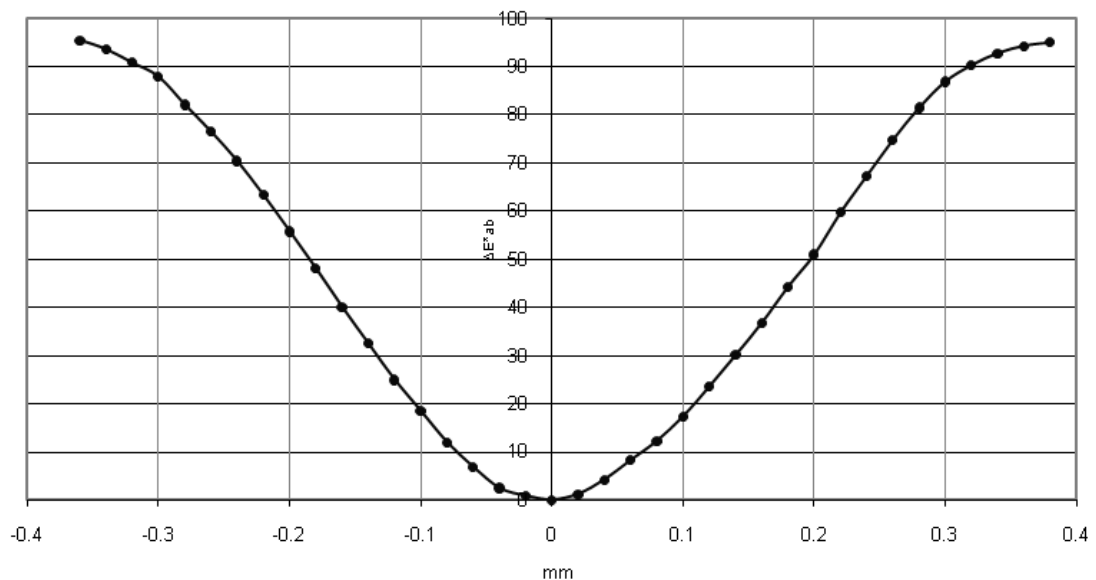


Figure 2.10. Alteration of colour measurements from micro-fadometer probe movements in 20 $\mu$ m increments through focus. Data is represented in  $\Delta E^*_{ab}$  when measuring a polished barium sulphate white standard.

Relative colour difference was also measured moving the probe in 50nm increments through focus when illuminating a polished barium sulphate white standard. Colour measurements are shown in figure 2.11, demonstrating that the colour measurements did not alter for 40 $\mu$ m through focus. From this analysis, colour measurement is shown to be more sensitive than the variation in size of the illuminated spot with probe position.

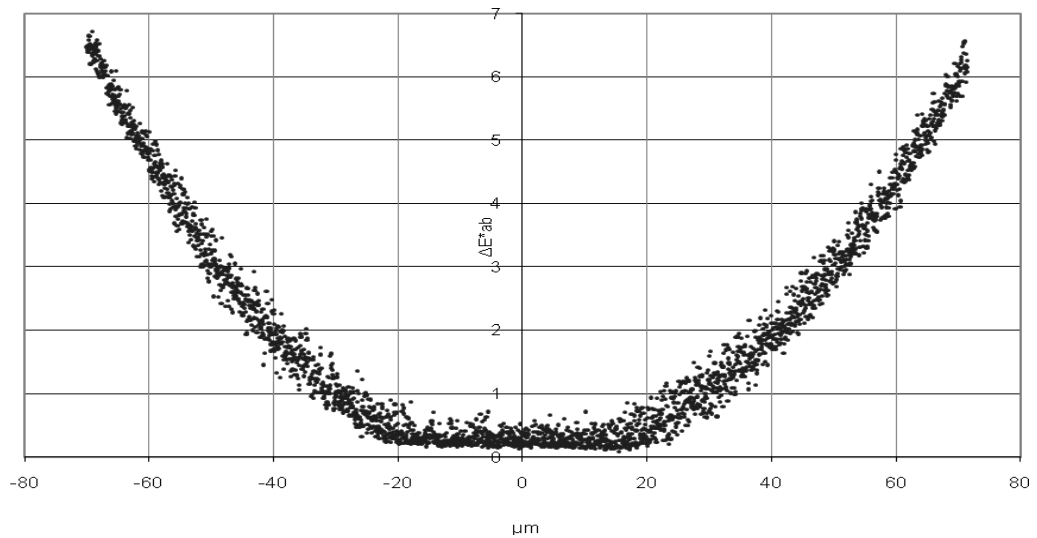


Figure 2.11. Alteration of colour measurements from micro-fadometer probe movements in 50nm increments through focus represented in  $\Delta E^*_{ab}$  values when measuring a pressed barium sulphate standard and comparing the colour measured with  $L^*=100$   $a^*=0$   $b^*=0$ .

The effect that small misalignments or alterations in geometry have on signal was also investigated. The sensitivity of positioning of the probe relative to the surface being sampled was determined. This was done by integrating the total counts of the received signal from a polished barium sulphate standard between 400nm and 700nm through focus (see figure 2.12). The signal is constant within approximately 10 $\mu$ m although variation in measured colour increases to larger values beyond this range

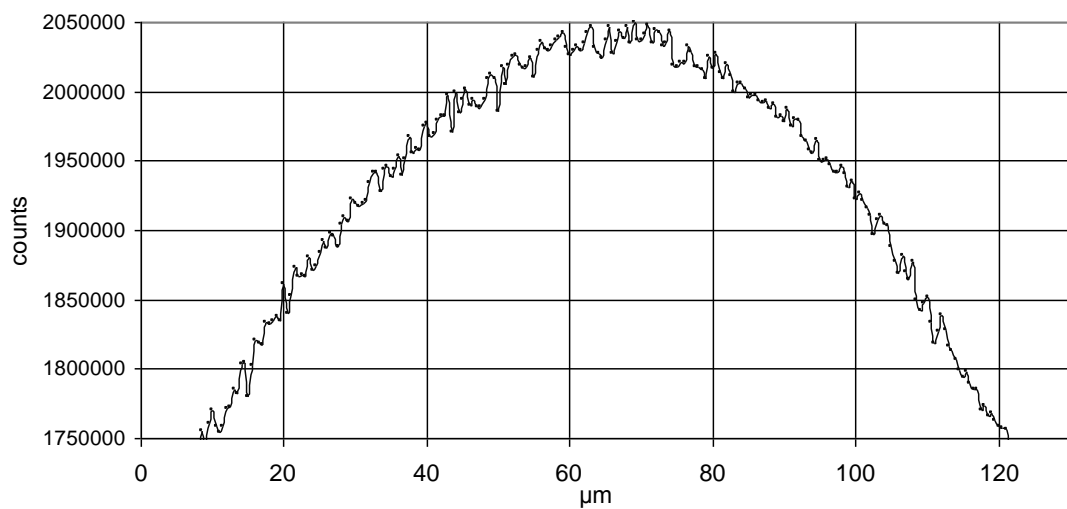


Figure 2.12. Total counts of the received signal from a polished barium sulphate standard integrated between 400nm and 700nm in 50nm movements of the probe through focus

The instrument used illuminating and receiving spots that were comparable, as the same fiber and lens systems were used for both probes. Alignment of the system was such as to ensure maximum signal was achieved when the spot size was 33 pixels FWHM. By ensuring this alignment, it was possible to remove the control of positioning of the probe head by eye thus removing human judgment of a sensitive sub-millimeter system. This alteration to the method does require accurate initial alignment of the probe head.

When considering the overlap of fading and sampling spots as shown in figure 2.5 a smaller sampling area than illuminating area could lead to the sampling spot being aligned at many locations and with many degrees of overlap on or around a non-uniformly illuminated area. Alternatively a smaller fading area and larger sampling area could lead to a variation in power density at the fading spot. This variation would be independent of signal strength as the illuminating spot could be of any size within the collecting optics sampling area. In other words maximum sample signal can be received from a large variation of overlapping spot sizes (even through the focus) of each lens system making repeatability of spot size an issue

### 2.2.6 Sample visibility and size

A series of faded spots were produced ranging from 1  $\Delta E^*_{ab}$  to 8  $\Delta E^*_{ab}$  on both Lightcheck ULTRA and Lightcheck Sensitive. The fading curve of Lightcheck Sensitive and the linear colour loss of Lightcheck ULTRA can be seen in figure 2.13. Lightcheck is made of a light sensitive coating on a paper or glass substrate. The colour changes of Lightcheck indicate the degree of exposure (Lavédrine 1998, Bacci *et al.* 2003, Romich and Martin, 2003, Dupont *et al.* 2008).

Reversion behavior in the case of both Lightcheck samples was observed. Faded spots created in this process were significantly less apparent or no longer visible when reviewed after 24 hours. Therefore all measurements were taken immediately after the fading process was complete.

Lightcheck was chosen as it provides an approximate worst case scenario with a very smooth highly fugitive surface. With both types of sample, it was possible to observe many spots in the series. It was found that 5 different observers of mixed ages and visual acuity when shown the location could see spots upto to a colour difference of 2 or 3  $\Delta E^*_{ab}$  units

(1 to 1.5  $\Delta E_{00}$ ) on a pristine Lightcheck surface under good lighting. This was in agreement with previous research on the subject where 2  $\Delta E_{ab}^*$  colour difference units are required before becoming visible (Michalski 1997) or a 50% probability for a colour difference of 1.5  $\Delta E_{00}$  (Pretzel 2000).

Importantly it was found that in situations where the Lightcheck surface was altered to reduce uniformity, for example by folding to vary the surface texture, it was impossible to see to such low levels of damage.

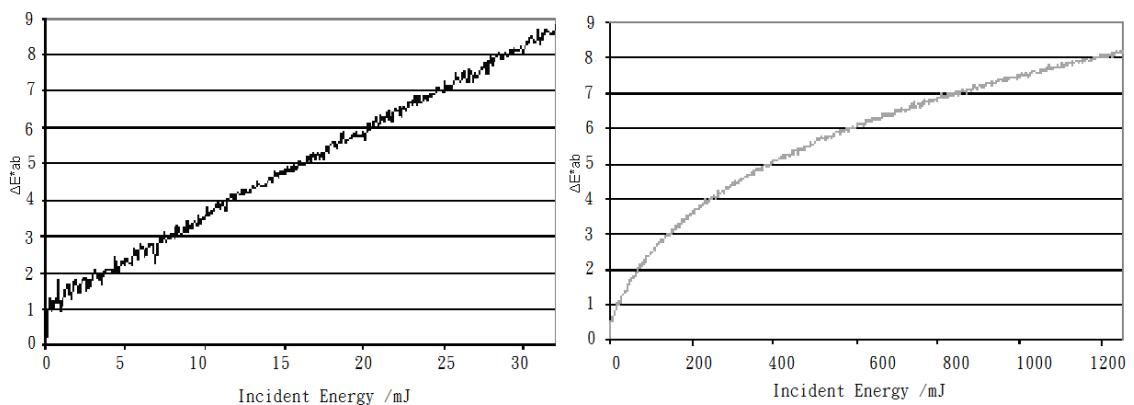


Figure 2.13. Colour change produced using the micro-fadometer on Lightcheck ULTRA (left) and Lightcheck Sensitive (right). Data presented in  $\Delta E_{ab}^*$  units.

Practically speaking, when fading rougher, more textured, varied surfaces, for example when fading samples of watercolour paint on rough paper, or oil paint brushed onto on canvas, it is possible at times to fade to 15  $\Delta E_{ab}^*$  and more and not observe any alteration as has been previously considered the case (Whitmore *et al.* 1999). This indicates that the damage is hidden by the texture in which it exists. Importantly, on many samples which were very uniform, such as various Prussian blues, a fade of 5 to 6  $\Delta E_{ab}^*$  (also 5 to 6  $\Delta E_{00}$ ) were visible on close inspection and often also at reading distance (25cm).

No change to the surface shape was observable to the human eye on fading to 5 to 6  $\Delta E_{ab}^*$  (5 to 6  $\Delta E_{00}$ ) for a Prussian blue sample. Further analysis of the faded spot using a Taicaan Xyris 3000 Interferometric surface profilometer (providing a 5nm resolution of the surface) provided no evidence of structural change. No alteration was observed to the profile of the surface of the faded area or the surrounding area.

An image of a faded spot of colour difference  $5\Delta E^*_{ab}$  ( $3.2 \Delta E_{00}$ ) on Lightcheck Sensitive was captured using a calibrated microscope. Analysis showed good uniformity of illumination and fading across the focal region. A typical example of the measured normalized profile of the faded spot, and a measured normalized profile of the incident illumination at best focus was also compared and shown to match well (see figure 2.14). The microscope camera was calibrated to 800 pixels per mm and this showed a variation in the FWHM spot size dependent on the degree to which we faded. This ranged from 0.22 for  $2 \Delta E^*_{ab}$  ( $1\Delta E_{00}$ ) to 0.25 for  $8 \Delta E^*_{ab}$  ( $3.2 \Delta E_{00}$ ). A separate investigation of spot size up to  $16 \Delta E^*_{ab}$  ( $12.8 \Delta E_{00}$ ) showed that continued fading led to continued increase of FWHM spot size.

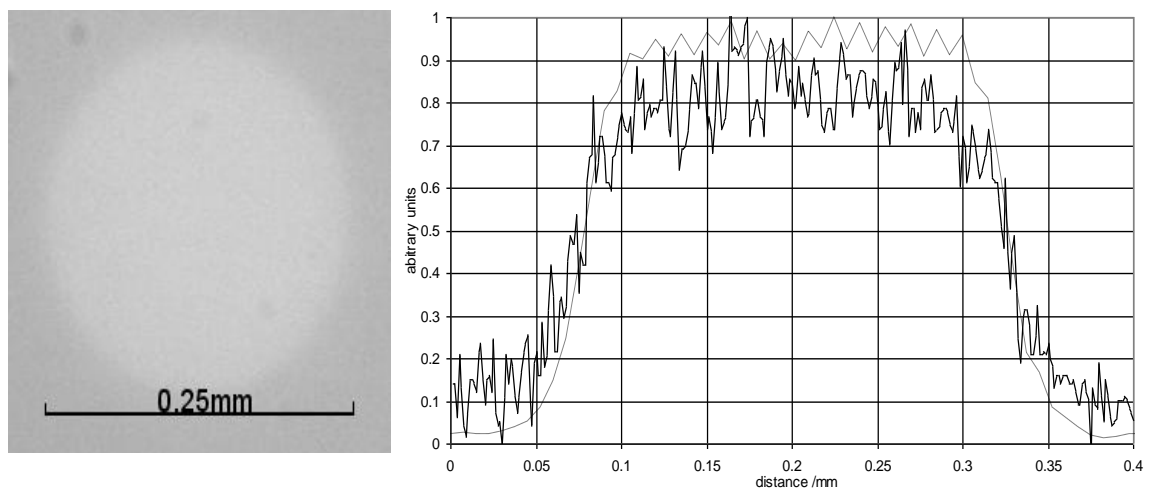


Figure 2.14. (Left) An image of a spot faded to a colour difference of  $5\Delta E^*_{ab}$  or  $3.2 \Delta E_{00}$  on Lightcheck ULTRA captured using a calibrated microscope. (Right). A typical example of the measured normalized profile of a  $5\Delta E^*_{ab}$  or  $3.2 \Delta E_{00}$  faded spot (indicated by the continuous line) and a measured normalized profile of the incident illumination at best focus (dashed line).

The sample size of 0.25mm corresponds well with the typical width of a textile thread. This can be seen in the case of Blue Wool standards (these standards are discussed further in the next section) where the woven texture has threads of approximately the same diameter. This is important as Blue Wool standards are of known relative lightfastness and are often used as a method of cross comparison in accelerated aging experiments (see British Standard 1006:1978). An example of thread width can be seen in figure 2.15.

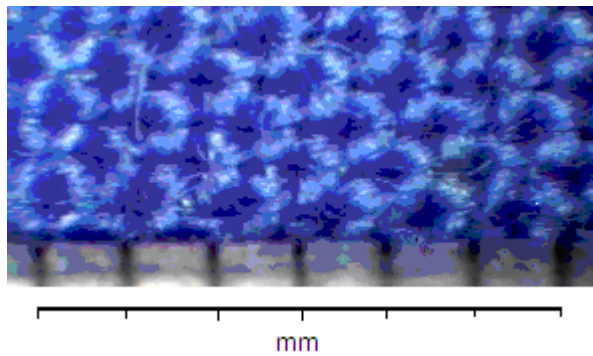


Figure 2.15. A magnified image of a Blue Wool standard sample. The scale seen on the bottom of the image is in millimeter increments.

## 2.3 Results and discussion

### 2.3.1 The rate of fading

ISO Standards are an internationally accepted method of measuring fading within the conservation science community (see British Standard 1006:1978). Eight different degrees of lightfast dyes can be used (with 1 being the least lightfast to 8 the most). The effect of fading Blue Wool samples 1, 2, and 3 by focusing 2.59mW to a 0.25mm diameter area can be seen in figure 2.16. This illustrates that the instrument is capable of fading Blue Wool 1 to 6  $\Delta E^*_{ab}$  in just over 5 minutes and Blue Wool 2 to the same level in twice that time period.

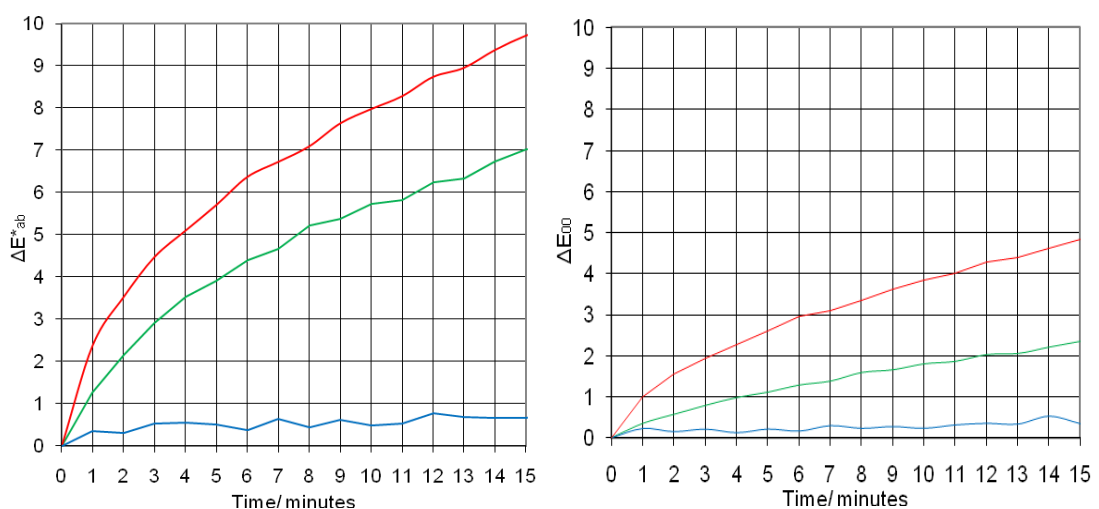
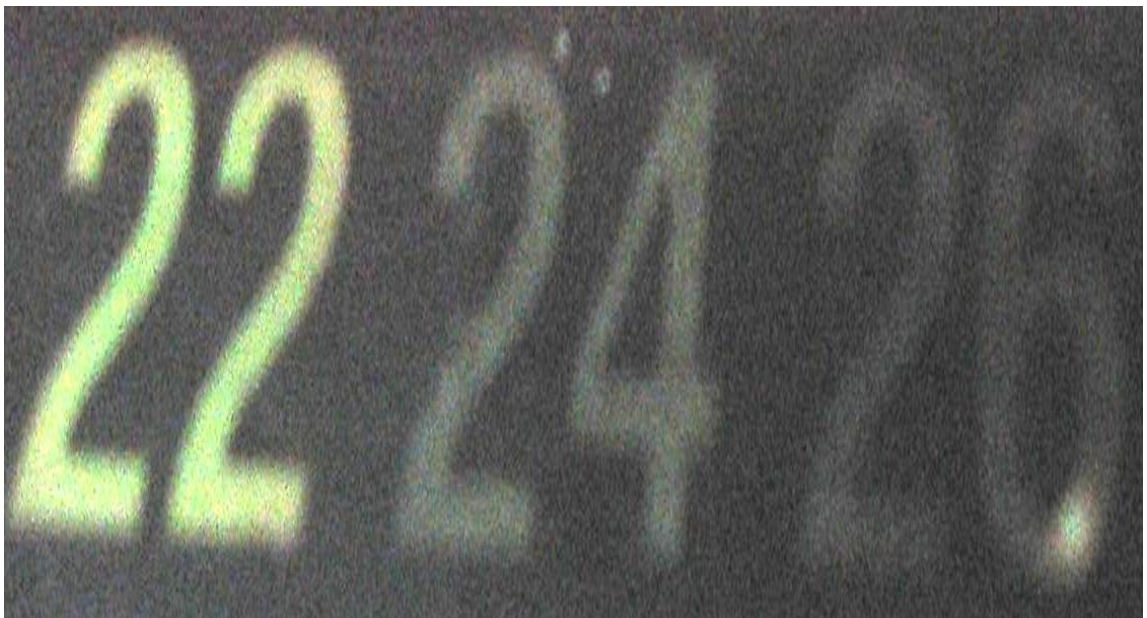


Figure 2.16. The fading rates of Blue Wool 1, 2 and 3 when fading using the broad spectrum. Results are shown using both colour difference units for clarity. Bluewool 1, 2 and 3 correspond with the red green and blue line respectively.

### 2.3.2 Temperature increase

In order to evaluate the safety of the instrument and to know to what degree temperature may play a part in any observed results, it was necessary to quantify the temperature increase caused by the focused radiation. Two techniques were employed. On separate occasions two different thermocouples were coated with various light and dark paint samples on paper and illuminated by the focused spot. A thermocouple was also lightly coated with a variety of paints as well as exposing the bare sensing junction. The same temperature increase of 3° to 4°C above room temperature was observed in all cases.

As a second method, a thermometer that contains heat-sensitive (thermochromic) liquid crystals that change colour to indicate different temperatures was used. A number in a series corresponding to the environmental temperature becomes translucent when it is reached. By focusing the probe onto the various temperature-sensitive numbers, 26°C clearly altered whereas all others from 12 to 34 (increments of 2 degrees) did not. The area heated by the radiation remained briefly unaltered after the light was removed by a shutter, before cooling. A photograph of this can be seen in figure 2.17.



*Figure 2.17. A liquid crystal thermometer immediately after being irradiated with the micro-fadometer. Note 22 is clearly visible at 22°C room temperature and the bottom right hand corner of the 26 showing a small circular area which has been increased in temperature to approximately 26°C by the focused probe*

### 2.3.3 Repeatability of results

In an investigation into the colour stability of digital prints a correlation between this micro-fadometer apparatus and bulk fading in a light box with a xenon lamp was found. It was possible to grade printed coloured papers according to lightfastness resulting in a linear relationship between the two (Sandahl 2009).

A variety of reflectance standards were used to investigate the colour measurement accuracy of the instrument and compared to results from other colour measurement techniques. This indicated that some standards are less accurate on the scale of measurement (0.25mm), with a significant variation in reflectance over the sub-millimeter scale.

The repeatability of measurements on different surface textures was investigated via three methods on 4 different samples. These samples were the smooth and diffuse sides of a pressed barium sulphate standard (Russian Opal), the considerably rougher surface of Whatman filter paper and also a faded spot created by the micro-fadometer of approximately  $6.5 \Delta E^*_{ab}$  or  $2.4 \Delta E_{00}$ .

Colour measurements were made at different locations on the same sample (refocusing at each location when the probe moved to a new area of the sample). Then repeat measurements of the probe when stationary were made on a sample surface to gauge the error connected with the system. Finally the same measurement location was revisited many times using an XYZ stage. With all these results the measured colour difference that was produced was monitored and calculated relative to the first reading in the sequence.

Results of the colour difference produced by the 3 processes are displayed in table 2.1 (the full data set can be found in appendix B). Maximum colour difference values over 10 measurements are displayed as well as the equivalent standard deviation to enable error analysis. Note that the standard deviation provided is an equivalent standard deviation as the data displayed an approximately rectangular distribution rather than a normal distribution when using cluster analysis. This equivalent standard deviation is calculated by dividing the maximum value of deviation by the cube root of 3.

	Smooth				Diffuse				Whatman Filter Paper				Colour Well			
	$\Delta E^*_{ab}$	St dev	$\Delta E_{00}$	St dev	$\Delta E^*_{ab}$	St dev	$\Delta E_{00}$	St dev	$\Delta E^*_{ab}$	St dev	$\Delta E_{00}$	St dev	$\Delta E^*_{ab}$	St dev	$\Delta E_{00}$	St dev
<b>A</b>	0.61	0.42	0.38	0.26	0.82	0.57	0.51	0.35	7.92	5.49	4.74	3.29				
<b>B</b>	0.1	0.07	0.1	0.07	0.07	0.05	0.2	0.14	0.06	0.04	0.07	0.05	0.08	0.06	0.04	0.03
<b>C</b>	0.14	0.01	0.2	0.14	0.14	0.01	0.1	0.07	0.14	0.1	0.14	0.1	0.07	0.05	0.03	0.02

Table 2.1. A summary of the results of accuracy tests of the instrument. Row A contains data from testing different locations on the same sample and refocusing at each location. Row B contains data from repeat measurements when stationary. Row C contains data from repeat measurements when returning to the same spot.

Results from the combination of all data obtained on the same location (rows B and C) resulted in a maximum observed error of  $0.14 \Delta E^*_{ab}$  with an equivalent standard deviation of  $0.1 \Delta E^*_{ab}$  or  $0.2 \Delta E_{00}$  with an equivalent standard deviation of  $0.14 \Delta E_{00}$ .

Lack of repeatability was seen to depend largely on the roughness of the target material. To investigate this sixty five historically accurate reproductions of pigments (as discussed in the introduction) were faded twice in order to appraise the repeatability of results gained from using the fadometer on real samples. The colour difference after 1 hour of exposure under illumination from the instrument is shown in the plots below.

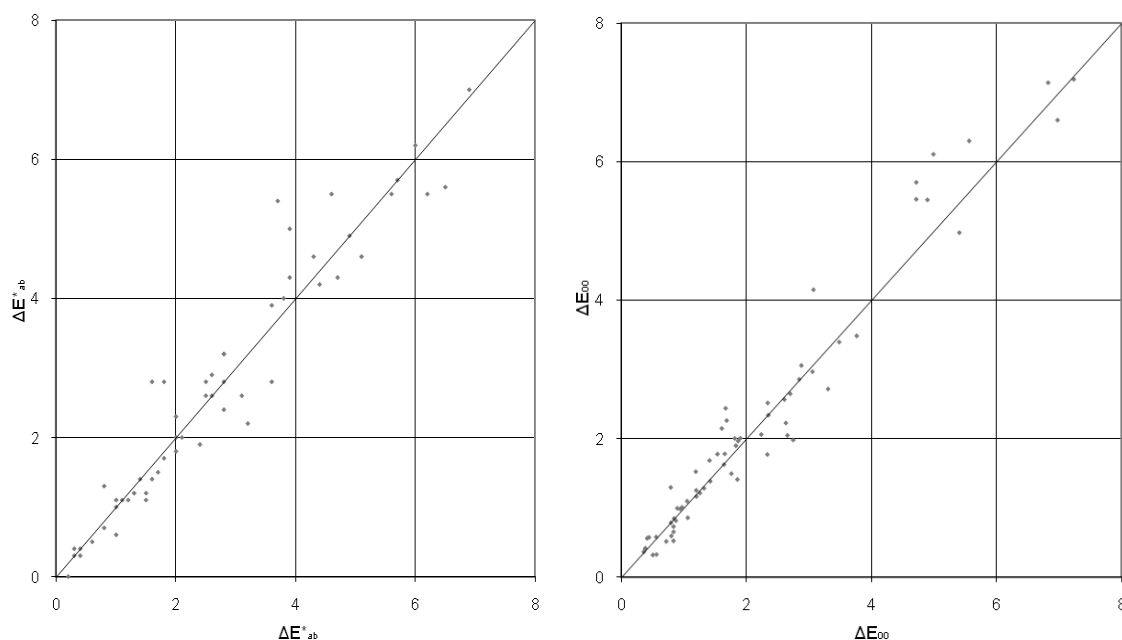


Figure 2.18. A illustration of the repeatability of the technique after application to a large number of historically accurate reproductions of traditional watercolour pigments ground in gum Arabic, on Ruscombe mill sized and glazed paper. Colour difference represented in  $\Delta E^*_{ab}$  (left) and  $\Delta E_{00}$  (right).

A correlation between the results, albeit with greater scatter than would be expected from measurement error alone can be observed. This provides some confidence that data obtained on real objects via this technique can provide reproducible information for this spot size, or for larger similar areas of the same work.

When comparing colour difference units the colour changes calculated in the CIE 1976 L\* a\* b\* colour space are significantly larger than the CIEDE2000 colour space as can be seen below in figure 2.19.

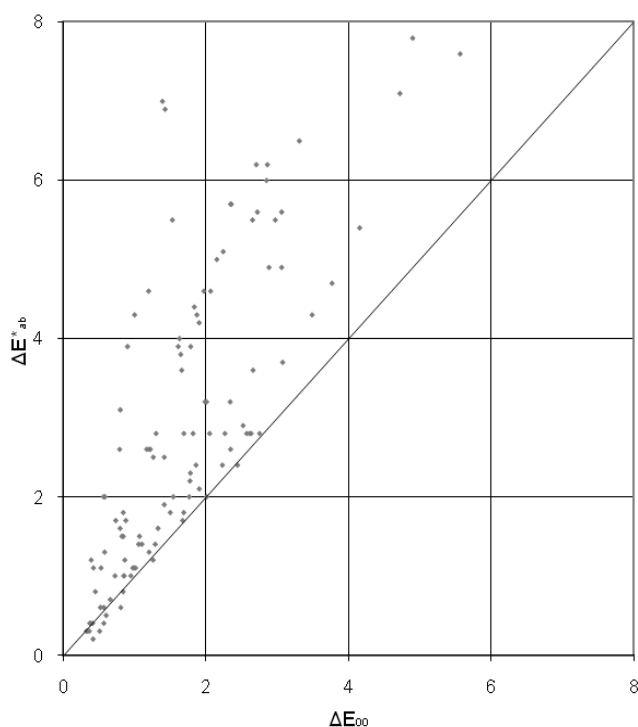


Figure 2.19. A comparison of the colour differences calculated for the same sample set as used in Fig. 2.18 in CIE 1976 L\* a\* b\* and CIEDE2000 colour difference units.

An individual example of this can be seen in figure 2.20 where a comparison of the 2 fading curves of verditer (CA21) and weld lake (NG3) are presented in different colour units. In the  $\Delta E_{00}$  case the two pigments would correctly be considered similar in their stability, however if the pigments were analysed using  $\Delta E_{ab}^*$  the conclusion drawn from the result would be the opposite. An issue that has had some previous discussion (Pretzel 2008).

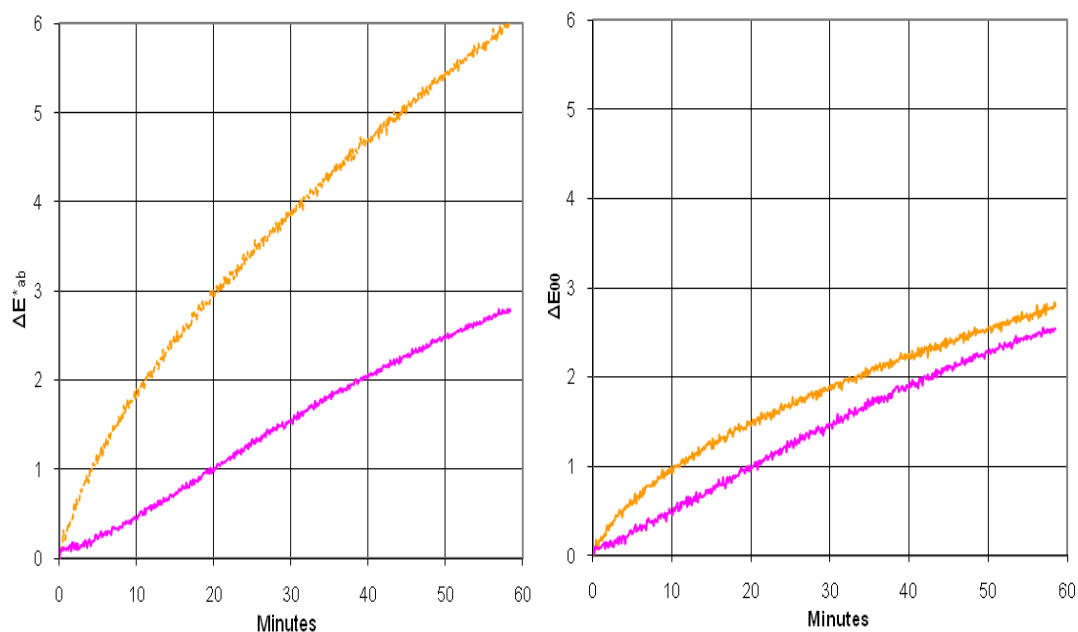


Figure 2.20. A comparison of the degrees of fading of verditer (code CA21) and weld lake (code NG3) (represented by the orange and pink lines respectively). Using  $\Delta E_{00}$  for analysis the two pigments are similar in their degree of stability, in  $\Delta E^*_{ab}$  the conclusion would be to the contrary.

### 2.3.4 Propagation of error

To investigate the effect of drift and noise on readings made by the instrument, spectra of the illuminant incident on a non-fugitive white tile were saved periodically over 7 hours. The percentage variation (from the initial illumination) of the lamp at each wavelength was calculated. The maximum drift and noise observed at any one point in time over the 7 hours was applied to typical pigment reflection spectra and the resultant colour difference calculated. A second technique was conducted by simulating drift and noise and creating a simulated spectral uncertainty. From data on the light source shown in section 2.2.4 a simulated 0.2% random Gaussian uncertainty at each measurement wavelength and a drift uncertainty of about 0.23% was applied. This resulted in a maximum peak to peak variation for the 100% signal of about 2% and an average variation of approximately 0.5% reflectance.

The results in terms of colour difference for both techniques were calculated for typical samples and also an ideal white ( $L^*=100$ ,  $a^*=0$ ,  $b^*=0$ ). The spectra selected for analysis are included in figures 3.4 and 3.5. The results can be seen in table 2.2.

Spectra	From Recorded Drift and Noise		Simulation of Drift and Noise			
	$\Delta E_{ab}^*$	$\Delta E_{00}$	$\Delta E_{ab}^*$		$\Delta E_{00}$	
			Mean	Max	Mean	Max
White	0.36	0.25	0.25	0.58	0.24	0.63
Prussian green (NGWC10)	0.17	0.14	0.19	0.43	0.17	0.4
Dragon's blood (NGWC7)	0.16	0.16	0.23	0.4	0.18	0.4
Weld (NG 2)	0.15	0.09	0.23	0.43	0.13	0.29
Rhodamine B	0.21	0.1	0.21	0.4	0.1	0.04
Blue Wool 1	0.19	0.07	0.15	0.42	0.17	0.07
Prussian blue (TTB6)	0.16	0.12	0.2	0.35	0.17	0.37
Litmus (NG L)	0.19	0.12	0.18	0.39	0.13	0.26

Table 2.2. A summary of the results of drift and noise analysis for the instrument. Firstly by the application of the maximum value of recorded drift and noise of the lamp over a 7 hour period and secondly via a simulation.

An error no greater than  $0.36 \Delta E_{ab}^*$  or  $0.25 \Delta E_{00}$  was calculated at any reading over the 7 hour period, and less when applied to typical samples.

The longer term stability of the entire system was investigated by monitoring the change in the signal received when illuminating a non fugitive white standard. This was conducted by taking an initial colour measurement and then when leaving the micro-fadometer running, periodically returning to make further measurements on the same location. It was found that colour measurement of a white tile did not exceed the maximum error previously observed for the 7 days tested. This meant a sufficient level of stability for this research.

When considering the previously observed and calculated errors connected with drift and noise as no greater than  $0.36 \Delta E_{ab}^*$  or  $0.25 \Delta E_{00}$  and a simulated maximum of approximately 0.6 in either colour difference unit, the large variation in results seen in figure 2.18 was largely considered due to the small sampling area of the instrument. Any variation in the sample was not averaged over as would happen with larger sampling areas.

Cluster analysis of error due to drift and noise did not display a Gaussian distribution via either method. Similar analysis of the distribution of tristimulus data and CIELAB data

indicated that the distribution of results became increasingly less normal in distribution at every step in the calculation of the error in colour difference values (see Pretzel 2008).

65 historically accurate reproductions were each faded twice as shown in figure 2.18. Distribution analysis of the percentage variations in fading for each individual pigment from its mean displayed an approximate normal distribution for the sample set (using a chi-squared test with a significance level of 5%). This was only for colour differences calculated in CIEDE2000 (with the risk to reject the hypothesis while it is true being 9.04%). Variation of CIELAB values did not follow a normal distribution (with the risk to reject the hypothesis while it is true lower than 0.01%) see figure 2.21.

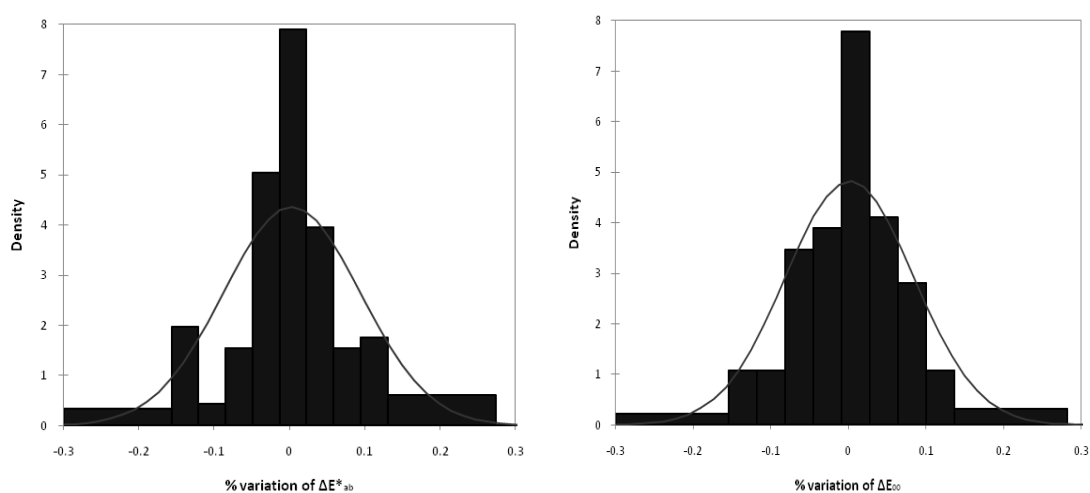


Figure 2.21. The percentage variation in the degree of fading of a large number of historically accurate reproductions of traditional watercolour pigments. Percentage colour difference represented for  $\Delta E^*_{ab}$  (left) and  $\Delta E_{00}$  (right) with the normal distribution shown as a red line. The extreme bins are pooled to create higher values necessary for a chi-squared test.

Variation in the sample has been shown to be a far more significant source of error than drift and noise. As the resultant variation in repeat measurements when calculated in CIEDE2000 show an approximate normal distribution and also in order to proceed a standard deviation was applied.

As the colour measurements that make up a single fading curve do not possess a normal distribution an approximate standard deviation was applied in this case (by dividing the maximum value of error by the cube root of 3). More significant analysis (although worthwhile) was not considered a suitable use of time within the context of the project.

## 3.0 The wavelength dependence of fading

### 3.1 Introduction

Colourants are chosen due to their absorption in the visible range as it is absorption in this wavelength range that gives them their useful property. Considering this, it can be argued that fugitive colourants must be faded predominantly by the visible region (McLaren 1956) especially in galleries where the ultraviolet wavelengths are filtered to protect artworks. Therefore the effect of visible radiation on deterioration of fugitive pigments warrants further investigation via a wavelength tunable fading system.

Early work investigating the influence of wavelength on colour change was produced by Russell and Abney (1888). Exploring the effects of blue, green and red light on selected watercolours; it was concluded that ‘the rays which produce by far the greatest change in a pigment are the blue and violet components of white light’.

Later Appel and Smith (1928) used various types of coloured filters to assess their effect on colour change. This technique was adopted in work in subsequent years by McLaren (1956) where the transmission of 5 filters which cut off radiation below 600nm, 460nm, 400nm, 360nm and 295nm were employed. This enabled the division of the incident spectrum into 5 wavelength sections to observe the relative degree of change in photochemical degradation when the changes in filter transmission occurred.

Further investigations which continued to use bulk fading were produced by Kenjo (1986) (1987) and Saunders and Kirby (1994a). In the work by Kenjo monochromatic light was employed to investigate the effect of radiation from 245nm to 699nm and via this the number of locations in the visible range increased to seven (located from 390 nm to 699 nm). Saunders and Kirby used broad band interference filters with bandwidths of 70nm (FWHM) at peak transmittances located at 50nm intervals in the visible range from 400nm to 700nm.

## 3.2 Technique introduction

### 3.2.1 Experimental arrangement

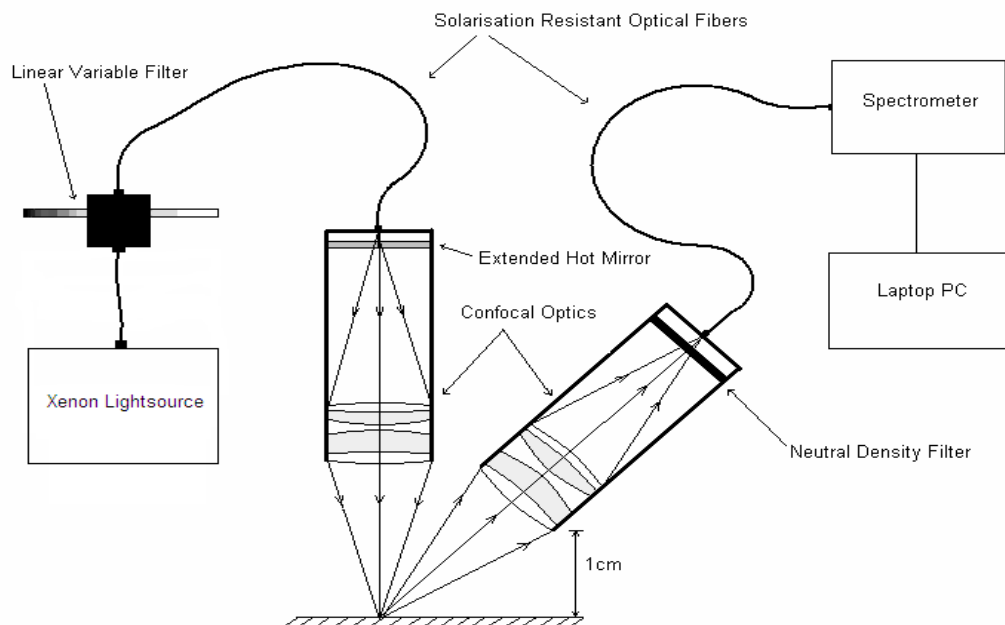


Figure 3.1. A representation of the schematic wavelength tunable micro-fadometer with linear variable filter.

An alteration to the micro-fading spectrometer (with the addition of a linear variable filter) can be seen in figure 3.1. The xenon lamp is filtered with an Ocean Optics LVF-UV-HL and LVF-HL filter. The filter bandwidth of this technique is 20 to 30nm FWHM and it is possible to vary the central wavelength of the filter in the visible range as in figure 3.2.

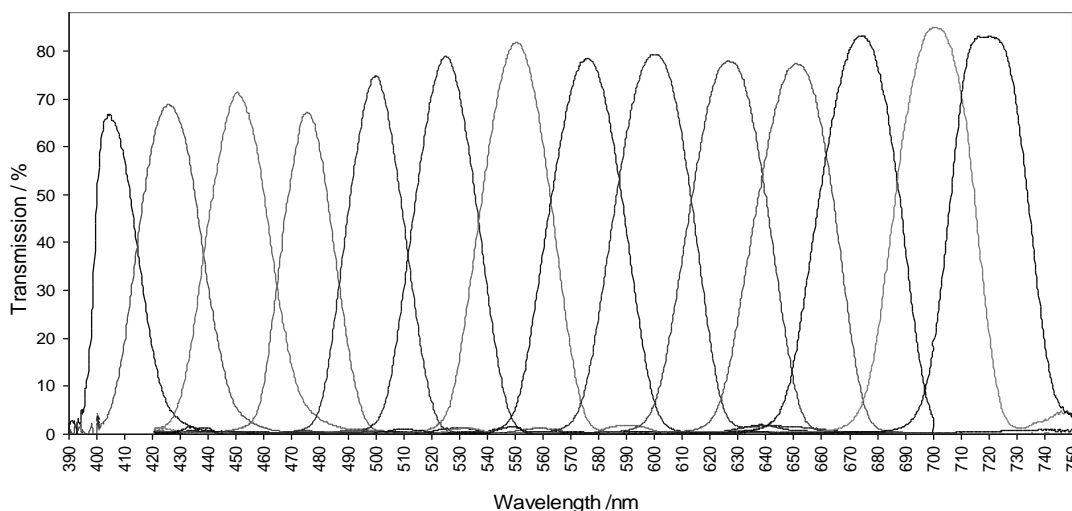


Figure 3.2. Tunable filter transmission at various wavelengths typically employed by the tunable instrument.

The power transmission was measured using a Melles Griot integrated 2 watt broadband power and energy meter system integrating over a wavelength range of 200nm to 20 $\mu$ m. The incident power measured when no variable filter was present is 1.46mW or 0.46 lumens at focus (losses due to the inclusion of the linear variable filter reduces the power of the instrument at focus from 2.59mW). Each sample is individually exposed to 13 wavelength peaks. Figure 3.2 contains measured data of the filter transmission employed by the instrument. Collectively these equate to approximately 1.46mW of power over the entire visible spectrum. Therefore the researcher is able to gain data using the full visible spectrum and then examine the degradation caused by individual sections of the spectrum for the same sample over that same exposure time.

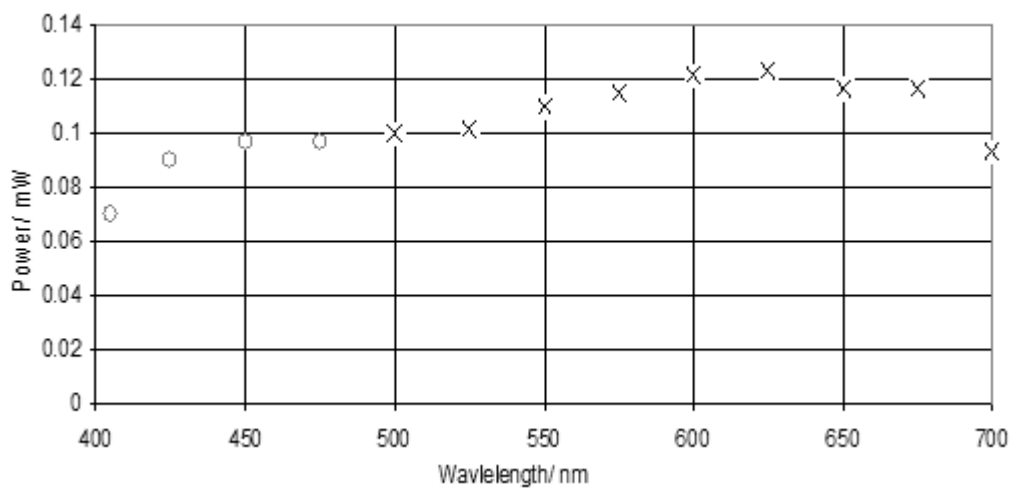


Figure 3.3. The power variation at focus of the wavelength tunable micro-fadometer. An Ocean Optics LVF-UV-HL is used from 405nm to 475nm and an LVF-HL filter from 500nm to 700nm .

The length of time for fading was altered at each wavelength. This was necessary in order to compensate for the variation in incident power with wavelength caused by the spectral power distribution of the lamp (see figure 2.6) and varying transmission of the filter at each wavelength (see figure 3.2). This resulted in a power distribution at focus as illustrated in figure 3.3.

With the linear variable filter in place, the temperature measured by a thermocouple substituted for the sample was found to increase by approximately 1°C independent of wavelength range. No alteration was observed when focusing on a liquid crystal thermometer with temperature increments of 2 degrees.

It was found that the fading spot size remains at 0.25mm when sampled using a CCD at intervals from 400nm to 700nm.

### **3.2.2 Experimental method**

The tunable instrument operates in a similar way to that described previously for the micro-fadometer. The spectra must be recorded before and after fading in order to obtain a value for the colour difference.

After an initial reading has been taken, the variable filter is adjusted to the chosen wavelength prior to fading. The filter is then removed after fading to take a spectral measurement. A neutral density filter was used prior to any exposure of the sample in the case of very fugitive materials. Due to the presence of the filter colour measurements are not possible during fading unless the shutter is opened, the filter removed and a measurement rapidly taken in order not to alter the degree of fading.

The technique of initially monitoring the sample lightfastness using a broad spectral fade enables the user to determine a suitable length of exposure. A 40 minute period has typically been used to fade samples as fugitive as Blue Wool 1 to 2.

## **3.3 Sample sets**

The sample selection could be separated into two sections – historically accurate reconstructions of traditional watercolour pigments that were selected because they were fugitive and Lightcheck ULTRA, Lightcheck Sensitive and Blue Wool Standards.

### **3.3.1 Artists' pigments**

Application of the instrument was extended to Prussian blue (Tate Gallery Archive 7315.6#6, Q04047 TTB6) and madder (Tate Gallery Archive 7315.6#13, Q04047 TTB13) taken from Turner's studio materials used before his death in 1851. Prussian green (NGWC10) and dragon's blood NGWC7 dated 1796-1826 were also tested. These were

taken from a dated Ackermann paint box and small samples of the watercolour cakes were mixed with water before painting out on the same paper.

Prussian green can be made in numerous ways; either by stopping the manufacturing process of Prussian blue at the stage when the sediment is green, or combining Prussian blue with a yellow pigment such as gamboge (Eastaugh *et al.* 2004), as is the case for this sample. All these pigments were prepared by grinding with gum Arabic, diluting with distilled water and applying in a wash onto Ruscombe mill paper (as discussed in the introduction).

Included in the pigment selection were weld NG 2 and litmus NG L; these pigments were produced and have been referred to by Saunders and Kirby (1994b). These samples were ground with gum Arabic, diluted with distilled water and applied in a thin wash on Whatman silversafe conservation grade paper. The results of wavelength specificity measurements were published (Saunders and Kirby 1994a).

Litmus is violet blue in colour and is derived from lichen. It is now used as an indicator dye; but records suggest it was used as a pigment in the 16th century (Eastaugh *et al.* 2004).

The reflectance spectra of the pigments can be found in figure 3.4.

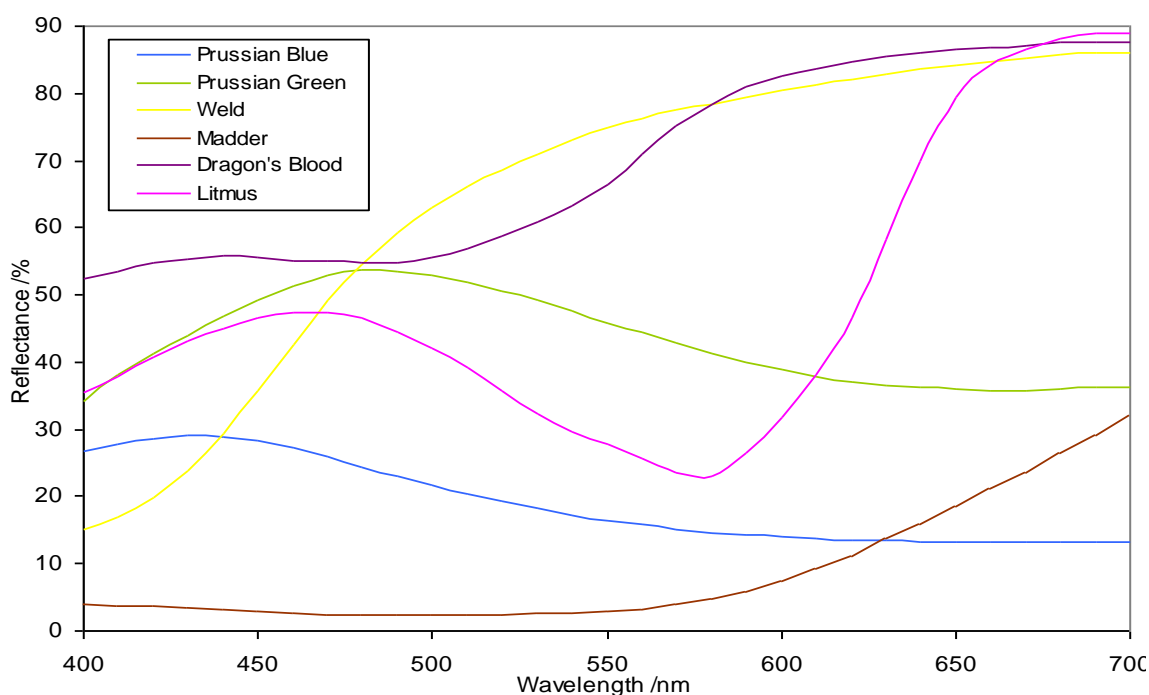


Figure 3.4. The reflection spectra of the pigments used for wavelength dependence fading.

### 3.3.2 Light dosimeters and standards

The investigation extended to dosimeters and standards currently used by heritage scientists. The light dosimeters and standards were selected to represent tools either having the potential to be used or often used by museums and galleries to assess the amount of light to which an object is exposed.

International Organization for Standardization (ISO) Blue Wools 1 & 2 were tested. These are commonly used in galleries to monitor lighting and consist of a combination of Eriochrome 2, Azurole B (colour index (CI) 43830) & Indigosol Blue AGG (CI 73801) dyed onto wool. Also Lightcheck Sensitive and Lightcheck Ultra were tested. These are two highly sensitive light dosimeters (constructed from a calibrated light sensitive coating printed on glass and paper respectively) developed and refined by the LiDo project; a collaboration between a number of European research institutes (Dupont *et al.* 2008, Lavédrine 1998, Bacci *et al.* 2003, Romich and Martin, 2003).

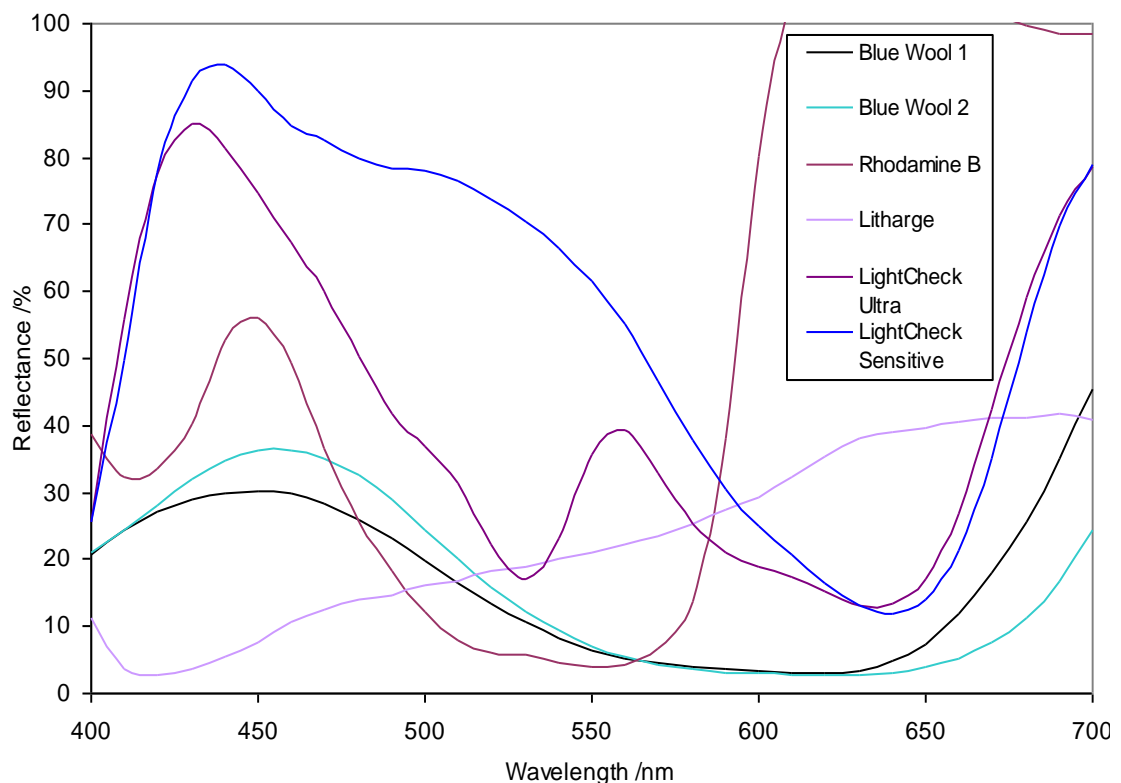


Figure 3.5. The 6 reflection spectra of the pigments used in the wavelength dependence fading tests.

Litharge and rhodamine B were 2 simple dosimeters for light level monitoring in galleries as suggested by Kenjo (1986) and these dosimeters were recreated from the published

recipe. As instructed litharge was mixed with a 10% aqueous solution of glue in order to make a soft paste and then applied to paper board cut to size. As a second dosimeter a 0.3% solution of rhodamine B was mixed with alcohol and a cotton blotting paper was immersed in the solution and dried in a dark room to produce a second sample.

Another standard investigated was a plastic UV absorbing foil coated with Paraloid B-72 and doped with Aberchrome 999P photochromic dye created as a potential dosimeter (Neeval 2008) and donated by its maker. This potential standard exhibits a major change in its absorption spectrum on irradiation at one wavelength, which later can be reversed either thermally or via exposure to a different (UV) wavelength (Heller 1986). The reflectance spectra of the dosimeters and standards can be found in figure 3.5.

### **3.4 Light exposure**

The majority of the samples were illuminated with the equivalent of approximately 3.5J of energy over approximately a forty minute period (total exposure time was depending on the filter response at the chosen wavelength as discussed earlier).

The exceptions to this were Blue Wool 2, Lightcheck Sensitive, Lightcheck Ultra, Aberchrome 999P photochromic dye and litmus. In the case of these samples, after initial fading experiments the exposure was either insufficient or far too great to acquire informative data.

In the case of blue wool 2 the standard exposure time of approximately 40 minutes or 3.5J was doubled to achieve a total energy of approximately 7 J in an 80 minute period

As Lightcheck Sensitive and Lightcheck Ultra were designed to have very low lightfastness, it was found they were too sensitive for a 3.5J exposure. In the case of Lightcheck Ultra it is reported that complete bleaching occurs within 120,000 lux hours. A 65 second fade provided this equivalent in lux hours (approximately 0.1 J of energy). Using the same model incident energy was reduced to approximately 0.3 J for Lightcheck Sensitive as it bleaches in 400,000 lux hours) (Lightcheck 2010).

The Plastic UV absorbing foil coated with Paraloid B-72 doped with Aberchrome 999P received a reduced dose of 0.1 J over 65 seconds.

Litmus proved to be an especially fugitive pigment and therefore exposure was halved to approximately 1.7J over approximately 20 minutes.

Prussian blue was exposed to 1.75J, 3.5J and 7J of over a 20, 40 and 60 minute exposure period (respectively), this was done in order to investigate effect of exposure on the damage function for the pigment.

A summary of incident energy and fading time can be found in table 3.1.

Sample	Sample Code	Total incident energy (J)	Fading time (s)
Madder	TTB13	3.5	2400
Prussian green	NGWC10	3.5	2400
Dragon's blood	NGWC7	3.5	2400
weld	NG 2	3.5	2400
rhodamine B	n/a	3.5	2400
litharge	n/a	3.5	2400
Blue Wool 1	n/a	3.5	2400
Blue Wool 2	n/a	5.25	3600
Prussian blue	TTB6	1.75 & 3.5 & 5.25	1200 & 2400 & 3600
Lightcheck Sensitive	n/a	0.3	195
Litmus	NG L	1.75	1200
Lightcheck ULTRA	n/a	0.1	65
Aberchrome 999P	n/a	0.1	65

Table 3.1. A summary of the illumination at each wavelength from the Micro-fadometer for each sample tested.

### 3.5 Results

Results relating to colour difference within this chapter are presented using the CIELAB colour space and the corresponding colour differences using  $\Delta E^*_{ab}$ .

#### 3.5.1 Appraisal of the technique

In order to assess the precision and repeatability of results from the technique complete measurements for Lightcheck Sensitive and the Aberchrome 999P photochromic dosimeter were repeated three times and five times respectively as shown in figure 3.6.

An approximate standard deviation was applied created by dividing the maximum value of deviation by the cube root of 3.

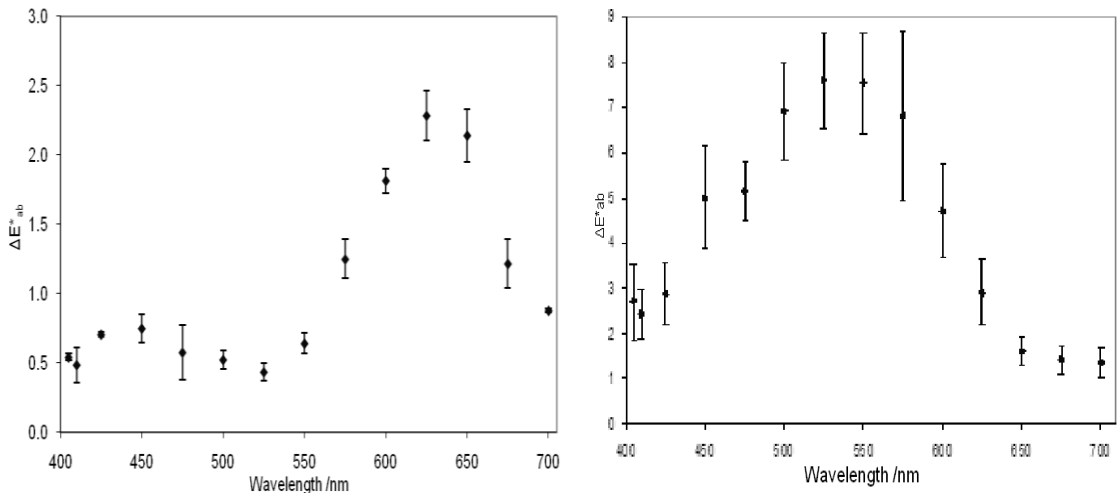


Figure 3.6 Lightcheck Sensitive (left) and Aberchrome 999P photochromic dosimeter (right) (error bars +/- 1 equivalent standard deviation of the numerous readings).

Using broadband filters the result for the wavelength dependency for Lightcheck Sensitive was confirmed. After a 40 minute exposure (with the same fadometer arrangement) using a blue transmitting filtered xenon source (with negligible light transmitted above 575nm) an average colour change of 2.6  $\Delta E^*_{ab}$  was observed after 5 measurements. After the same period of exposure under a red transmitting filtered lamp (with negligible light transmitted below 575nm) an average colour change of 7.1  $\Delta E^*_{ab}$  was measured after 5 measurements.

The result clearly illustrates the wavelength sensitivity that Lightcheck displays. The Aberchrome 999P photochromic dosimeter illustrates a potential to be used as a lux meter with a response to wavelength similar to the photopic response of the human eye.

To investigate any effect incident energy or fading time may have on the resulting damage function, the Prussian blue sample was exposed to 1.75J, 3.5J and 5.25J over a 20, 40 and 60 minute period respectively. The three results as shown in figure 3.7 show good agreement as similar information was achieved for the damage function at each exposure.

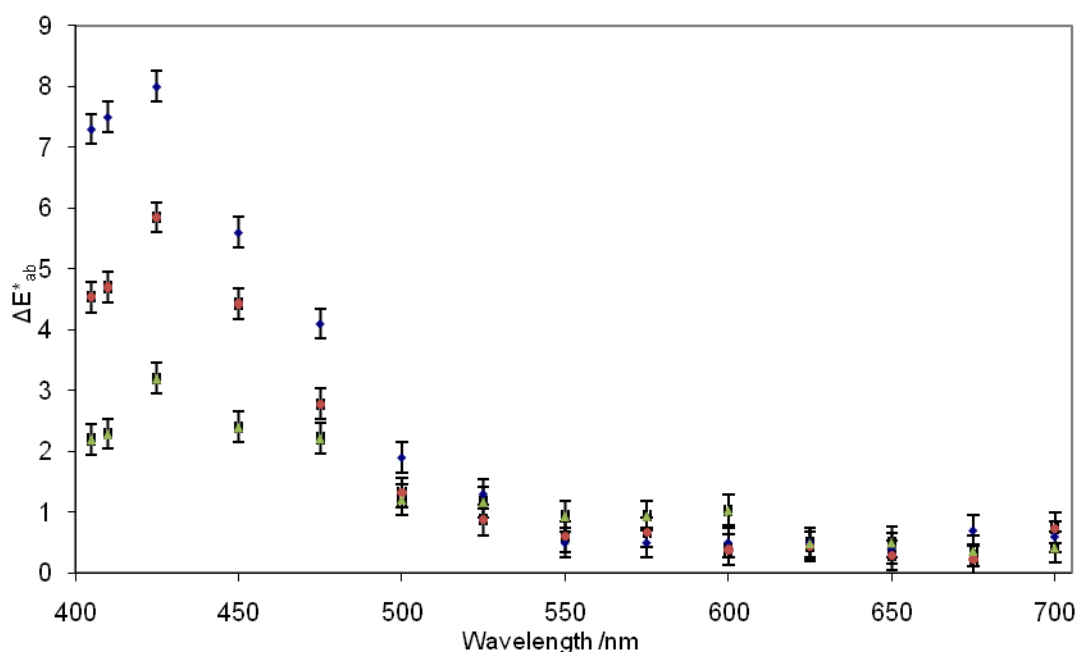


Figure 3.7. Results from application of the instrument to Prussian blue over different exposure times. The 20, 40 and 60 minute period fades are shown in green red and blue respectively. Error bars +/- 1 equivalent standard deviation for drift and noise.

In order to appraise the reliability of information achievable with this technique, results were compared to previous work using bulk optical filters by Kenjo (1986). Where a similar investigation was conducted using a number of monochromatic lights (over a broader range of wavelengths than in this work). Comparisons are shown in the visible range between data collected using monochromatic lights and the micro-fadometer (see figures 3.8 and 3.9).

In the case of the monochromatic lights colour difference measurements after exposures of approximately  $15 \text{ J cm}^{-2}$  for rhodamine B and  $46 \text{ J cm}^{-2}$  in the case of litharge were made.

Despite the fact that previously the results were measured after a greater colour change, these comparisons demonstrate the similarity of results from the two different techniques with respect to the effect of wavelength. The level of colour change differed between the two samples. This was thought to be due to differing concentrations of colourant on the sample surfaces. This variable was not controlled in the instructions given for the creation of the sample.

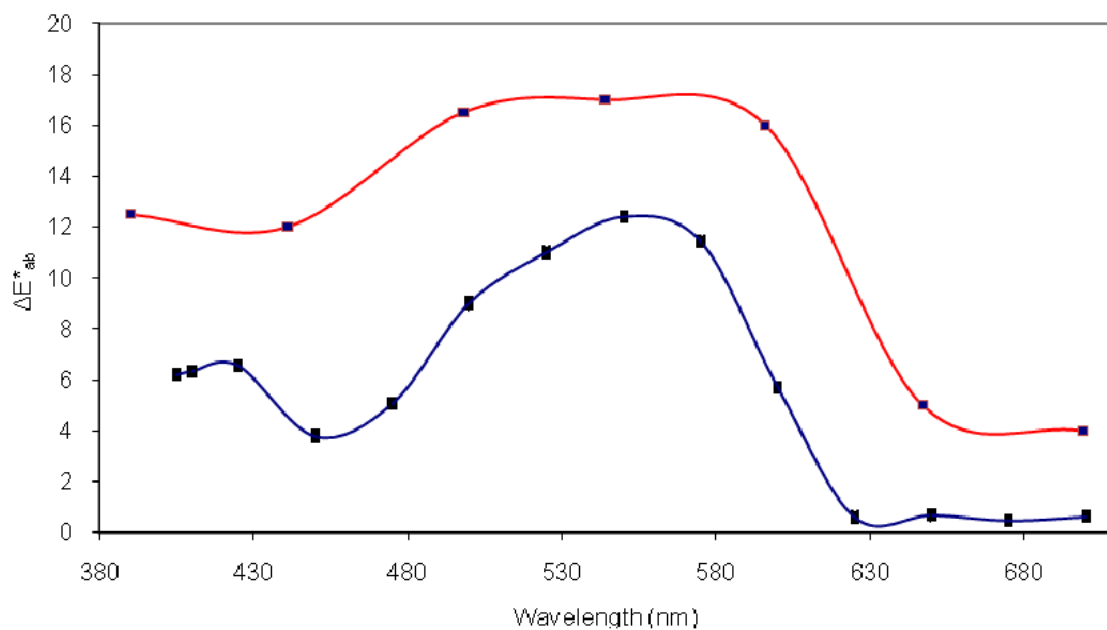


Figure 3.8 Results from application of the instrument to rhodamine B (in blue) in comparison to similar research using monochromatic lights (red). Error bars are too small to be seen.

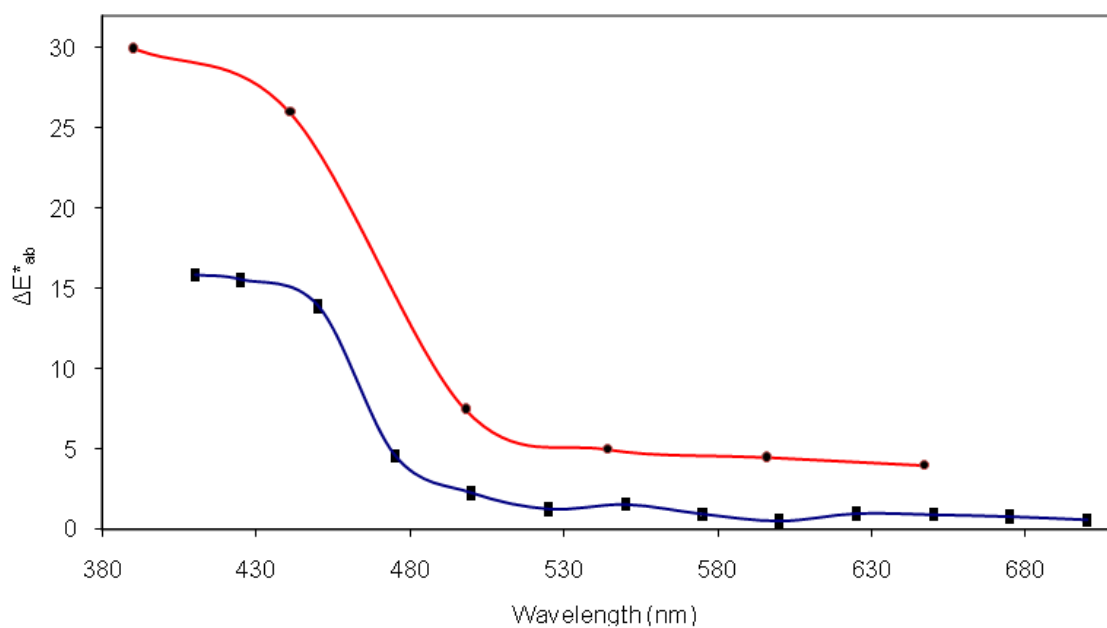


Figure 3.9. Results from application of the instrument to litharge (in blue) compared to similar research using monochromatic lights (red). Error bars are too small to be seen.

### 3.5.2 Comparison of results with reflection spectra

The technique was applied to the full sample set of dosimeters and artist's pigments, described previously.

As data acquisition was time consuming measurements were repeated solely to confirm significant peaks or troughs.

Results for the individual pigments along with their reflection spectra can be found in figures 3.10 to 3.21

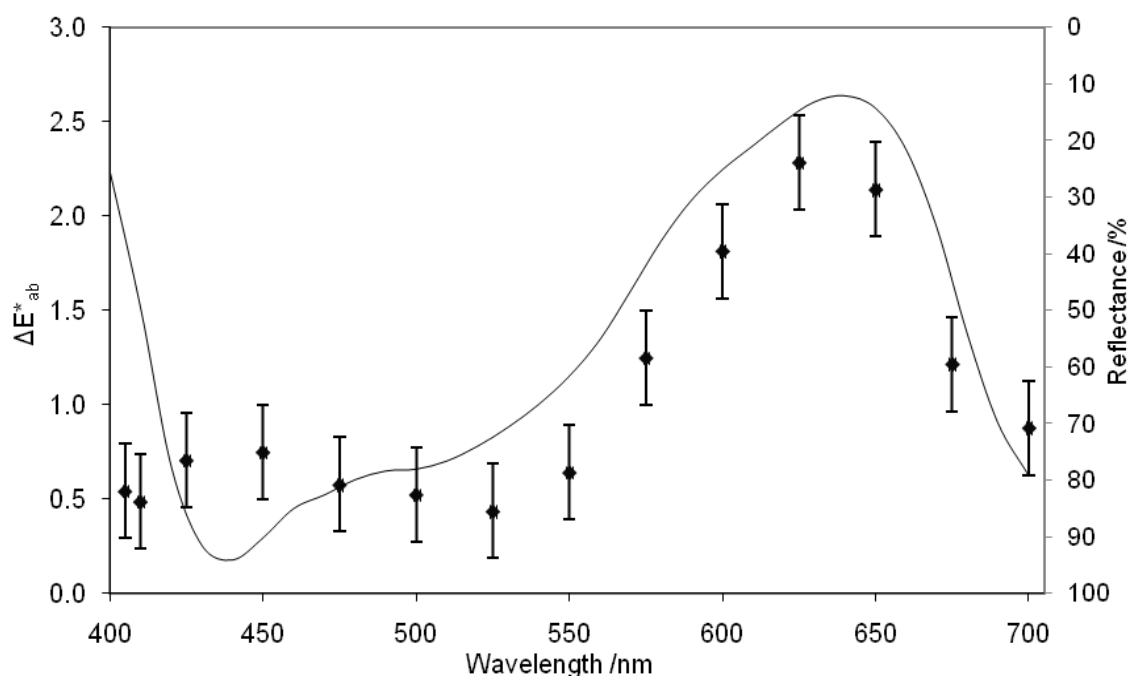


Figure 3.10 Results from application of the instrument to Lightcheck Sensitive (error bars +/- 1 equivalent standard deviation for drift and noise) and the corresponding reflectance curve of the sample represented on the secondary inverted y axis.

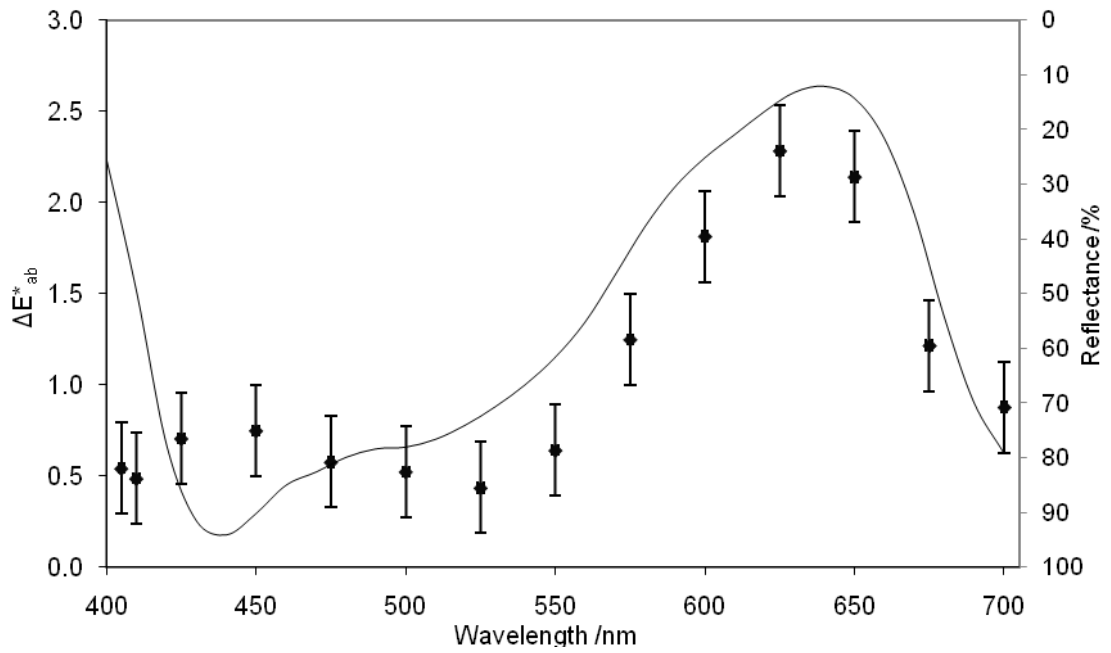


Figure 3.11. Results from application of the instrument to Lightcheck Ultra Sensitive (error bars +/- 1 equivalent standard deviation for drift and noise) and the corresponding reflectance curve of the sample represented on the secondary inverted y axis.

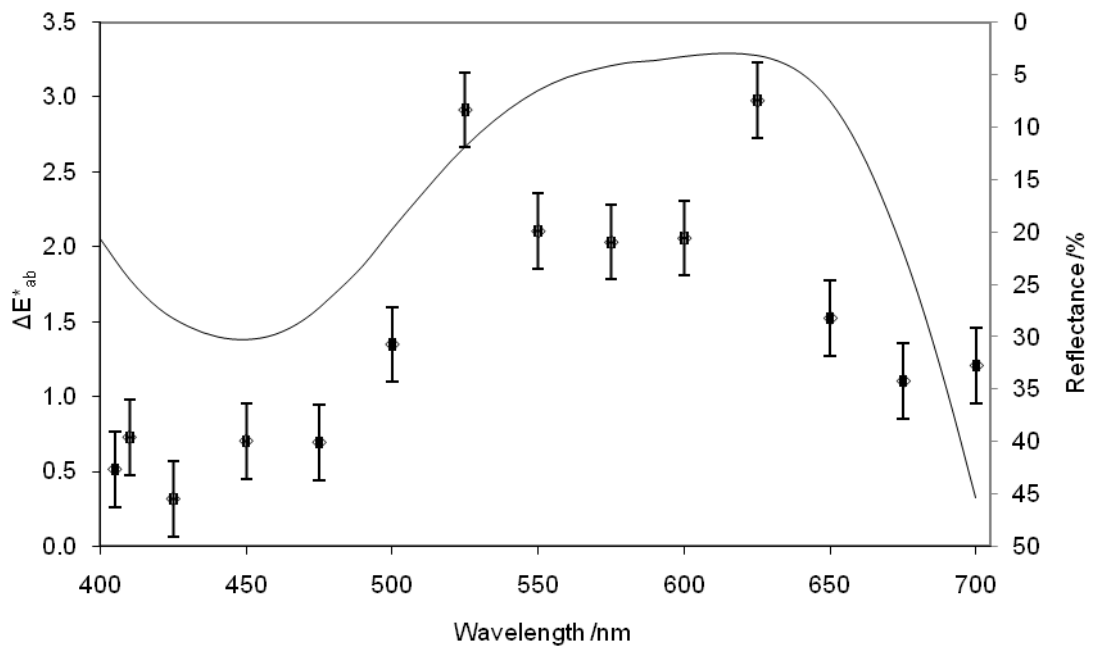


Figure 3.12. Results from application of the instrument to Blue Wool 1 (error bars +/- 1 equivalent standard deviation for drift and noise) and the corresponding reflectance curve of the sample represented on the secondary inverted y axis.

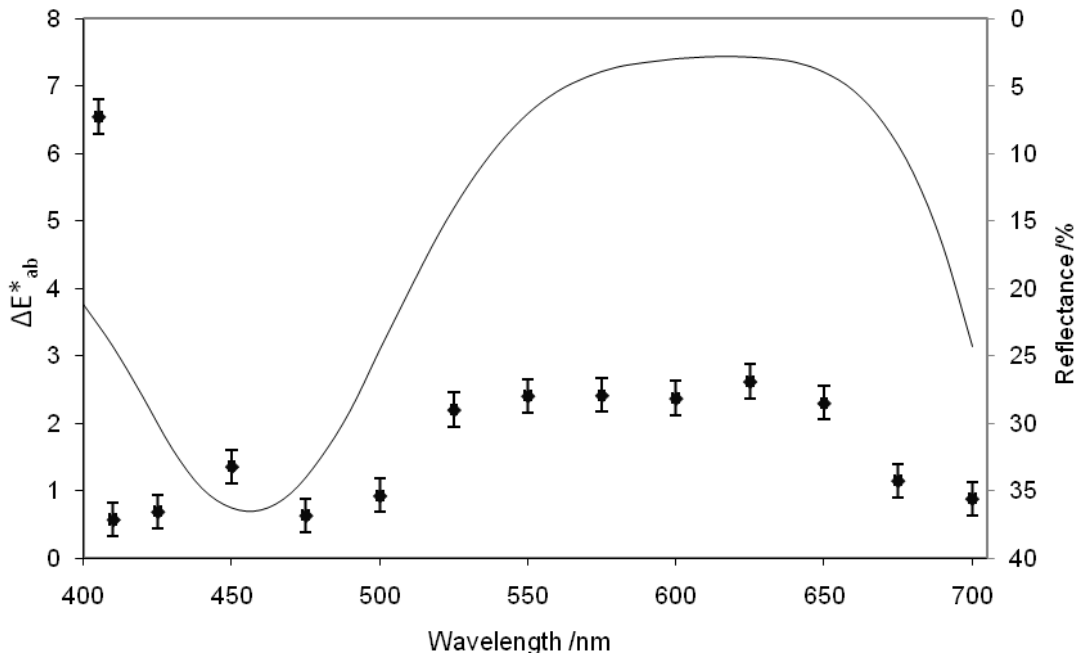


Figure 3.13. Results from application of the instrument Blue Wool 2 (error bars +/- 1 equivalent standard deviation for drift and noise) and the corresponding reflectance curve of the sample represented on the secondary inverted y axis.

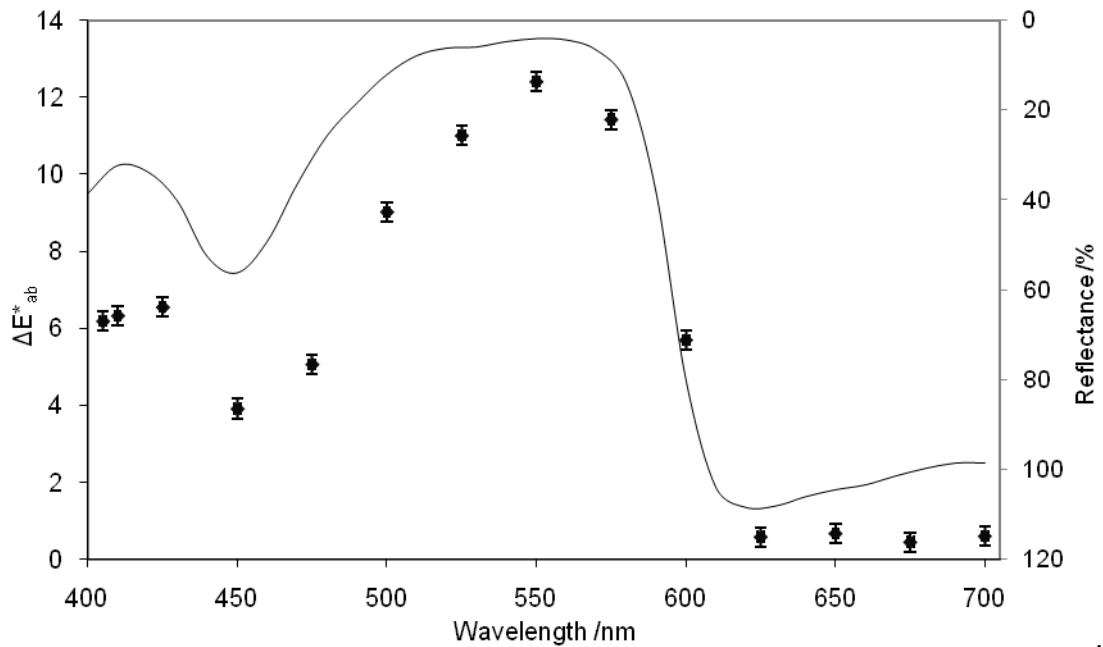


Figure 3.14. Results from application of the instrument to a 0.3 % solution of Rhodamine-B mixed with alcohol on cotton blotting paper (error bars +/- 1 equivalent standard deviation for drift and noise) and the corresponding reflectance curve of the sample represented on the secondary inverted y axis.

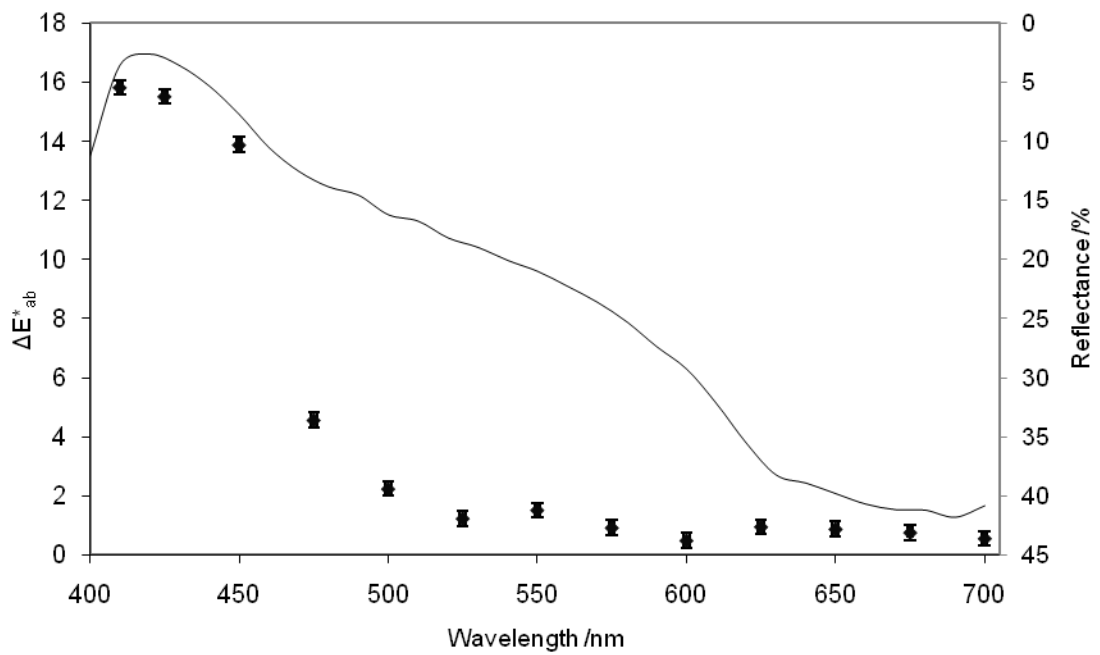


Figure 3.15. Results from application of the instrument to litharge mixed with a 10% aqueous solution of glue to make a soft paste applied to paper board and the corresponding reflectance curve of the sample represented on the secondary inverted y axis (error bars +/- 1 equivalent standard deviation for drift and noise).

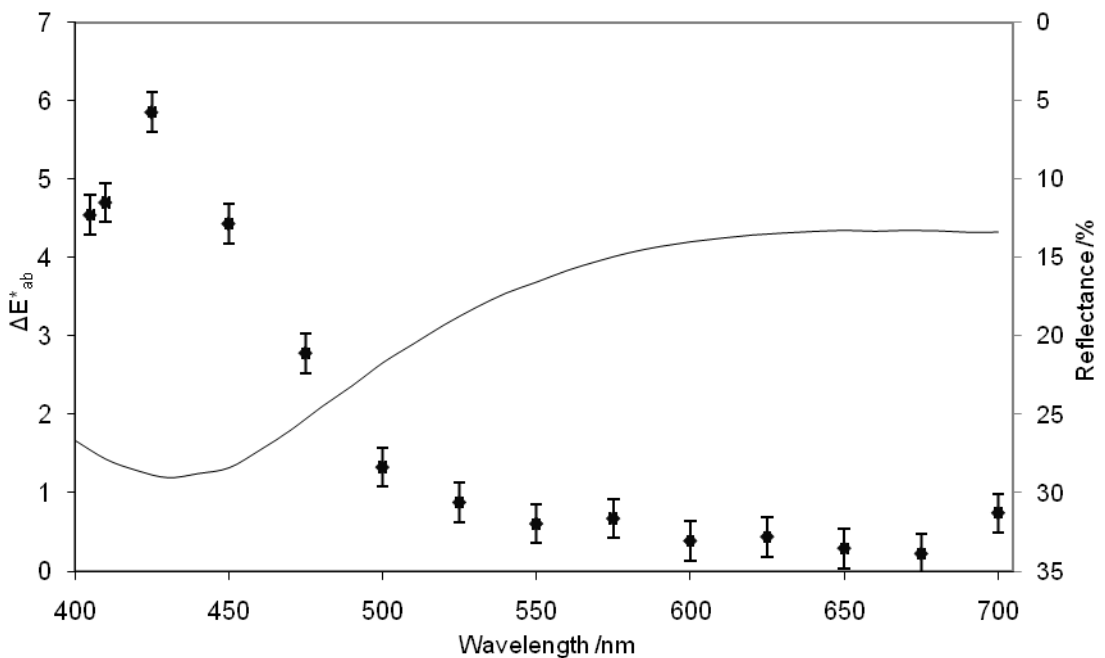


Figure 3.16. Results from application of the instrument to Prussian blue for an exposure of 5.25J of over a 60 minute period and the corresponding reflectance curve of the sample represented on the secondary inverted y axis (error bars +/- 1 equivalent standard deviation for drift and noise).

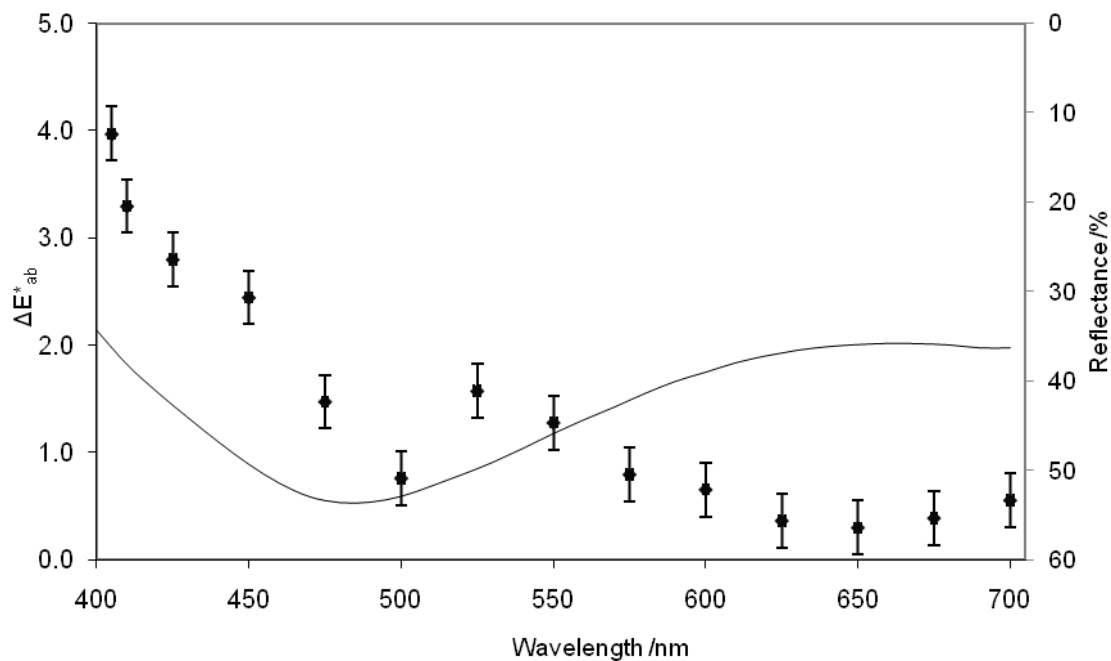


Figure 3.17. Results from application of the instrument to Prussian green and the corresponding reflectance curve of the sample represented on the secondary inverted y axis (error bars +/- 1 equivalent standard deviation for drift and noise).

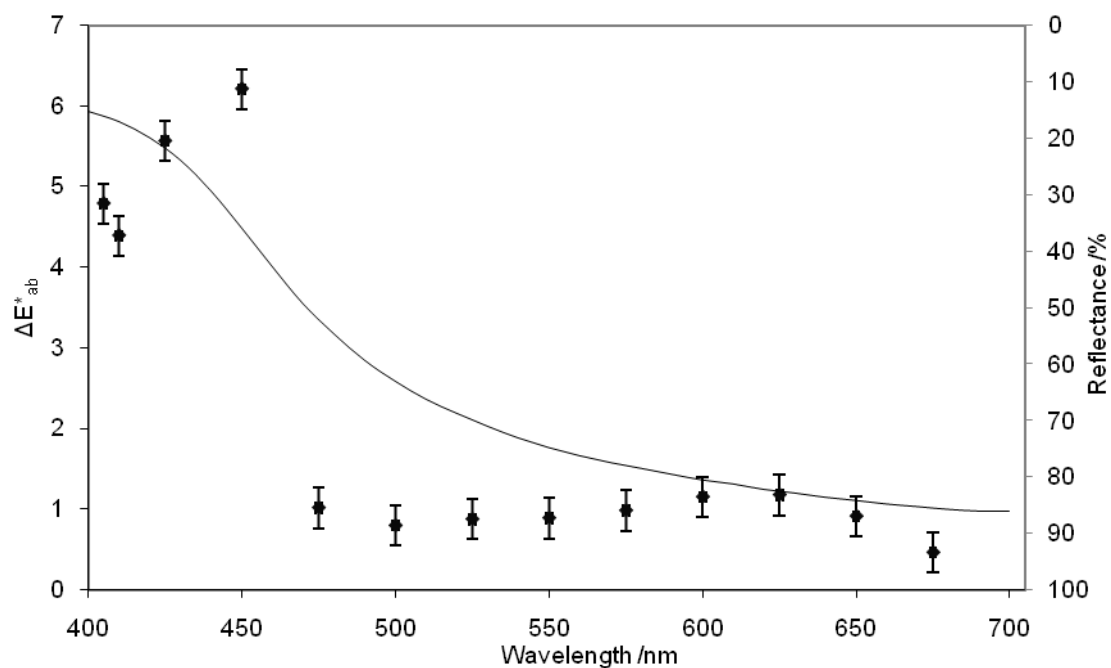


Figure 3.18. Results from application of the instrument to weld (error bars +/- 1 equivalent standard deviation for drift and noise) and the corresponding reflectance curve of the sample represented on the secondary inverted y axis.

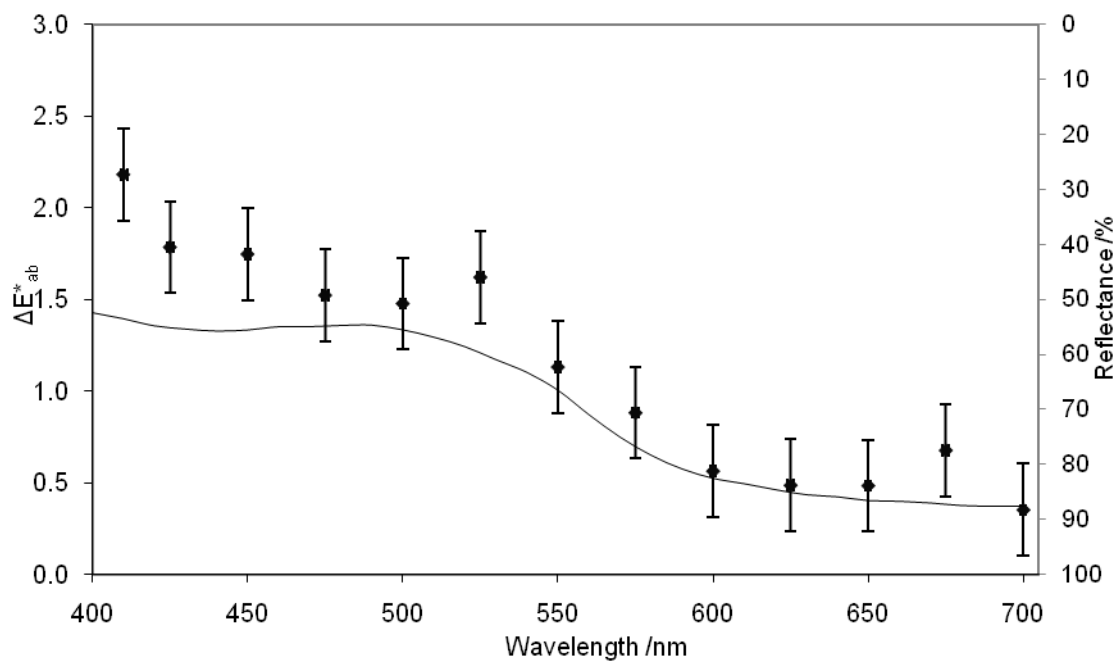


Figure 3.19. Results from application of the instrument to dragon's blood pigment (error bars +/- 1 equivalent standard deviation for drift and noise) and the corresponding reflectance curve of the sample represented on the secondary inverted y axis.

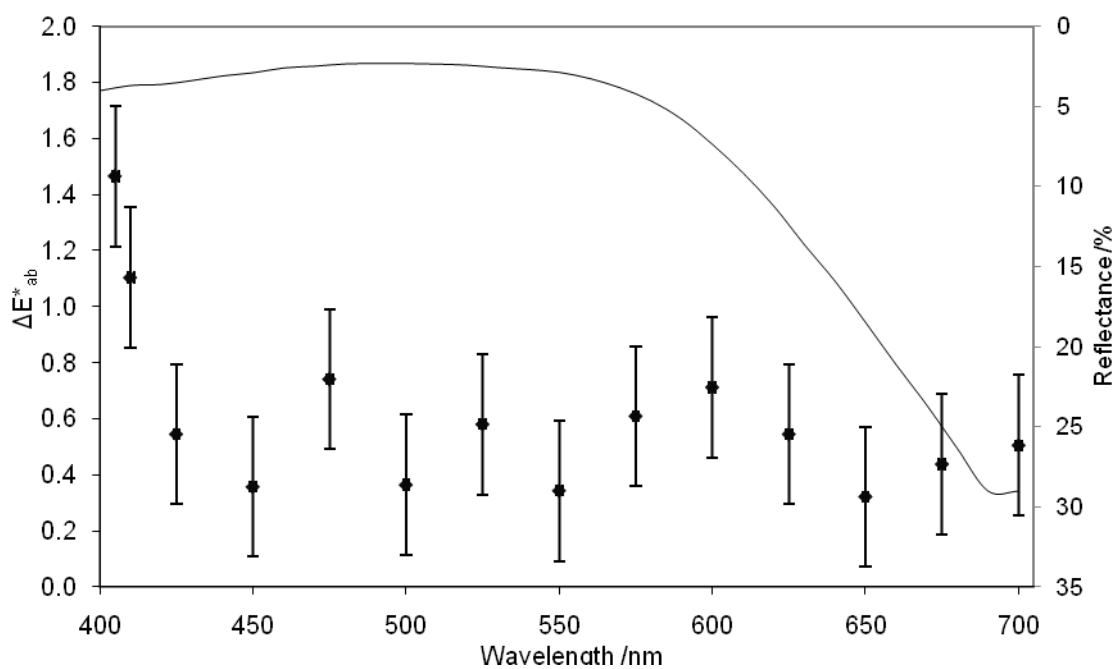


Figure 3.20. Results from application of the instrument to madder and the corresponding reflectance curve of the sample represented on the secondary inverted y axis (error bars +/- 1 equivalent standard deviation for drift and noise).

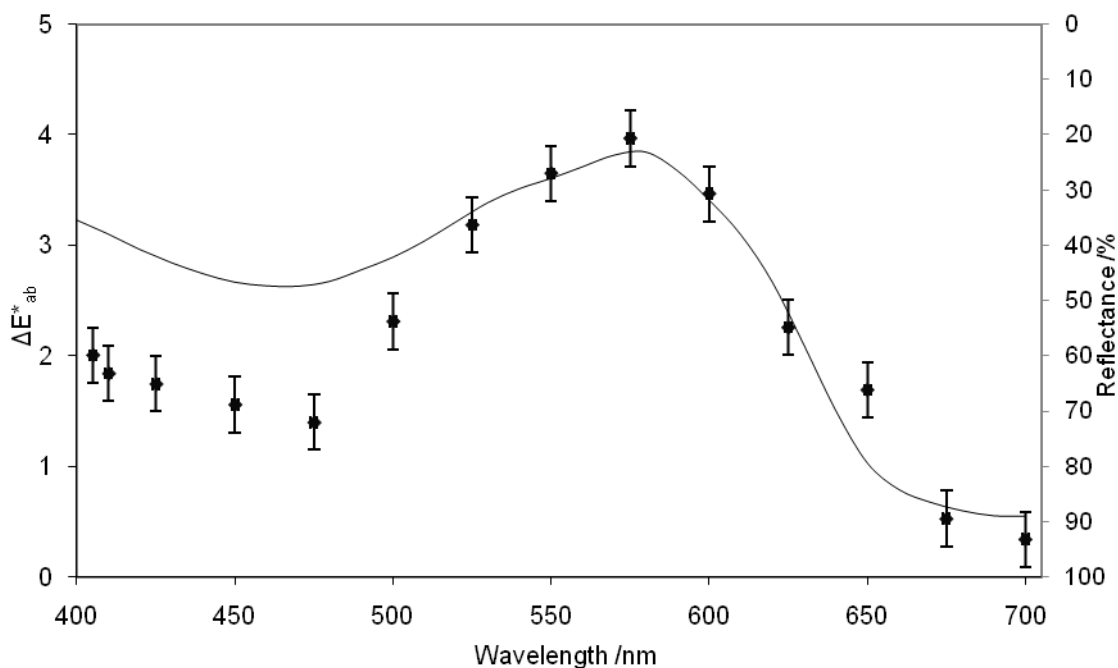


Figure 3.21. Results from application of the instrument to litmus (error bars +/- 1 equivalent standard deviation for drift and noise) and the corresponding reflectance curve of the sample represented on the secondary inverted y axis.

### 3.6 Discussion

The time required to gain repeated values for every data point was too great to justify. It is therefore necessary to consider error relating to variation in the sample in analysis of the results.

In the entire sample set no general correlation is apparent between fading and incident wavelength and this result provides little justification for a damage function.

In contrast to the other materials examined here, the widely used Blue Wool Standards and Lightcheck dosimeters were more vulnerable to the longer wavelength regions of the visible spectrum (as has previously been found). Alternative dosimeters have previously been suggested by Tennent and Townsend (1987), Allen *et al.* (1993) and Smith (1991) although they remain unexamined for wavelength sensitivity.

Previous research in this area has shown that the wavelength dependence of fading correlates well with the absorption spectra of each pigment and this was also strongly the case in this investigation. Exceptions were found when testing Prussian blue and Prussian green. In these cases fading appears to decrease with the wavelength of incident radiation rather than having any correlation with the pigment's absorption spectra. Potentially fading can be caused by the absorption of radiation which can then be passed on to the colourant. Under these circumstances; an absorption curve of Prussian blue would not correspond to those wavelengths that initiated the process of colour change.

With respect to Prussian blue and Prussian green, there is an apparent cut off wavelength at 550nm. Below this wavelength photo-degradation occurs. If this behavior extends to other Prussian blues, reducing lighting levels below the cutoff wavelength could significantly reduce damage. It is possible to state that as only photons with wavelengths below 550nm seem to induce the damage observed an activation energy of approximately 2.3eV per photon or 218kJ/mol is required to initiate photosensitized fading in this instance.

The fading properties of Prussian blue are similar to Prussian green, which is to be expected since the latter includes the former pigment.

The damage of the pigments other than Prussian blue and Prussian green decrease with wavelength, therefore based on this data a conclusion could be drawn that fading decreases with increasing wavelength.

Unsurprisingly the Aberchrome 999P Photochromic dosimeter, litmus and rhodamine B damage functions illustrate the greatest suitability for use as lux meters due to the peak of the damage function present at the centre of the visible range.

The Blue Wool results illustrate that they are most sensitive between approximately 500nm and 650nm. Due to the higher spectral resolution of fading via this technique, two peaks in the spectrum are revealed at 525nm and 625nm in the assessment of Blue Wool 1: possibly the two dyes Eriochrome Azurole B (CI 43830) and Indigosol Blue AGG (CI 73801) used in its production. These peaks were confirmed with numerous repeat measurements.

Previously Blue Wool 1 and 2 were assessed by McLaren (1956) and Saunders and Kirby (1994a) with comparable results. Both reported peaks at 600nm in the red region, however

McLaren reported no significant colour change in the blue end of the spectrum whereas Saunders and Kirby reported an equal or greater colour change than that seen at 600nm. The results of the research carried out using the micro-fadometer confirmed significant colour change in the red region in the case of Blue Wool 1 and conformed to McLaren's results by showing no considerable change in the blue region. A greater colour change was observed at 405nm in the case of Blue Wool 2 via this technique.

Similarly no considerable colour change was observed via this method in the blue region for Litmus and weld as reported by Saunders and Kirby (1994a).

When comparing these results with other research, different filtered bandwidths of illumination have been used to acquire similarly positioned data points in different published experiments, despite experimental difference between the investigations. For example negligible light below 400nm was present in the fading process for this research. This was not the case for results reported by Saunders and Kirby (1994a) where filtering permitted the transmission of light well below 400nm. It could be the presence or absence of critical frequencies that explain the differences observed.

Variation may also in some cases be due to difference between samples.

A possible improvement to the technique would be to increase the degree to which fading occurs in order to limit the effect of error.

Wavelength dependent fading is a time consuming experimental method, however this novel technique means a larger number of samples can be tested faster making it possible to improve upon the existing damage functions that are limited by the lack of suitable data available.

## 4 Investigation of Prussian blue

### 4.1 Introduction

Some colourants have been reported to perform poorly in anoxia (Townsend *et al.* 2008). A widely reported problematic pigment is Prussian blue (which can be considered as the first modern synthetic pigment and found widely in a variety of objects).

The poor stability of Prussian blue as a textile dye in anoxia was reported by Chevreul (1837). It has been noted that exposure of Prussian blue (in particular watercolours) to light under anoxic conditions results in fading followed at least partially by reversion of colour loss (Rowe 2004).

#### 4.1.1 The prevalence of the pigment

The original method for the creation of Prussian blue was published in the early 1700s (Kirby 1993). The creation of the pigment was announced in 1710 and it has had widespread use since the early part of the 18<sup>th</sup> century (Kirby and Saunders 2004). The watercolours of J. M. W. Turner widely contain the pigment (Townsend 1993). The pigment can be found used in many cultures since the eighteenth century and variants are commonly employed in paint manufacture. It has been documented in Japanese prints (Leona and Winter 2003) and Chinese, Indian and other south east Asian works of art from the nineteenth century.

A major source of Prussian blue in collections are objects created via the cyanotype process. As Prussian blue is the colourant formed during this process, cyanotypes are not considered suitable for storage in anoxia. The cyanotype process was employed to copy large drawings (for example engineering drawings leading to the term blueprint). The process was in regular use after 1842 until the 1950s (Ware 1999a) (Ware 1999b).

Prussian blue was also used as a textile dye between the early nineteenth and the late twentieth century (Rowe 2004), and as a printing ink and in many other types of ink until the middle of the previous century (Townsend *et al.* 2008).

Prussian blue has a high tinting strength and when used at full strength is almost black in appearance. Therefore extenders and/or white pigments are often added to the pigment as supplied, which may increase the impermanence of the colour (Kirby and Saunders 2004).

#### 4.1.2 Fading and reversion characteristics

Prussian blue is reported to be phototropic (it loses colour due to light exposure, and then regains it in the dark). Prussian blue is also reported to lose colour in enclosed containers by reduction due to lack of oxygen (it is also reported to reduce when in proximity to reducing materials (Berrie 1997)). Any colour loss is reported to be reversible when the material is re-exposed to air. The time for this reversion in relation to the time to lose colour is rarely discussed.

Reports of fading in light in the presence of normal air and/or nitrogen have been summarised by Kirby (1993), Kirby and Saunders (2004) and Rowe (2004). Complete colour loss in 100% hydrogen environments was noted by Russell and Abney (1888). A report of slightly opening a sealed environment to permit a small amount of air to induce reversion for a faded Cyanotype is reported by Ware (2003).

#### 4.1.3 Prussian blue manufacture and chemical structure

Prussian blue is a type II mixed valence transition metal complex; ferric ferrocyanide, iron (III) hexacyanoferrate (II) conventionally represented as  $\text{Fe}_4[\text{Fe}(\text{CN})_6]_3 \cdot x\text{H}_2\text{O}$  (where x is 14-16). This is known as “insoluble” Prussian blue. The formula quoted by Berrie (1997) could be considered more correct:  $\text{M}^{\text{I}}\text{Fe}^{\text{III}}\text{Fe}^{\text{II}}(\text{CN})_6 \cdot n\text{H}_2\text{O}$ , where  $\text{M}^{\text{I}}$  is a potassium ( $\text{K}^+$ ), ammonium ( $\text{NH}_4^+$ ) or sodium ( $\text{Na}^+$ ) ion (depending on the method of manufacture), and  $n=14-16$ . The potassium containing variant is known as “soluble”.

The Prussian blue pigment may be precipitated from aqueous media via any of these 3 reactions (Ware 1999b).

- 1, Iron (III) salts,  $\text{Fe}^{3+}$  (aq) with hexacyanoferrate(II),  $[\text{Fe}(\text{CN})_6]^{4-}$
- 2, Iron (II) salts,  $\text{Fe}^{2+}$  (aq) with hexacyanoferrate(III),  $[\text{Fe}(\text{CN})_6]^{3-}$

### 3, Iron (II) salts, $\text{Fe}^{2+}$ (aq) with hexcyanoferrate(II), $[\text{Fe}(\text{CN})_6]^{4-}$

This results in iron (II) hexcyanoferrate(II) known as Prussian white or Berlin white. It is then oxidized to Prussian blue by an oxidant.

The colour of the pigment arises from the charge transfer transition between the two valence states of the iron from  $\text{Fe}^{\text{II}}$  to  $\text{Fe}^{\text{III}}$  (the structural element of the pigment framework being  $\text{Fe}^{\text{III}}\text{-N-C-Fe}^{\text{II}}$ ) (Ware 1999b) (see figure 4.1).

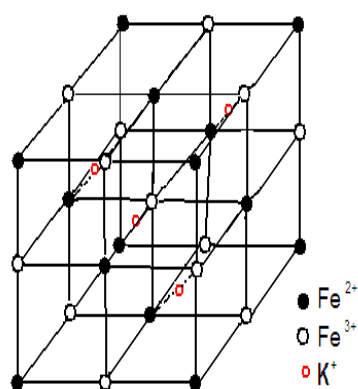


Figure 4.1. The structural element of the Prussian blue pigment framework.

The chemistry associated with the pigment remains not fully understood. The preparation of Prussian blue results in colloidal precipitates which preclude the use of single crystals in analysis. The lattice structure of Prussian blue contain both vacancies and impurities which creates additional complexity (Ware 1999b).

#### 4.1.4 The fading and reversion mechanisms

Fading of the pigment is considered as a cumulative result of more than one degradation pathway, a reversible reaction and hypothetical irreversible reaction(s). Of the two processes active in the fading of Prussian blue one is rapid and creates a reversible loss of colour and the second produces irreversible colour change to grey. Irradiation of Prussian blue is considered to induce three reactions that are presently considered to be responsible for observed colour change and discussed comprehensively by Kirby and Saunders (2004).

Two experiments were conducted (the first reported in section 4.2 and the second in section 4.3)

## 4.2 Experimental method

### 4.2.1 The micro-fadometer arrangement

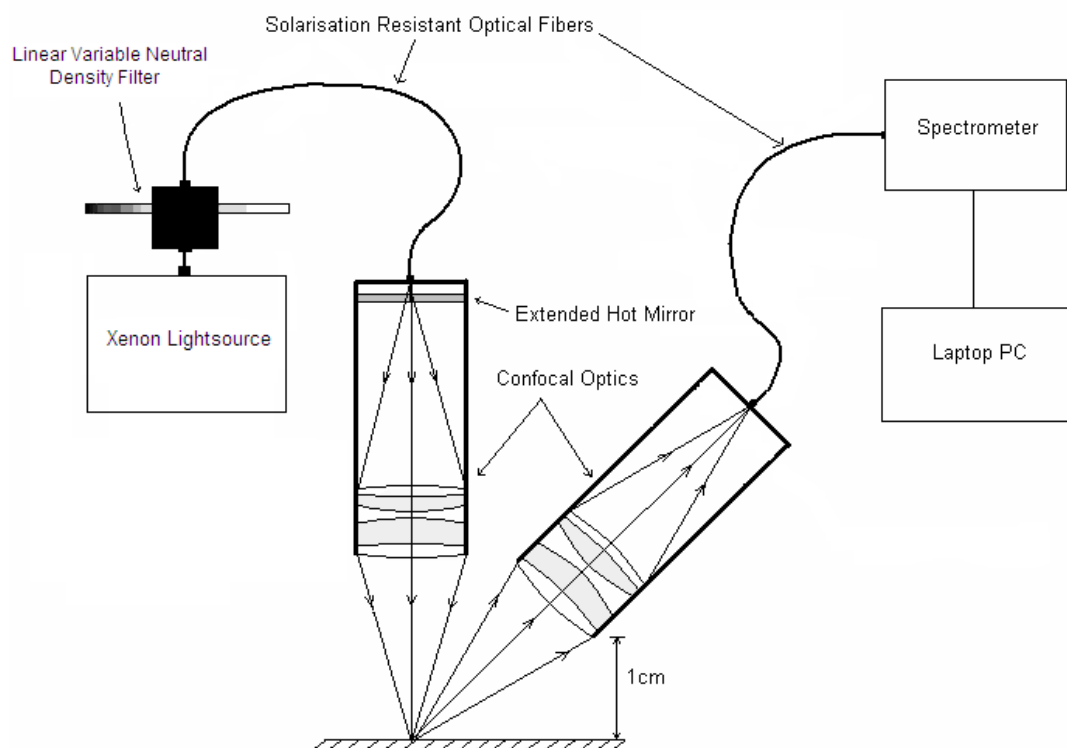


Figure 4.2. A schematic representation of the micro-fadometer optical arrangement for the investigation of reversion behaviour for Prussian blue.

The Prussian blue was analysed using a modified micro-fading technique. A schematic of the instrument is shown in figure 4.2. This instrument differs from that in figure 3.1 as no filter was placed in the receiving probe and a linear variable neutral density filter was placed before the illumination fiber.

In order to conduct the experimental investigation the sample was faded using the micro-fadometer and the colour difference created by the fading process was recorded. Following

this light was prevented from contact with the sample using a black cloth and over a 2 day period the cloth was removed at intervals and the reverted colour was measured.

The high light intensity of the system was reduced for all measurements using a linear variable neutral density filter (removing 99% of the lamp output). This was done in order to reduce the intensity of illumination on the sample to a power level that enabled a rapid measurement of the colour, while not allowing the incident radiation necessary for measurement to re-fade the sample area and harm the reversion process. The filter was removed when fading and replaced afterwards.

After initially defining the reversion characteristics of Prussian blue in air and analysing the pigments reversion behaviour, the investigation was extended to a variety of fade durations (15 minutes, 1 hour, 3 hours, and 15 hours). At each fade duration the oxygen concentration was controlled at either 0%, 2%, 3.5%, 5%, 10% (the remainder of the gas being nitrogen) or was provided by air at approximately 21% oxygen. To create accurate oxygen levels modified environments were created by flushing a valved anoxic chamber with a premixed gas (supplied by BOC) of the desired oxygen levels. The housing was built from glass, stainless steel and butyl rubber (see figure 4.3). Fading took place through glass in all instances. A white reference for colour measurement was taken through the glass so the transmission of the glass did not harm colour measurement. In the case of 21% oxygen the pigment was tested in the same chamber with the valves open to the room atmosphere.

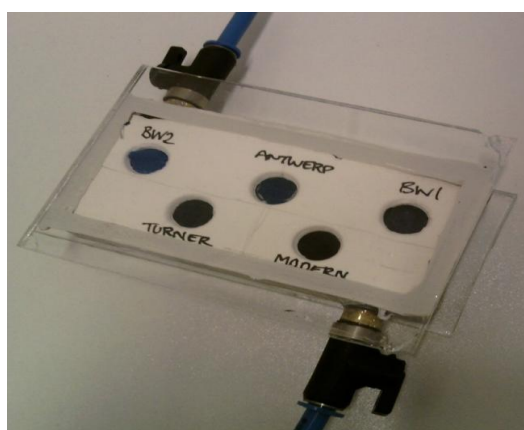


*Figure 4.3. The valved anoxic chamber built from glass, stainless steel and butyl rubber (here shown containing a variety of samples).*

Any link between the degree of fading of Prussian blues for a given illumination and the level of relative humidity has been reported to be non-detectable previously (Saunders 2009). Therefore in this instance purging gas used in the experiment was not humidified.

The reversion behaviour of the Prussian blue pigment was investigated in the CIE 1976 L\* a\* b\* colour space. This was done in order to compare the results with previous leading research (Kirby and Saunders 2004).

#### **4.2.2 Error connected with the method**

In order to quantify any error connected to the addition and removal of a filter in the optical axis (which as stated, was necessary to fade the sample). The instrument was focused onto a pressed barium sulphate white standard and the colour difference connected with the combined removal and replacement of the neutral density filter was measured 10 times. The maximum error connected with the process was  $0.33\Delta E^*_{ab}$  with an equivalent standard deviation of  $0.23\Delta E^*_{ab}$ . Another source of error was due to drift and noise of the system. In section 2.3.4 an error no greater than  $0.36 \Delta E^*_{ab}$  was shown to take place due to this over a 7 day period the equivalent standard deviation being  $0.25 \Delta E^*_{ab}$ . Combining these errors results in a error for any reading of  $0.42 \Delta E^*_{ab}$  (the error bars shown within graphs for this research are  $\pm 0.42 \Delta E^*_{ab}$ ).

#### **4.2.3 Results**

##### **4.2.4 Reversion behaviour**

A typical example of Prussian blue pigment behaviour (TTB6) showing a combined fading and reversion curve can be seen in figure 4.4 (created by combining a data set for each process). As reversion takes place over a significantly greater period compared to the fading process, data is presented on a logarithmic scale.

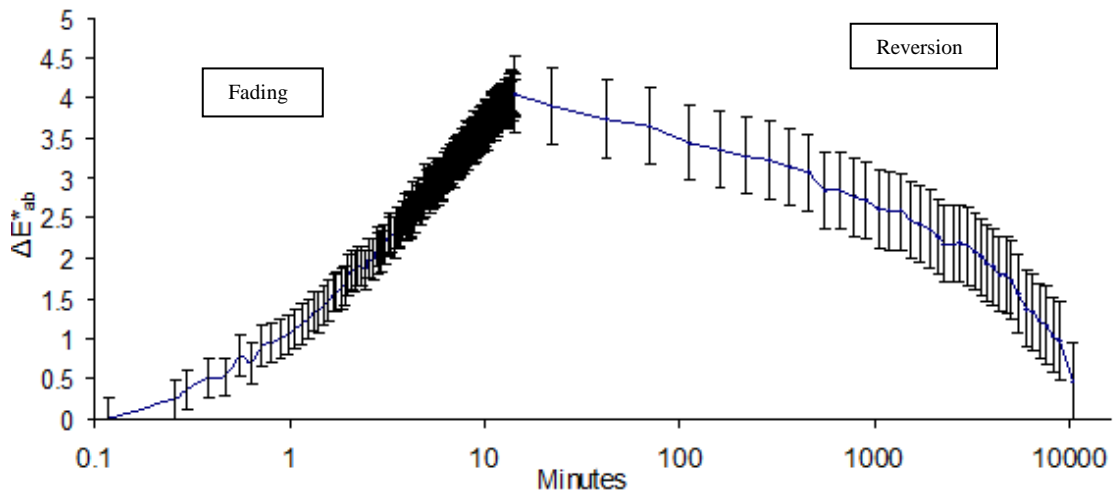


Figure 4.4. An example of the colour change measured for TTB6 Prussian blue pigment when undergoing fading and reversion processes.

An example of the typical reversion behaviour of the Prussian blue pigment in the CIE 1976  $L^* a^* b^*$  colour space can be seen in figure 4.5. A circle marks the initial measured colour of the pigment before any fading and the path of the reverting pigment colour is plotted as it returns closer to the location of the initial value.

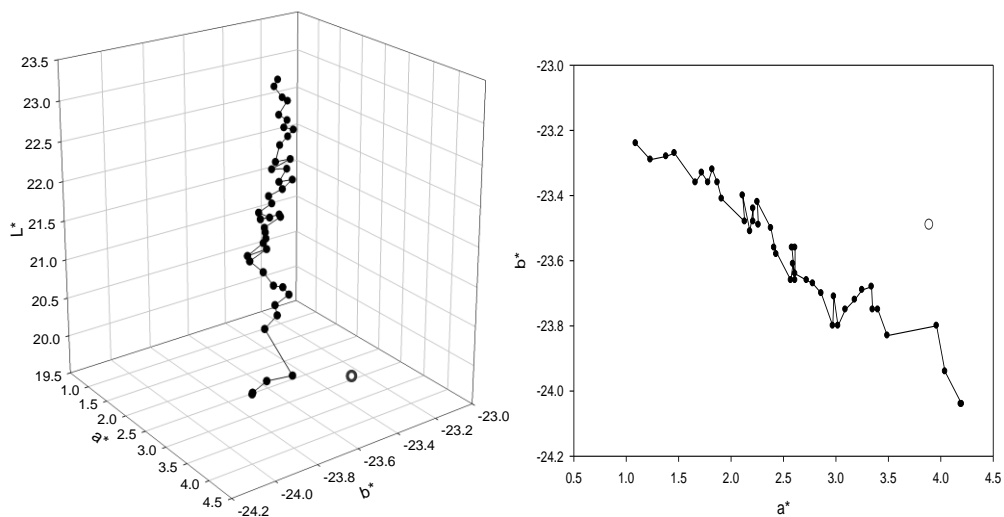


Figure 4.5. An example of the measured reversion behaviour of TTB6 in the 3 colour dimensions  $L^*a^*b^*$  (left) and an illustration of the reversion in 2 dimensions in the  $a^* b^*$  plane (right). The path of colour reversion follows from top to bottom or left to right respectively as the measured value returns closer to the circle which denotes the initial measured colour before fading.

#### 4.2.5 Modeling reversion behaviour

When studied in various environments the TTB6 Prussian blue sample was found to regain colour exponentially as seen in Figure 4.6. Reversion was not complete and a degree of colour change was measurable after reversion.

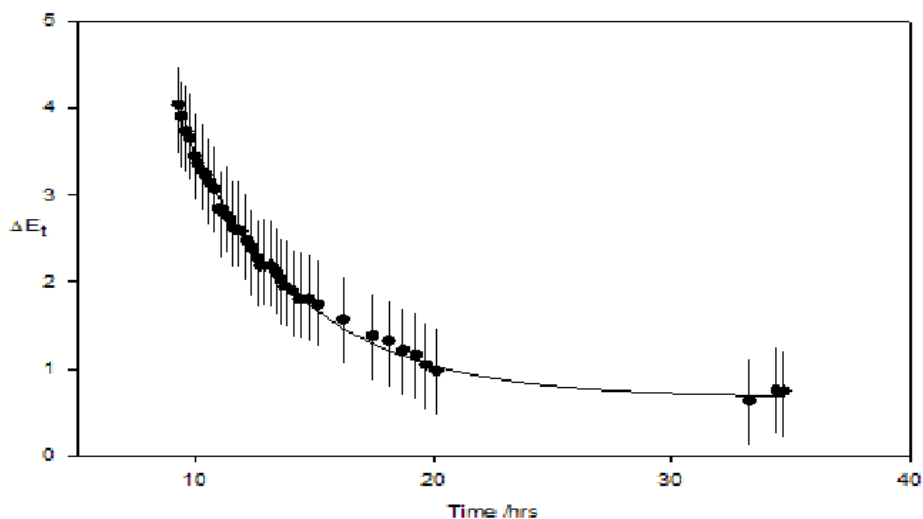


Figure 4.6. An example of the colour reversion characteristic of the Prussian blue sample.

The reversion behaviour could be modeled using the following equation.

$$\Delta E(t) = \Delta E_f + (\Delta E_0 - \Delta E_f)e^{-\beta t}$$

Where:

$\Delta E_0$  is the colour change immediately after fading relative to original reference colour.

$\Delta E(t)$  is the reverted colour of the pigment at time (t) relative to the initial colour prior to fading.

t is the time in hours since the reversion process began.

$\Delta E_f$  is the baseline of  $\Delta E(t)$  vs. t graph this can be viewed as the final colour difference of the pigment relative to original colour after reversion is complete.

$\beta$  is the rate of reversion (obtained via a first-order exponential fit of the  $\Delta E(t)$  vs. t graph).

As an aside the fading rather than the reversion behaviour of Prussian blue was also modeled. The result of the modeling can be found summarized, along with an example in appendix C.

#### 4.2.6 Effect of oxygen concentration on behaviour

The reversion curves for light-faded TTb6 Prussian blue samples (graphs plotting  $\Delta E(t)$  vs  $t$ ) were analyzed to obtain reversion rate ( $\beta$ ) and colour change after reversion ( $\Delta E_r$ ). The influence of oxygen concentration and fade duration upon these parameters was investigated in.

The results of this investigation are summarized in the table 4.1 (further graphs of the results can be found in appendix D). Column 1 corresponds to oxygen concentration of the environment in which the experiment was conducted. The fade duration is in column 2. The colour difference after the fade duration  $\Delta E_0$  is in column 3.  $\Delta E_r$  is in column 4. Column 5 contains  $\beta$  (the rate of reversion).

The R-squared ( $R^2$ ) values provide a statistical measure of the standard of fit connected to the regression line approximation. If  $R^2$  equates to 1, the regression line can be considered to match the data exactly.

O <sub>2</sub> %	Fade time	$\Delta E_0 \pm 0.42$	$\Delta E_f \pm 0.42$	$\beta$	R <sup>2</sup>
21	15 minutes	2.1	1.0	0.396 ± 0.039	0.959
21	1 hours	2.4	0.7	0.275 ± 0.023	0.989
21	3 hours	4.2	1.3	0.267 ± 0.014	0.993
21	15 hours	4.0	0.7	0.202 ± 0.006	0.994
Average		3.2	0.9	0.285	

O <sub>2</sub> %	Fade time	$\Delta E_0 \pm 0.42$	$\Delta E_f \pm 0.42$	$\beta$	R <sup>2</sup>
10	15 minutes	2.2	1.5	0.191 ± 0.034	0.938
10	1 hours	2.0	0.5	0.245 ± 0.021	0.988
10	3 hours	5.5	0.1	0.073 ± 0.003	0.999
10	15 hours	1.4	1.0	0.374 ± 0.175	0.925
Average		2.8	0.8	0.221	

O <sub>2</sub> %	Fade time	$\Delta E_0 \pm 0.42$	$\Delta E_f \pm 0.42$	$\beta$	R <sup>2</sup>
5	15 minutes	2.5	1.0	0.222 ± 0.016	0.983
5	1 hours	2.2	0.6	0.321 ± 0.053	0.985
5	3 hours	6.6	0.7	0.093 ± 0.013	0.986
5	15 hours	3.0	1.7	0.232 ± 0.826	0.967
Average		3.6	1.01	0.217	

O <sub>2</sub> %	Fade time	$\Delta E_0 \pm 0.42$	$\Delta E_f \pm 0.42$	$\beta$	R <sup>2</sup>
3.5	15 minutes	2.2	0.8	0.029 ± 0.014	0.975
3.5	1 hours	1.6	1.5	0.318 ± 0	0.429
3.5	3 hours	2.4	0.8	0.145 ± 0.016	0.989
3.5	15 hours	7.3	1.5	0.020 ± 0.001	0.998
Average		3.4	1.3	0.128	

O <sub>2</sub> %	Fade time	$\Delta E_0 \pm 0.42$	$\Delta E_f \pm 0.42$	$\beta$	R <sup>2</sup>
2	15 minutes	4.3	2.9	0.134 ± 0.024	0.915
2	1 hours	4.8	2.1	0.104 ± 0.007	0.993
2	3 hours	7.3	3.2	0.093 ± 0.008	0.992
2	15 hours	4.2	2.0	0.071 ± 0.006	0.995
Average		5.1	2.6	0.100	

O <sub>2</sub> %	Fade time	$\Delta E_0 \pm 0.42$	$\Delta E_f \pm 0.42$	$\beta$	R <sup>2</sup>
0	15 minutes	4.8	2.4	0.397 ± 0.039	0.978
0	1 hours	3.2	2.6	0.396 ± 0.058	0.964
0	3 hours	6.6	3.0	0.160 ± 0.001	0.990
0	15 hours	13.1	10.1	0.048 ± 0.003	0.994
Average		7.0	4.5	0.250	

Table 4.1. Reversion values of light-faded TTB6, interpreted R-Squared values indicate how well the regression line approximates to the data points.

#### 4.2.7 Influence of fade duration upon $\Delta E_f$ , $\Delta E_0$ , and $\beta$

$\Delta E_0$  was found to increase with fade duration at all oxygen concentrations and colour change typically reached a plateau or reduced after 3 hours of fading, however in anoxic conditions the colour difference observed increased to larger values not seen at other oxygen levels (see figure 4.7).

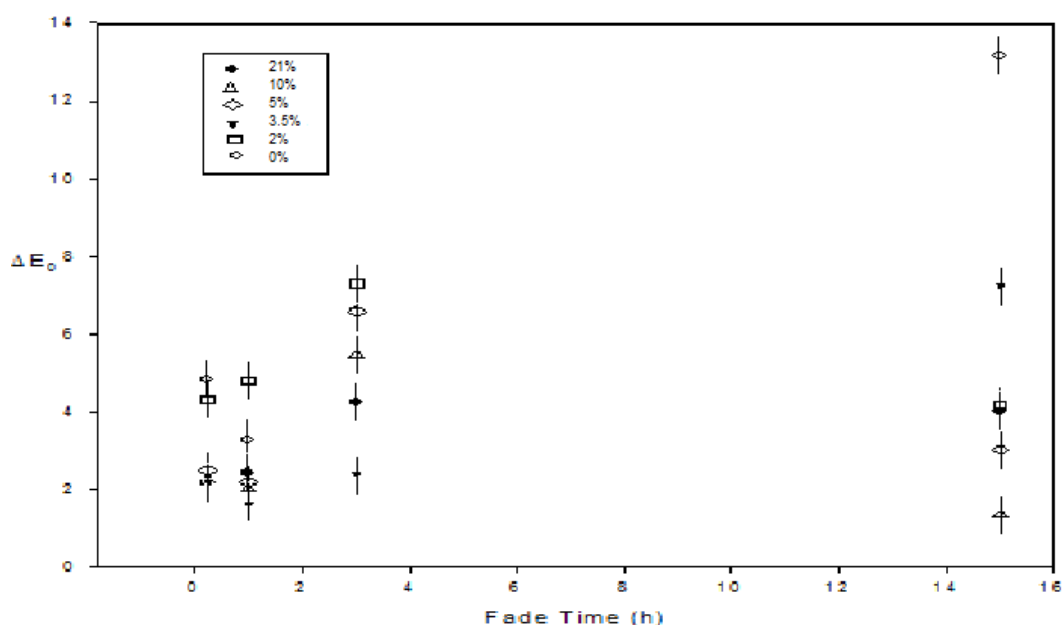


Figure 4.7. The relationship between  $\Delta E_0$  and fade duration under various oxygen levels

The colour change for anoxia after 15 hours is significantly larger than the rest of those measured. This large value was rechecked 3 times and was found to be repeatable. This significant fading of Prussian blue to a visible white in anoxia has been widely reported.

No clear relationship was found between  $\Delta E_f$  and the duration of fade or between  $\beta$  and fade duration as shown in figures 4.8 and 4.9 respectively. Again  $\Delta E_f$  was seen to be large in anoxic conditions when compared to the degree of reversion in other oxygen levels. This value was rechecked and was repeatable. This behaviour reflects previous reports where Prussian blue does not revert until exposed to oxygen (generally from room atmosphere exposure).

There was also no relationship observed between the reverted colour's hue (which could be considered as the orientation of  $\Delta E_f$  in the colour space) and fade duration.

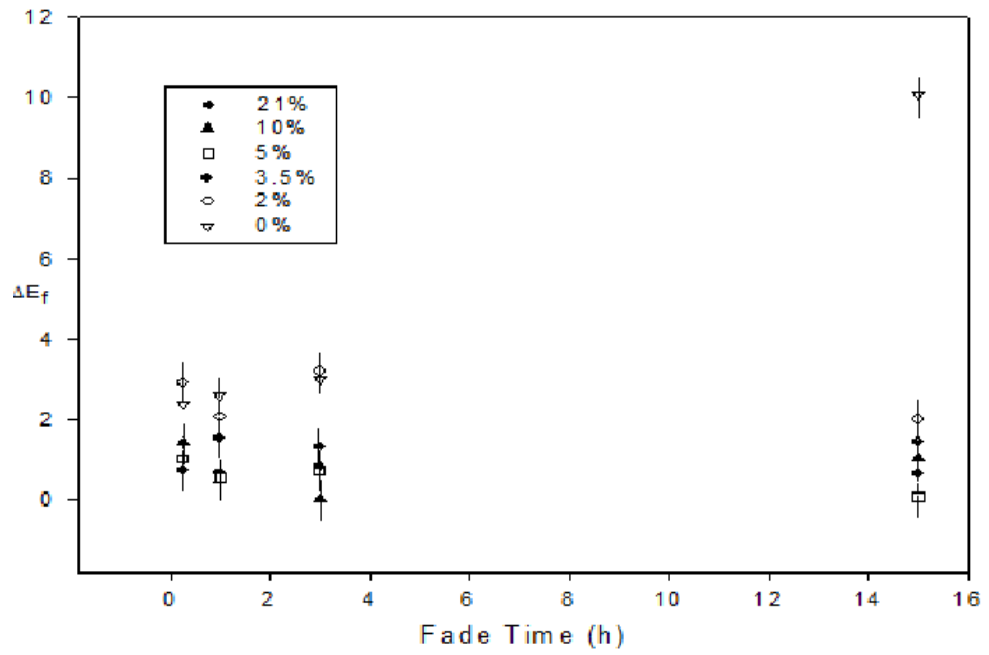


Figure 4.8. The relationship between  $\Delta E_f$  and fade duration under various oxygen levels.

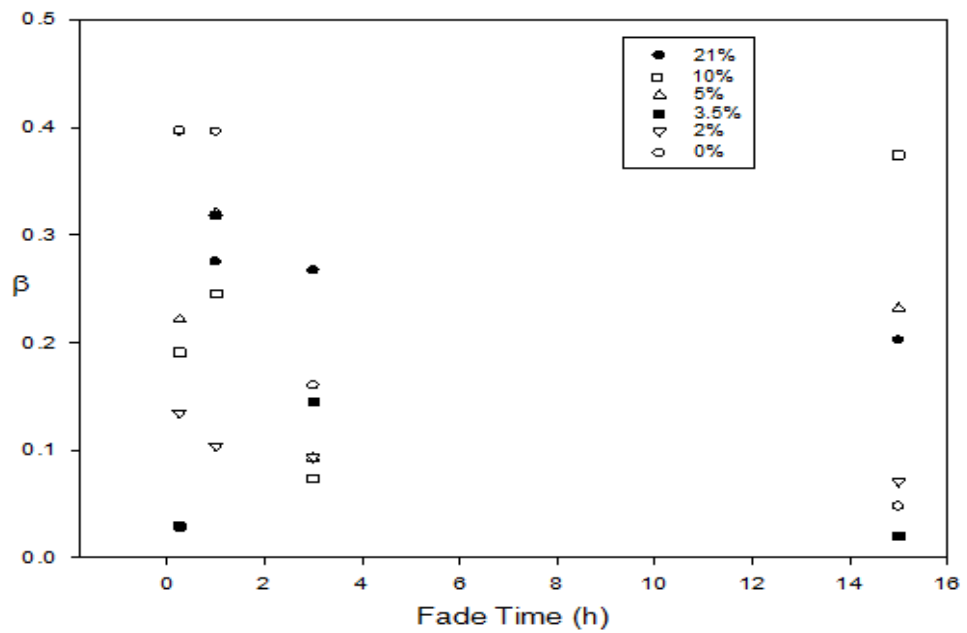


Figure 4.9. The relationship between  $\beta$  and fade duration under various oxygen levels.

#### 4.2.8 Influence of $O_2$ concentration upon $\Delta E_f$ , $\beta$ .

As no correlation between fade duration and  $\Delta E_f$  or  $\beta$  was found we proceed by assuming random variables between samples only. It was therefore possible to investigate the

relationship with oxygen concentration using the average values of  $\Delta E_f$  and  $\beta$  that were obtained using all fade durations at each oxygen concentration.

Importantly it was found that  $\Delta E_f$  increases with decreasing oxygen concentration at the lower percentages tested as shown in figure 4.10 with reverted values lowest at 5%.

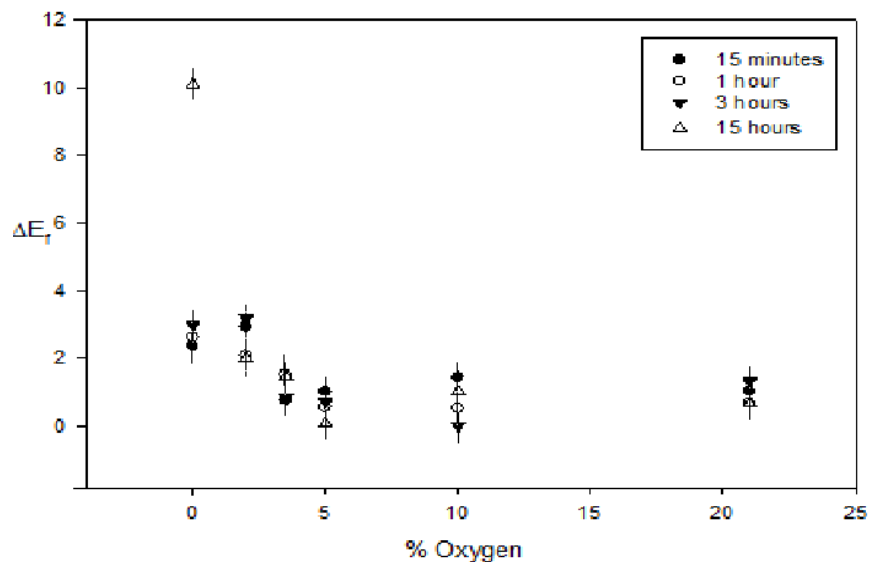


Figure 4.10. The relationship between  $\Delta E_f$  for the different lengths of exposure and the various oxygen levels for the TTB6 Prussian blue sample.

There was also no discernable relationship between the reverted hue and oxygen concentration. The rate of reversion,  $\beta$ , showed no correlation with oxygen concentration as shown in figure 4.11.

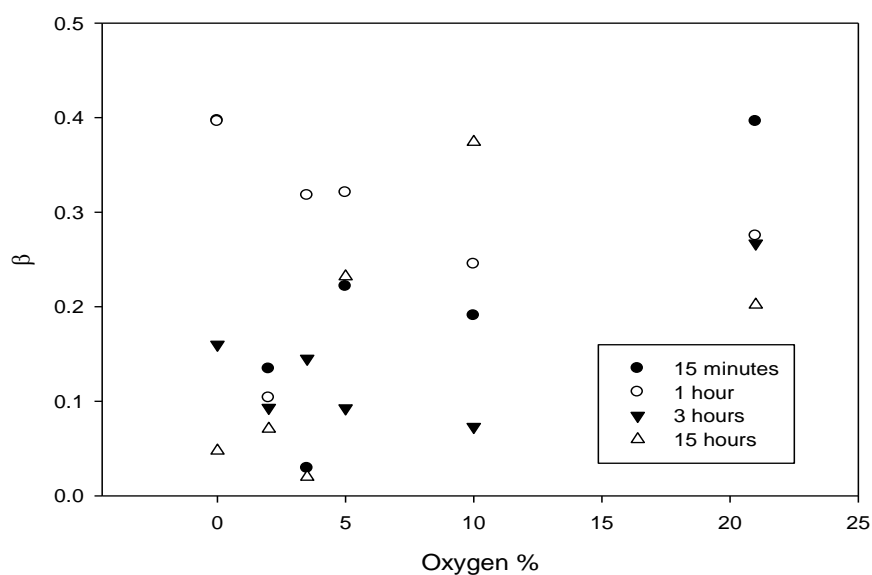


Figure 4.11. The relationship between average  $\beta$  for the different lengths of exposure and the various oxygen levels for the TTB6 Prussian blue sample.

### 4.3 Experimental extension to other Prussian blue samples.

Previously an hypoxic 5% oxygen environment was shown to be a suitable oxygen concentration for a particular historic Prussian blue pigment (see figure 4.10). This section describes an automated micro-fadometer experiment applied to a greater number of Prussian blues (both traditional and modern). All the pigments were prepared by grinding with gum Arabic, diluting with distilled water and applying in a wash onto Ruscombe mill paper (or Whatman silversafe paper when stated). Further detailed information on the sample set of 56 Prussian blue pigments ground in gum Arabic and painted onto paper can be found in the introduction and appendix E.

#### 4.3.1 Experimental technique

The automated micro-fadometer system was employed which utilized Thorlabs ATP positioning software to control movement of the probe head attached to the XYZ stage as shown in figure 4.12. Via the use of the automated system the probe was automatically moved and repositioned at best focus for each sample in a matrix. Using this instrumentation it was possible to revisit any location to monitor colour change after a period of time.

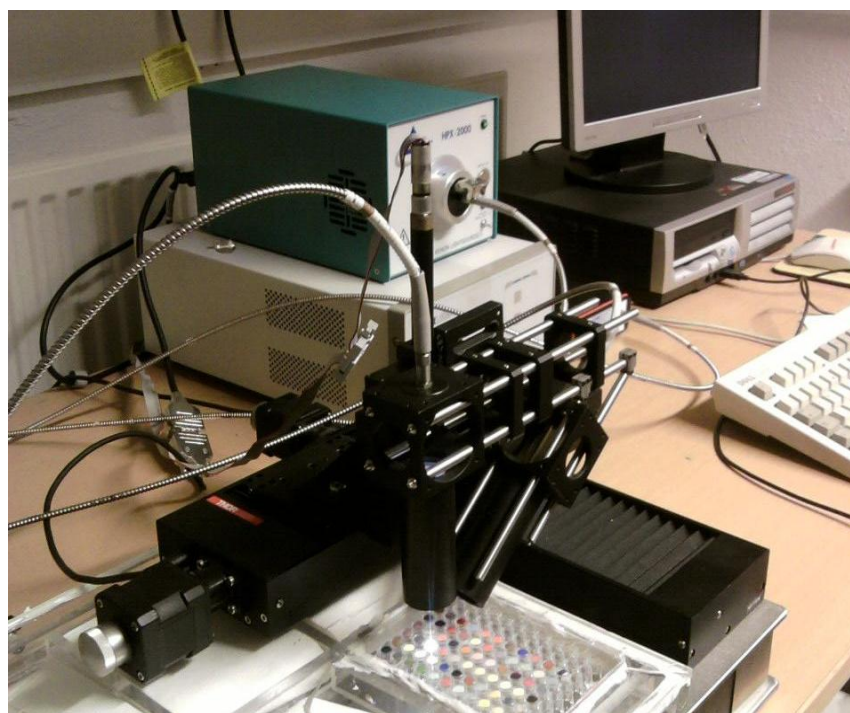


*Figure 4.12. The automated micro-fadometer system which controls movement of the probe head via the attached XYZ stage.*

It was possible to enter position control data into the spreadsheet function of the program. The probe would pause to fade each pigment for one hour while  $L^*a^*b^*$  values were continuously recorded. The first  $L^*a^*b^*$  values recorded at each new position were used as the reference colour, from which all colour differences could be calculated. It was considered too time consuming to produce an automated focusing system for the instrument. With a neutral density filter in place to reduce illumination and the integration time increased to compensate for the resulting low signal, the instrument was focused and the position of the probe in the Z plane recorded at each position. This position of best focus was entered into the APT software movement spreadsheet for each pigment.

The samples were mounted in a braced gas valved chamber manufactured to control the oxygen level as shown in figure 4.13. To maintain the desired environmental conditions the fading experiments were run under a slight positive pressure of 100% nitrogen or 5% oxygen and 95% nitrogen to avoid oxygen ingress. The purging gas was split such that a fraction flowed through a water bubbler and some directly to the controlled chamber; the portion running through each segment was then valve-regulated and the humidity of the resultant gas stream was measured using a Tinytag humidity meter. Humidity remained within desirable limits of  $40\% \pm 5\%$  throughout the experimental process. In the case of fading in air the valves were left open to allow air flow.



*Figure 4.13. Some samples mounted in a braced gas valved chamber manufactured to control the oxygen level in the environment surrounding the samples.*

3 similar and separate fading experiments were conducted at 3 different oxygen levels for the sample set. In air, anoxia or 5% hypoxic environments Prussian blue colour change was measured following a 1 hour fadometer exposure and then measured after remaining housed for 3 days in the same environment they were faded in. In a further step the pigments that were faded and housed in anoxia or hypoxia during the experiment were exposed to air. In this further step they were monitored for further colour change after another 3 days.

A period of 3 days was chosen as the length of time between the various steps in the experiments. This decision was based on the behaviour of the Prussian blue pigment discussed previously (Tate Gallery Archive 7315.7, Q04047 TTB6). In the case of this pigment any colour change in the reversion process was typically no longer observable after a day (with a maximum of one and a half days). It was thought doubling the typical time period previously required would be adequate for no further change via reversion to be taking place.

The instrument remained running during the experiment in order to remain calibrated and repeat measurements of the same locations were possible using the high positional repeatability (40nm) of the micro-fadometer probe head using the XYZ stage.

### 4.3.2 Results

In order to understand to what degree the paper substrate may affect the result the Ruscombe mill paper was faded without any pigment applied. The paper was shown not to be fugitive after fading for 140 minutes using the micro-fadometer (see figure 4.14).

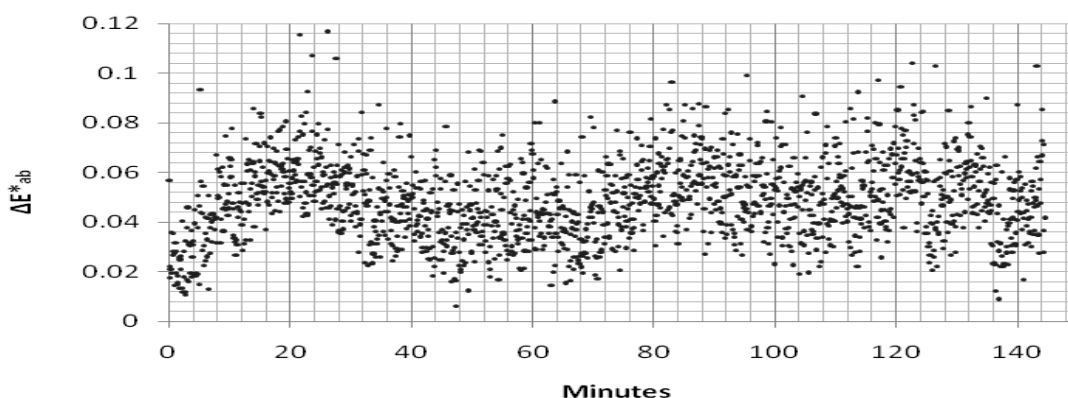


Figure 4.14. The results of fading the Ruscombe mill paper without any pigment applied after fading for 140 minutes using the Micro-fadometer.

### 4.3.2.1 Fading and reversion in air

In table 4.2 overleaf the first two columns contain the name and code of the pigments tested. The third column shows the degree of fading of the Prussian blue pigments in air after 1 hour using the micro-fadometer. The fourth column contains data on the reverted colour of each pigment in air when given over 3 days in low light to revert. Results are summarized via a histogram in figure 4.15.

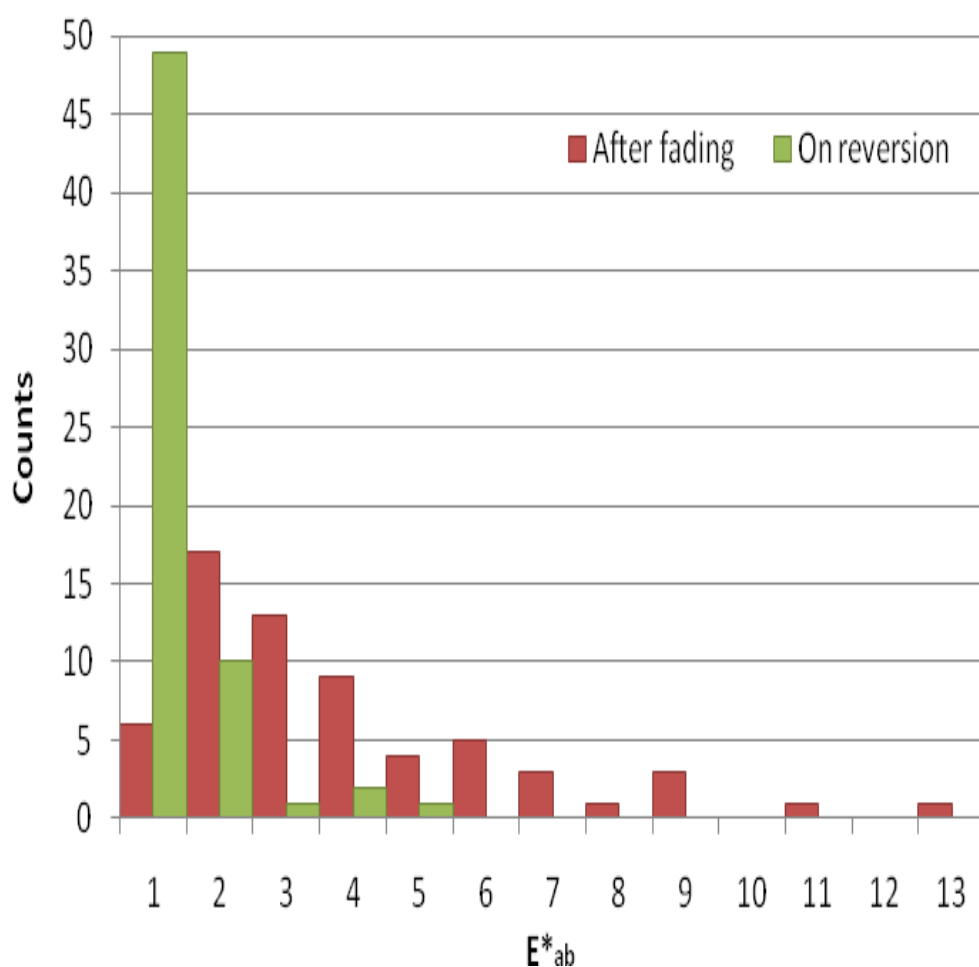


Table 4.15. A histogram representation of the degree of colour difference the Prussian blue sample set after fading in air (red) and after 3 days in low light to revert (green).

Code	Prussian blue sample name	$\Delta E^*_{ab}$ after fading in air $\pm 0.25$	$\Delta E^*_{ab}$ after reversion in air $\pm 0.25$
CA15	Prussian blue	6.8	1
D&C 8/01	Blue de Prusse	1.7	0.7
HKI 1	Prussian blue	1.8	0.4
HKI 2	Prussian blue	2.1	0.2
HKI 3	Antwerp blue	3.4	1.9
HKI 4	Prussian blue	2	0.6
HKI 5	Prussian blue	1.1	0.4
MB 1	Prussian blue (Berlijns Blauw)	1.6	0.4
MB 8	Prussian blue (Berlijns Blauw)	1.3	0.5
MB 8	Prussian blue	3	0.7
MB A1	Prussian blue	0.7	0.5
MB A5	Antwerp blue	2.4	0.7
MB BA1	Prussian blue	1.7	0.3
NG 12a	Prussian blue	5.8	0.4
NG 12b	Prussian blue	10.7	1.4
NG AA (NG WC2)	Ackermann ' Antwerp blue	1.2	0.3
NG ALP	Prussian blue	2.5	0.1
NG AR	Prussian blue	5.4	1.2
NG BA	Good Berlin blue from Weimar	8.2	1.3
NG BB	Berlin blue	4.2	1.5
NG BCB	Prussian blue	2.4	0.5
NG GA	Prussian blue	6.2	0.4
NG JSM	Prussian blue	8.3	0.1
NG K7	Prussian blue	1.6	0.2
NG MA	Prussian blue	5.1	0.2
NG MB	Prussian blue	1.7	0.6
NG NB	Blue	3.1	0.3
NG NP	Prussian blue	2.4	1
NG OZ	Prussian blue	5.9	0.4
NG RA	Prussian blue, barytes, gypsum	2.8	0.2
NG RC	Prussian blue, gypsum	4.2	0.8
NG RD	Prussian blue, kaolin, quartz	12.6	2.6
NG RE	Prussian blue, barites	3.8	0.5
NG RG	Prussian blue, barites	6.1	1.5
NG SA	Prussian blue	0.8	1.2
NG SB	Prussian blue	2.4	0.8
NG SC	Prussian blue	4.5	0.4
NG SD	Prussian blue	7.7	0.2
NG TB	Turnbull's blue'	0.9	0.5
NG VA	Prussian blue	8.5	0.5
NG VB	Prussian blue	4	0.6
NG WC1, (AP)	Prussian blue	2.9	0.3
NG WN	Prussian blue, alkalie ferric ferrocyanide	3.3	0.4
OH2	Prussian blue (Chinese Blue)	1	0.7
OH4	Prussian blue (Blue de Prusse)	1.1	0.3
OH6	Prussian blue (Parijs blauw)	1.5	0.3
OH8	Prussian blue (Mineraalblauw)	2.2	0.3
OH9	Prussian blue (ijzercyaan Berlijns blauw)	2.4	0.1
RC ICN1	Prussian blue	5.2	0.7
RC ICN2	Chinese blue	3.6	1.8
RK14	Prussian blue	1.4	0.1
T CA1	Antwerp Blue	1.3	0.7
T CA7	Chinese Blue 23	1.7	0.5
T RR1	Prussian blue	0.9	0.3
T1	Prussian blue (Berlijns Blauw)	3.5	0.5

Table 4.2. The degree of fading of the Prussian blue sample set in air and after 3 days in low light to revert.

### 4.3.2.2 Fading and storage in anoxia and reversion in air

The results of the anoxic analysis for the Prussian blue sample set are shown Table 4.3 overleaf. The first results columns show the degree of fading of the pigments in anoxia after 1 hour using the micro-fadometer. The second results column illustrates the colour difference of each pigment when kept in anoxic conditions in low light after 3 days. The final column shows the degree of reversion of the 56 Prussian blues after fading and housing in anoxia on exposure to air. Results are summarized via a histogram in figure 4.16.

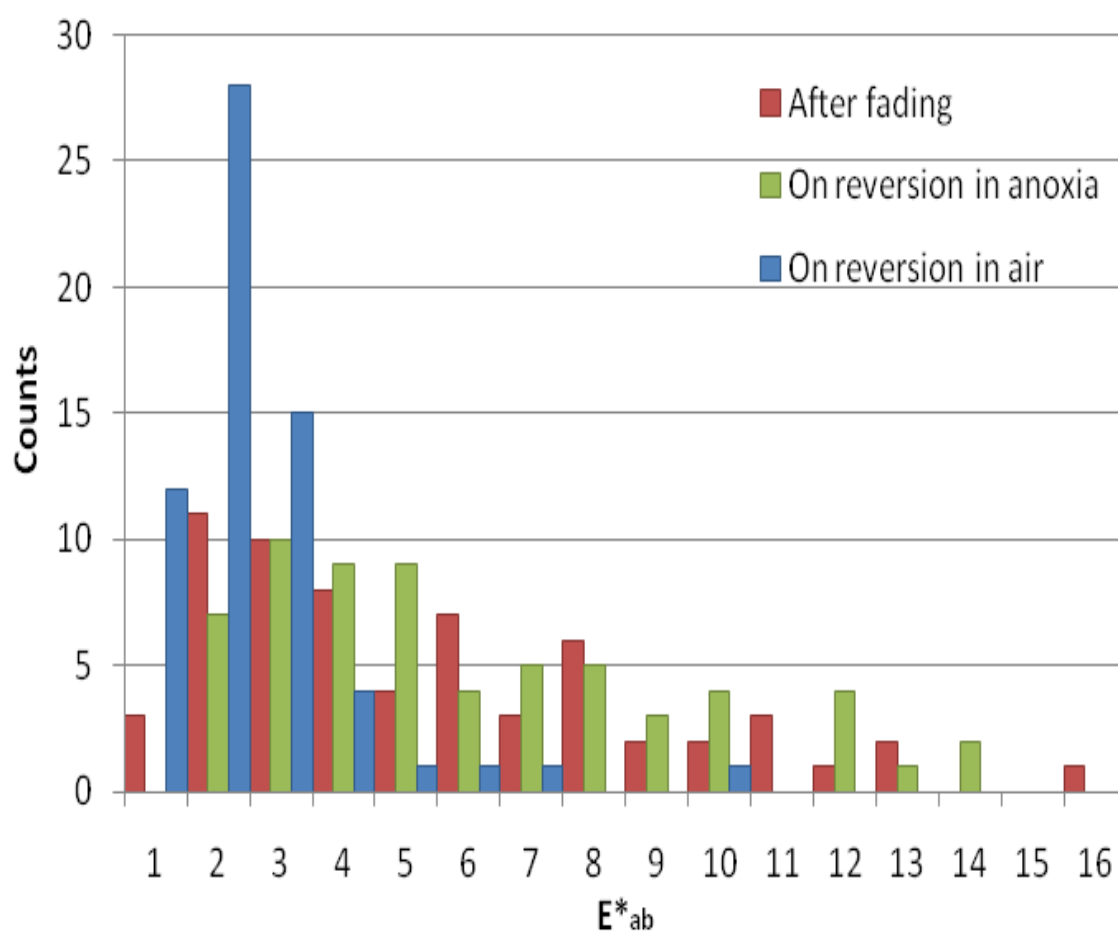


Table 4.16. A histogram representation of the degree of colour difference shown by the Prussian blue sample set in anoxia (red), after 3 days in anoxia in low light to revert (green) and after reexposure to air after 3 days in low light to revert (blue).

CODE	Prussian blue sample name	$\Delta E^*_{ab}$ after fading in anoxia $\pm 0.25$	$\Delta E^*_{ab}$ after reversion in anoxia $\pm 0.25$	$\Delta E^*_{ab}$ after reversion in air $\pm 0.25$
CA15	Prussian blue	9.4	11.5	1.2
D&C 8/01	Blue de Prusse	1.5	3.5	2.1
HKI 1	Prussian blue	2.3	3.7	1.9
HKI 2	Prussian blue	2.4	2	1.3
HKI 3	Antwerp blue	2.5	4.6	1.2
HKI 4	Prussian blue	1.3	1.3	1
HKI 5	Prussian blue	1.4	1.4	1.4
MB 1	Prussian blue (Berlijns Blauw)	2.9	7.8	2.9
MB 8	Prussian blue (Berlijns Blauw)	1.6	2.8	2
MB 9	Prussian blue	3.9	7.5	2.6
MB A1	Prussian blue	2.1	3.4	1.3
MB A5	Antwerp blue	2.3	2.1	1.3
MB BA1	Prussian blue	8.8	8.9	2.9
NG 12a	Prussian blue	7.9	8.3	2.3
NG 12b	Prussian blue	11.3	12.4	1.5
NG AA (NG WC2)	Ackermann ' Antwerp blue	4.6	5.4	3.9
NG ALP	Prussian blue	3.9	2.6	2.4
NG AR	Prussian blue	5.3	4.9	2.1
NG BA	Good Berlin blue from Weimar	15.7	13.1	9.6
NG BB	Berlin blue	3.3	7.5	4.3
NG BCB	Prussian blue	2.3	3.4	1.8
NG GA	Prussian blue	12.8	11.8	1.9
NG JSM	Prussian blue	10	9.2	0.9
NG K7	Prussian blue	3.1	3.3	1
NG MA	Prussian blue	7.1	6.6	0.4
NG MB	Prussian blue	1.7	1.9	1.7
NG NB	Blue	5.5	6.8	2
NG NP	Prussian blue	5.2	5.4	1
NG OZ	Prussian blue	10.9	8.2	2.5
NG RA	Prussian blue, barytes, gypsum	4.1	4.3	1.6
NG RC	Prussian blue, gypsum	6.3	7.4	0.9
NG RD	Prussian blue, kaolin, quartz	12.8	13.4	5.4
NG RE	Prussian blue, barites	8	9.1	1.8
NG RG	Prussian blue, barites	7.2	11.4	6.3
NG SA	Prussian blue	1.6	2.6	2.2
NG SB	Prussian blue	5.1	3.5	1.3
NG SC	Prussian blue	5.8	7.4	1.5
NG SD	Prussian blue	8.5	9.1	1.1
NG TB	Turnbull's blue	1.8	2.7	1.9
NG VA	Prussian blue	10.6	9	0.5
NG VB	Prussian blue	7.1	5.5	1.2
NG WC1, (AP)	Prussian blue	5.2	5.2	0.8
NG WN	Prussian blue, alkalie ferric ferrocyanide	6.7	6.5	2.5
OH2	Prussian blue (Chinese Blue)	1.2	2.5	1.7
OH4	Prussian blue (Blue de Prusse)	2.3	1.8	1.2
OH6	Prussian blue (Parijs blauw)	1.4	1.3	0.3
OH8	Prussian blue (Mineraalblauw)	3.1	2.2	2.3
OH9	Prussian blue (ijzercyaan Berlijns blauw)	5	4.2	3.2
RC ICN1	Prussian blue	8	7	0.7
RC ICN2	Chinese blue	3.8	4.9	1.4
RK14	Prussian blue	2.3	2.8	1.1
T CA1	Antwerp blue	2.7	3.3	3.1
T CA7	Chinese Blue 23	1.7	2.2	0.6
T RR1	Prussian blue	1	3.7	2.6
T1	Prussian blue (Berlijns Blauw)	5.8	6.8	2.5

Table 4.3. The degree of fading after 1 hour using the micro-fadometer, the colour difference after storage in anoxic conditions in low light after 3 days, and the degree of reversion on re-exposure to air.

### 4.3.2.3 Fading and storage in hypoxia and reversion air

The results for fading and storage in hypoxia and reversion in air are shown in table 4.4 overleaf. The first results column shows the colour difference of the pigment immediately after exposure. The second results column represents the colour difference after 3 days of storage in the hypoxic environment. The final column is the colour difference after 3 days of exposure to air after the seal of the test chamber was breached in order to readmit oxygen. Results are summarized via a histogram in figure 4.17.

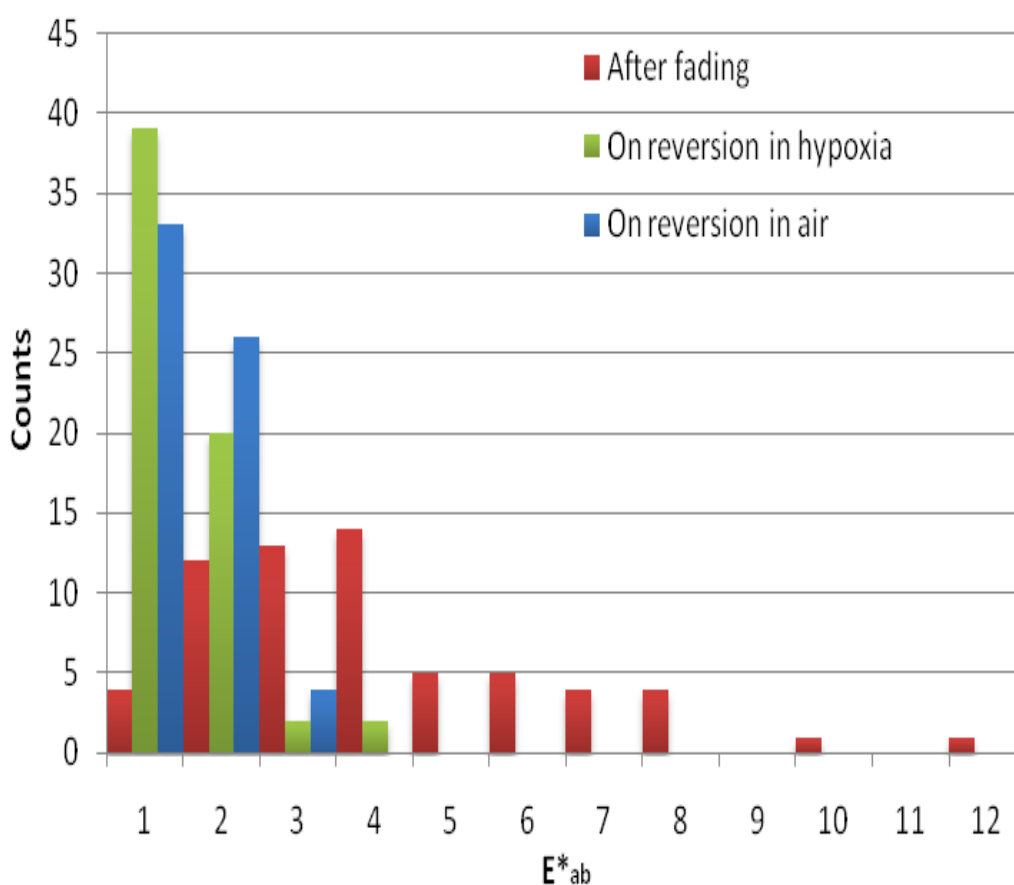


Figure 4.17 A histogram representation of the degree of colour difference the Prussian blue sample set after fading in hypoxia (red), after 3 days in hypoxia in low light to revert (green) and after reexposure to air after 3 days in low light to revert (blue).

CODE	Prussian blue sample name	$\Delta E^*_{ab}$ after fading in hypoxia $\pm 0.25$	$\Delta E^*_{ab}$ after reversion in hypoxia $\pm 0.25$	$\Delta E^*_{ab}$ after reversion in air $\pm 0.25$
CA15	Prussian blue	5.7	0.7	2.3
D&C 8/01	Blue de Prusse	1.6	1.6	0.8
HKI 1	Prussian blue	2.5	2.2	1.3
HKI 2	Prussian blue	2.5	0.6	0.5
HKI 3	Antwerp blue	3.2	2.1	1.4
HKI 4	Prussian blue	2	0.4	0.5
HKI 5	Prussian blue	1.7	0.7	1.8
MB 1	Prussian blue (Berlijns Blauw)	2.2	1.7	0.7
MB 8	Prussian blue (Berlijns Blauw)	1.6	0.5	1
MB 9	Prussian blue	2.2	0.7	0.5
MB A1	Prussian blue	0.9	0.3	0.3
MB A5	Antwerp blue	2.1	0.6	0.6
MB BA1	Prussian blue	5.3	0.4	1.2
NG 12a	Prussian blue	5.9	1.7	2.6
NG 12b	Prussian blue	7.8	0.5	0.5
NG AA (NG WC2)	Ackermann ' Antwerp blue	2.8	1.7	1
NG ALP	Prussian blue	3.1	1.5	1.7
NG AR	Prussian blue	4.2	1.7	1.5
NG BA	Good Berlin blue from Weimar	7.5	0.7	2.8
NG BB	Berlin blue	3.9	1.5	1.3
NG BCB	Prussian blue	3.9	1.7	1.3
NG GA	Prussian blue	9.2	0.2	0.5
NG JSM	Prussian blue	6.2	1	1
NG K7	Prussian blue	2.5	1	1.3
NG MA	Prussian blue	3.7	1.4	1.8
NG MB	Prussian blue	2.3	1.7	1.8
NG NB	Blue	4.5	0.8	0.5
NG NP	Prussian blue	3	1.1	1.8
NG OZ	Prussian blue	4	0.7	1.2
NG RA	Prussian blue, barytes, gypsum	3.5	1.3	0.6
NG RC	Prussian blue, gypsum	4.5	0.5	0.6
NG RD	Prussian blue, kaolin, quartz	11.1	3.7	1.2
NG RE	Prussian blue, barites	5.3	0.4	1.6
NG RG	Prussian blue, barites	7.1	3.8	2
NG SA	Prussian blue	0.2	0.5	1.4
NG SB	Prussian blue	3.4	1.2	1.7
NG SC	Prussian blue	4.1	1	2.3
NG SD	Prussian blue	6.9	0.6	1
NG TB	Turnbull's blue	1.4	0.5	0.5
NG VA	Prussian blue	7.1	1.6	1.6
NG VB	Prussian blue	3.5	1.7	1.7
NG WC1, (AP)	Prussian blue	4.4	0.6	1.1
NG WN	Prussian blue, alkalie ferric ferrocyanide	3.9	0.6	0.6
OH2	Prussian blue (Chinese Blue)	1.2	1.2	1.2
OH4	Prussian blue (Blue de Prusse)	2	0.7	0.9
OH6	Prussian blue (Parijs blauw)	1.7	0.5	0.5
OH8	Prussian blue (Mineraalblauw)	3.2	0.5	0.4
OH9	Prussian blue (ijzercyaan Berlijns blauw)	3.1	1	0.9
RC ICN1	Prussian blue	6.5	1	0.6
RC ICN2	Chinese blue	2.8	0.9	1.3
RK14	Prussian blue	1.4	0.7	0.4
T CA1	Antwerp blue	1.4	1.1	0.8
T CA7	Chinese Blue 23	1.8	0.8	0.5
T RR1	Prussian blue	2.6	1.6	1.3
T1	Prussian blue (Berlijns Blauw)	3	1.1	1

Table 4.4. The colour difference of the Prussian blue sample set immediately after exposure in hypoxia, after 3 days in the hypoxic environment and 3 days after the readmission of oxygen.

#### 4.3.2.4 Comparison of the 3 environments for fading and storage.

In order to analyze the data acquired a series of graphs comparing the colour difference at different stages of the experiments are shown. Each data point represents a single pigment in the Prussian blue sample set.

#### 4.3.2.5 Comparison of the degree of fading

A comparison of the colour difference produced by the micro-fading technique immediately after fading for 1 hour in air and anoxic environments can be seen in figure 4.18. An increase in colour difference is produced by anoxic conditions for the same light exposure. Comparing fading in air and hypoxia produced no clear trend.

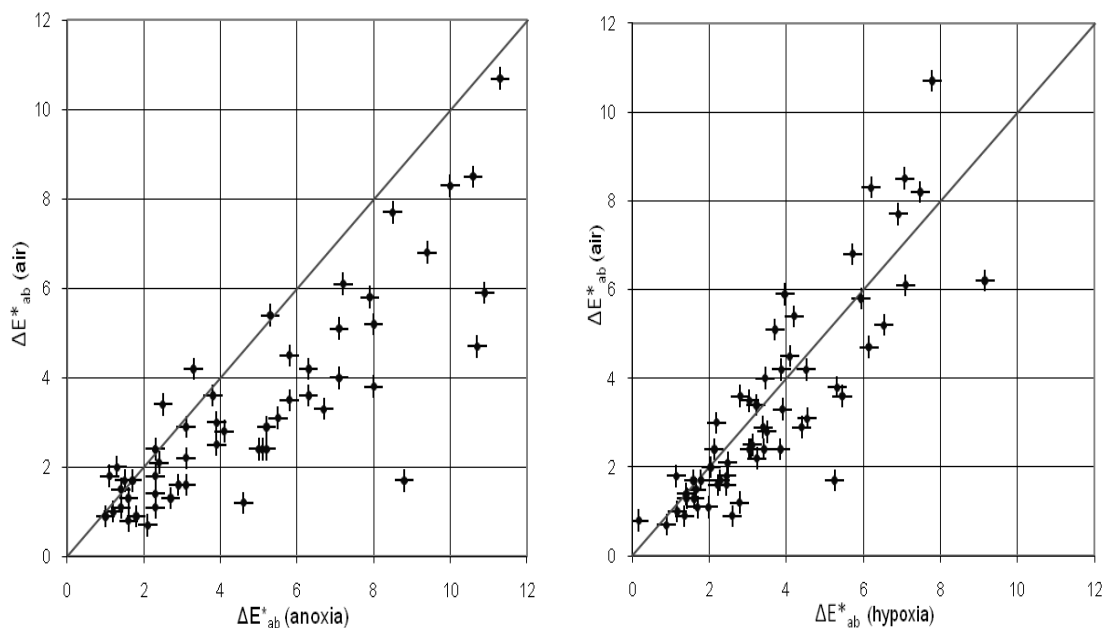


Figure 4.18. A comparison of the colour difference produced by the microfading technique immediately after fading for 1 hour in air and anoxia (left), and a comparison for the same set of Prussian blue pigments immediately after fading in 5% hypoxia and air (right). Error bars +/- 1 equivalent standard deviation for drift and noise.

When comparing the colour difference created by light exposure in 5% oxygen and in anoxia, a similar relationship is illustrated as that seen when comparing anoxia to room atmospheric conditions. A larger degree of change is induced by the anoxic housing than that observed in 5% oxygen (see figure 4.19).

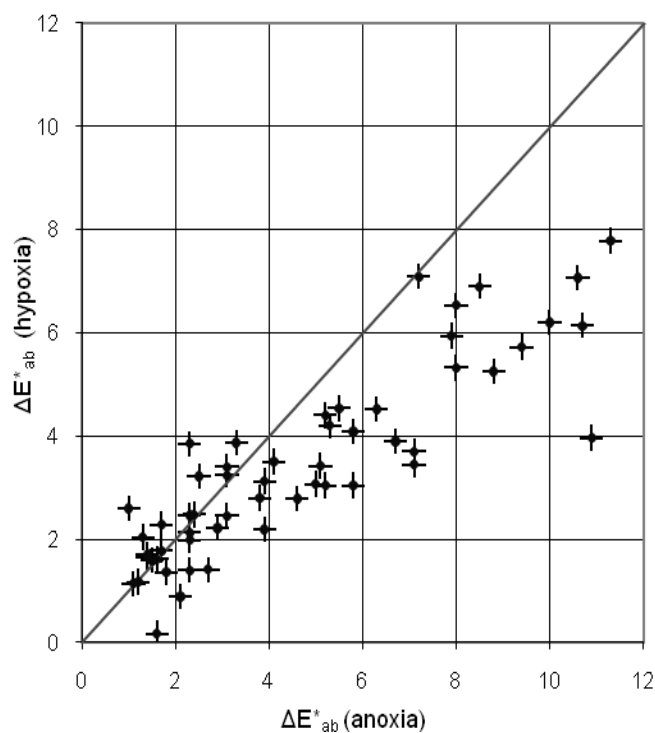


Figure 4.19. Comparison of colour difference produced by the microfading technique for the same set of Prussian blue samples immediately after fading in 5% oxygen (hypoxia) and 0% anoxic conditions (anoxia). Error bars +/- 1 equivalent standard deviation for drift and noise.

#### 4.3.2.6 Reversion within modified environments

The colour difference of the pigments after 3 days storage in both anoxic and room atmosphere environments are shown in figure 4.20. Those pigments housed for the 3 day period in air have reverted however the samples under anoxic purge maintained a significant colour difference.

The colour difference of the pigments after 3 days storage in both hypoxic environments and room atmosphere is also shown. The pigments when stored in air have reverted and the samples under hypoxic purge have also reverted removing any significant colour difference.

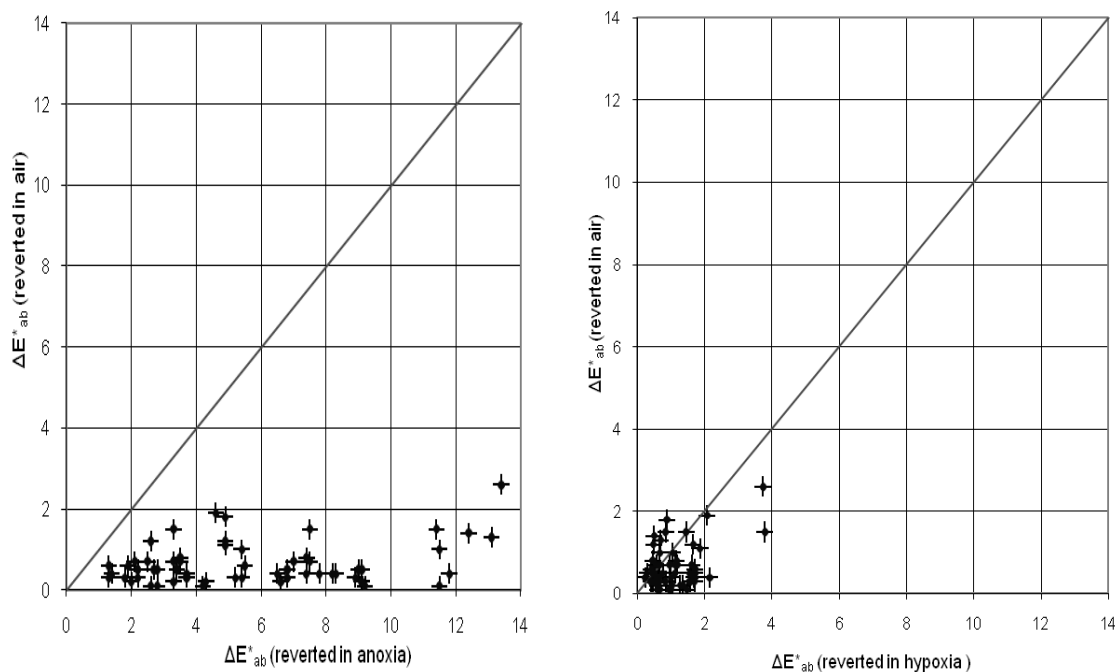


Figure 4.20. Comparison of colour difference produced by the microfading technique for the same set of Prussian blue samples after fading in air and anoxia and after 3 days low light storage in both environments (left) and after fading in air and hypoxia and after 3 days low light storage in both environments (right). Error bars +/- 1 equivalent standard deviation for drift and noise.

#### 4.3.2.7 Reversion after exposure to air.

When the anoxic housed pigments were re-exposed to air the colour difference between the pigments in the two experiments decreased (see figure 4.21). Those pigments that were in anoxic housing regain some of the colour lost via the reversion process over the 3 day period, (a phenomenon that has been widely reported previously).

A number of those pigments faded and stored in anoxia maintain a greater degree of colour difference after this process than those exposed to air and permitted to revert. This indicates that removing Prussian blues from anoxia and allowing lost colour to revert is not a solution to the widely reported damaging effects of anoxic housings.

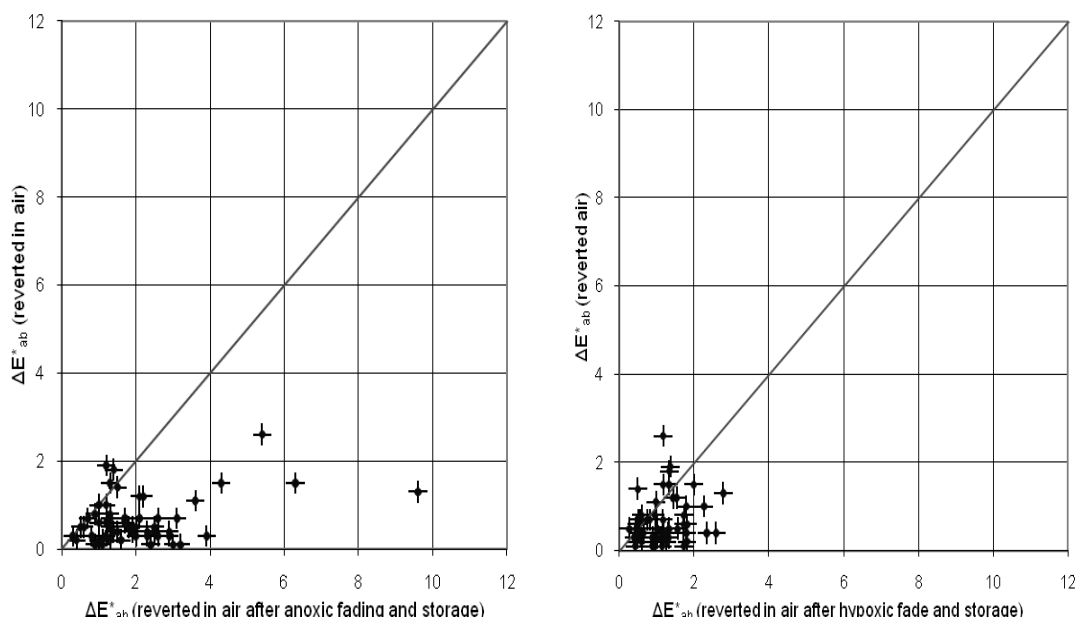


Figure 4.21. Colour difference after fading and reversion in air (y axis) and 3 days after the anoxic chamber has been exposed to air after the faded pigments had 3 days storage in anoxia (x axis) (left), and after fading and reversion in air (y axis), and 3 days after the hypoxic chamber has been exposed to air after the faded pigments had 3 days storage in 5% oxygen (x axis) (right). Error bars +/- 1 equivalent standard deviation for drift and noise.

When the hypoxic housed pigments were re-exposed to air the colour difference between the pigments in the two experiments is further reduced and the damage from light exposure when using a 5% hypoxic storage environment for Prussian blue rather than no housing seem comparable. The pigments largely remain no more faded by the initial hour of micro-fadometer exposure after the hypoxic process than those exposed only to air during the experiment. This indicates the use of 5% hypoxia is not a damaging method for the storage of Prussian blues, as the increased colour difference observed after storage in anoxia is not present at this oxygen level. The variation observed is no greater than that typically observed when fading pigments using this technique.

When comparing Prussian blue pigments that have been housed, faded and stored in anoxic and hypoxic conditions and then re-exposed to air the difference between 5% hypoxia and anoxia is evident. Some pigments display a greater degree of damage due to anoxic storage (see figure 4.22).

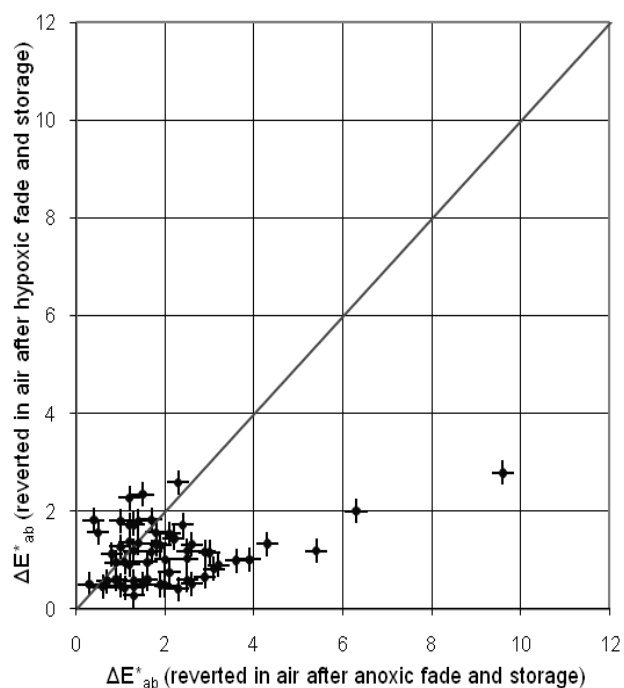


Figure 4.22. Comparison of colour difference produced by the microfading technique for the same set of Prussian blue samples by fading in the respective oxygen level after 3 days storage and 3 days after exposure to air. Error bars  $\pm 1$  equivalent standard deviation for drift and noise.

#### 4.4 Discussion

The sample of Turners Prussian blue TTB6 showed similar behaviour in the two different experiments. The pigment exhibits limited reversion in anoxic conditions. No greater colour difference was observed due to anoxic storage after the fading process ends and the illumination removed.

When Turners Prussian blue TTB6 was faded at 0%, 2%, 3.5%, 5%, 10% or 21% oxygen concentration a plateau of fading was observed in all cases other than at 0% oxygen. When oxygen is present in the controlled hypoxic fading environments the rate of colour change with time becomes increasingly small, however in anoxic conditions this observed decrease in colour change with time is not present. This difference created by the different oxygen level is considerably more pronounced after longer periods of time and only under anoxic conditions is fading to an observable white colour observed.

Under both lower hypoxic conditions and anoxia, fading of Prussian blue appears to be accelerated. This effect is more pronounced after longer periods of time. Within shorter

fading periods there is no observable difference. When oxygen is present in the controlled fading environments the rate of colour change with length of time of exposure becomes increasingly small, however in anoxic conditions this decrease in colour change with time is not present.

At 21% 10% 5% and 3.5% oxygen,  $\Delta E_f$  has the same calculated value of colour change and can be regarded as similar to that under ambient atmosphere. At 0% and 2% oxygen concentrations, however, it is higher than at ambient atmosphere. With this data set, it appears as though overall colour change increases in a non-linear manner with decreasing oxygen concentration. This indicates that the deleterious effects of hypoxia may only become relevant at low oxygen concentrations (beginning at an hypoxic level above 2% and below 3.5%), and that relatively low concentrations of oxygen (around 5%) may be tolerated by Prussian-blue containing works of art.

When the study in this pattern of behaviour was extended to a larger number of Prussian blues and the behaviour of the pigment at 0% and 5% oxygen was compared to behaviour in room atmosphere, it is indicated that a 5% oxygen concentration is widely applicable. The deleterious effect of anoxia was not observed for 5% oxygen when the investigation was widely extended.

Importantly, further insight has been gained in to the necessity of a novel storage atmosphere for Prussian blue.

## 5 Reduced oxygen for watercolour pigments

### 5.1 Introduction

Anoxia is a method of housing objects that is commonly expected to retard the oxidative degradation pathway (Russell and Abney 1888, Thomas *et al.* 2009). This pathway is often associated with light exposure. Anoxia is potentially a highly suitable conservation method for display and storage of collections (Maekawa 1998, Townsend *et al.* 2008). This is especially the case for those collection materials highly susceptible to oxidation as photo-oxidation of most colourants (whether or not they are in binding media) will be reduced by anoxia. Organic dyes, lakes and pigments should benefit from anoxia as most undergo oxidative fading (Hackney 2006). The majority of inorganic pigments should not be negatively affected by storage in anoxia, though some can undergo reductive colour change.

Research is required in order to further assess the effects of anoxia for paper-based works of art and to provide data to gain insight and understanding regarding pigments that have may be harmed by anoxic display. As a result of a literature review (see Townsend *et al.* 2008) many problematic pigments were identified. In the Russell and Abney (1888) report the affect of anoxia on traditional artists pigments was investigated. Those single colours that altered when faded within a vacuum were vermilion, purple madder, purple carmine, violet carmine, Prussian blue, raw sienna and sepia. Brommelle (1964) has referenced work contemporary to the Russell and Abney report by chemist A. Richardson, illustrating cadmium yellow, cadmium orange, king's yellow, crimson lake, indigo, Prussian blue, vermilion and the chrome yellows all undergo reducing reactions independent of air. Arney (1979) found vermilion azo and Prussian blue to perform poorly in anoxia. Yellow lead oxide (lead(II) oxide), and to a lesser extent red lead (lead(II) lead (IV) oxide), show colour changes in anoxic environments (Saunders *et al.* 2002). Korenberg (2008) illustrated the damaging effects of anoxia for modern Prussian blue and Antwerp blue pigments. Work by Beltran *et al.* (2008) illustrated negative effects of anoxia on red lead, verdigris and rose madder as well as Prussian blue. Pascoe *et al.* (1994) studied the effects of reduction bleaching on traditional pigments in gum Arabic and reported changes in vermilion, chromates, iron oxides and ultramarine violet.

Norville-Day *et al.* (1994) found harmful effects of reducing bleaches with respect to vermilion, brown madder, red lead, madder, sap green and gamboge. Chrome yellow, vermilion, lead white, Naples yellow, zinc white and malachite has been reported to reduce to oxides by Chappé *et al.* (2003) and Pouli *et al.* (2003). Kenjo (1980) discussed the storage of pigments that are stable in normal atmospheric surroundings but are reduced in inert gases in atmospheres having low oxygen concentrations up to 4.5 to 5.5%.

A comprehensive literature review of the behaviour of colourants in anoxia was presented by Thomas *et al.* (2009).

The benefits and risks of anoxia for paper falls outside the scope of this research, although work continues in this area (Thomas 2011). No comprehensive published study on the effect of anoxia on binding media is available.

## **5.2 The pigments selected for study**

Often only one example of a pigment type is tested in any investigation, and the provenance and independent analysis of pigments in question is not always presented. It was hoped that this research would address these two issues to some degree.

The pigment sample set was based on those pigments that had previously been reported to behave poorly in anoxia. The most important pigment considered for study was Prussian blue (dealt with in greater detail in chapter 4). Other important pigments chosen for the research were indigo, logwood, vermilion, cadmium yellows, lead chromates (chrome yellows), lead oxides (red lead and massicot/litharge) and madders on various substrates.

All the pigments were prepared by Caspers (2008) by grinding with gum Arabic, diluting with distilled water and applying in a wash onto Ruscombe mill paper (or Whatman silversafe paper when stated). Appendix E and Caspers (2008) detail the provenance of the samples collected, and the results of elemental and sometimes FTIR analysis used to confirm that they were as labeled. This group is styled as ‘characterised pigments’. In a few cases, these screening methods did not serve to give a positive identification, e.g. for sepia. In these cases, examples that matched in terms expected EDX and published FTIR results were used, and less consistent samples of the same name were rejected from the set. If

strenuous efforts had not led to a group of three such pigments of the same type, the one or two examples are styled as ‘uncharacterised’ here.

No strict controls were placed on many variables originating from the historically informed reconstructions that could alter the rate of fading, such as the thickness of the paint layer tested, particle size or uniformity of colour of the paper substrate. Variations in accelerated aging results are often due to differences in specimen preparation, surface irregularities, colour measurement and conditions of exposure (ASTM 2006). This variation led to a reduction in the repeatability of results and meant repeat measurements were required in order to distinguish variation in pigment behaviour between the various environments.

Groups of pigments that were well characterised were brazilwood, cochineal, gamboge, indigo, madder, orpiment, Prussian green, sap green, vermilion, weld, Indian yellow, quercitron, cadmium, massicot, sepia, and zinc oxide. Also thought as suitable grouping in terms of composition were lakes pigments, chromate pigments and iron oxides.

Pigments that were poorly characterised were bistre, black, buckthorns, brown pink, burnt umber, carmine, Van Dyke brown verditer, smalt, yellow ochre, lead white, red lead and Kopp’s purpurine.

Many of the pigments contained within this study independently warranted further analysis due to their reported photosensitivity. Schaeffer (2001) produced a list of light-sensitive traditional pigments in a review. The list contained vermilion, lead(II) oxide, lead chromate, copper greens, and Prussian blue (a selection of pigments with a strong overlap with those chosen for this anoxic research).

Confusingly for the newcomer to pigments (in particular lake pigments) the use of the term substrate can lead to some confusion. Lake pigments are produced by precipitating colourants upon alumina, chalks or starch, or occasionally metal oxides of copper, iron or tin (all of which are known as substrates) (Eastaugh *et al.* 2004). This description of a lake pigment substrate is not to be confused with the alternative use to the term as used when referring to the material upon which any pigment is applied.

### 5.3 The experimental method

Previous work in the field often lacks detailed information with respect to the degree of exposure that was incident to produce the colour changes reported. Larger exposures make it possible to distinguish differences of behaviour because they become more apparent the greater that degree of colour change. In this research it was hoped to use light exposures that are equivalent and more representative of the 10 year period an art work may experience when contained within an anoxic frame (Townsend *et al.* 2008).

To simulate the effect of modified environmental framing the fading characteristics of a large sample set was analysed using automated micro-fadometry using the technique as discussed in the previous chapter.

Results of colour change for 1 hour of fading (corresponding to an exposure of approximately 93 kilojoules or  $1.7 \times 10^7$  lux-hours) in air or anoxia were analysed for all pigments. This was done in order to appraise the degree of damage that had been induced by illumination. If a colour difference less than  $1 \Delta E_{00}$  was measured in both air and anoxia for this fade duration, the testing of the pigment was discontinued. A colour change on this scale was deemed not suitably significant and therefore any further information was not of concern.

Those pigments that faded to a colour difference greater than  $1 \Delta E_{00}$  were further faded in oxygen concentrations of 0%, 5% and room atmospheric conditions (air). Fades were repeated 3 times, 3 times and 5 times respectively. Repeats of the fade were necessary to obtain information and overcome the dominant uncertainty caused by sample non-uniformity.

The monitored spectrum is converted using the Commission International de l'Eclairage (CIE) 1976  $L^*a^*b^*$  equation for the 2° standard observer under the standard illuminant D65. The  $L^*a^*b^*$  values were then used to calculate colour difference for the samples in CIEDE2000. All numerical data presented in this chapter is in these units.

## 5.4 Results

For each pigment category results are grouped and tabled to summarise the investigation. They are arranged by common chemical type as analysed and not by label. If no standard deviations or colour difference values in 5% oxygen are displayed this is because the colour difference created in air and anoxia was than 1  $\Delta E_{00}$  for the individual pigment. In this case the values below 1  $\Delta E_{00}$  will be displayed for the behaviour in air and anoxia in the average cell of the table.

To enable a comparison of final colour difference in air and anoxia and air and hypoxia comparative graphs of the pigments data set is also provided. Final colour differences after the hour exposure in a particular oxygen concentration are plotted on different axis to enable comparison for an entire pigment grouping.

In all graphs the blue line represents the behaviour of the pigment in air. The pink line represents the behaviour in anoxia and the yellow line represents the behaviour in a 5% oxygen concentration. Every error bar shown represents  $\pm 1$  standard deviation of the result.

### 5.4.1 Fugitive characterised pigment groups

#### Brazilwood

Brazilwood is a red dyestuff derived from a particular genus of hard brown red wood trees. Results from the fading of this sample set can be seen in table 5.1.

The main colouring matter present is brazilein (Eastaugh *et al.* 2004). An evident lack of colour permanence has been reported (Kirby and White 1996) (Ford 1992) (Padfield and Landi 1966).

All pigments were considered likely to be brazilwood, given their provenance, but were not however independently verified.

Brazilwood was shown to benefit from anoxia. Some benefit was still present when using a 5% oxygen concentration.

Analysis indicated that the logwood lake (code NG10) was actually brazilwood on an Alum based substrate.

NAME	CODE	Air		0%		5%	
		Average	St Dev	Average	St Dev	Average	St Dev
Brazilwood	RK8	0.5	0.1	1.1	0.3	0.7	0.1
Brazilwood, BR12	NG9	4.7	1.2	1.9	0.4	3.1	0.2
Brazilwood and madder	RC-ICN-BM	5.3	1	2.0	0.5	3.8	0.2
Logwood lake	NG10	2.4	0.2	1.6	0.3	1.6	0.1

Table 5.1. The behaviour of brazilwood at the 3 oxygen concentrations.

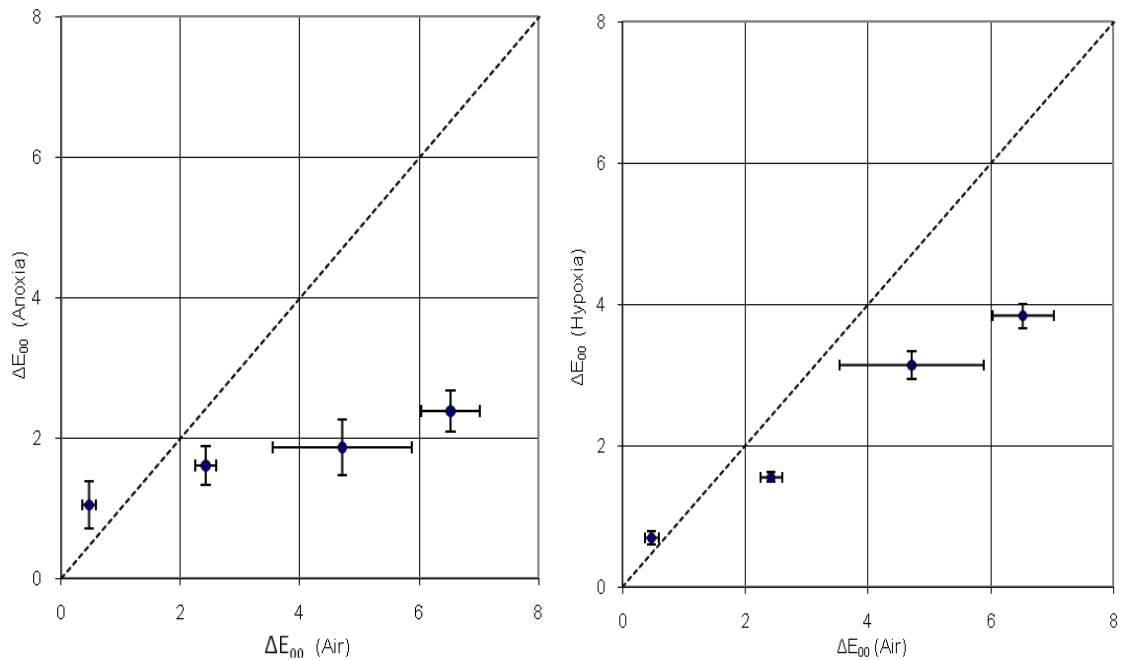


Figure 5.1. Brazilwood: colour difference in air and anoxia after the fade period (left) and a comparison of final colour difference in air and hypoxia for the same fade duration (right)

The graphs below show the fading behaviour of the brazilwood pigments. Data is presented averaged with the standard deviation of the fades presented and also shown individually in separate plots.

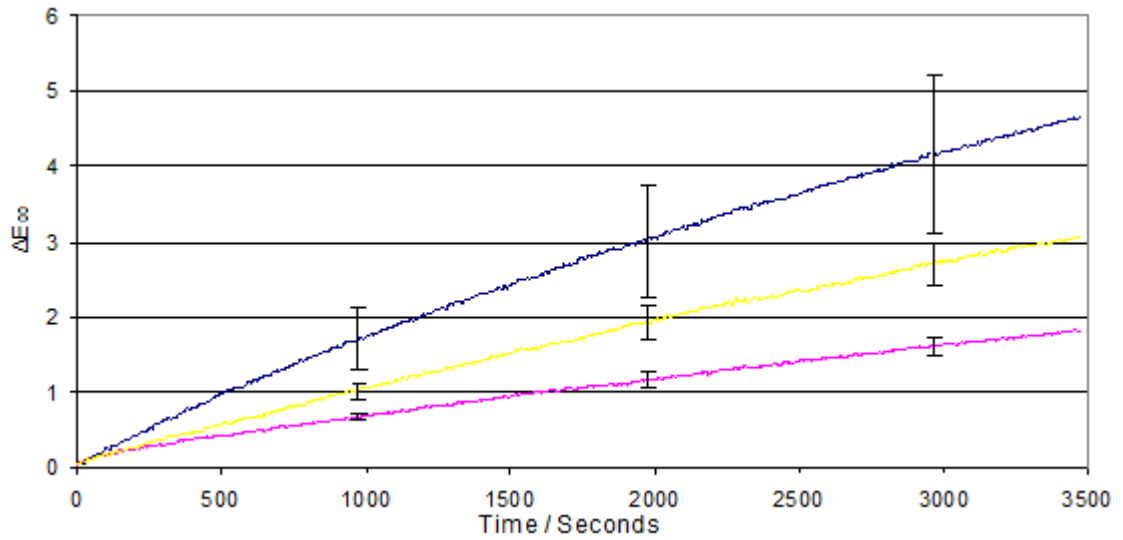


Figure 5.2. The colour difference created over the duration of the fade for a brazilwood, BR12 (code NG9) pigment in the 3 different oxygen concentrations. The blue, pink and yellow lines represent fading in air, anoxia and 5% hypoxia respectively.

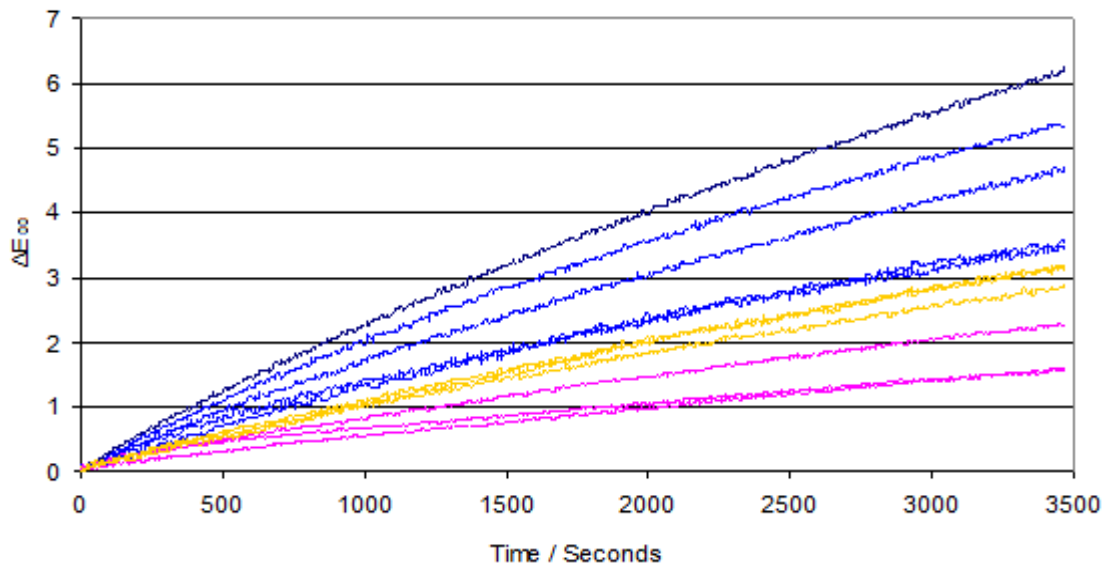


Figure 5.3. Individual plots of the colour difference created over the duration of the fade for a brazilwood, BR12 (code NG9) pigment in the 3 different oxygen concentrations.

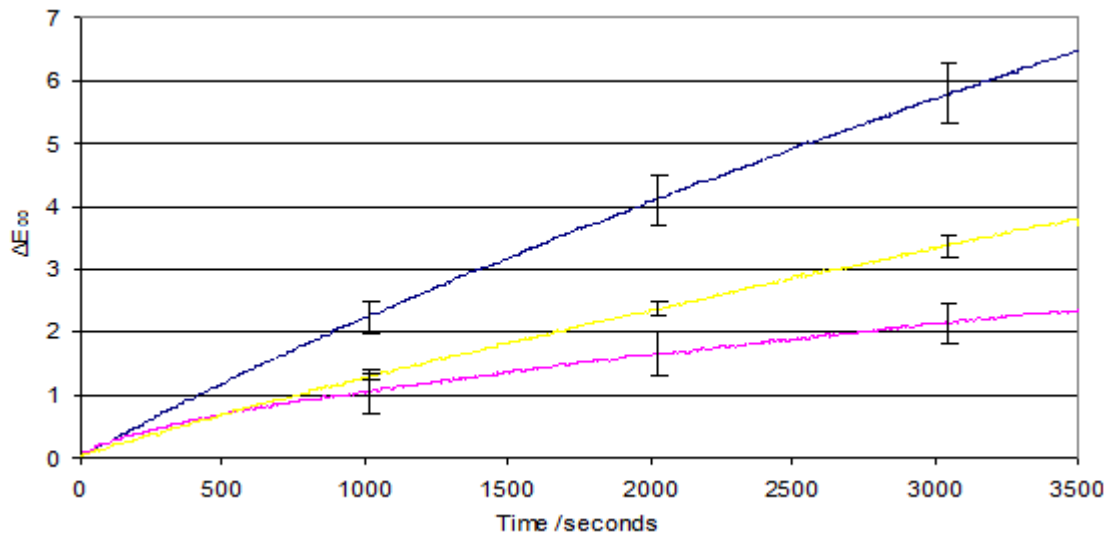


Figure 5.4. Colour difference measured with time for a brazilwood on potas (code RC-ICN-B2) pigment in 3 oxygen concentrations.

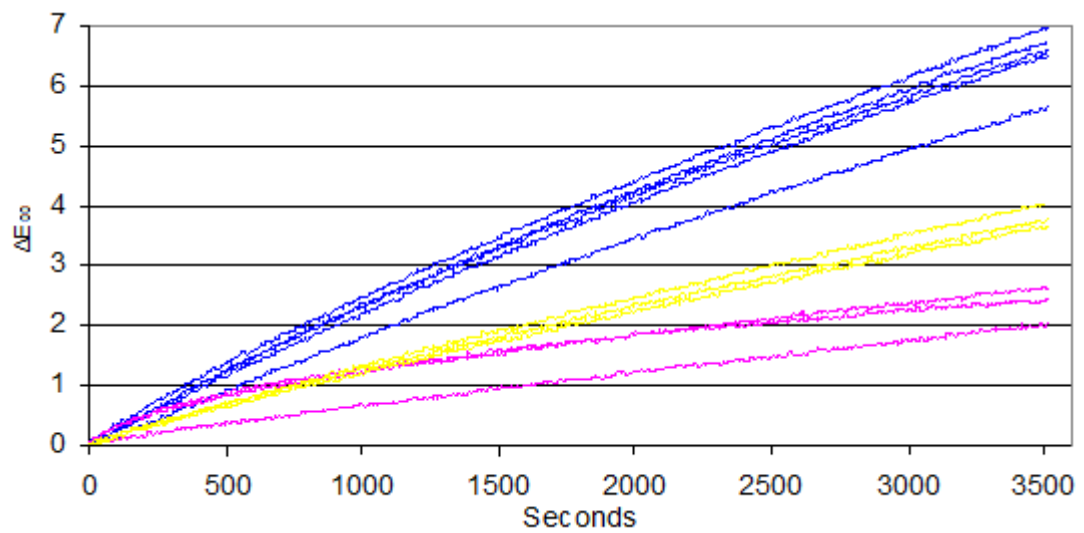


Figure 5.5. Individual plots of the colour difference measured with time for a brazilwood on a potassium-based substrate (code RC-ICN-B2) pigment in 3 oxygen concentrations.

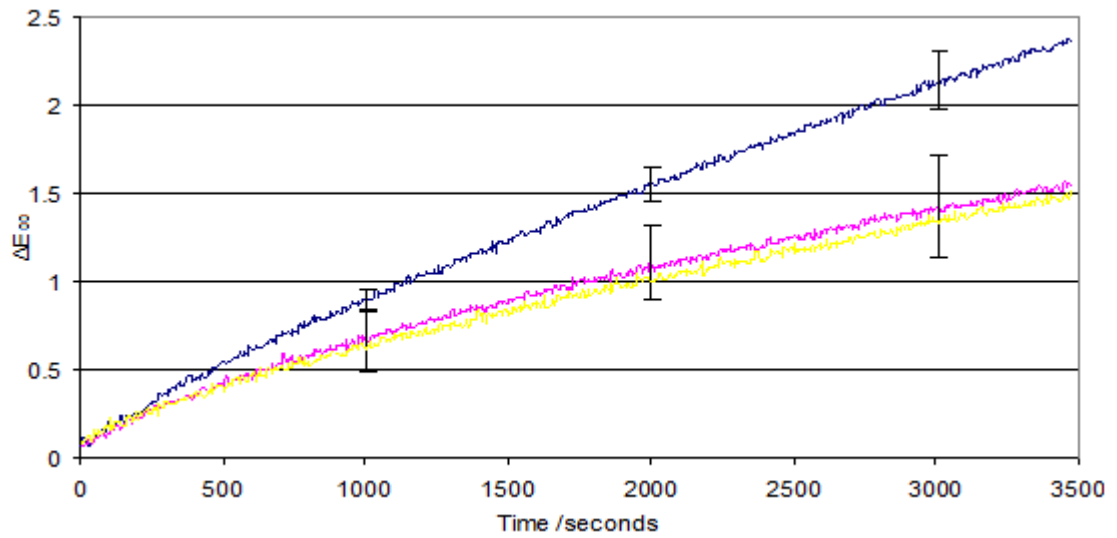


Figure 5.6. Colour difference measured over time for logwood lake (code NG 10) pigment in the 3 different oxygen concentrations. The error bars represent  $\pm 1$  standard deviation of the 5 results from fading the pigment in air and anoxia.

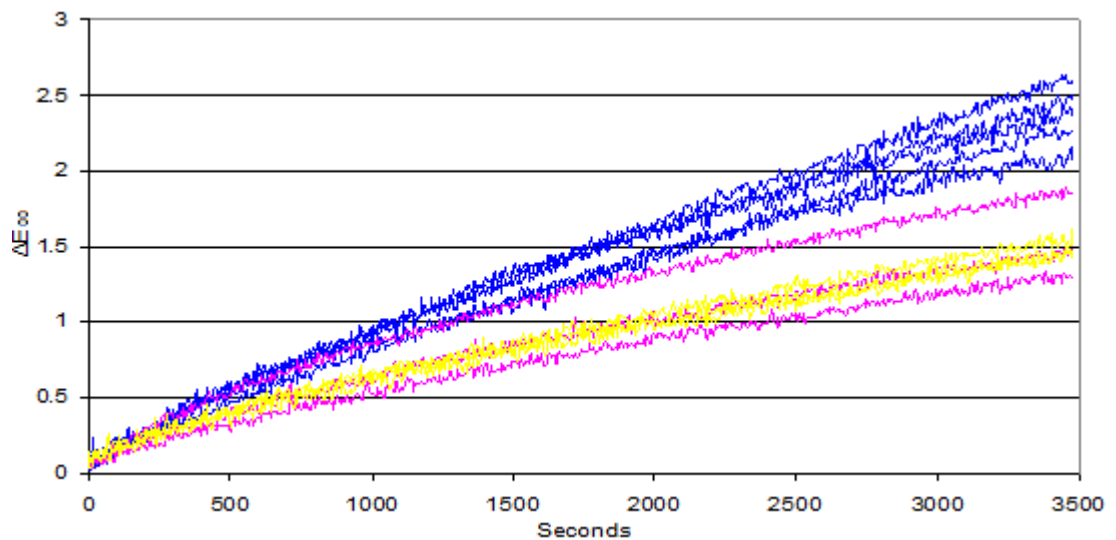


Figure 5.7. Individual plots of the colour difference measured over time for logwood lake (code NG 10) pigment in the 3 different oxygen concentrations.

## Chromate pigments

Chromates are a group of pigments of yellow/orange/red colours in which a variety of elements combine with chromate ( $\text{CrO}_4$ ) or dichromate ( $\text{Cr}_2\text{O}_7$ ) ions (Eastaugh *et al.* 2004). Results from the fading of this sample set can be seen in table 5.2.

Previous work indicates that chrome red (lead chromate (VI) oxide,  $\text{PbCrO}_4 \cdot \text{Pb}(\text{OH})_2$ ) can be considered as lightfast (as has been found in here). This is in contrast to chrome yellow (lead chromate(VI)  $\text{PbCrO}_4 \cdot \text{Pb}(\text{OH})_2$  or lead chromate(VI) sulfate  $\text{PbCrO}_4 \cdot x\text{PbSO}_4$ ) which are reported to darken to a brown on exposure to light (Kühn and Curran 1986) although only one of the chrome yellows displayed instability to light.

Four chrome pigments analysed displayed little colour change. Mid chrome yellow displayed fading independent of oxygen concentration used during the process. Fading independent of oxygen concentration for chrome yellow has previously been reported as discussed.

Analysis found that Indian yellow (code NG4) was in fact a chrome yellow.

NAME	CODE	Air		0%		5%	
		Average	St Dev	Average	St Dev	Average	St Dev
Chrome red	OH11	0.4		0.2			
Chrome clair	D&C 8/05	0.5		0.4			
Chrome yellow	OH12	0.6		0.5			
Mid chrome yellow	T TB12	2.0	0.5	1.9	0.2	2.0	0.1
Indian yellow	NG4	0.3		0.4			

Table 5.2. The behaviour of the chrome pigments at the 3 oxygen concentrations.

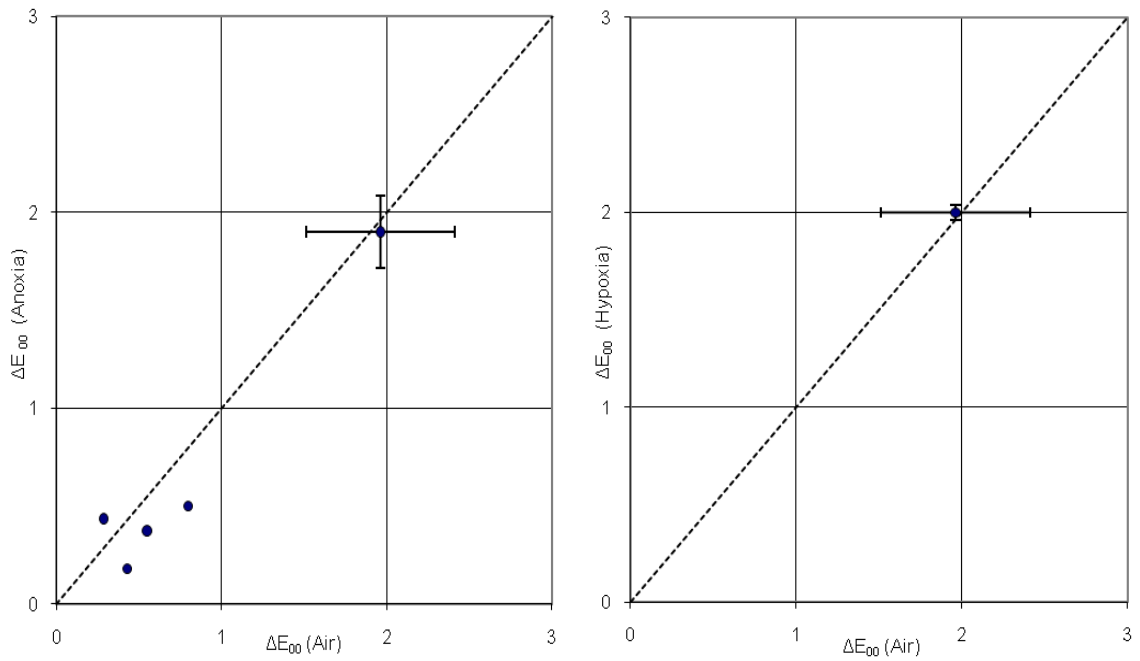


Figure 5.8. Chrome pigments: final colour difference in air and anoxia (left) and a comparison of final colour difference in air and hypoxia (right) No error bars are displayed for values below 1 colour difference unit as no repeat measurements were made for these values.

The following graphs illustrate the fading behaviour of the pigments that showed colour change above 1 colour difference unit. Results are both averaged with the standard deviation of the fades presented and also shown individually in separate plots.

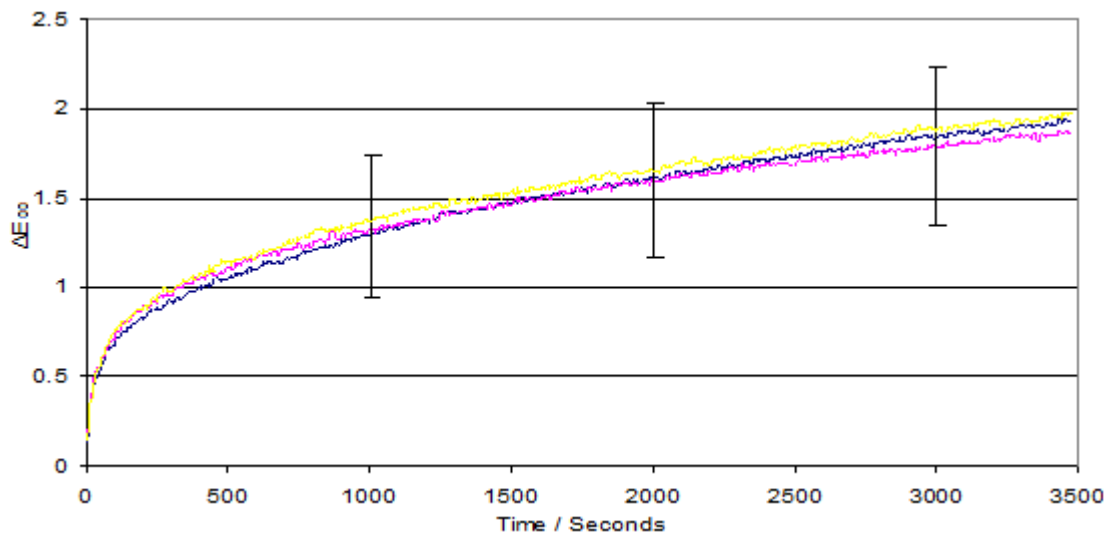


Figure 5.9. Fading behaviour of mid chrome yellow (code T TB12) pigment in different oxygen concentrations. The error bars represent  $\pm 1$  standard deviation of the 5 results from fading the pigment in air.

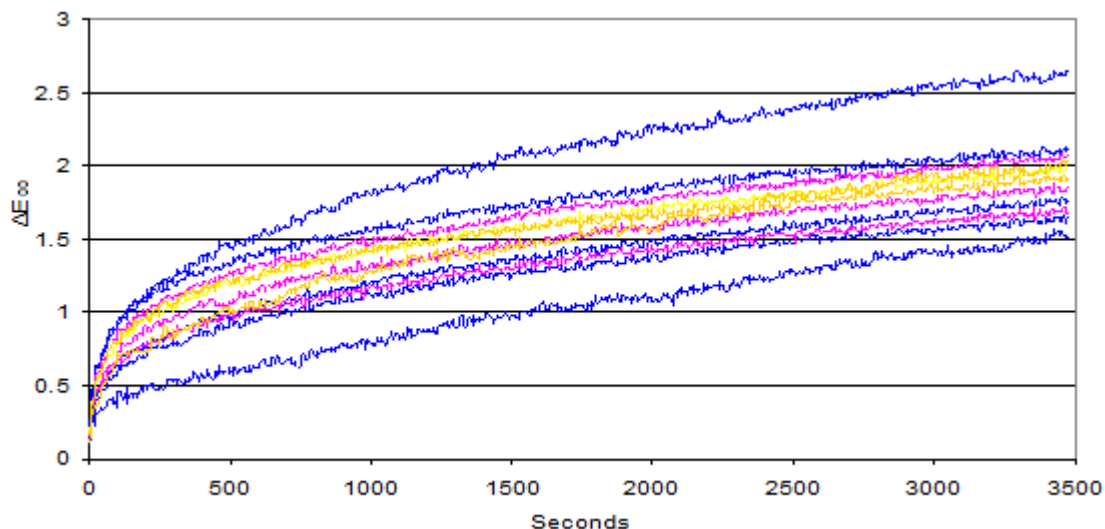


Figure 5.10. Individual plots of the fading behaviour of mid chrome yellow (code T TB12) pigment in different oxygen concentrations.

### Cochineal

Cochineal is a red dye stuff derived from species of scale insects (Eastaugh *et al.* 2004). All samples were considered likely to be cochineal due to their provenance but were not independently verified. Results from the fading of this sample set can be seen in table 5.3.

Cochineal has been reported to display a good degree of lightfastness (Harrison 1957) and is reported to become bluer on fading by Duff (1977) and Padfield and Landi (1966).

Cochineal was shown to benefit from anoxia as has previously been reported. A benefit was still present when using a 5% oxygen concentration.

NAME	CODE	Air		0%		5%	
		Average	St Dev	Average	St Dev	Average	St Dev
Cochineal lake	CD 1b	0.9		0.2		0.3	
Cochineal on Al	C1	1.3	0.1	0.2	0.1	0.6	0.1
Cochineal lake	C8	1.7	0.5	0.4	0.1	0.6	0.3

Table 5.3. A summary of the behaviour of cochineal at the 3 oxygen concentrations.

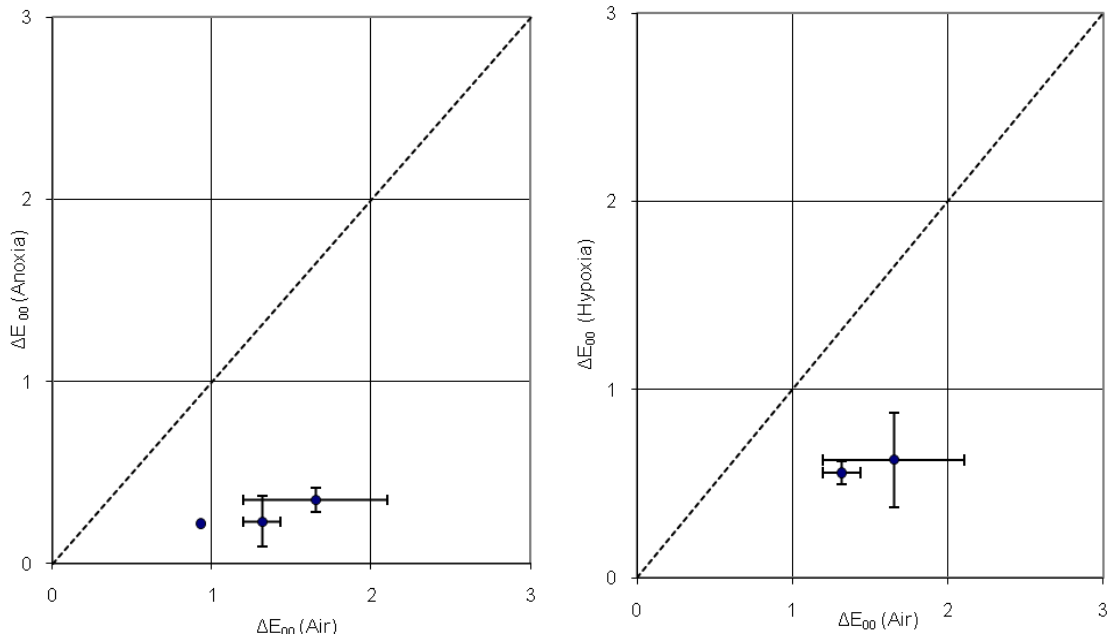


Figure 5.11. Cochineal: final colour difference in air and anoxia (left) and a comparison of final colour difference in air and hypoxia (right)

The graphs below show the fading behaviour of the cochineal pigments that showed colour change greater than 1 colour difference unit, both averaged with the standard deviation of the fades presented and also shown individually in separate plots.

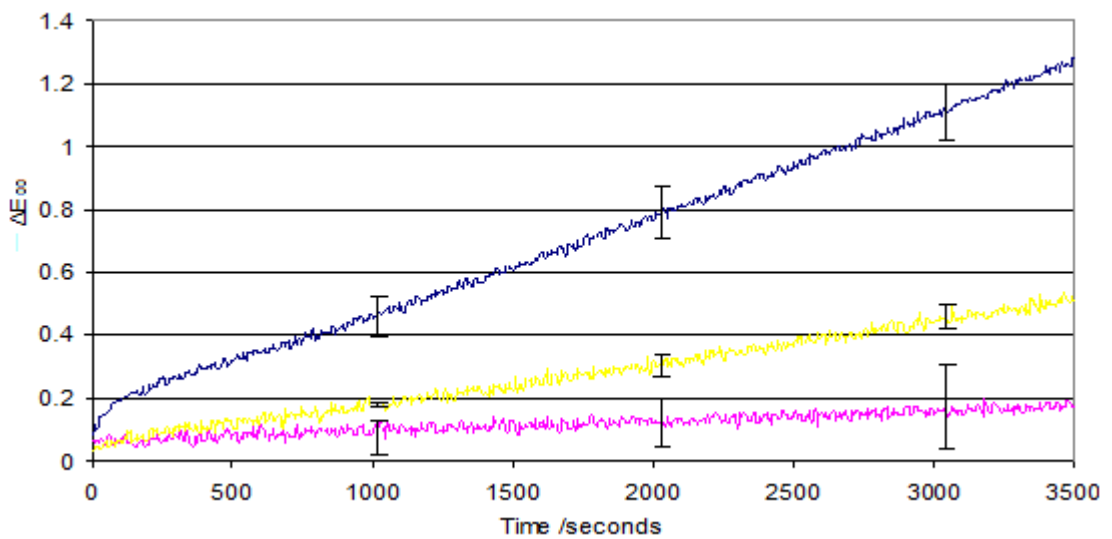


Figure 5.12. Fading curve of cochineal on alum (code C1) pigment in different oxygen concentrations.

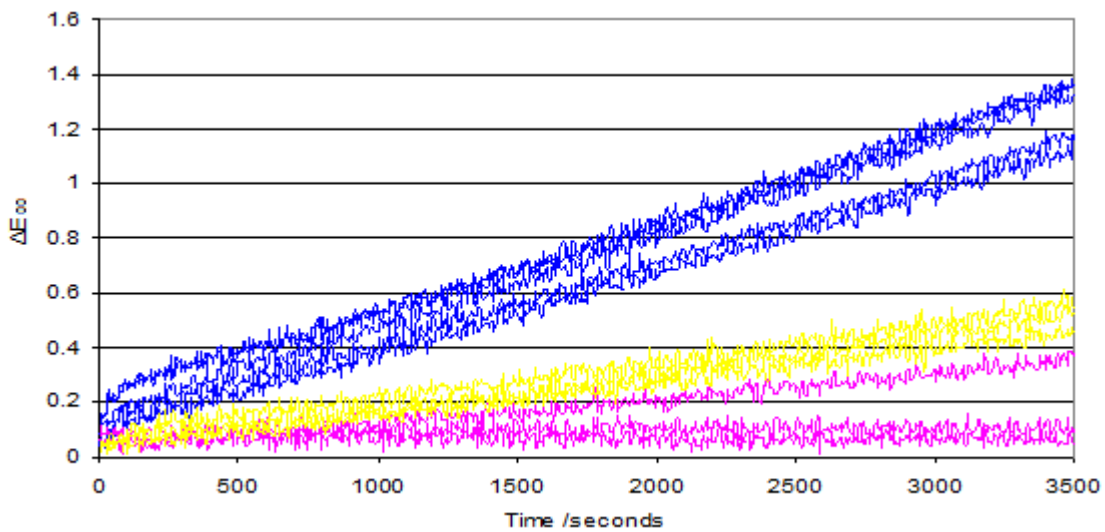


Figure 5.13. Individual fading curves of cochineal on alum (code C1) pigment in different oxygen concentrations.

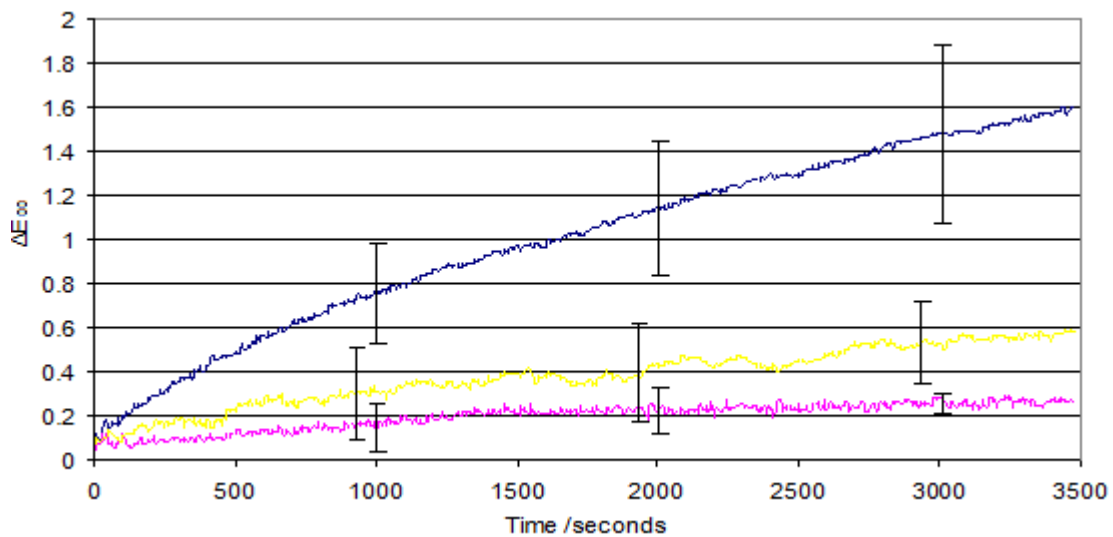


Figure 5.14. Colour change for cochineal lake (code C8) pigment in different oxygen concentrations.

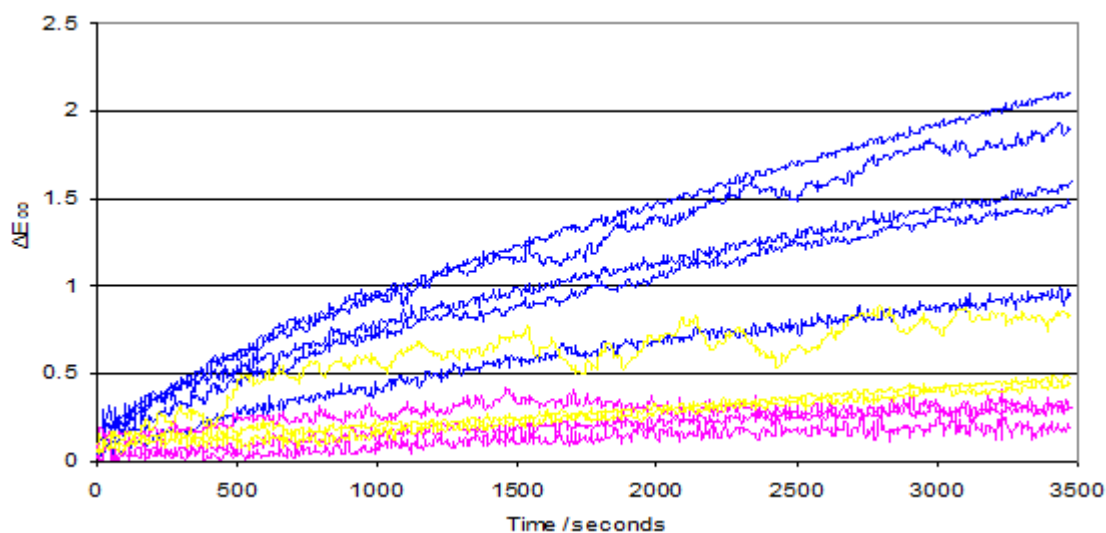


Figure 5.15. Individual colour changes for cochineal lake (code C8) pigment in different oxygen concentrations.

## Gamboge

Gamboge is a brown resin derived from certain evergreen trees (Eastaugh *et al.* 2004). It is widely regarded as fugitive (Winter 2007) although the durability of the pigment varies between samples (Harley 2001). Results from the fading of this sample set can be seen in table 5.4.

The sample set was light stable contrary to previous reports. Some benefit from anoxia over the fade duration was observed for gamboge (code MB A3) which was also contrary to previous reports; this clear benefit was still present when using a 5% oxygen concentration.

NAME	CODE	Air		0%		5%	
		Average	St Dev	Average	St Dev	Average	St Dev
Gamboge	RC ICN9	0.2		0.1			
Gamboge	T TB3	0.3		0.2			
Gamboge	NG WC3	0.4		0.2			
Gamboge	NG1	0.5		0.2			
Gamboge	TRS7	0.9	0.1	1.1	0.2	0.9	0.1
Gamboge	MB A3	1.1	0.1	0.5	0.1	0.6	0.1

Table 5.4. The behaviour of the gamboge at the 3 oxygen concentrations.

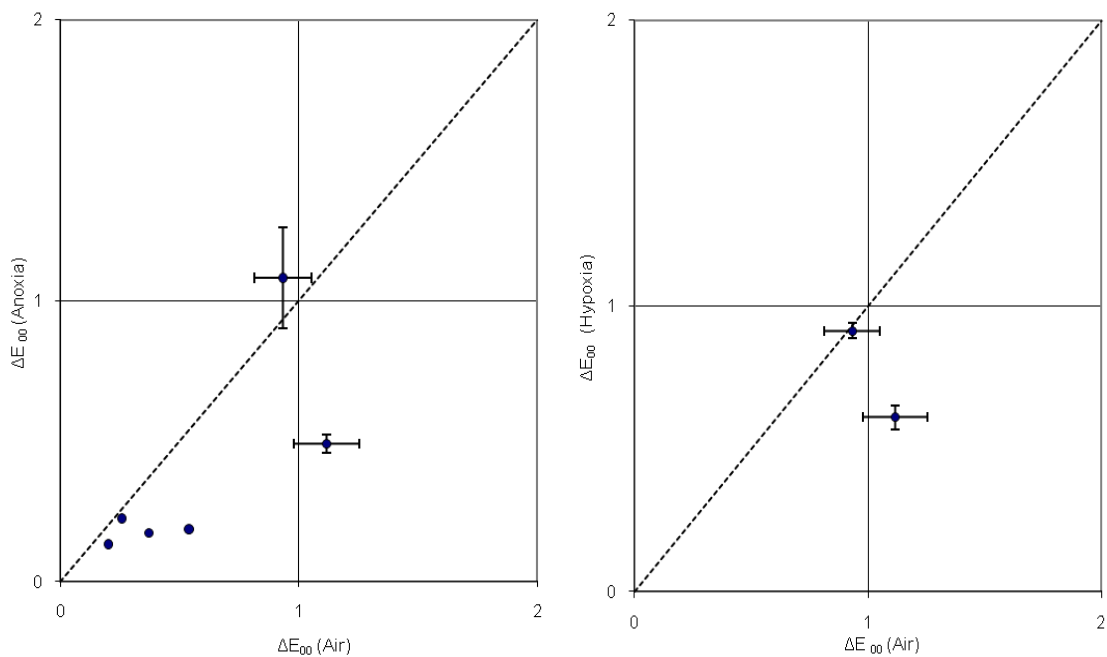


Figure 5.16. Gamboge: final colour difference in air and anoxia (left) and a comparison of final colour difference in air and hypoxia (right)

The graphs below illustrate the fading behaviour of the gamboge pigments that showed colour change greater than 1  $\Delta E_{00}$  in either air or anoxia. The graphs show the data both averaged with the standard deviation of the fades presented and also shown individually in separate plots.

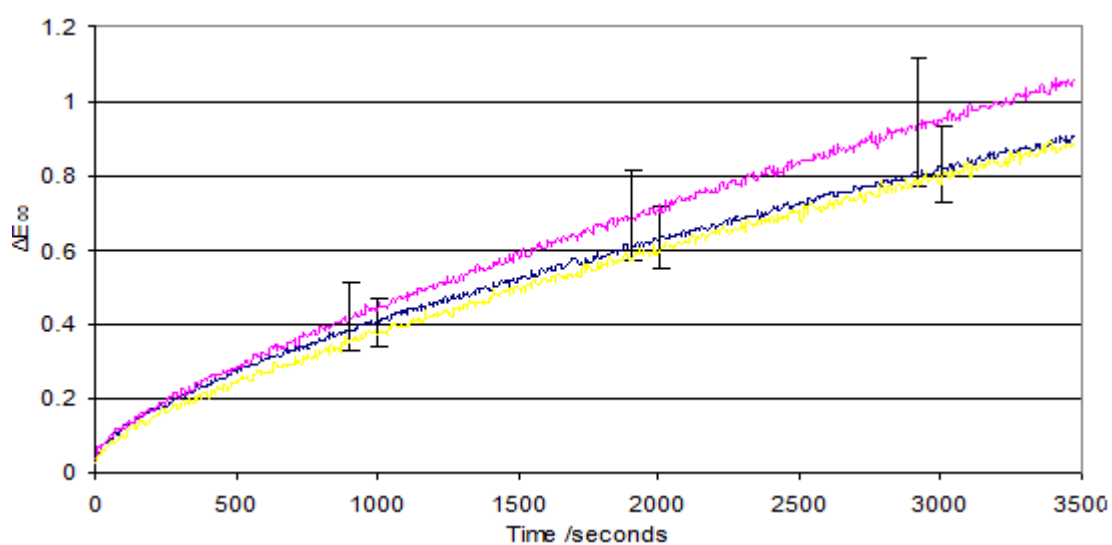


Figure 5.17. Fading behaviour of gamboge (code TRS7) pigment in different oxygen concentrations. The error bars represent  $\pm 1$  standard deviation of the results from fading the pigment in air and anoxia.

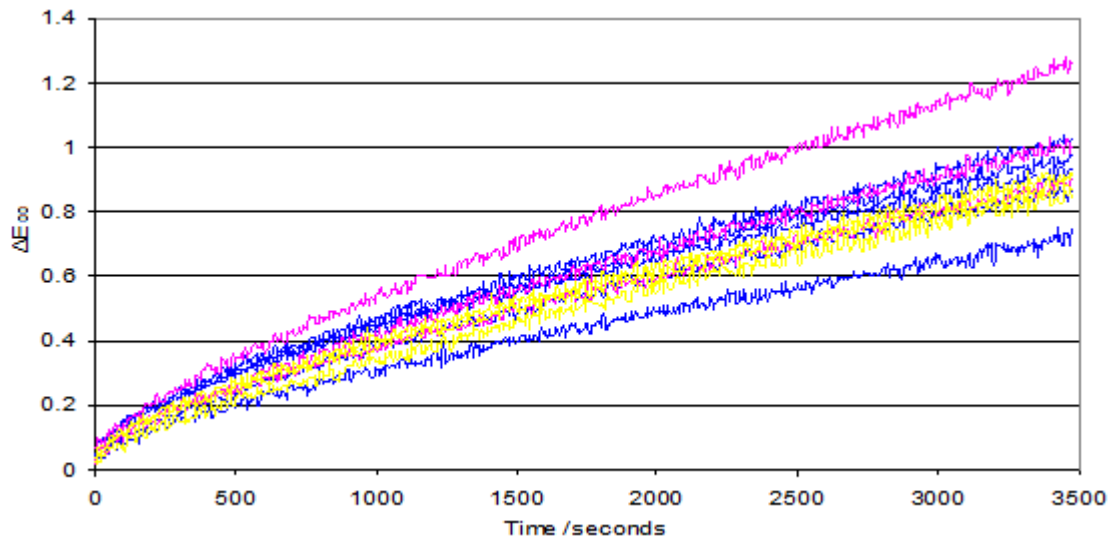


Figure 5.18. Individual fading curves of gamboge (code TRS7) pigment in different oxygen concentrations.

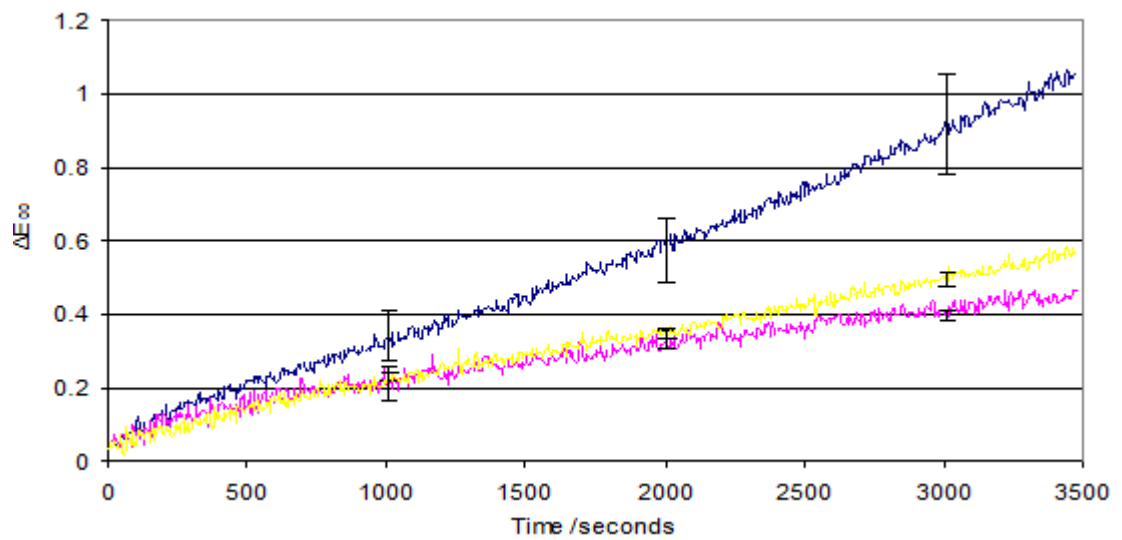


Figure 5.19. The colour difference measured over time for a gamboge (code MB A3) pigment in different oxygen concentrations.

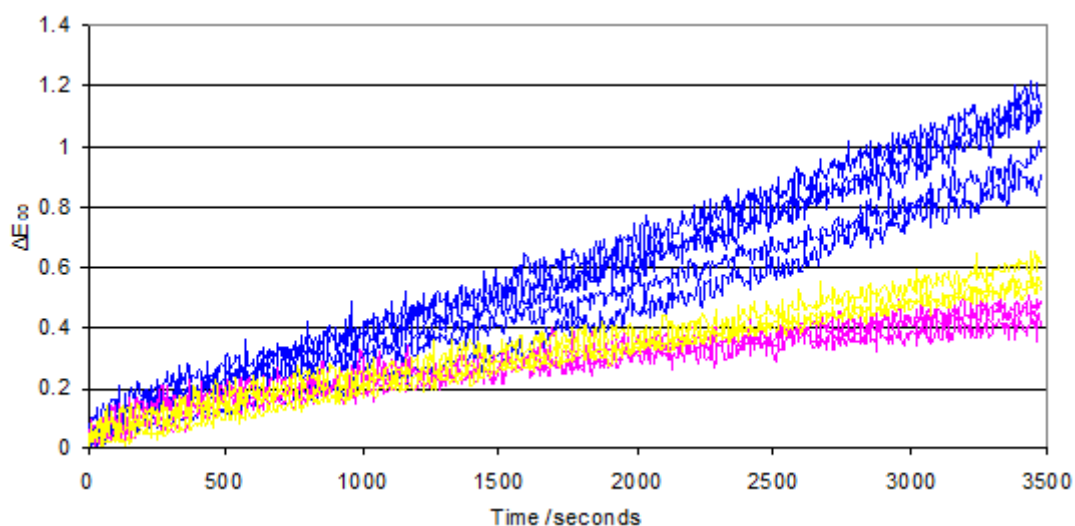


Figure 5.20. The individual colour differences created from fading measured over time for a gamboge (code MB A3) pigment in different oxygen concentrations.

## Lake pigments

Harrison (1957) describes a lake pigment as any coloured substance produced by the precipitation of an organic dyestuff onto a substrate, giving a pigment which is more or less translucent insoluble in the particular vehicle in which it is to be used and non-bleeding in water. The fugitive nature of red and yellow lake pigments has been investigated and reported on by Saunders and Kirby (1994b).

The lake pigments tested displayed a reduced degree of colour change in anoxia and this was also the case in hypoxia where a clear difference was observed. Results from the fading of this sample set can be seen in table 5.5.

NAME	CODE	Air		0%		5%		Substrate
		Average	St Dev	Average	St Dev	Average	St Dev	
Fine lake (red)	CA18	0.8		0.5				Al
Crimson lake	T RR2	0.9		0.9				Al/Sn
Green lake	T R5	0.9		0.8				Al
Brown/red lake	T R10	1.9	0.3	0.8	0.3	0.8	0.2	Al
Fustic lake (yellow)	NG7	2.6	0.3	1.0	0.3	1.6	0.1	Al

Table 5.5. A summary of the behaviour of lake pigments at the 3 oxygen concentrations.

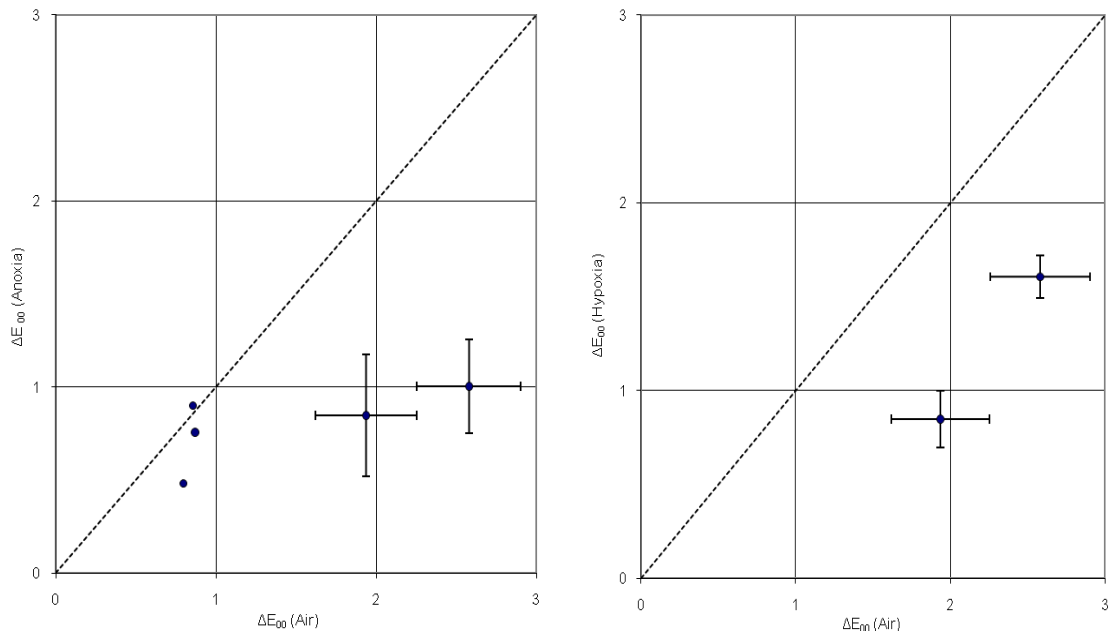


Figure 5.21. Lake pigments: a comparison of final colour difference in air and anoxia (left) and a comparison of final colour difference in air and hypoxia (right)

The following graphs illustrate the fading behaviour of the lake pigments that showed visible colour change, both averaged with the standard deviation of the fades presented and also shown individually in separate plots.

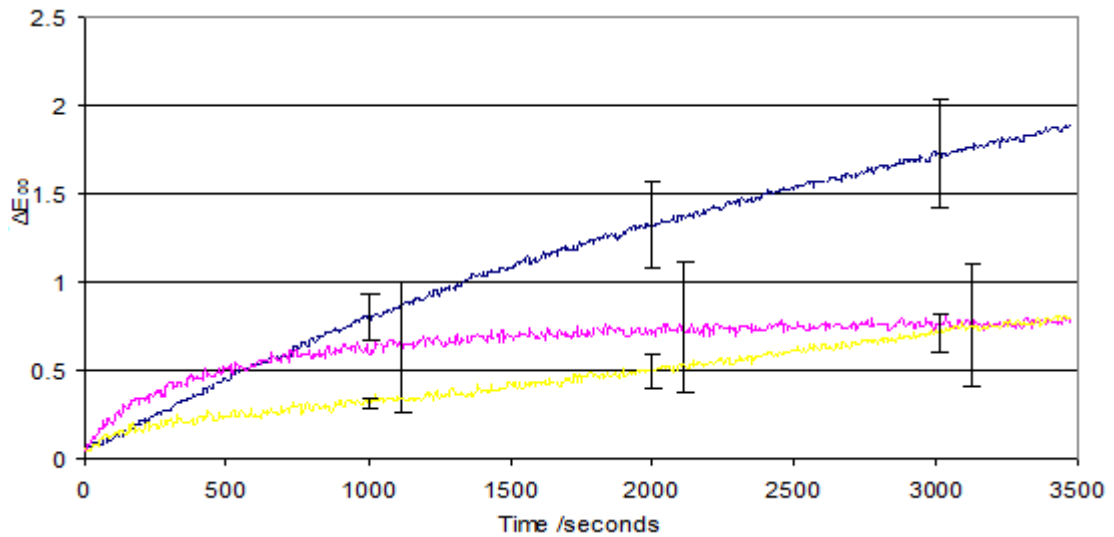


Figure 5.22. The fading curve for a brown/red lake (code T R10) pigment in the 3 different oxygen concentrations.

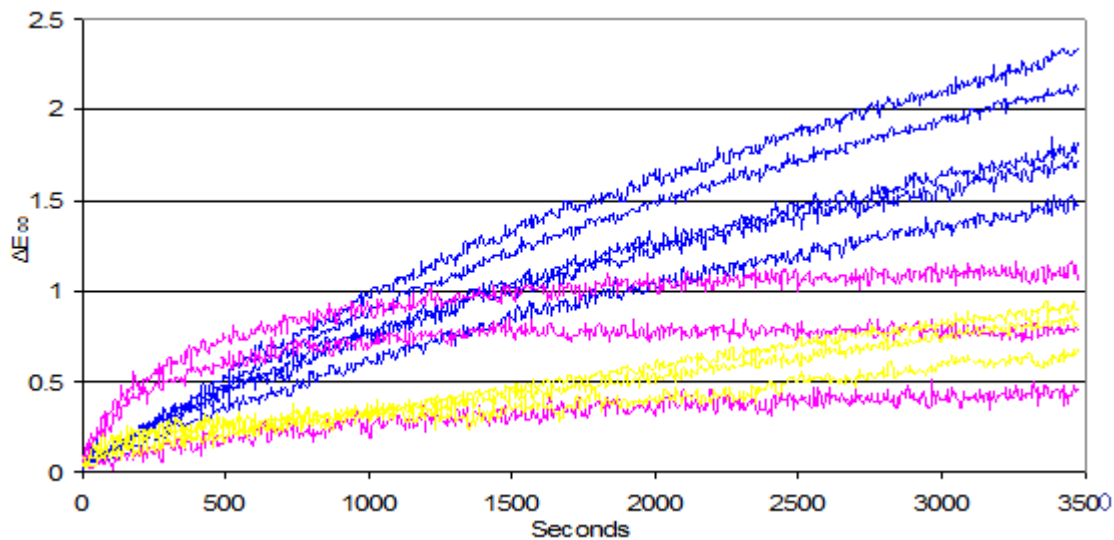


Figure 5.23. The individual fading curves for a brown/red lake (code T R10) pigment in the 3 different oxygen concentrations.

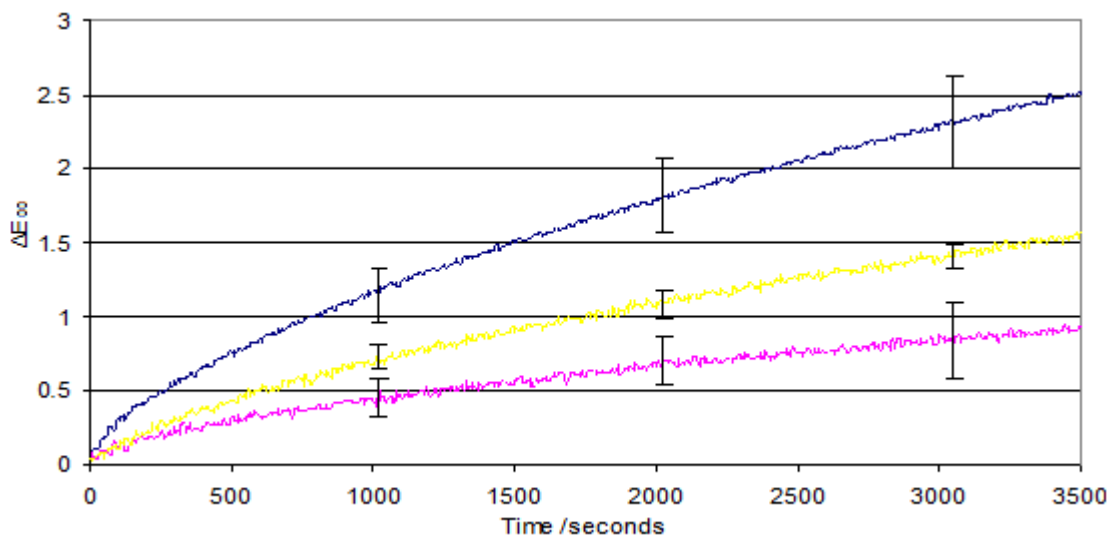


Figure 5.24. The fading curve for a yellow fustic lake (code NG7) pigment in the 3 different oxygen concentrations.

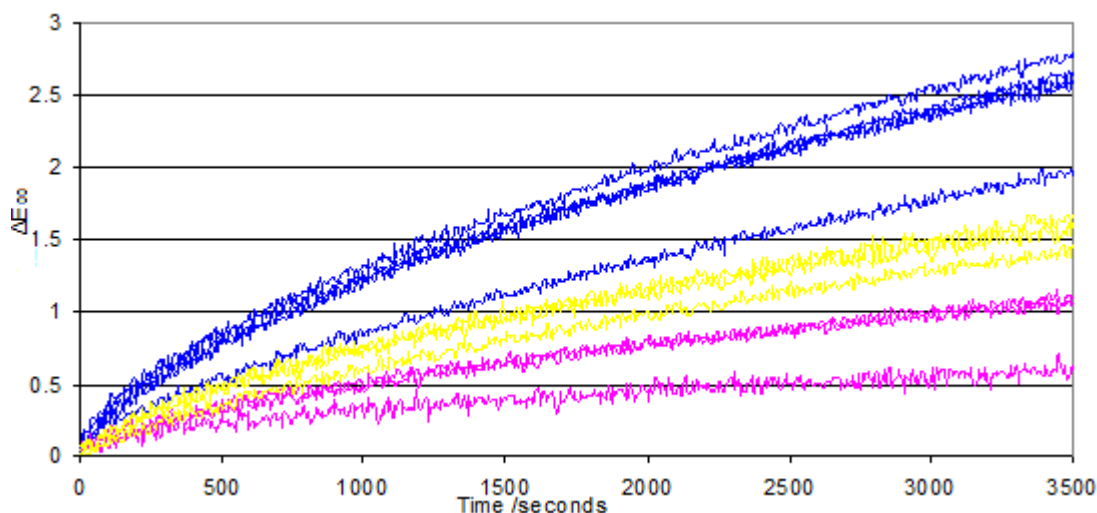


Figure 5.25. The individual fading curves for a yellow fustic lake (code NG7) pigment in the 3 different oxygen concentrations.

### Madder lakes

Madder is a dyestuff derived from the root of the *Rubiaceae* species (Chenciner 2000). They are regarded as having good lightfastness (Schweppe and Winter 1997) and experiment has found them to be amongst the more stable of the red lakes see Saunders and Kirby (1994a) (1994b). Results from the fading of this sample set can be seen in table 5.6.

In the case of the madders tested, they were largely light stable confirming previous reports. Madder TTB14 was found to be a rose madder and showed clear benefit in both anoxia and hypoxia contrary to what has been previously been reported by Beltran *et al.* (2008), Russell and Abney (1888) and Brommelle (1964).

Analysis indicated that Scarlet madder (code TTB1) was madder carmine. The substrate is shown in the final column.

NAME	CODE	Air		0%		5%		Substrate
		Average	St Dev	Average	St Dev	Average	St Dev	
Rose madder	RK9	0.3		0.1				Al
Brown madder	T TB 16	0.4		0.7				Sn
Brown madder	T TB5	0.5		1.0				Fe/Ca/Si
Madder	T TB4	0.5		0.3				Al/Cu
Madder	RK6	0.5		0.3				Al
Garance cerise	D&C 8/02	0.7		0.6				Al
Scarlet madder	T TB1	0.8		0.5				Al/Fe/Cu
Madder carmine	T PC6	0.8		0.5				Al
Madder	T TB14	2.4	0.2	0.5	0.2	1.2	0.2	Al
Madder	T TB2	0.5		0.1				Al

Table 5.6. A summary of the behaviour of the madder lakes at the 3 oxygen concentrations.

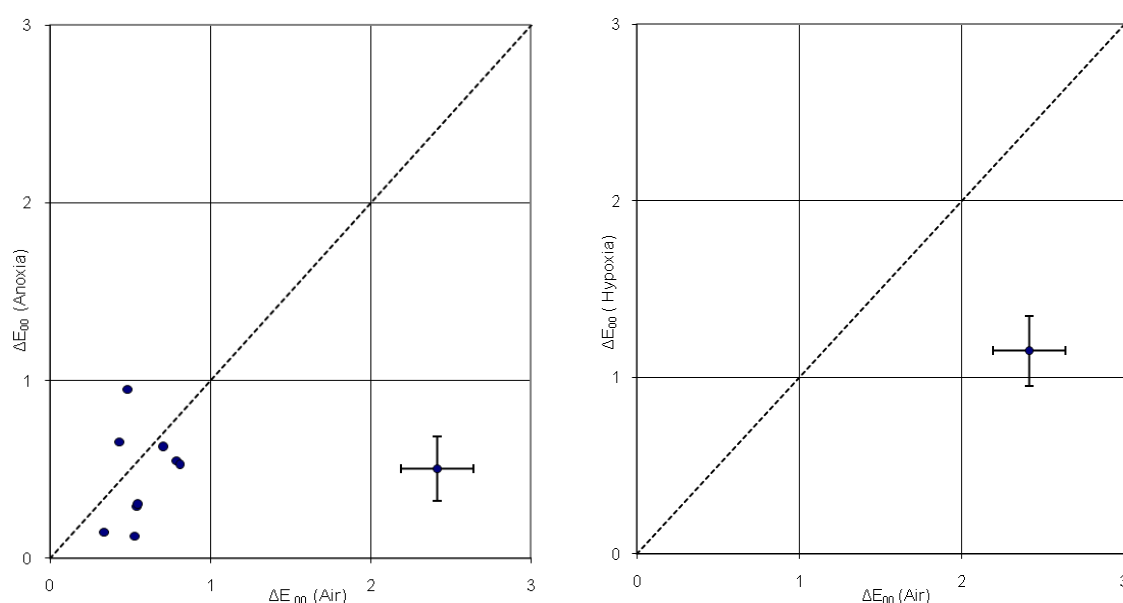


Figure 5.26. Madder lakes: a comparison of final colour difference in air and anoxia (left) and a comparison of final colour difference in air and hypoxia (right)

The graphs below show the fading behaviour of the madder lakes with colour change greater than a colour difference unit, both averaged with the standard deviation of the fades presented and also shown individually in separate plots.

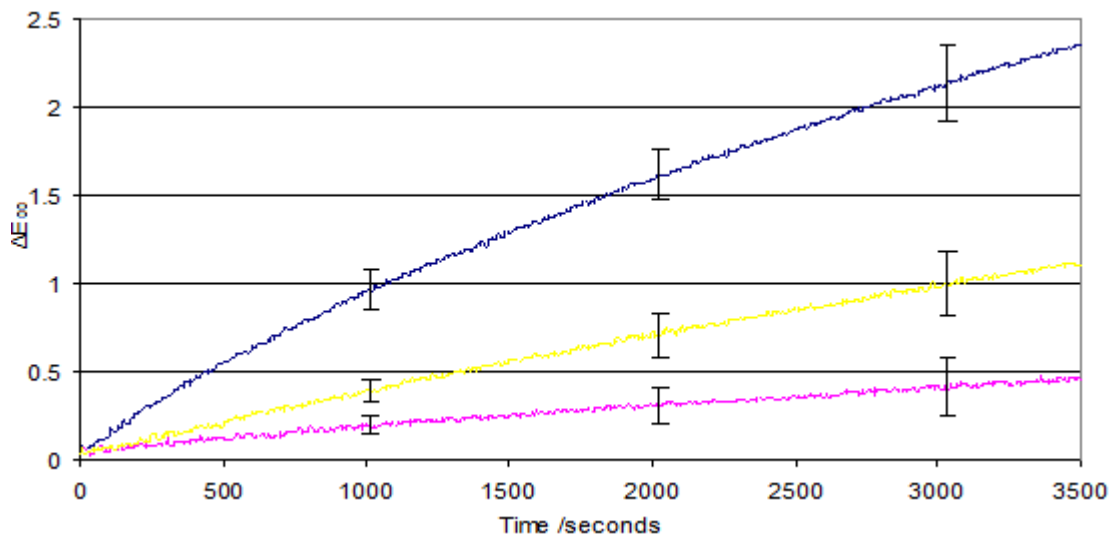


Figure 5.27. The colour difference measured over time for madder (code T TB14) pigment in the 3 different oxygen concentrations.

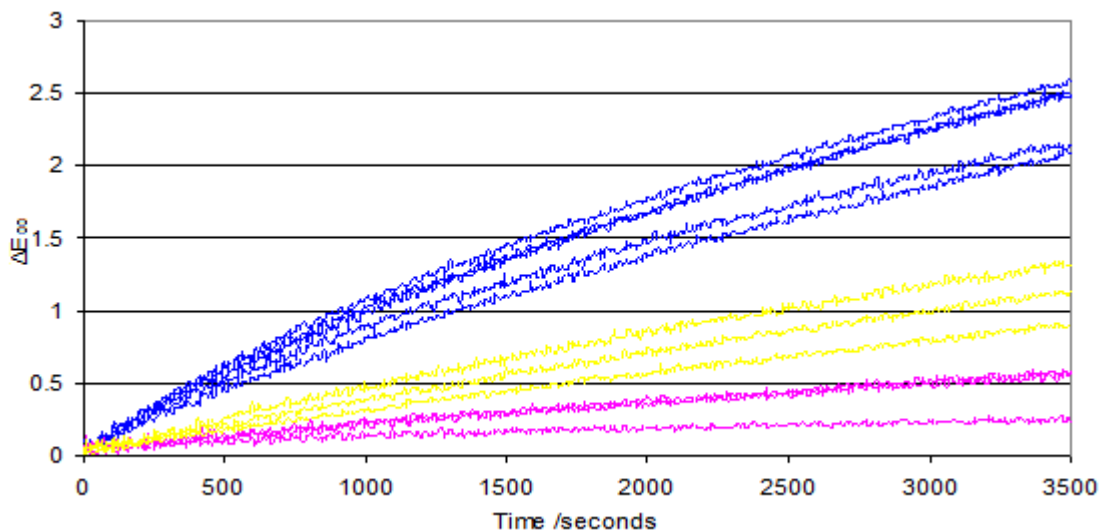


Figure 5.28. The individual colour differences measured over time for Madder (code T TB14) pigment in the 3 different oxygen concentrations.

## Orpiment

Orpiment is a yellow arsenic sulfide ( $\text{As}_2\text{S}_3$ ) (Eastaugh *et al.* 2004). Reports of the lightfastness of orpiment describe it as fading easily (Weber 1923), or to some degree after light exposure showing a yellow orange alteration. (Fitzhugh 1997). Results from the fading of this sample set can be seen in table 5.7.

Although fugitive, no clear relationship was observed between the degree of fading and oxygen concentration, leading to the conclusion that the degradation pathway is likely to be independent of oxygen concentration.

NAME	CODE	Air		0%		5%	
		Average	St Dev	Average	St Dev	Average	St Dev
Orpiment red	CA20	2.1	1	1.6	0.7	1.3	0.5
Kings yellow	NG WC13	2.2	0.8	2.6	0.4	2.7	0.5
Orpiment (yellow)	CA13	4.8	1.2	5.5	0.3	4.9	0.4

Table 5.7. A summary of the behaviour of orpiment at the 3 oxygen concentrations.

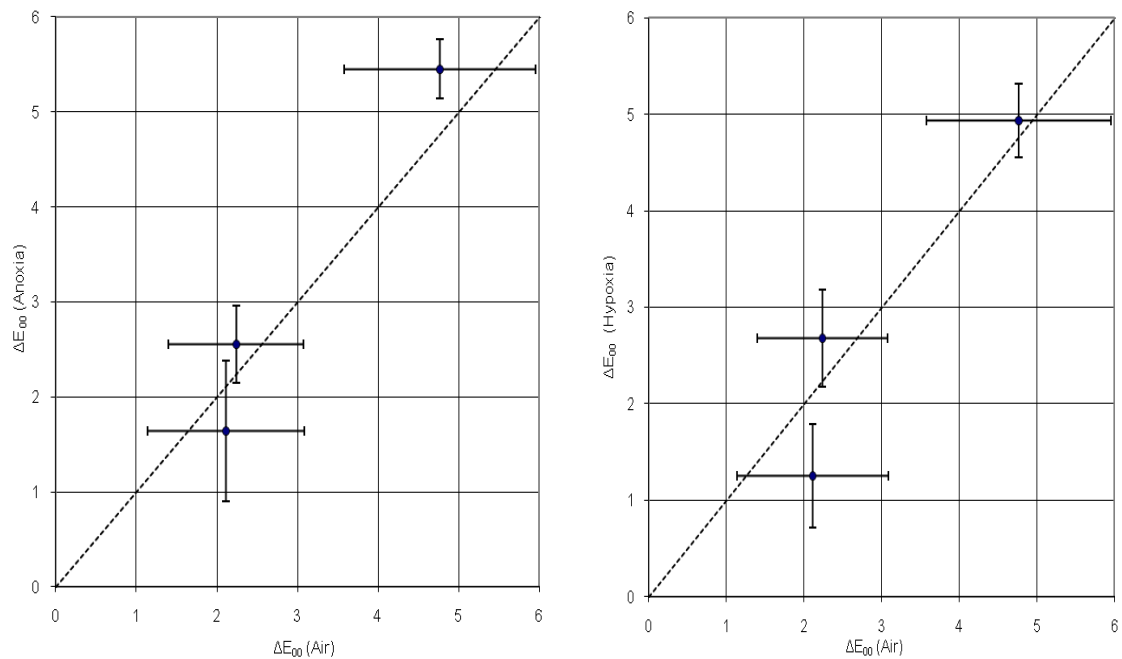


Figure 5.29. Orpiment: a comparison of final colour difference in air and anoxia (left) and a comparison of final colour difference in air and hypoxia (right)

The graphs following show the fading behaviour of orpiment that showed colour change above 1 colour difference unit, both averaged with the standard deviation of the fades presented and also shown individually in separate plots.

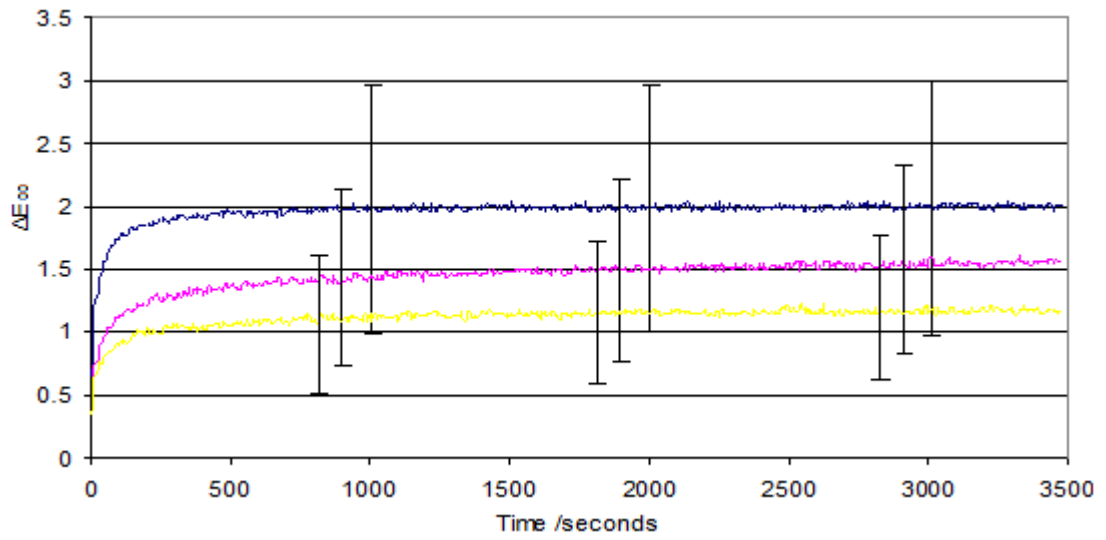


Figure 5.30. The colour difference measured over time for orpiment red (code CA20) pigment in the 3 different oxygen concentrations.

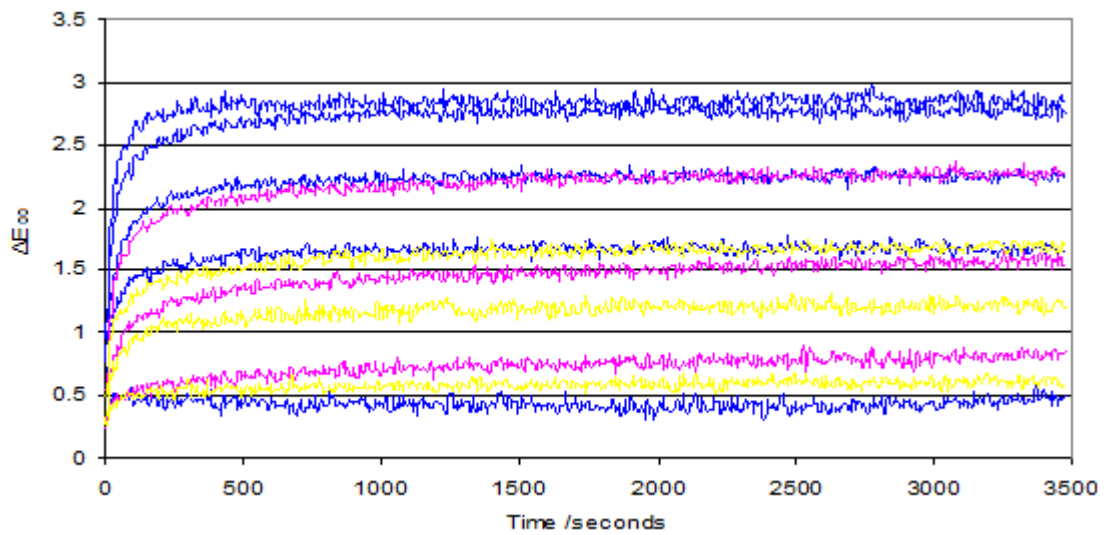


Figure 5.31. The individual colour differences measured over time for orpiment red (code CA20) pigment in the 3 different oxygen concentrations.

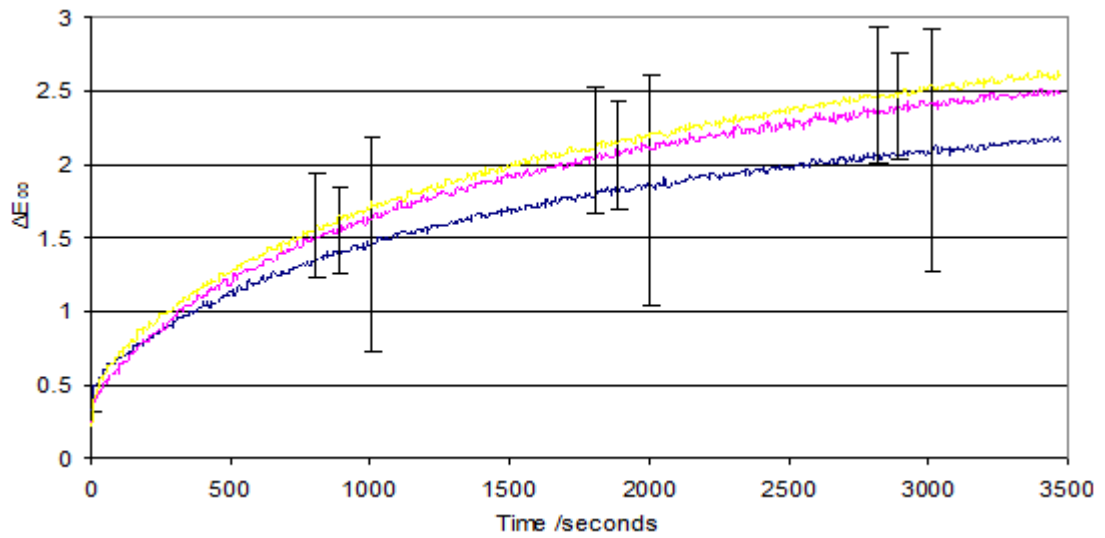


Figure 5.32. The colour difference measured over time for kings yellow (code NG WC13) pigment in the 3 different oxygen concentrations.

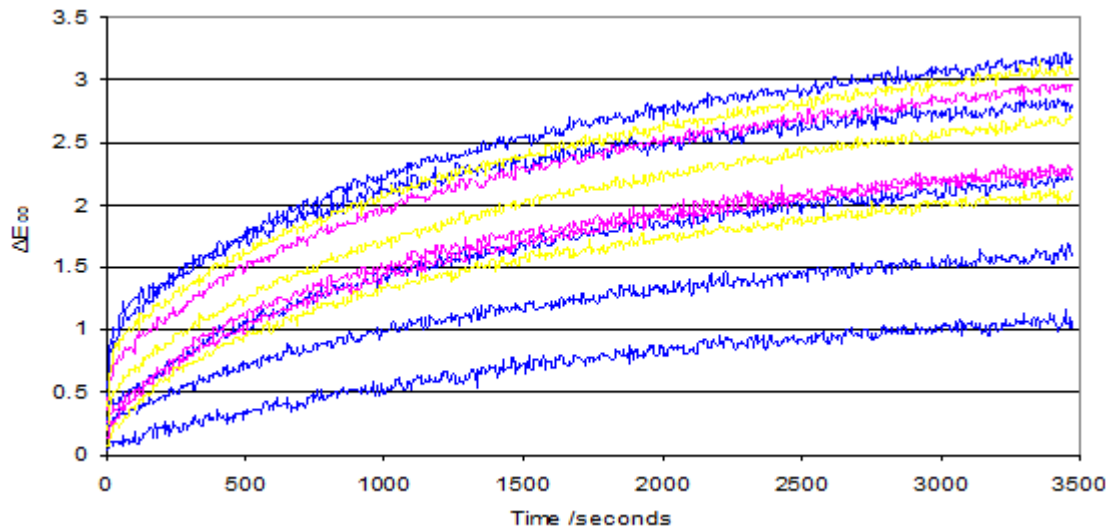


Figure 5.33 The individual colour difference measured over time for kings yellow (code NG WC13) pigment in the 3 different oxygen concentrations.

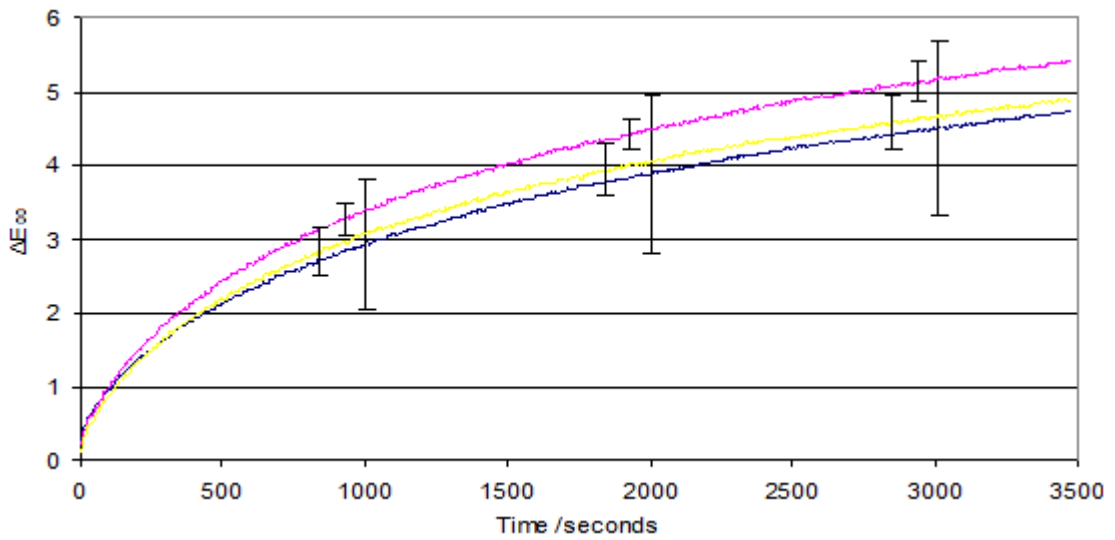


Figure 5.34. The colour differences measured over time for orpiment yellow (code CA13) pigment in the 3 different oxygen concentrations.

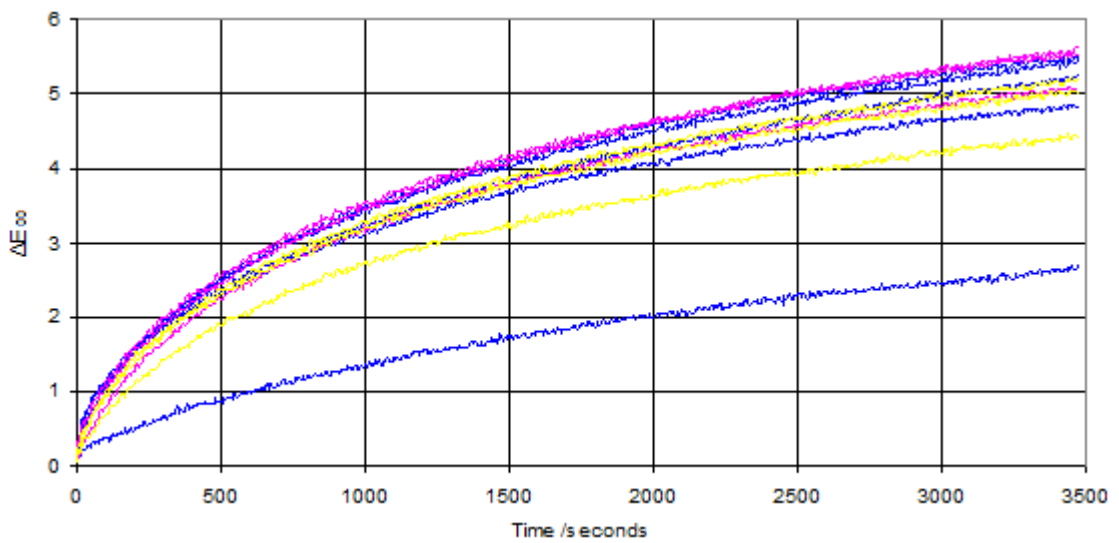


Figure 5.35. The individual colour differences measured over time for orpiment yellow (code CA13) pigment in the 3 different oxygen concentrations.

### Prussian green

Prussian green can be created via 2 methods; either by stopping the manufacturing process of Prussian blue at the stage when the sediment is green before adding hydrochloric acid to turn the pigment blue, or by combining Prussian blue with a yellow pigment such as yellow

ochre or gamboge (Eastaugh *et al.* 2004). The latter process of combination was extremely dominant and the former can be regarded as insignificant (Harley 2001). All the examples studied here included Prussian blue and nearly all also had a yellow pigment present. Results from the fading of this sample set can be seen in table 5.8.

The behaviour of the pigment mirrored that reported for Prussian blue. Prussian green was a largely fugitive pigment and faded to a colour change that was greater in anoxia than air. The significance of the difference was reduced in 5% oxygen.

Analysis of green lake showed it to be Prussian green containing Prussian blue.

NAME	CODE	Air		0%		5%	
		Average	St Dev	Average	St Dev	Average	St Dev
Green lake	T CA 7	2.8	1.2	4.9	0.8	3.8	0.2
Prussian green	MB BA2	0.4		0.4			
Prussian green	MB A2	1.6	0.2	2.8	0.6	2.2	0.2
Prussian green	CA1	2.2	0.4	3.7	0.8	2.4	0.2

Table 5.8. A summary of the behaviour of Prussian greens at the 3 oxygen concentrations.

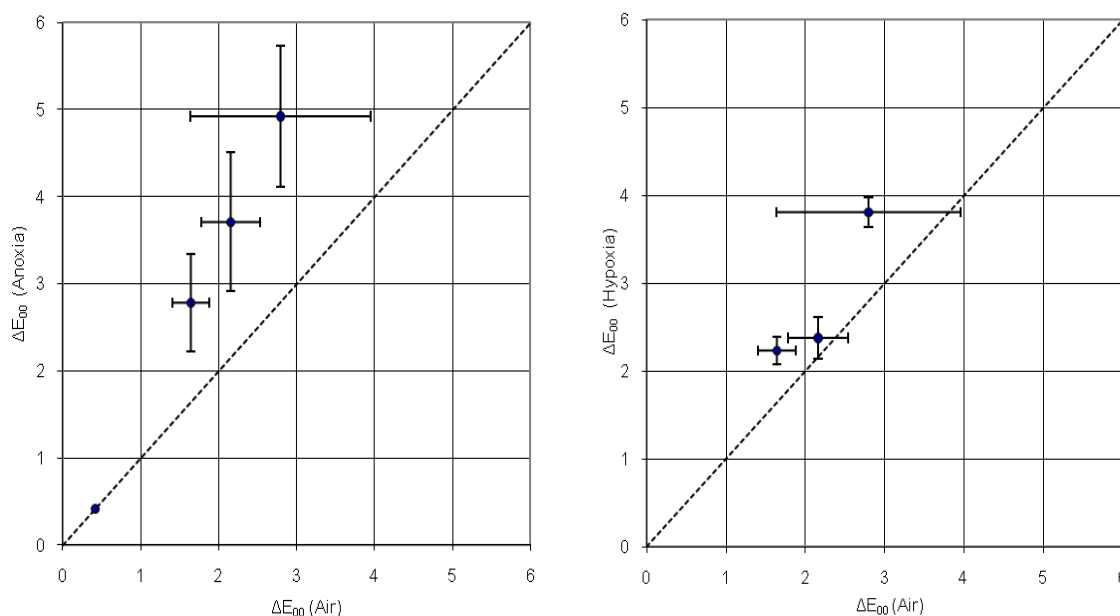


Figure 5.36. Prussian greens: a comparison of final colour difference in air and anoxia (left) and a comparison of final colour difference in air and hypoxia (right)

The graphs following display results for Prussian green that showed visible colour change, both averaged with the standard deviation of the fades presented and also shown individually in separate plots.

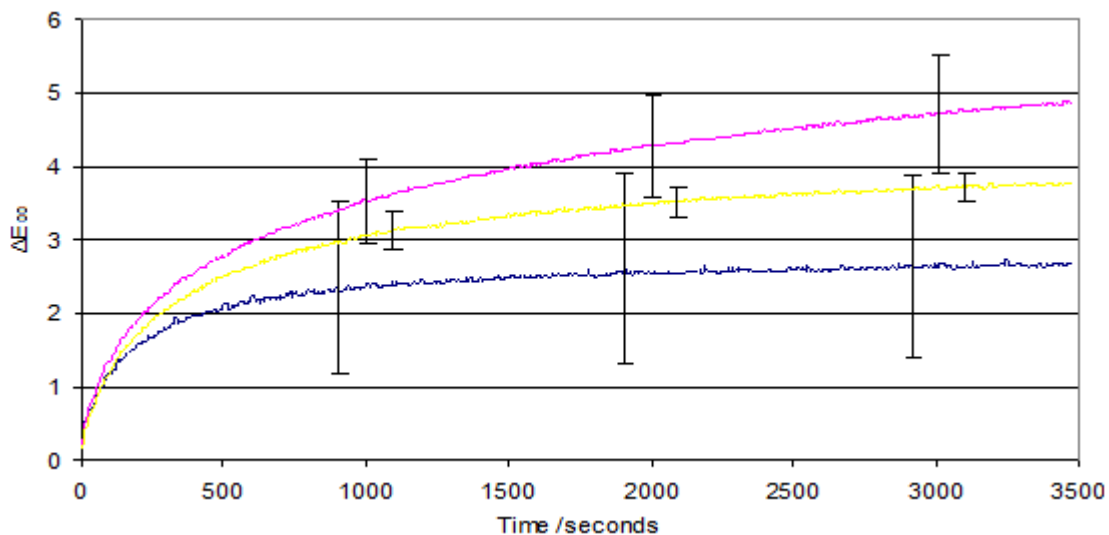


Figure 5.37. The colour difference measured over time for green lake (code CA7) pigment in the 3 different oxygen concentrations.

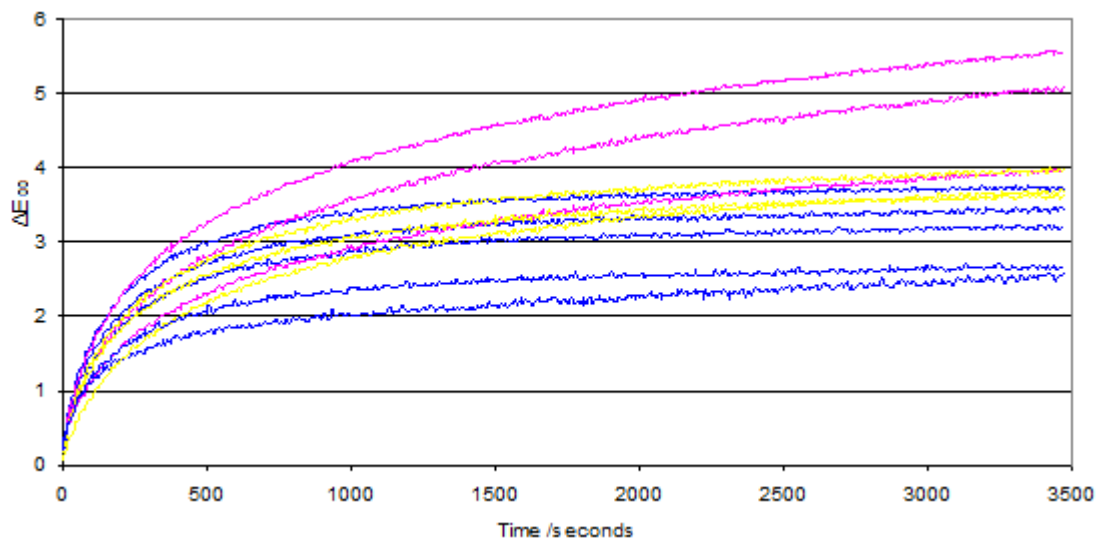


Figure 5.38. The individual colour differences measured over time for green lake (code CA7) pigment in the 3 different oxygen concentrations.

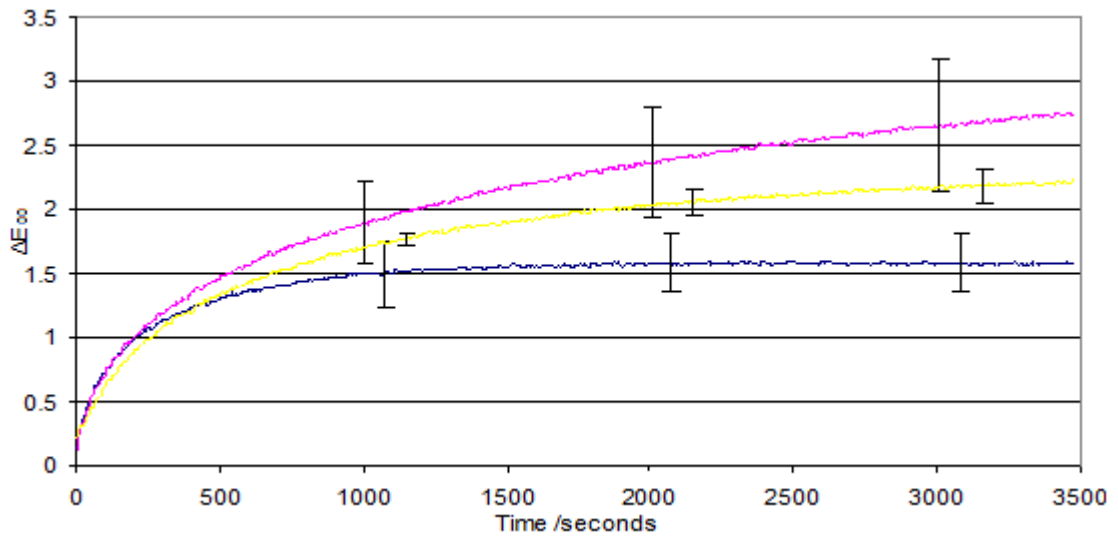


Figure 5.39. The colour difference measured over time for Prussian green (code MB A2) pigment in the 3 different oxygen concentrations.

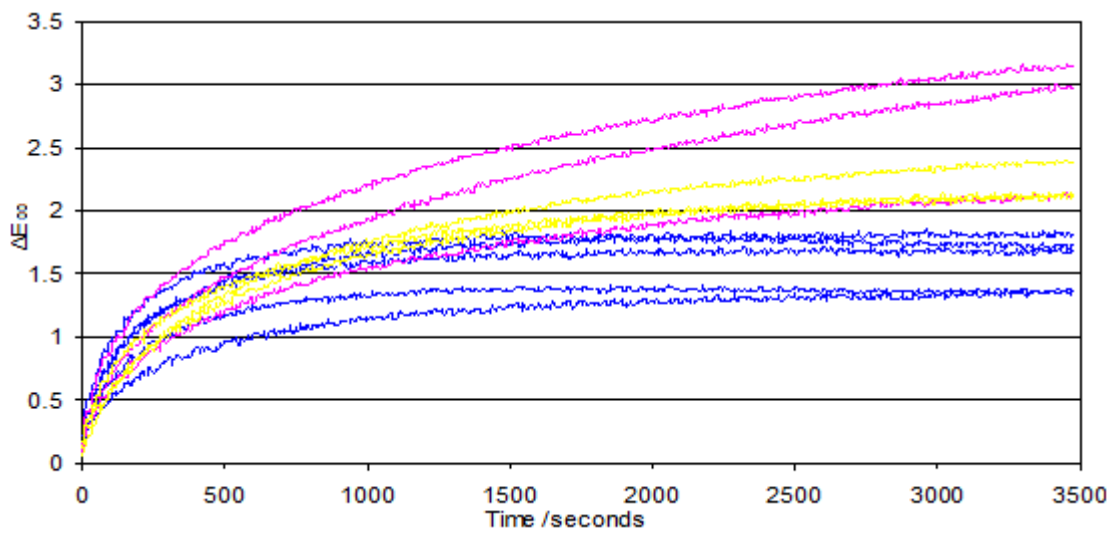


Figure 5.40. The individual colour differences measured over time for Prussian green (code MB A2) pigment in the 3 different oxygen concentrations.

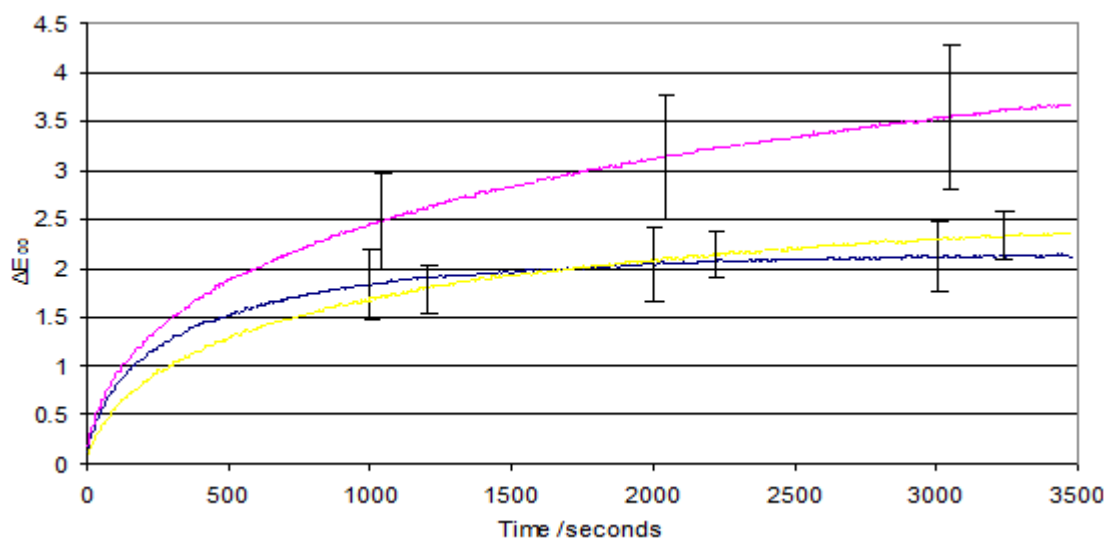


Figure 5.41. The colour difference measured over time for Prussian green (code CA1) pigment in the 3 different oxygen concentrations.

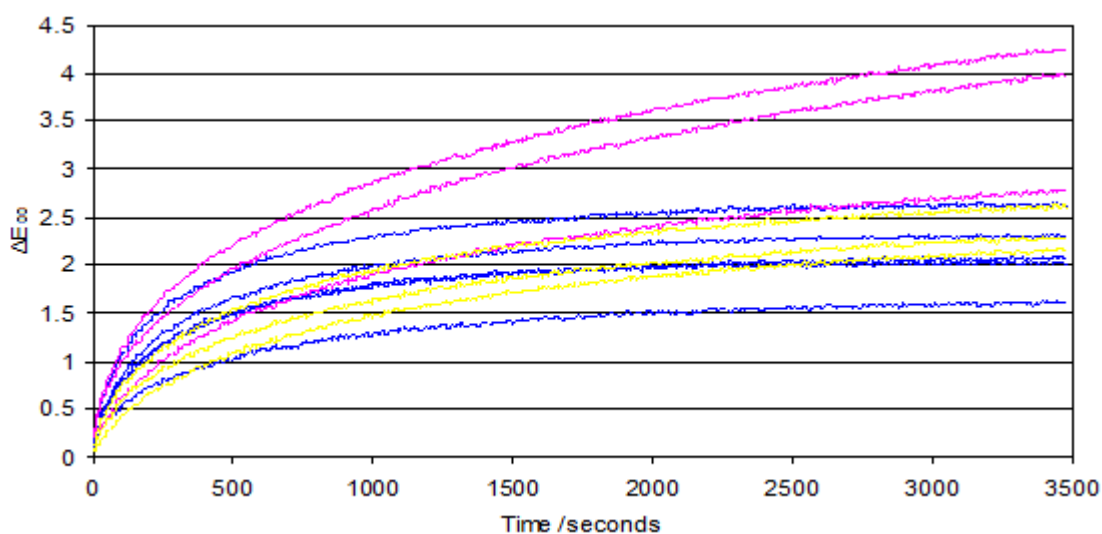


Figure 5.42. The individual colour differences measured over time for Prussian green (code CA1) pigment in the 3 different oxygen concentrations.

### Sap green

Sap green is a green flavonoid dye derived from the ripe berries of the *Rhamnus* and *Frangula* species. The colour derived from chlorophyll (Mills and White 1994). Historically

sap green has been reported to be a problematic fugitive pigment (Harley 2001). Results from the fading of this sample set can be seen in table 5.9.

The sap green pigments were largely fugitive. Any differences between the environments over this degree of fading are not clear within the variation in results observed.

NAME	CODE	Air		0%		5%	
		Average	St Dev	Average	St Dev	Average	St Dev
Sap green	OH1	2.8	0.5	3.0	0.4	2.8	0.1
Sap green	RK4	1.4	0.3	1.7	0.4	1.4	0.2
Sap green	RK5	2.9	0.4	3.6	0.5	3.0	0.1
Sap green lake	NG11	0.7		0.8			

Table 5.9. A summary of the behaviour of sap green at the 3 oxygen concentrations.

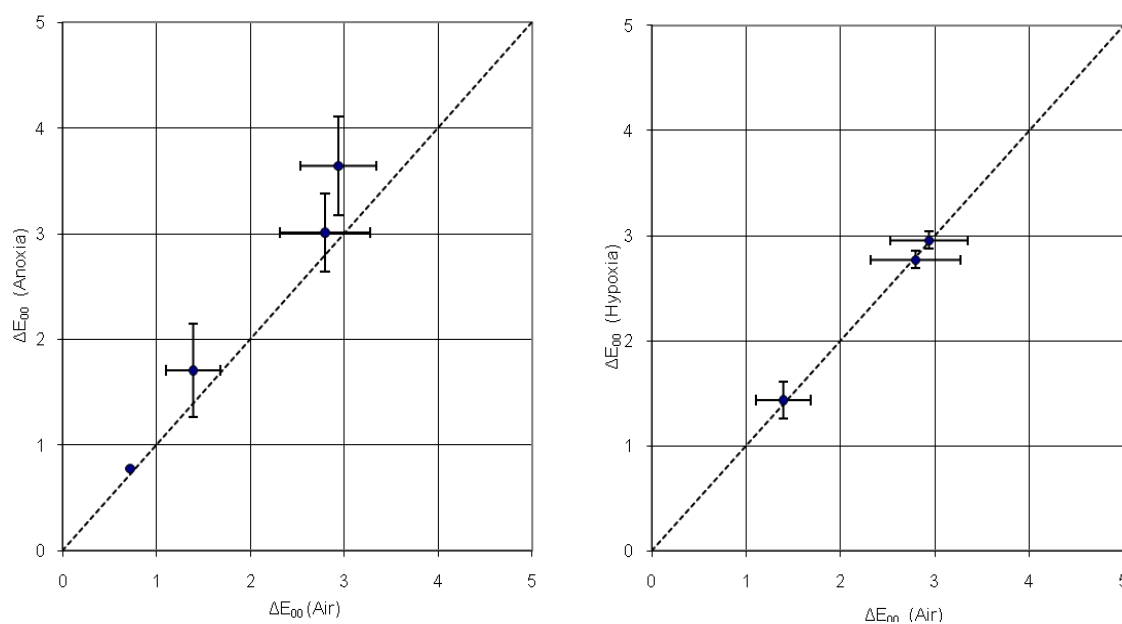


Figure 5.43. Sap green: colour difference after an hour fade in air and anoxia (left) and a comparison of final colour difference in air and hypoxia (right)

The graphs following show the fading behaviour of sap greens that showed visible colour change, both averaged with the standard deviation of the fades presented and also shown individually in separate plots.

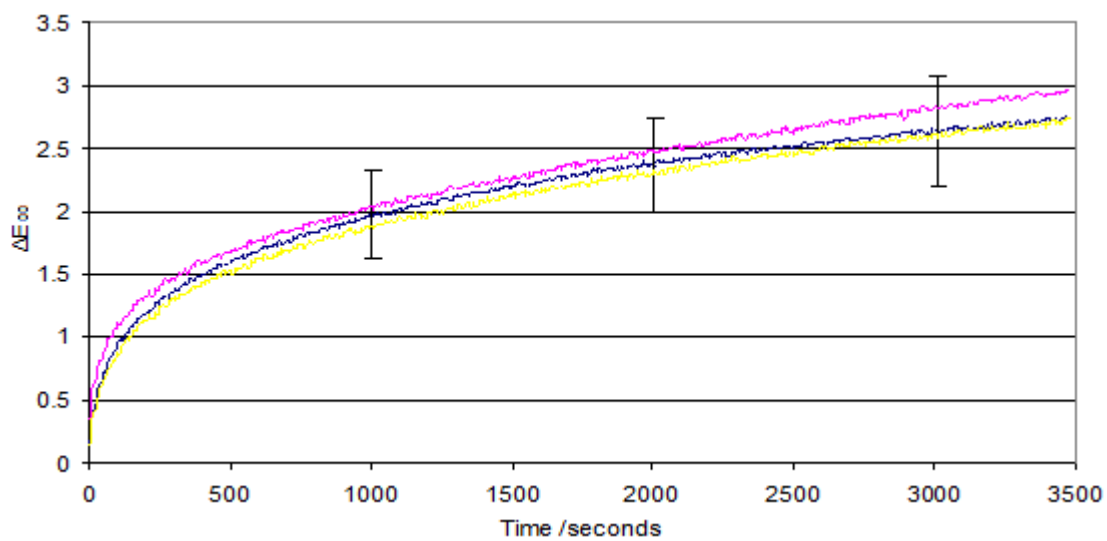


Figure 5.44. The colour difference measured over time for a sap green (code OH1) pigment in different oxygen concentrations. The error bars represent  $\pm 1$  standard deviation of the 5 results from fading the pigment in air.

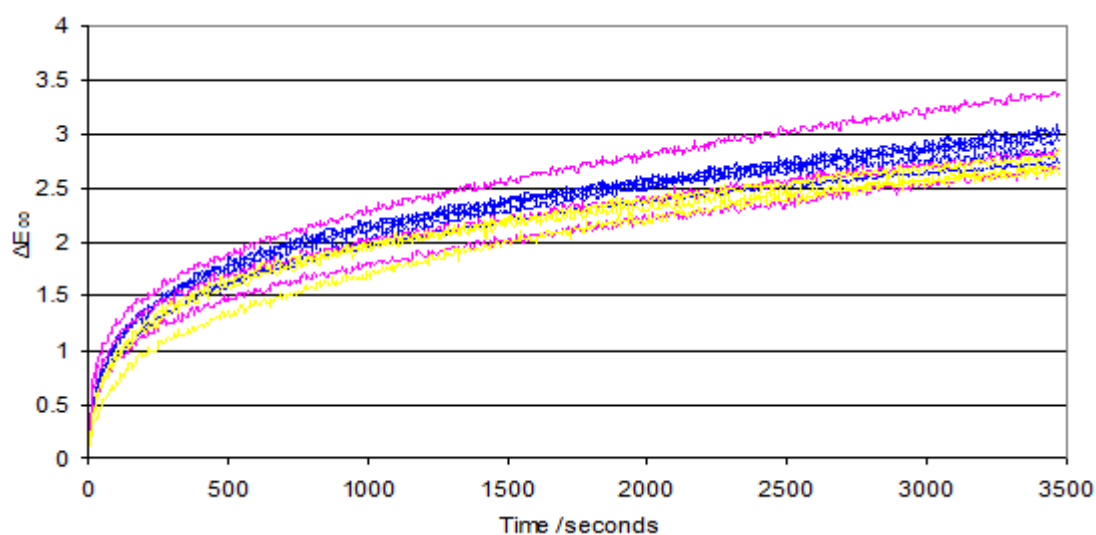


Figure 5.45. The individual colour differences measured over time for a sap green (code OH1) pigment in different oxygen concentrations.

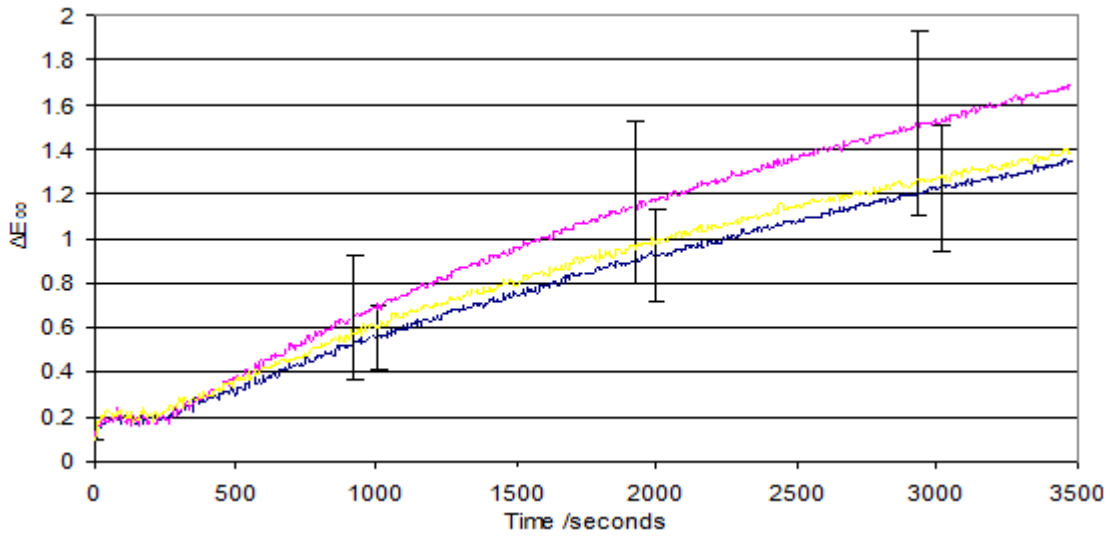


Figure 5.46. The colour difference measured over time for a sap green (code RK4) pigment in different oxygen concentrations. The error bars represent  $\pm 1$  standard deviation of the results from fading the pigment in air and anoxia.

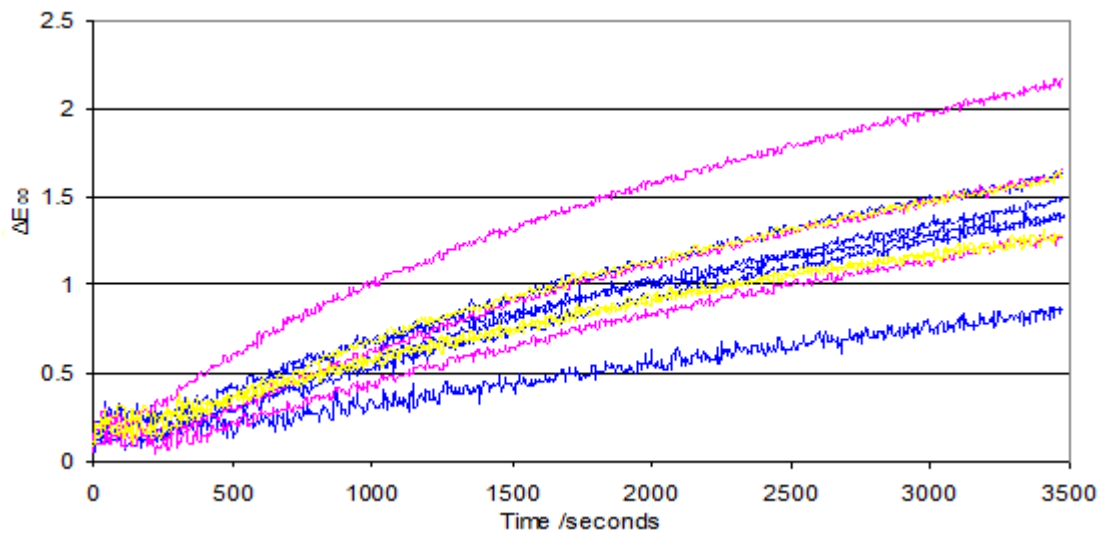


Figure 5.47. The individual colour differences measured over time for sap green (code RK4) pigment in different oxygen concentrations.

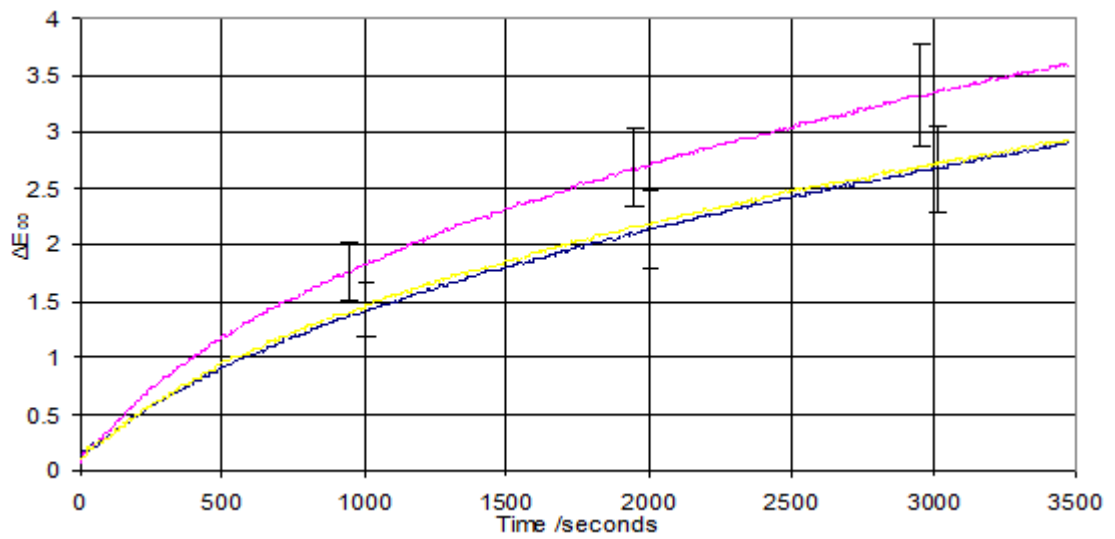


Figure 5.48. The colour difference measured over time for a sap green (code RK5) pigment in different oxygen concentrations. The error bars represent  $\pm 1$  standard deviation of the results from fading the pigment in air and anoxia.

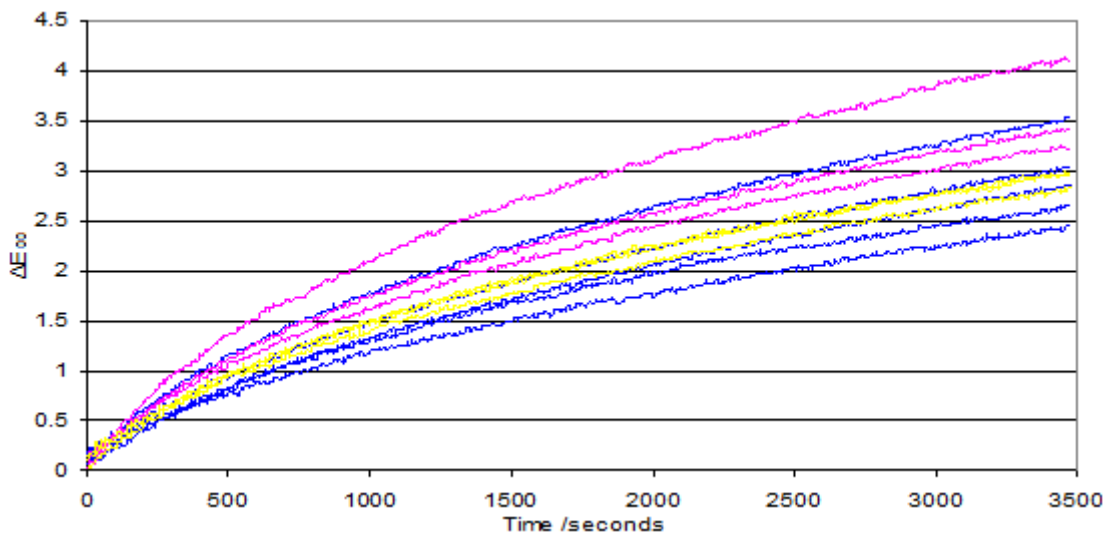


Figure 5.49. The individual colour differences measured over time for a sap green (code RK5) pigment in different oxygen concentrations.

## Vermillion

The mineral cinnabar (mercury (II) sulphide) or vermilion pigment when processed has been widely reported to change colour to black (Eastaugh *et al.* 2004) and is not presently considered to be a permanent pigment (Schaeffer 2001) despite examples of stability (Gettens *et al.* 1993). Results from the fading of this sample set can be seen in table 5.10.

The large numbers of vermilion pigments were overall rated highly fugitive. Studies cited in the introductory section also reported significant colour change: these findings imply that the fading of vermilion may be greater than expected at high irradiance, a point worthy of further study. Fading of pigment was independent of oxygen level as no greater degrees of fading were observed (as was the case in previous reports).

Vermillion (code T RR4) faded to a greater degree in anoxia (although no result was clear within the variation observed), however this difference was removed in 5% oxygen and overall no difference between 5% oxygen and air was observed.

Analysis indicated red (code T R11) was a vermilion and zinc white mixture.

NAME	CODE	Air		0%		5%	
		Average	St Dev	Average	St Dev	Average	St Dev
C. vermilion	NG WC11	1.5	0.4	2.2	0.2	1.9	0.2
Red	T R11	2.0	0.1	2.2	0.2	1.9	0.1
Vermilion	T2	2.2	0.1	2.4	0.1	2.1	0.4
Vermillion	CA22	2.3	0.1	2.6	0.2	2.2	0.2
Vermillion	MB A7	3.2	0.2	3.7	0.1	3.5	0.3
Vermillion 4	RC ICN8	5.0	0.6	4.9	0.5	4.8	0.1
Vermilion	T RR4	5.1	0.4	6.2	0.7	4.9	0.2

Table 5.10. A summary of the behaviour of vermilion at the 3 oxygen concentrations.

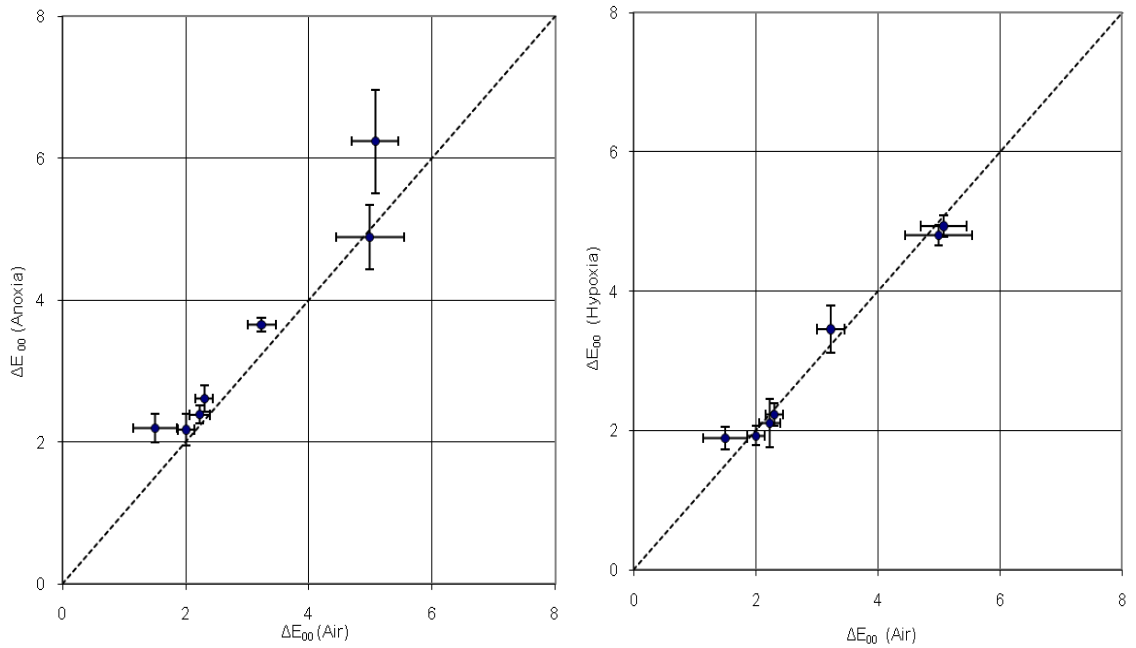


Figure 5.50. Vermilion: the final colour difference in air and anoxia (left) and a comparison of final colour difference in air and hypoxia (right)

The graphs below show the fading behaviour of vermilions that showed visible colour change, both averaged with the standard deviation of the fades presented and also shown individually in separate plots.

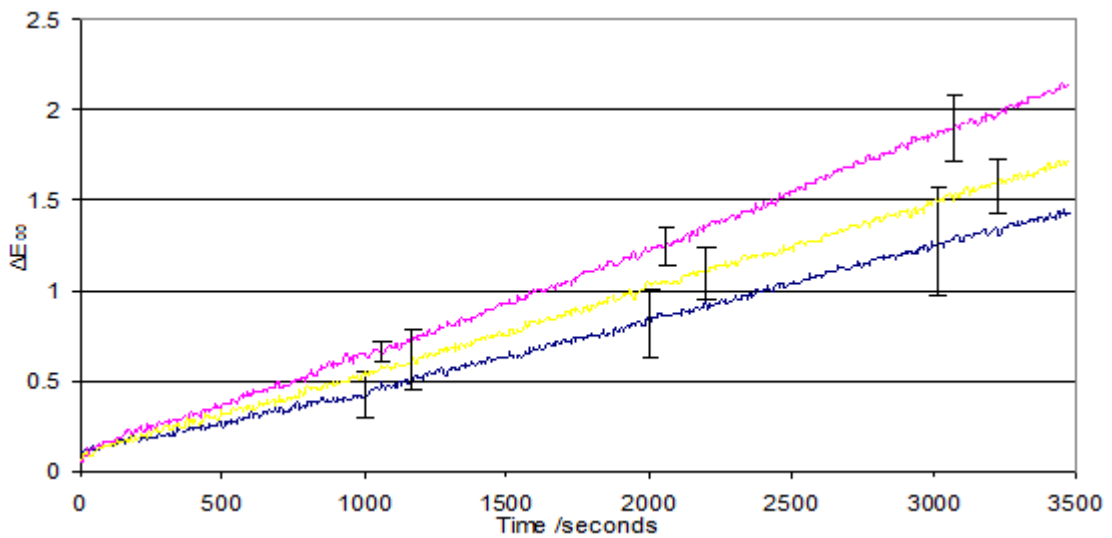


Figure 5.51. The colour difference measured over time for *C. vermilion* (code NG WC11) pigment in the 3 different oxygen concentrations.

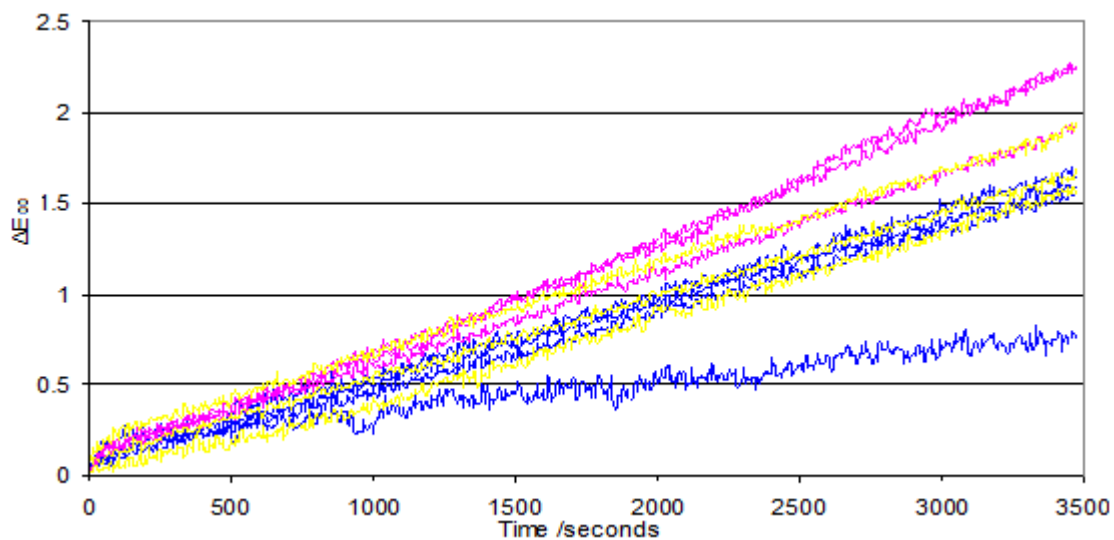


Figure 5.52. The individual colour differences measured over time for *C. vermillon* (code NG WC11) pigment in the 3 different oxygen concentrations.

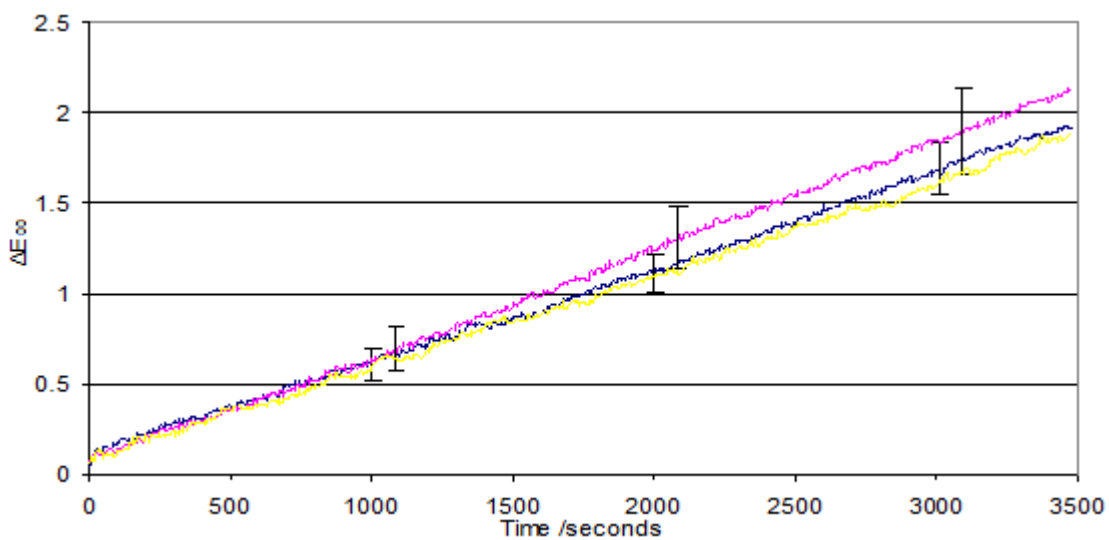


Figure 5.53. The colour difference measured over time for a red (code TR11) pigment in the 3 different oxygen concentrations. The error bars represent  $\pm 1$  standard deviation of the results from fading the pigment in air and anoxia.

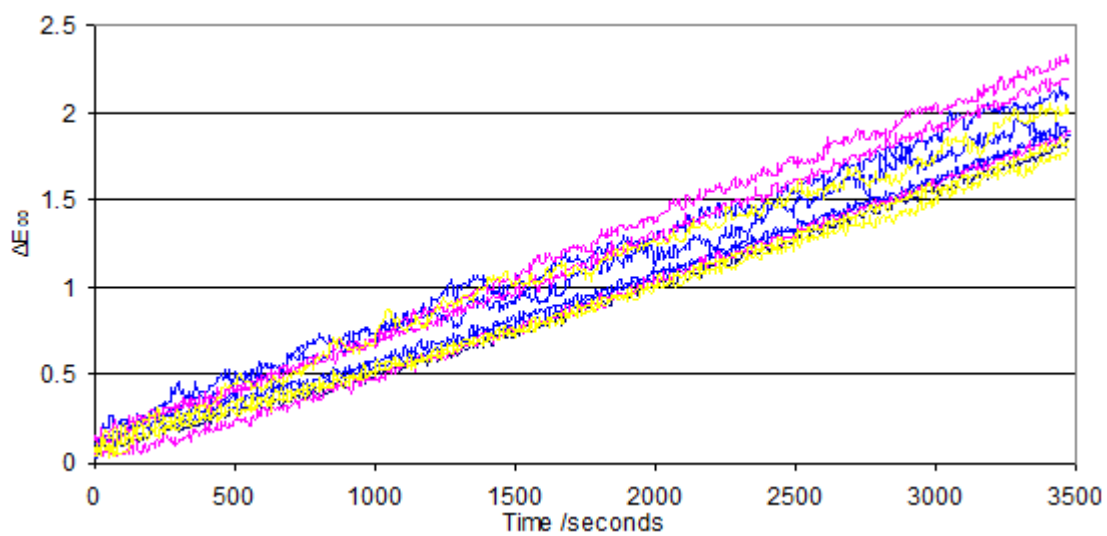


Figure 5.54. The individual colour difference measured over time for a red (code TR11) pigment in the 3 different oxygen concentrations

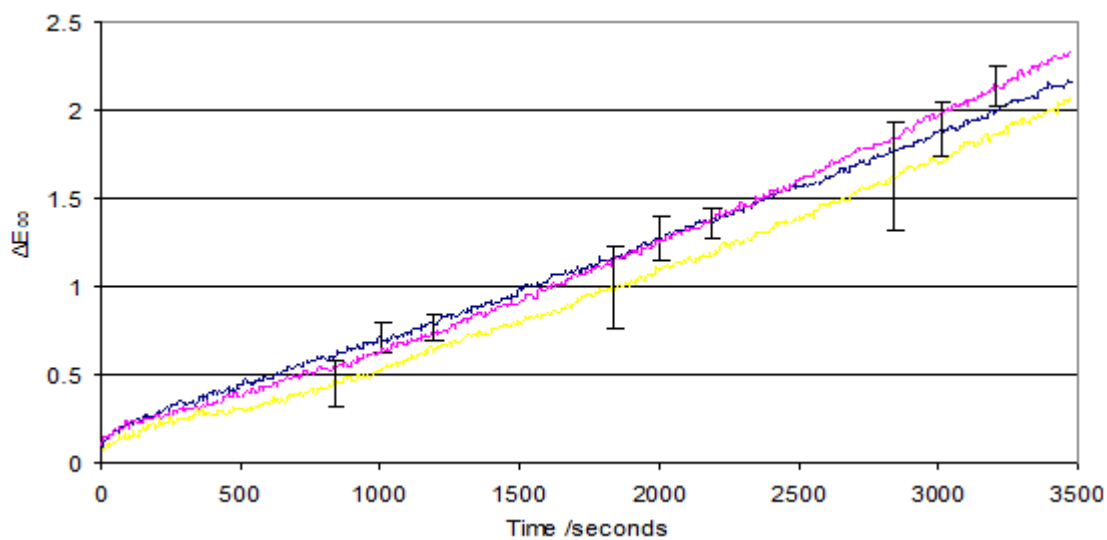


Figure 5.55. The colour difference measured over time for a vermilion (code 2T) pigment in the 3 different oxygen concentrations.

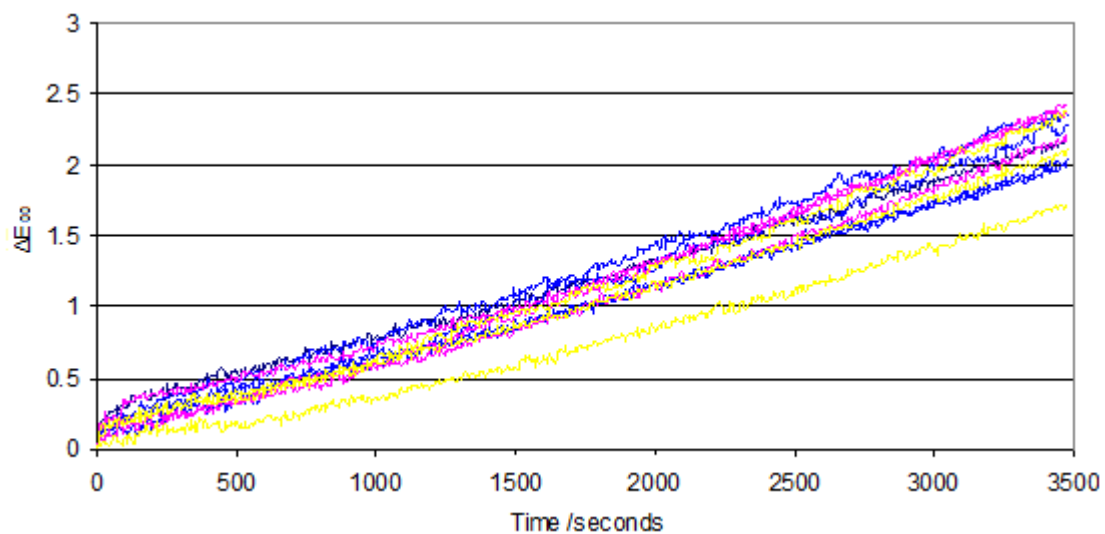


Figure 5.56. The individual colour differences measured over time for a vermilion (code 2T) pigment in the 3 different oxygen concentrations.

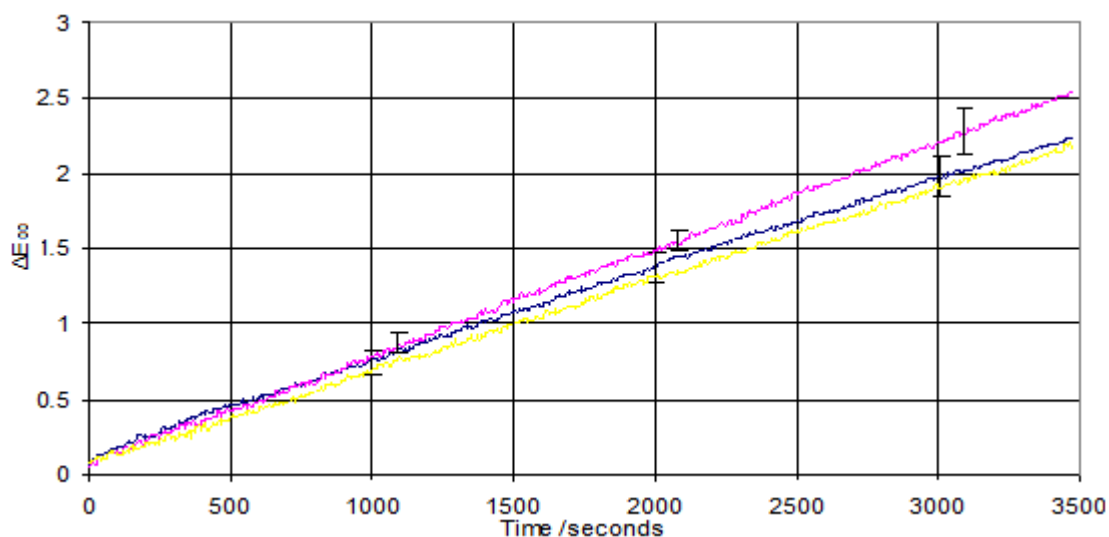


Figure 5.57. Colour difference measured with time for a vermilion (code CA22) pigment in the 3 different oxygen concentrations. The error bars represent  $\pm 1$  standard deviation of the results from fading the pigment in air and anoxia.

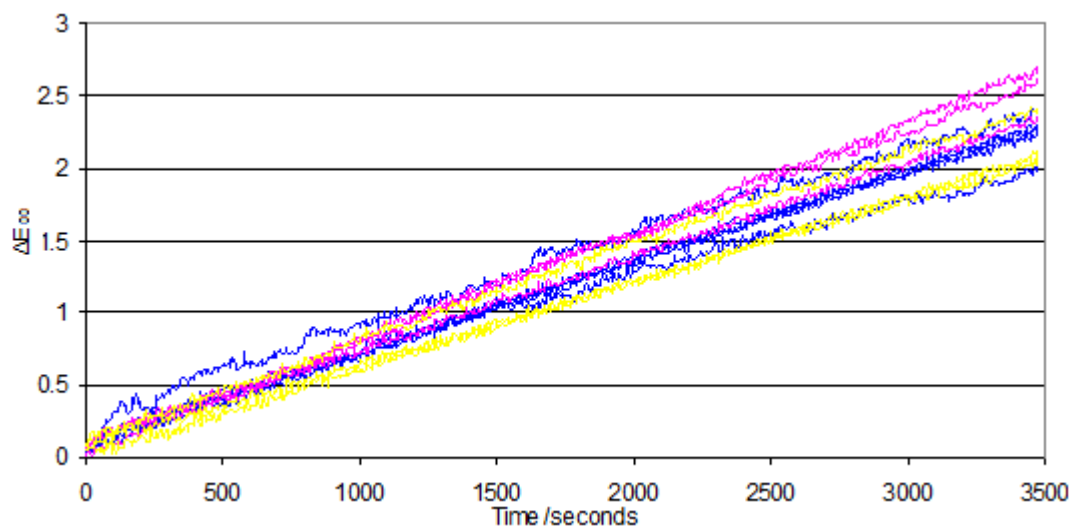


Figure 5.58. The individual colour difference measured with time for a vermilion (code CA22) pigment in the 3 different oxygen concentrations.

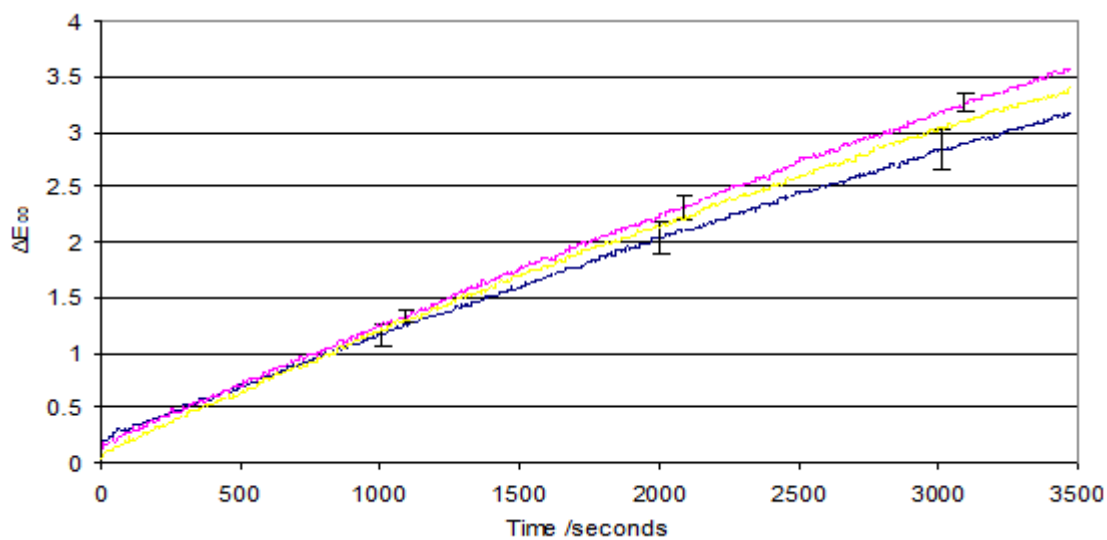


Figure 5.59. The colour difference measured over time for a vermilion (code MB A7) pigment in the 3 different oxygen concentrations. The error bars represent  $\pm 1$  standard deviation of the results from fading the pigment in air and anoxia.

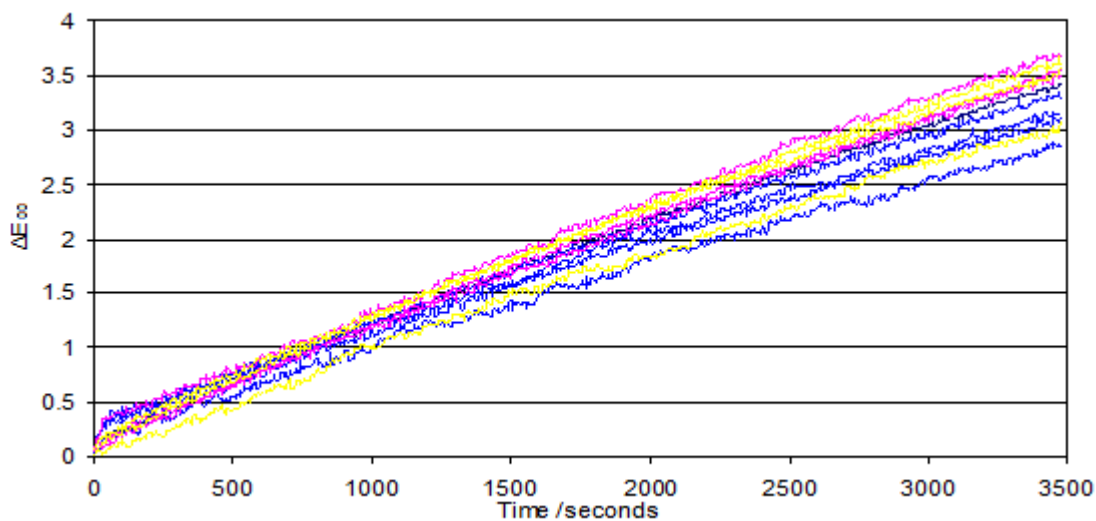


Figure 5.60. The individual colour difference measured over time for a vermillion (code MB A7) pigment in the 3 different oxygen concentrations.

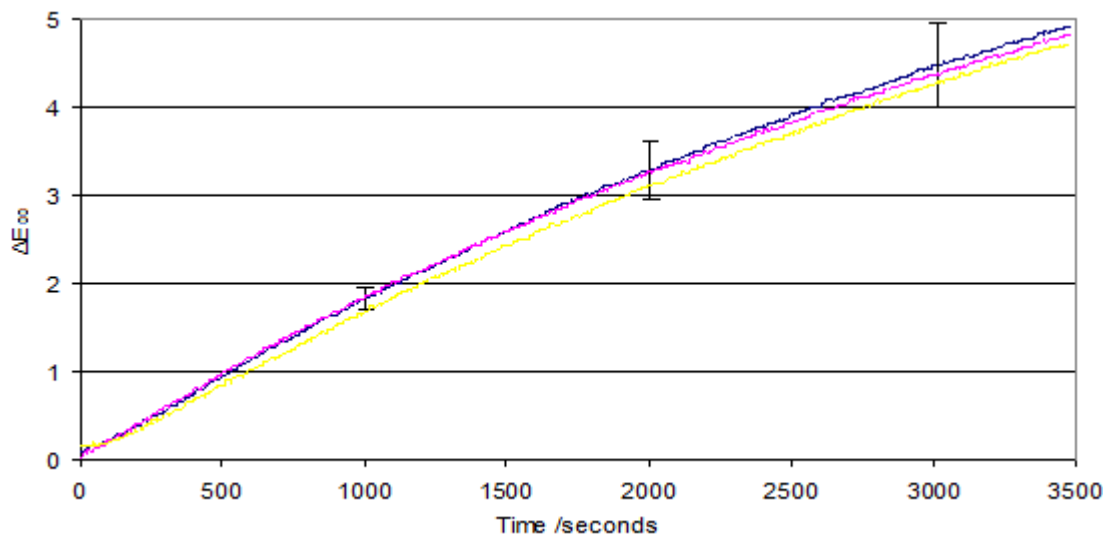


Figure 5.61. The colour difference measured over time for a vermillion 4 (code RC ICN8) pigment in the 3 different oxygen concentrations. The error bars represent  $\pm 1$  standard deviation of the 5 results from fading the pigment in air.

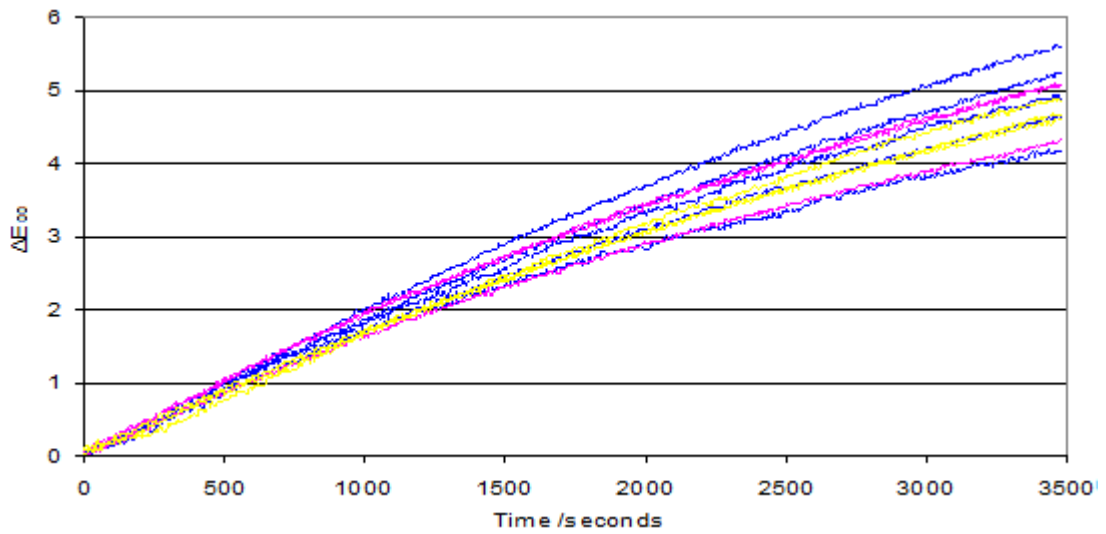


Figure 5.62. The individual colour difference measured over time for a vermilion 4 (code RC ICN8) pigment in the 3 different oxygen concentrations.

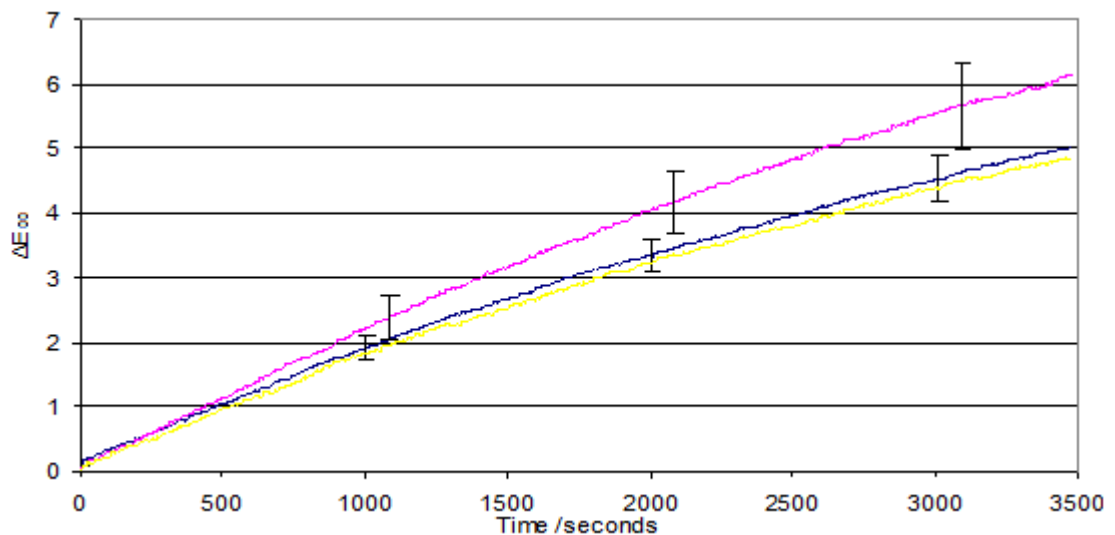


Figure 5.63. The colour difference measured over time for a vermilion (code T RR4) pigment in the 3 different oxygen concentrations. The error bars represent  $\pm 1$  standard deviation of the 5 results from fading the pigment in air and anoxia.

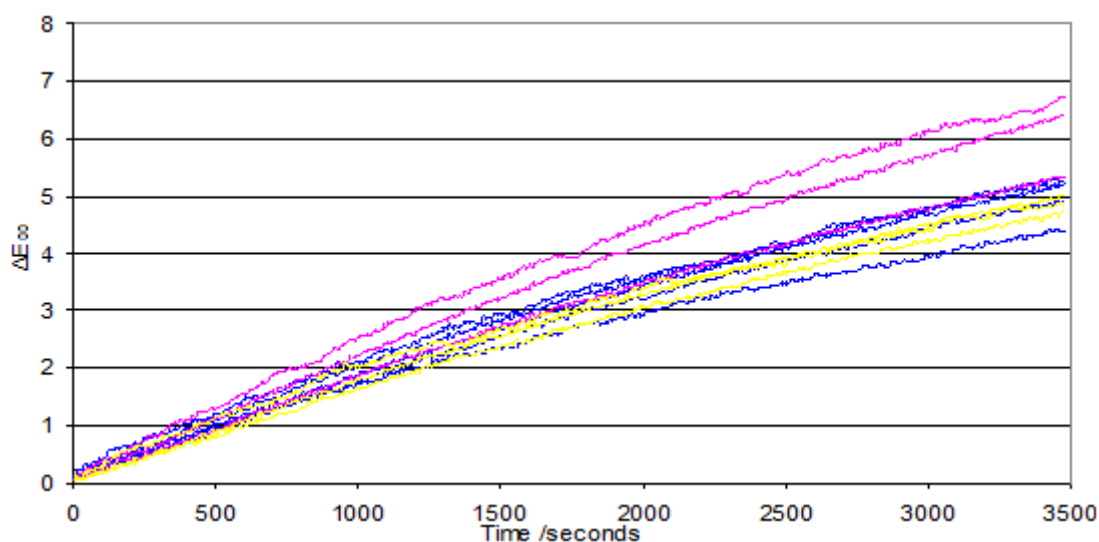


Figure 5.64. The individual colour difference measured over time for a vermillion (code T RR4) pigment in the 3 different oxygen concentrations.

## Weld

A yellow flavonoid dye derived from *Reseda luteola* or the dyers herb (Eastaugh *et al.* 2004). Weld is the most lightfast bright yellow natural dye (Crews 1987) and has been found to have a lightfastness similar to that of ISO Blue Wool 3 and fades without a change in hue (Padfield and Landi 1966). Weld (code NG2) has been shown to be fugitive by Saunders and Kirby (1994b). Results from the fading of this sample set can be seen in table 5.11.

A similar level of stability to that previously reported was observed for a number of the weld pigments tested. A clear benefit was observed for weld in anoxia and this was also the case in hypoxia although the benefit was slightly reduced.

NAME	CODE	Air		0%		5%	
		Average	St Dev	Average	St Dev	Average	St Dev
weld	RK2	0.4		0.3			
weld	RK1	0.9		0.4			
weld lake	NG3	2.6	0.3	0.8	0.1	1.3	0.3
weld	NG2	3.2	0.6	1.1	0.6	2.2	0.4

Table 5.11. A summary of the behaviour of weld at the 3 oxygen concentrations.

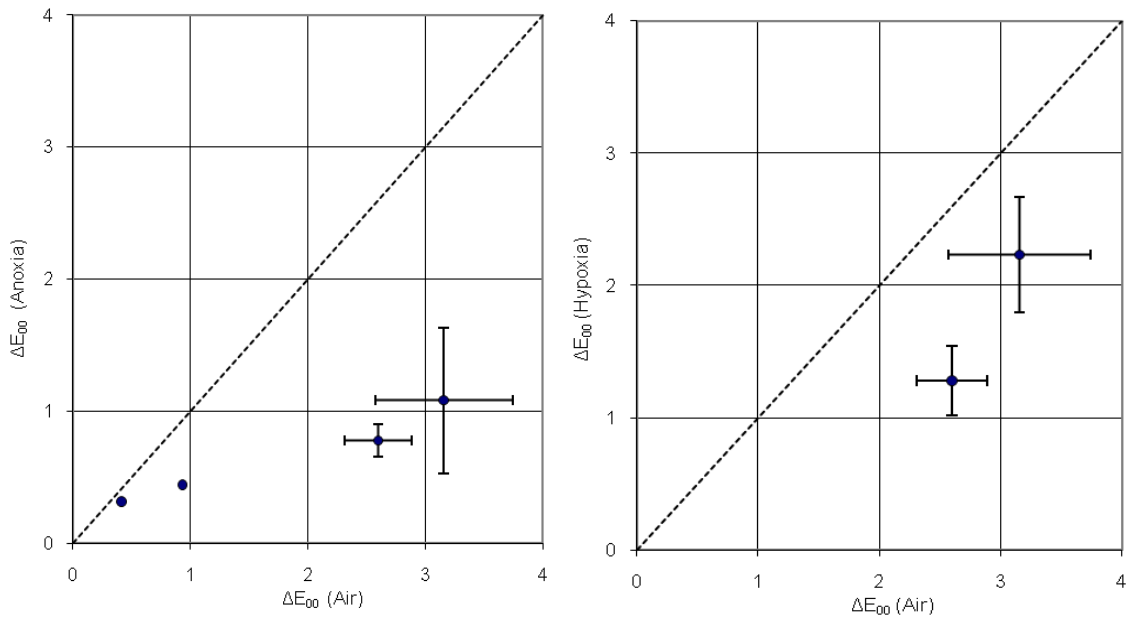


Figure 5.65. Weld: a comparison of final colour difference in air and anoxia (left) and a comparison of final colour difference in air and hypoxia (right)

The graphs below show the fading behaviour of weld pigments with significant colour change, both averaged with the standard deviation of the fades presented and also shown individually in separate plots.

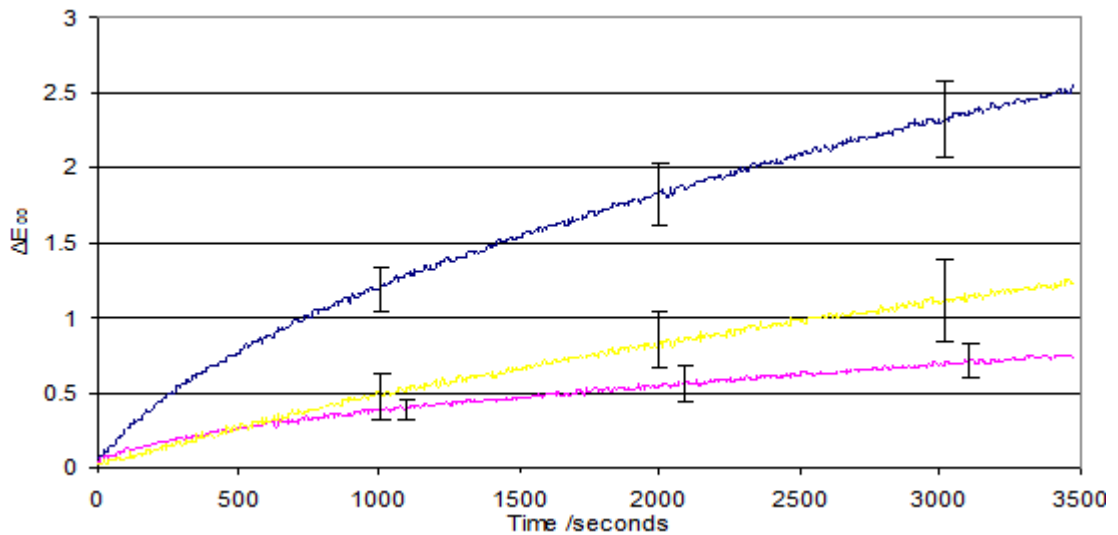


Figure 5.66. The colour difference measured over time for a weld lake (code NG3) pigment in the 3 different oxygen concentrations.

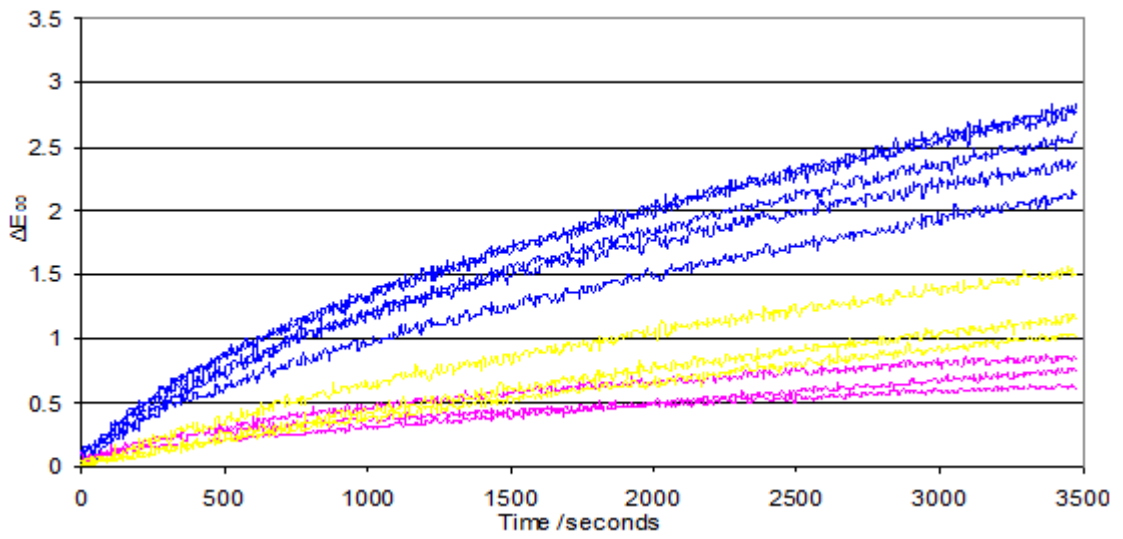


Figure 5.67. The individual colour differences measured over time for a weld lake (code NG3) pigment in the 3 different oxygen concentrations.

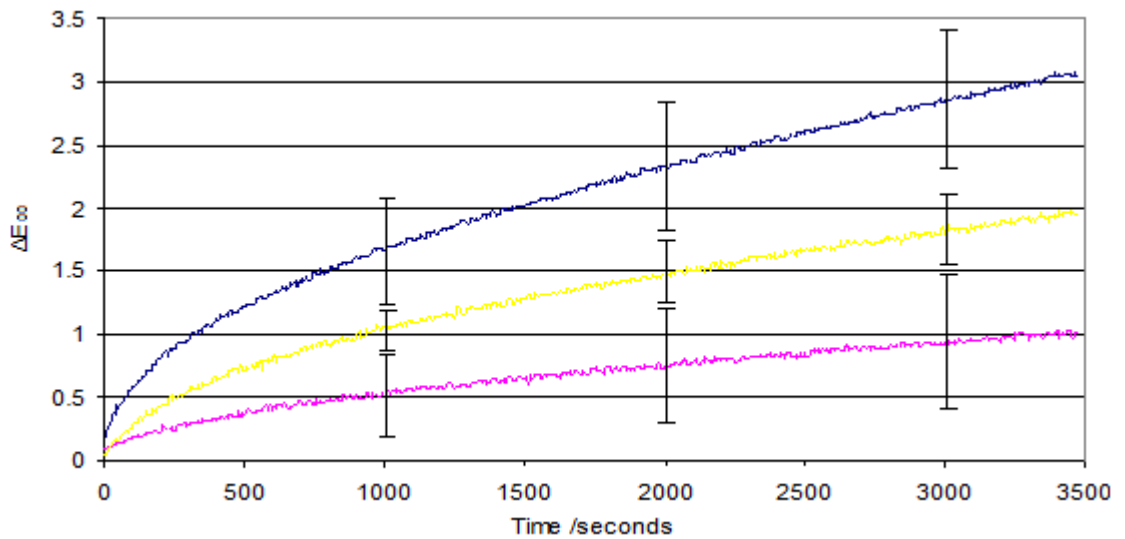


Figure 5.68. The colour difference measured over time for a weld (code NG2) pigment in the 3 different oxygen concentrations.

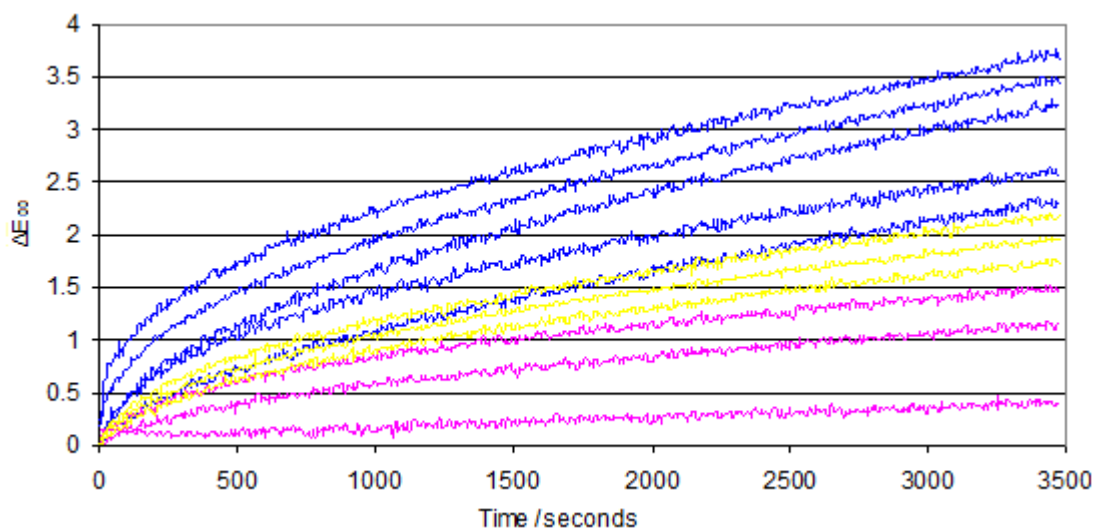


Figure 5.69. The individual colour differences measured over time for a weld (code NG2) pigment in the 3 different oxygen concentrations.

#### 5.4.2 Light stable characterised pigment groups

##### Cadmium group

The cadmium group contains cadmium sulfide, early forms of which were reported to darken due to light exposure, this was thought due to impurities and additives. Later pigments in dark red and brown shades were greatly improved and were considered permanent as has been found here (Fiedler and Bayard 1986). Results from the fading of this sample set can be seen in table 5.12.

NAME	CODE	Air	Anoxia
Cadmium yellow	RK12	0.2	0.1
Cadmium orange	RK10	0.2	0.2

Table 5.12. The behaviour of cadmium yellows at the 2 oxygen concentrations.

##### Emerald green

Emerald green most commonly refers to copper aceto arsenite  $3\text{Cu}(\text{AsO}_2)_2 \cdot \text{Cu}(\text{CH}_3\text{COO})_2$ . Sources consider emerald green to be light stable (as has been found here). Historically it was considered unstable due to susceptibility to pollution. Russell and Abney (1888) found

the pigment to fade slightly towards brown on exposure (Fiedler and Bayard 1997). Results from the fading of this sample set can be seen in table 5.13.

NAME	CODE	Air	Anoxia
Green	T RS2	0.2	0.3
Green	T R9	0.5	0.8

Table 5.13. The behaviour of emerald green at the 2 oxygen concentrations.

### Indian Yellow

Indian yellow is a complex compound derived from the urine of cows fed on mango leaves, the colouration coming from calcium and magnesium salts of euxanthic acid (Eastaugh *et al.* 2004). Reports of good stability in watercolours are reported. Experimental evidence indicates the pigment has stability on a par with ISO Blue Wool 5-6 (Baer *et al.* 1986). Results from the fading of this sample set can be seen in table 5.14.

NAME	CODE	Air	Anoxia
Indian yellow	NG WC6	0.5	0.4
Yellow lake	TR7	0.2	0.2

Table 5.14. The behaviour of genuine Indian yellow at the 2 oxygen concentrations.

### Indigo

Indigo is a blue dye derived from the leaves of the *Indigofera* species (Eastaugh *et al.* 2004) and is one of the most stable natural dyes (Crews 1987).

The sample set was light stable as has been previously reported. The degree of fading seemed to be largely unaffected by anoxia over the fade duration as had also previously been reported.

MvEH1 was found to be natural indigo and MB A6 was found to be a synthetic indigo.

Results from the fading of this sample set can be seen in table 5.15.

NAME	CODE	Air	Anoxia
Indigo	OH14	0.3	0.3
Indigo 2	MvEH1	0.4	0.2
Indigo	T PC5	0.4	0.4
Indigo	T3	0.4	0.4
Indigo	MB A6	0.5	0.4
Natural indigo	RC ICN3	0.7	0.2

*Table 5.15. The behaviour of indigo at the 2 oxygen concentrations.*

### Iron oxides

Indian red TRR3 was a natural iron oxide; the colour was originally derived from a purple ochre in the Persian gulf. Iron oxides have long been considered among the very most permanent of pigments available (Helwig 2007) as was the case in this research.

Analysis indicated that light red (TRS10) was a synthetic iron oxide. Results from the fading of this sample set can be seen in table 5.16.

NAME	CODE	Air	Anoxia
Light red	T RS10	0.1	0.4
Indian red	T RR3	0.2	0.2

*Table 5.16. The behaviour of iron oxides at the 2 oxygen concentrations.*

### Massicot

Massicot refers to an orthorhombic lead (II) oxide mineral (PbO) and is derived from a yellow material found associated with iron ore deposits (Eastaugh *et al.* 2004). It is considered as a chemically stable compound (Petushkova and Lyalikova 1986). Results from the fading of this sample set can be seen in table 5.17.

NAME	CODE	Air	Anoxia
Mineral yellow	CA23	0.3	0.2
Jaune de Naples	D&C 8/07	0.8	0.7
Naples yellow	RK11	0.1	0.2

Table 5.17. The behaviour of massicot at the 2 oxygen concentrations.

## Quercitron

A yellow naturally occurring dye derived from the bark of the black oak. The major colouring matter being the flavonoid dyestuff quercetin (Eastaugh *et al.* 2004). Quercitron is reported to redden before fading (Duff 1977) or darken before fading (Padfield and Landi 1966). Feller (1963) found the pigment to be fugitive to an ISO Blue Wool level of 2-4., a result not observed here. Results from the fading of this sample set can be seen in table 5.18.

NAME	CODE	Air	Anoxia	Substrate
Quercitron lake 1	NG8	0.5	0.7	Al
Quercitron lake 2	NG Q2	0.6	0.9	
Ackermann's yellow	NG WC4	0.8	0.6	

Table 5.18. The behaviour of quercitron at the 2 oxygen concentrations.

## Sepia

Sepia is derived from the ink sac of the cuttle fish and other cephalopods, the pigment produced contains melanin (Eastaugh *et al.* 2004). Feller (1963) found sepia paint to be fugitive to an ISO Blue Wool level of 4-5 (not contradicted here). Results from the fading of this sample set can be seen in table 5.19.

NAME	CODE	Air	Anoxia
Sepia 12400	T PC10	0.6	0.6
Sepia	RK15	0.7	0.4
Sepia	CA12	0.8	0.6

Table 5.19. The behaviour of sepia at the 2 oxygen concentrations.

## Zinc oxide

Chinese white is a more opaque variety of zinc oxide. Similar to what has been observed here, during aging zinc whites in watercolour tend to maintain colour and not yellow (Kühn 1986). Results from the fading of this sample set can be seen in table 5.20.

NAME	CODE	Air	Anoxia
Zinc white	MoL 1	0.3	0.3
Zinc white	HKI 16	0.5	0.5
Chinese white	MoL 3	0.6	0.2
Zinc white	SO/11	0.7	0.7
Chinese white	MoL 2	0.7	0.6

Table 5.20. The behaviour of the zinc white at the 2 oxygen concentrations.

### 5.4.3 Poorly identified pigments

A number of pigments could not be well characterised by the screening methods used here, or else two samples of equally good provenance gave conflicting analytical results. Being the best samples obtainable from a thorough search they were tested nonetheless and the results are presented here.

## Bister

The black pigment of bister was historically prepared from wood soot (beechwood was preferred) (Eastaugh *et al.* 2004). Carbon based pigments are widely reported to be unaffected by light, although bister in particular may lighten with time due to oxidation (Winter and Fitzhugh 2007). Results from the fading of this sample set can be seen in table 5.21.

NAME	CODE	Air		0%		5%	
		Average	St Dev	Average	St Dev	Average	St Dev
Bister	NG WC9	1.0	0.1	1.4	0.1	1.2	0.2

Table 5.21. The behaviour of bister at the 3 oxygen concentrations.

The graphs below show the fading behaviour of the pigment both averaged with the standard deviation of the fades presented and also shown individually in separate plots.

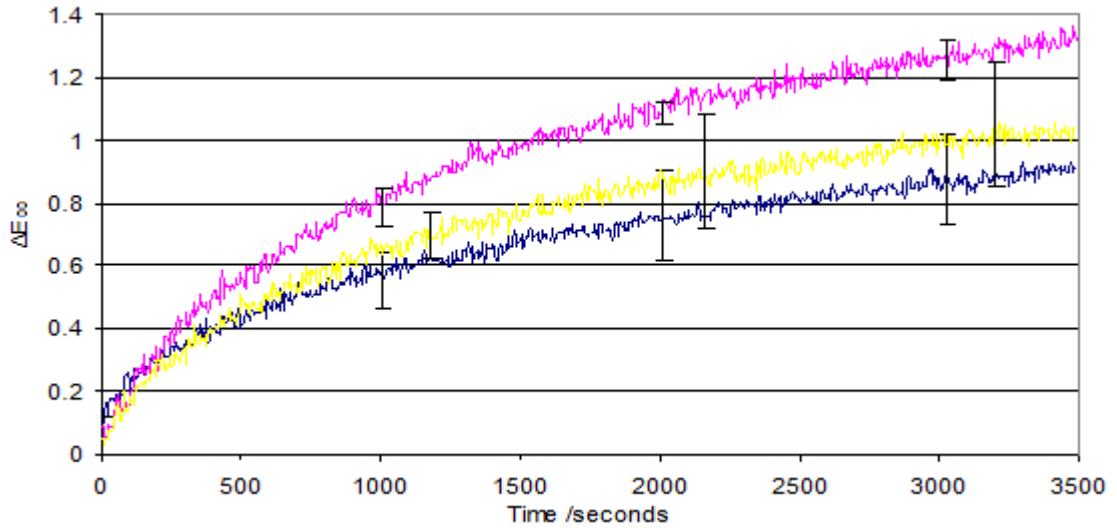


Figure 5.70. The colour difference measured over time for Bistre (code NG WC9) pigment in the 3 different oxygen concentrations.

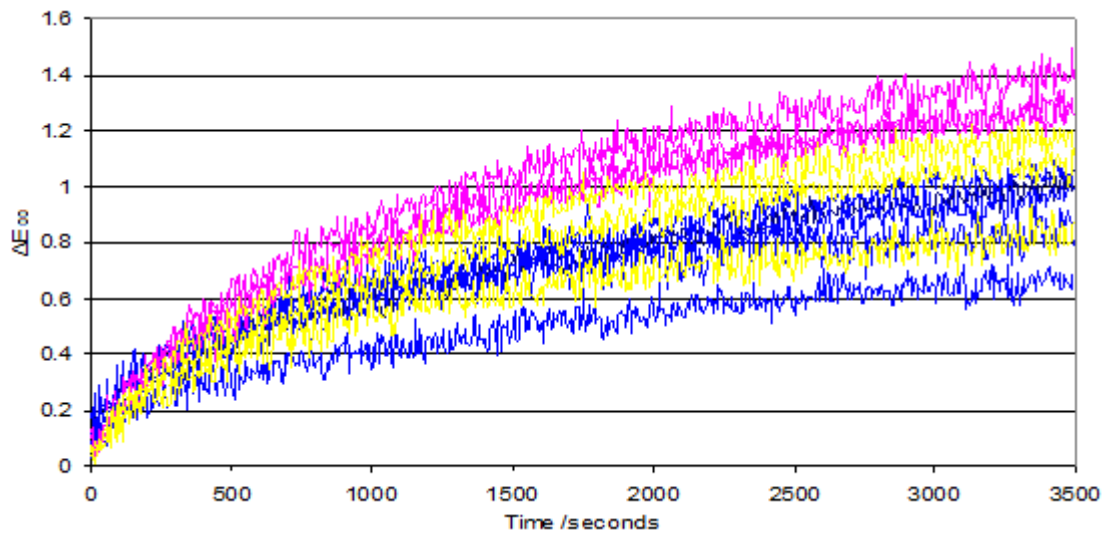


Figure 5.71. The individual colour difference measured over time for Bister (code NG WC9) pigment in the 3 different oxygen concentrations.

### Bone Black

Created by the burning of bone, this black is usually calcium phosphate  $\text{Ca}_5(\text{PO}_4)_{3x}(\text{CO}_3)_x\text{OH}_{x+1}$  (Reich *et al.*, 2002). Results from the fading of this sample set can be seen in table 5.22.

NAME	CODE	Air		0%		5%	
		Average	St Dev	Average	St Dev	Average	St Dev
Carbon black	T RS3	1.0	0.1	1.3	0.1	1.1	0.1

Table 5.22. A summary of the behaviour of bone black at the 3 oxygen concentrations.

The graphs below show the fading behaviour of bone black, both averaged with the standard deviation of the fades presented and also shown individually in separate plots.

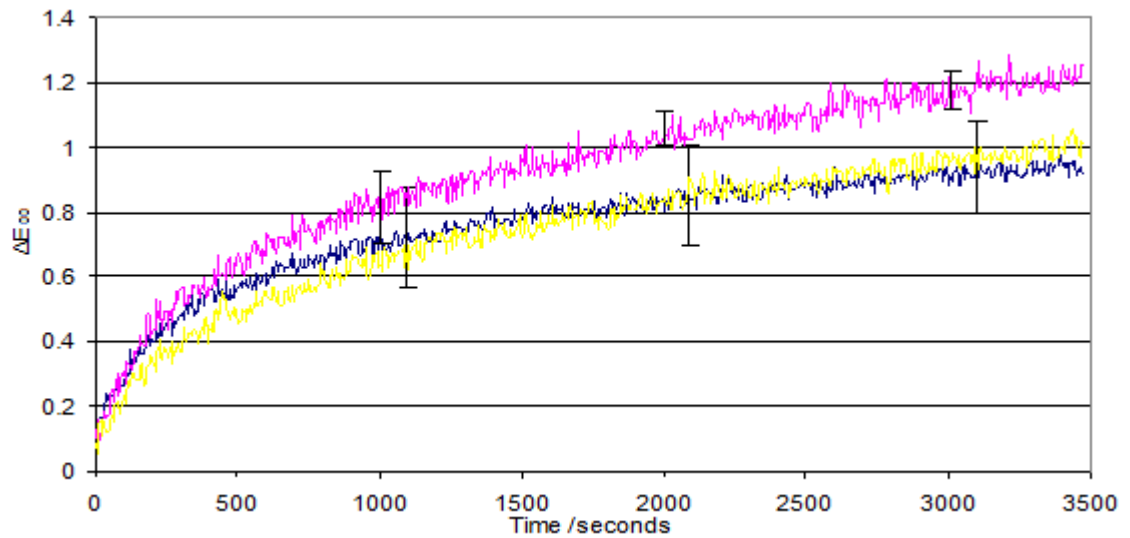


Figure 5.72. The colour difference measured over time for a black (code TRS3) pigment in the 3 different oxygen concentrations. The error bars represent  $\pm 1$  standard deviation of the results from fading the pigment in air and anoxia.

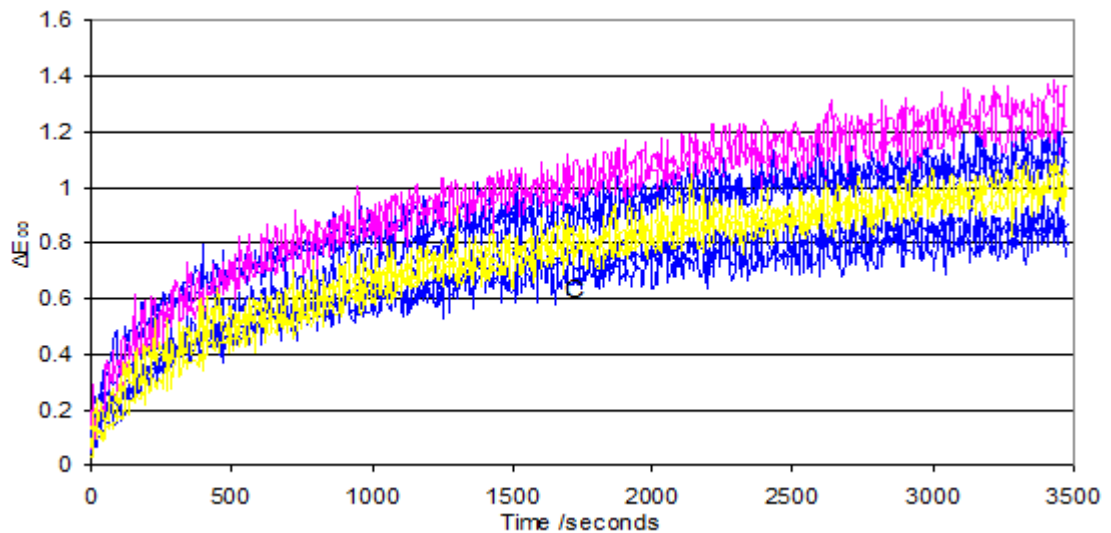


Figure 5.73. The individual colour difference measured over time for a black (code TRS3) pigment in the 3 different oxygen concentrations.

## Buckthorns

A yellow or green flavonoid dye derived from the berries of the buckthorn tree and other *Rhamnus* and *Frangula* species (Eastaugh *et al.* 2004). Examples of the fading of yellow buckthorn lake pigments have been summarised by Saunders and Kirby (1994b) where the important role of substrate on the degree of fading was made evident. Padfield and Landi (1966) tested dyes from the *Rhaimnus saxatilis* and *Rhamnus utilis* and found them to possess poor lightfastness similar to Blue Wool 1 or 2. Results from the fading of this sample set can be seen in table 5.23.

The buckthorn pigments showed little colour change (contrary to previous findings for buckthorn based pigments). The small colour difference observed for buckthorn lake (code NG5) was higher after fading in anoxia rather than air. This result seemed to show improvement when using a 5% oxygen concentration. Analysis indicated RK5 and NG5 were non standard buckthorn. NGB differed from NG5.

NAME	ODE	Air		0%		5%	
		Average	St Dev	Average	St Dev	Average	St Dev
Buckthorn yellow	RK3	0.4		0.8			
Buckthorn on alumina	NG B	0.8		0.8			
Buckthorn lake	NG5	0.8	0.1	1.4	0.1	0.9	0.1

Table 5.23. A summary of the behaviour of buckthorns at the 3 oxygen concentrations.

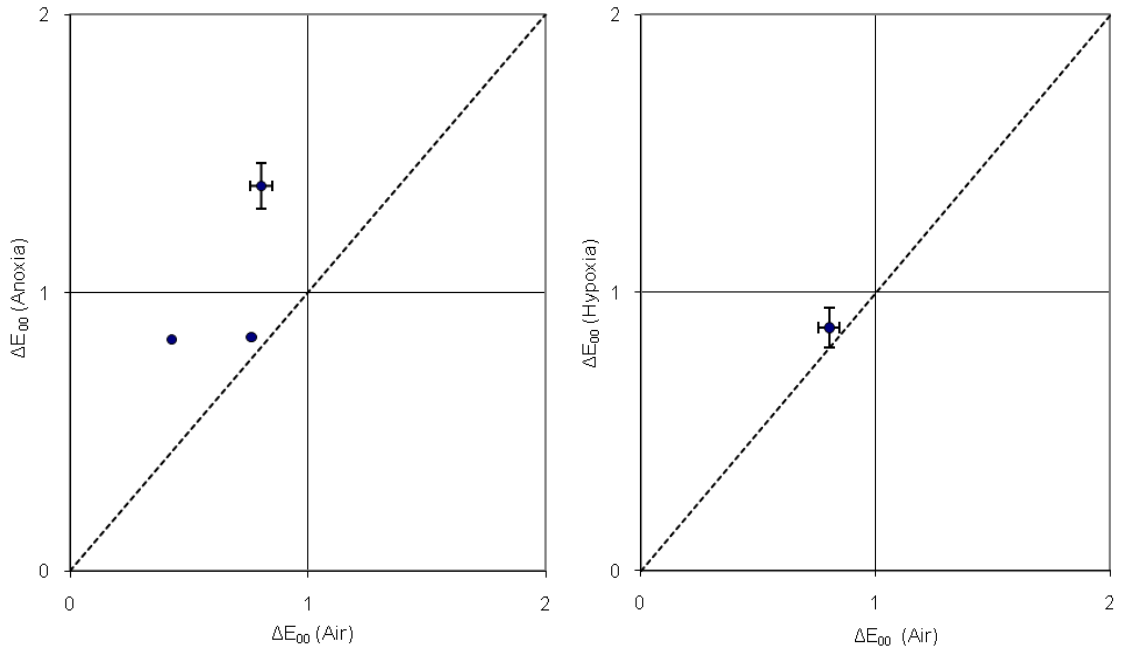


Figure 5.74. Buckthorn; final colour difference in air and anoxia (left) and a comparison of final colour difference in air and hypoxia (right).

The graphs below show the fading behaviour of buckthorn lake code NG5 both averaged with the standard deviation of the fades presented and also shown individually in separate plots.

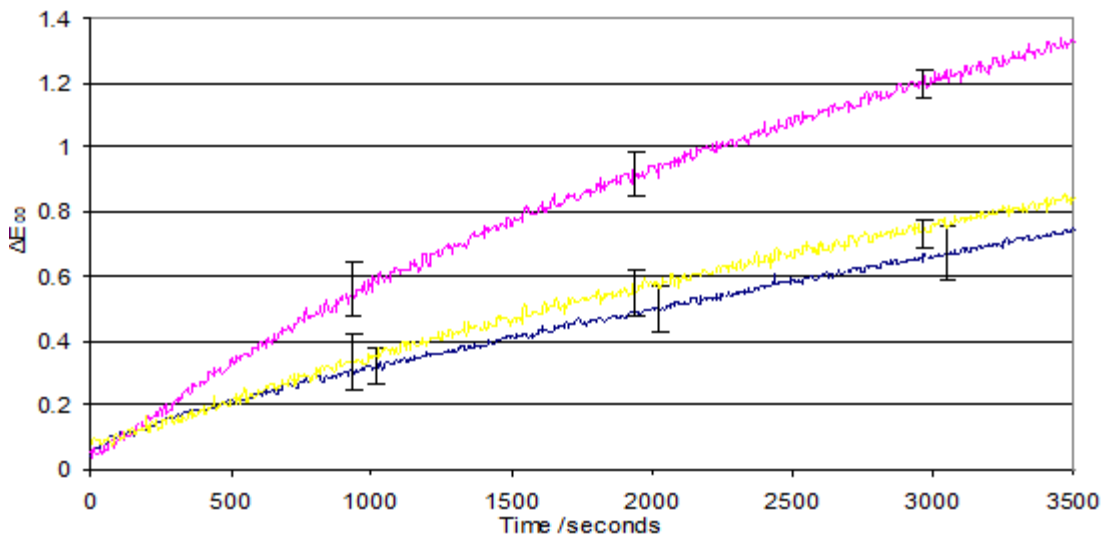


Figure 5.75. The fading curves of buckthorn lake (code NG5) pigment in 3 different oxygen concentrations.

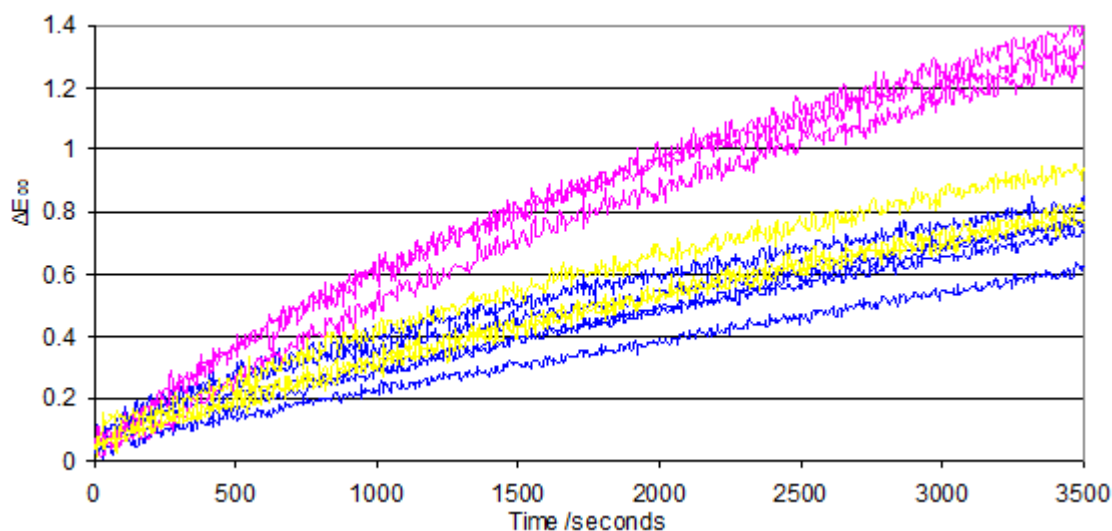


Figure 5.76. The individual fading curves of buckthorn lake (code NG5) pigment in 3 different oxygen concentrations.

### Van Dyke Brown

A particular brown earth containing iron oxide, a hydrate and humus or bituminous matter is most commonly referred to as the compound from which Van Dyke brown is derived (Eastaugh *et al.* 2004). When considering modern research into the lightfastness of the pigment results indicates a tendency to fade with an intermediate lightfastness. (Feller and Johnston-Feller 1997). Results from the fading of this sample can be seen in table 5.24.

The Van Dyke brown analysed clearly displayed colour difference over the fade duration independent of oxygen level.

NAME	CODE	Air		0%		5%	
		Average	St Dev	Average	St Dev	Average	St Dev
Van Dyke brown	T RS9	1.4	0.2	1.6	0.2	1.5	0.2

Table 5.24. The fading behaviour of Van Dyke brown code (T RS9) in 3 different oxygen concentrations.

The graphs below show the fading behaviour of the pigment both averaged with the standard deviation of the fades presented and also shown individually in separate plots.

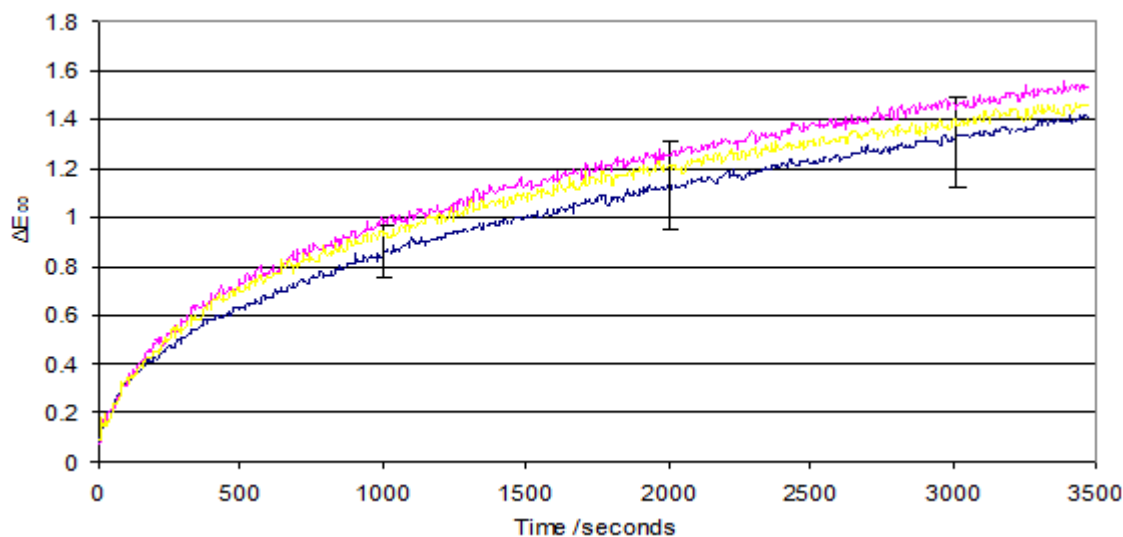


Figure 5.77. The colour difference measured over time for Van Dyke brown (code T RS9). The error bars represent  $\pm 1$  standard deviation of the results from fading the pigment in air.

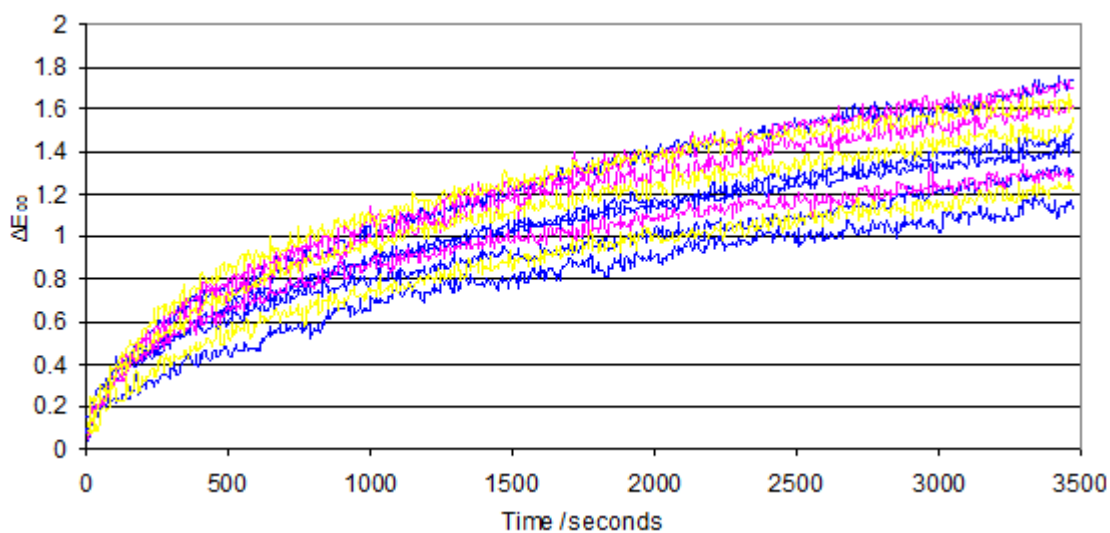


Figure 5.78. The individual colour difference measured over time for Van Dyke brown (code T RS9).

## Verditer

Verditer is a synthetic copper carbonate hydroxide pigment and has the same chemistry as the natural malachite and azurite pigments (which it was synthesized to replace) (Eastaugh *et al.* 2004). The pigment is regarded as moderately permanent as evidence suggests. Results from the fading of this sample can be seen in table 5.25.

No relationship between oxygen concentration and the degree of fade duration was observed in the case of verditer.

		Air		0%		5%	
NAME	CODE	Average	St Dev	Average	St Dev	Average	St Dev
Verditer	CA21	2.2	0.3	1.7	0.8	2.2	1.1

Table 5.25. A summary of the behaviour of verditer at the 3 oxygen concentrations.

The graphs below show the fading behaviour of the pigment both averaged with the standard deviation of the fades presented and also shown individually in separate plots.

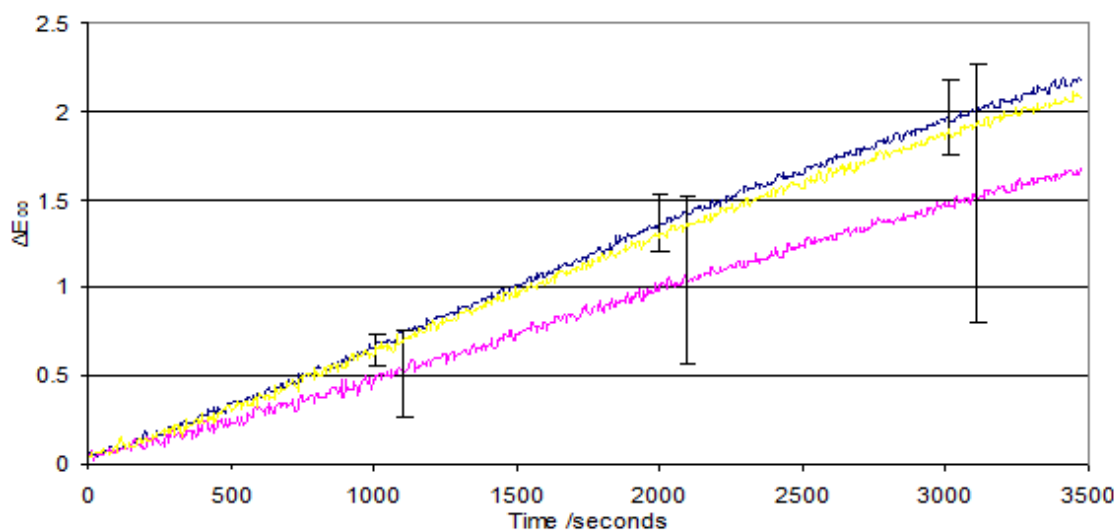


Figure 5.79. The colour difference measured over time for verditer (code CA21) pigment in the 3 different oxygen concentrations. The error bars represent  $\pm 1$  standard deviation of the results from fading the pigment in air.

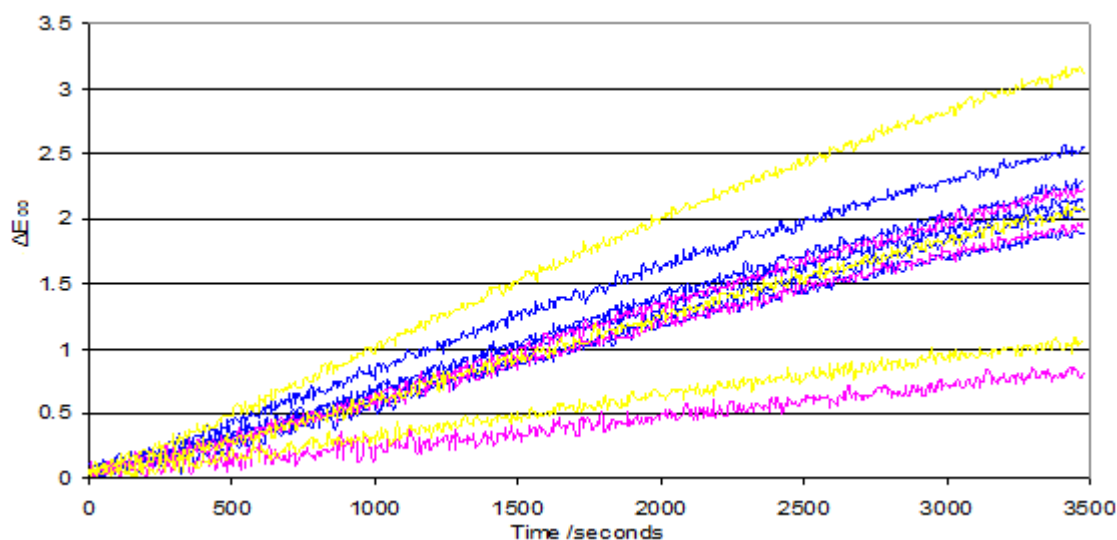


Figure 5.80. The individual colour difference measured over time for verditer (code CA21) pigment in the 3 different oxygen concentrations.

#### 5.4.4 Uncharacterised stable pigments

##### Burnt Umber

The brown pigment of burnt umber is created by roasting raw umber (a naturally occurring mineral) (Weber 1923). It is permanent and therefore suitable for use as a watercolour pigment (Harley 2001).

Results from the fading of this sample can be seen in table 5.26. Analysis indicated the sample was produced from a natural umber.

NAME	CODE	Air	Anoxia
Burnt Umber	T RR7	0.2	0.2

Table 5.26. The behaviour of burnt umber at the 2 oxygen concentrations.

##### Brown Pink

Brown pink is a yellow pigment derived from the berries of the Avignon (*Rhamnus infectorius*) (Salter 1869) and one would expect the pigment to be fugitive (Levison 1976). Results from the fading of this sample can be seen in table 5.27.

NAME	CODE	Air	Anoxia
Brown pink	MB A4	0.8	0.4

Table 5.27. The behaviour of brown pink at the 2 oxygen concentrations.

## Carmines

Carmine can be regarded as a cochineal lake (since the end of the 17<sup>th</sup> century). Cochineal is a red dye stuff derived from species of scale insects and exhibits a high degree of lightfastness (Schweppe and Roosen-Runge 1986). Watercolours based on carmine have been found to exhibit a lightfastness of 1 or 2 on the ISO Blue Wool scale (Feller 1963). Results from the fading of this sample set can be seen in table 5.28.

NAME	CODE	Air	Anoxia	Substrate
Carmines extra	D&C 8/08	0.5	0.4	Al and/or Ca
Carmines	OH13	0.6	0.5	Al

Table 5.28. The behaviour of carmine at the 2 oxygen concentrations.

## Kopp's Purpurin

Purpurine is 1,2,4-trihydroxyanthraquinone and is found in dye stuffs derived from the *Rubiaceae* species (madder). Kopp's Purpurin is produced when the madder is soaked and heated in sulfuric acid (Eastaugh *et al.* 2004). Despite remaining relatively stable in work by Russell and Abney (1888) the pigment would be expected to fade Levison (1976).

The conclusion of analysis indicated the pigment was synthetic. Results from the fading of this sample can be seen in table 5.29.

NAME	CODE	Air	Anoxia	Substrate
Kopp's purpurine	RC-ICN-M2	0.7	0.2	Al

Table 5.29. The behaviour of Kopp's purpurine at the 2 oxygen concentrations.

## Lead White

Lead white is a manufactured and synthesized pigment and normally refers to lead carbonate hydroxide ( $2\text{PbCO}_3 \cdot \text{Pb}(\text{OH})_2$ ) (Eastaugh *et al.* 2004). The pigment has a record of permanence and is not affected by light (Gettens *et al.* 1993). Results from the fading of this sample can be seen in table 5.30.

NAME	CODE	Air	Anoxia
Lead white	CA24	0.8	0.5

Table 5.30. The behaviour of lead white at the 2 oxygen concentrations.

## Red Lead

Red lead is lead tetroxide ( $\text{Pb}_3\text{O}_3$ ) and is derived from a material found surrounding lead ore deposits (Eastaugh *et al.* 2004). It is considered unsuitable as a watercolour pigment due to its lightfastness and is reported to change colour to a brown or black (Fitzhugh 1986). Results from the fading of this sample can be seen in table 5.31.

NAME	CODE	Air	Anoxia
Rouge de Saturne	D&C 8/04	0.2	0.2

Table 5.31. The behaviour of red lead at the 2 oxygen concentrations.

## Smalt

Smalt is cobalt doped glass. It is considered to be light stable unless improperly prepared though in oil medium it can lose colour. There are examples of the pigment showing fugitive behavior (Mühlethaler and Thissen 1993). Results from the fading of this sample can be seen in table 5.32.

NAME	CODE	Air	Anoxia
Smalt	MB3	0.5	0.5

Table 5.32. The behaviour of smalt at the 2 oxygen concentrations.

## Yellow Ochre

Yellow ochre contains the colouring matter iron oxide hydroxide goethite (Eastaugh *et al.* 2004). As an ochre the pigment can be considered as reliably lightfast (Levison 1976).

Results from the fading of this sample set can be seen in table 5.33. Analysis indicated this pigment was derived from a naturally occurring earth pigment.

NAME	CODE	Air	Anoxia
Yellow ochre	T RS4	0.4	0.7

*Table 5.33. The behaviour of yellow ochre at the 2 oxygen concentrations.*

## 5.5 Discussion

Of the well characterised pigments, brazilwood, gamboge, madder, weld cochineal and the lake pigments all benefited (showed reduced fading) in anoxia and the benefits observed were still present in hypoxia.

The characterised pigment of Prussian green performed poorly in anoxia, however this damage was reduced significantly in an hypoxic environment. The uncharacterised pigments that exhibited this behaviour were bister and buckthorn.

In the case of the chromate pigments, sap green, orpiment and vermillion no difference was observed due to the presence of oxygen with regards to the degree of damage caused by the fading. Therefore the fading of the pigments were independent of oxygen concentration. The uncharacterised pigments that exhibited the same behaviour were Van Dyke brown and verditer.

A large number of pigments displayed a low sensitivity to light in either air or anoxia, this higher stability would lessen the effect that the exclusion of oxygen would have on the sample. Those characterised pigment groups that did not display any visible colour difference due to the fading process were the cadmium group of pigments, emerald green, Indian yellow, indigo, iron oxides, massicot, quercitron, sepia and zinc oxide. All these

displayed no visible change. The uncharacterised pigments that also displayed this behaviour were black, burnt umber, brown pink, carmines, Kopps' purpurine, lead white, red lead, smalt and yellow ochre.

Vermillion illustrated a low level of light stability agreeing well with previous findings for the pigment. Brazilwood also displayed a low degree of stability as did sap green.

The colour differences due to the use of altered oxygen content over this degree of exposure are subtle and at no point has the colour change observed been catastrophic for the pigment under test. This result is important as it can be considered as justification for the use of monitored anoxic framing of watercolours.

The pigments fading behaviour was often altered by the 5% oxygen concentration, usually performing in a similar way to the behaviour in air (although this was not always the case). Interestingly this result is a significant departure from that as discussed in the introduction; that the degree of oxidative degradation of most organic pigments would show little or no decrease in the rate of degradation until an oxygen level of parts per million was achieved. The finding of this research is similar to the later work of Arney *et al.* (1979) whose results indicated the relationship was dependent upon the sample under test.

With the large quantity of data acquired and numerous examples of the same type of pigment tested, clear patterns were observed. The variation sometimes seen in the degree of fading for an individual group of pigments indicate that caution should be employed when making overarching statements about a particular pigment type stability.

Often a large variation in the degree of fading was created by variation in the sample. This error was often significant and resulted in a degree of variation that often made differences created by altering the atmosphere unobservable. This spread in data could aid a strong case for increasing the size of the sampling spot size.

## 6 Conclusions

In this thesis, a micro-fading instrument that addresses and corrects the problems as summarised by Neeval (2008) has been presented and employed that enables the investigation of photosensitive samples and works of art. Several new experimental methods have been illustrated.

The instrument demonstrates increased structural stability increasing the portability over an earlier design, broadening the scope of locations at which data can be acquired, enabling insitu investigation of light sensitivity. This enables more informed decisions on light sensitivity to be made. Increased precision of probe positioning relative to the sample, homogeneity of illumination across the faded area, controlled intensity at the illuminated surface from the lamp, and an ease of confocal probe alignment are present in the new design. Two different measurement methods indicate a temperature increase of 3 to 4 degrees during fading experiments, an improvement on the degree of increase previously reported.

An investigation of the error in colour measurement and colour difference calculations produced by small differences in position, indicated that alignment by eye may be a significant cause of error in measurements.

Incorporating a linear variable filter enables the investigation of the wavelength dependence of fading of many samples to a greater resolution than previously attempted, and the novel wavelength dependent technique has been shown to produce repeatable data that compares very well with previous research conducted in the same area using other techniques.

The wavelength dependence of fading for the samples tested correlates well with the absorption spectra although exceptions were found when testing Prussian blue, where fading decreases with the wavelength of incident radiation (possibly due to photosensitized fading). There is an apparent cut off wavelength at 550nm. Below this wavelength Prussian blue photo-degradation occurs. If this behaviour extends to other Prussian blues, reducing lighting levels below the cutoff wavelength could significantly reduce damage typically associated with anoxic storage environments for this pigment. As it is possible to state that as only photons with wavelengths below 550nm seem to induce the damage

observed an activation energy of 218kJ/mol or approximately 2.3eV per photon is required to initiate the possible photosensitized fading of the Prussian blue.

Filtering the blue end of the visible spectrum has been previously suggested in numerous publications including Hilbert (1987), Harrison (1953), and Cuttle (1988) and the application of a “yellow filter” removing light from the ultraviolet region up to 460nm was employed by the United States Library of Congress (National Bureau of Standards 1951) (Nicholson and Ritzenthaler 2005). This method would be of benefit in the case of Prussian blue in anoxia.

By mathematically simulating an alteration of illumination it is possible to indicate how harmful any filtering of the illuminant would be on colour perception. Comparisons between pigment spectra with and without filtering of the D65 illuminant were made and the colour difference created by such filtering was calculated in  $\Delta E_{00}$  units for blue and white pigments. For a blue pigment removing illumination below 420nm would result in an observed colour difference of less than 1  $\Delta E_{00}$  and if removing illumination below 430nm a resulting colour difference of less than 3.5  $\Delta E_{00}$  would be observed. When analysing a white pigment cutting radiation below 420 nm would produce a colour difference of approximately 3  $\Delta E_{00}$  units and over 8  $\Delta E_{00}$  units was the calculated result for a cut-off at 430nm. This indicated the degree of fading could be greatly reduced by filtering below 420nm with a limited alteration to the perceived colour. The difference would be too great if filtering was extended to 430nm. As all these calculations are concerned with blue and white pigments, the degree of observed colour difference created by such filtering would be at its greatest for these colours and much reduced for many others. Colour rendering (see CIE 1995b) when cutting illumination below 420nm remains within acceptable limits producing a General Color Rendering Index (Ra) of 99.

The fading and reversion behaviour of a traditional Prussian blue pigment ground in gum Arabic was investigated at 0%, 2%, 3.5%, 5%, 10% or 21% oxygen concentrations. Results indicated that the deleterious effects of hypoxia may only become relevant at low oxygen concentrations (beginning at an hypoxic oxygen level above 2% and below 3.5%), and that relatively low concentrations of oxygen (around 5%) may be tolerated by Prussian-blue containing works of art.

When the study in this pattern of behaviour was extended to a larger number of traditional Prussian blues and the behaviour of the pigment at 0% and 5% oxygen was compared to

behaviour in room atmosphere, it is indicated that a 5% oxygen concentration is widely applicable to a variety of Prussian blue pigments. Results also indicated that anoxic storage is more damaging for Prussian blue than air or 5% hypoxic storage.

An investigation of the effect of housing in anoxia and 5% hypoxia was extended to most traditional watercolour pigments. This revealed encouraging results to overcoming some of the problems of reduced oxygen storage for a wider variety of watercolour pigments. A large sample set was employed when possible to constitute many variants of the same pigment type.

Results led to the classification of pigment behaviour into 4 groups; those pigment which showed reduced fading in anoxia, where the benefits observed were still present in hypoxia. Those that faded to a greater degree in anoxia, where this damage was reduced significantly in an hypoxic environment. Those for which fading was independent of oxygen concentration and also pigments which displayed a low sensitivity to light in either air or anoxia.

At no point was the colour change “catastrophic” indicating that monitored trials of anoxic or hypoxic framing for watercolours works are justifiable via the data.

## 7 References

Allen, N.S., Pratt, E., McCormick, D.M. and Davis, A., 1993. 'Development of a visible light dosimeter film based on a crystal violet dye'. *Conservation News*, 52, pp.10-11.

Appel. W.D., Smith. W.C., 1928. 'Report of the Sub-committee on Light Fastness: The Fading of Dyed Textiles in the Light Transmitted by Various Glasses'. *American Dyestuff Reporter*, 17, pp.410-422.

Arney, J.S., Jacobs, A.J. and Newman, R., 1979. 'The influence of oxygen on the fading of organic colourants'. *Journal of the American Institute of Conservation*, 18, pp.108–117.

Ashley-Smith, J., Derbyshire, A. and Pretzel, B., 2002. 'The continuing development of a practical lighting policy for works of art on paper and other object types at the Victoria and Albert Museum'. *ICOM-CC13th Triennial Meeting preprints*, London: James & James, pp.3-8.

American Society for Testing and Materials 1993a 'Standard practice for obtaining spectrophotometric data for object-color evaluation, E 1164-91'. *Annual Book of ASTM Standards*, Vol 6.01, ASTM, Philadelphia pp 834-840.

American Society for Testing and Materials 1993b, 'Standard test method for reflectance factor and color by spectrophotometry using bidirectional geometry E 1349-90'. *Annual Book of ASTM Standards*, Vol 6.01, Philadelphia pp 863-865.

American Society for Testing and Materials 2006. 'Standard methods for testing the lightfastness of pigments used in artists materials D4303-06'. *Annual Book of ASTM Standards*, Vol. 6.02, Philadelphia, pp.295-304.

Aydinli, S., Krochmann, E., Hilbert, G.S. and Krochmann, J., 1990. 'On the deterioration of exhibited museum objects by optical radiation'. CIE Publication 89/3, *CIE Technical Collection*.

Aydinli, S., Hilbert, G. S. and Krochmann. J., 1983. '*Licht-Forschung*'. 5, (1), pp.35.

Bacci M *et al.* 2003. 'Disposable indicators for monitoring Lighting Conditions in Museums' *Environmental Science and Technology*, 37, pp.5687-5694.

Baer N.S., Joel, A., Feller. R.L and Indictor. N., 1986. *Artists' Pigments. A handbook of their history and characteristics*. R.L. Feller, ed. National Gallery of Art, Washington and Cambridge University Press. Cambridge, pp.17-46.

Bansa, H. 2002. 'Accelerated aging of paper: Some ideas on its practical benefit'. *Restaurator* 23, 106-117

Beltran. V., Druzic, J. and Maekawa, S., 2008. Poster abstract 'An extended investigation of the influence of oxygen on colour fading'. *ICOM-CC 15<sup>th</sup> Triennial Meeting*, I Braher. ed. London: James and James, pp.820.

Berric, B., 1997, *Artists' Pigments: a Handbook of their History and Characteristics*. E.W. Fitzhugh, ed. National Gallery of Art, Washington, pp.191-217.

Berson D. M., Dunn F. A. and Takao M. 2002 'Phototransduction by retinal ganglion cells that set the circadian clock'. *Science* 295, 1070.

Billmeyer, F. W., Saltzman, M., 2000. '*Principles of colour technology*'. R.S. Berns, ed. Wiley, New York.

Bowen, C., Mangum, B.J. and Montague, M., 2002. 'Pursuing the Fugitive: The User's Point of View: Micro-Fading Test Results and the Shaping of Exhibition Policy'. *The Broad Spectrum: Studies in The Materials Techniques and Conservation of Colour on Paper*, H.K. Stratis and B. Salvesen, eds. Archetype Publications, London, pp.245-251.

Brommelle, N.S., 1964. 'The Russell and Abney report on the action of light on water colours'. *Studies in Conservation*, 9, pp.140-152.

British Standards Institution, 1978. *Methods of test for colour fastness of textiles and leather, BS 1006: 1978*. BSI, London.

British Standards Institution, 1988. *Calculation of small colour differences, BS 6923:1988*. BSI, London.

Burns, R.S., Grum F., 1987. 'Exhibiting Artwork: Consider the Illuminating Source'. Presented at the Inter-society Color Council Conference Color:Then and Now,

Williamsburg, Virginia, 1985. *COLOR research and application*. Volume 12, Number 2, pp 63-72.

Burnstock, A., Lanfear, I., v.d. Berg K.J., 2005. 'Comparison of the fading and surface deterioration of red lake pigments in six paintings by Vincent van Gogh with artificially aged paint reconstructions'. *ICOM-CC14<sup>th</sup> Triennial Meeting Preprints*, I. Verger, ed. London: James and James, pp.459-466.

Caspers, C., 2008. *Reconstructing 19th -century British watercolour paint*. (Masters Thesis) Stichting Restauratie Atelier Limburg (SRAL). University of Amsterdam, The Netherlands.

Castillejo, M., Martin, M., Oujja, M., Santamaria, J., Silva, D., Torres, R., Manousaki, A., Zafirooulos, V., Van den brink, O.F., Heeren, R.M.A., Teule, R. and Silva, A., 2003. 'Evaluation of the chemical and physical changes induced by KrF laser irradiation of tempera paints'. *Journal of Cultural Heritage*, 4, pp.257–263.

Chappé, M., Hildenhagen, J., Dickmann, K., and Bredol, M., 2003. 'Laser irradiation of medieval pigments at IR, VIS and UV wavelengths'. *Journal of Cultural Heritage*, 4, pp.264–270.

Chenciner, R., 2000. *Madder Red: A history of luxury and trade*. Curzon Press, London.

Chevreul, M., 1837. 'Recherches chiniques sur la teinture'. *Mémoires de l'Académie Royale des Sciences de l'Institut de France*, 16, pp.41–116.

Commission Internationale de l'Éclairage, 1931. *Commission Internationale de l'Éclairage Proceedings*. Cambridge University Press, Cambridge.

Commission Internationale de l'Éclairage, 1986. *CIE 15.2, Colorimetry. 2<sup>nd</sup> ed*, Central de la Commission Internationale de l'Éclairage. Vienna, Austria.

Commission Internationale de l'Éclairage, 1987. *Recommendations on uniform colour spaces, colour difference equations, psychometric colour terms*. Supplement No.2 to CIE publication No 15 (E-2.3.1), 1971/(TC-1.3).

Commission Internationale de l'Éclairage, 1995 . *CIE 116–1995, Industrial Colour-Difference Evaluation*. Vienna: Bureau Central de la Commission Internationale de l'Éclairage.

Commission Internationale de l'Éclairage, 1995b. *CIE 13.3-1995, Method of Measuring and Specifying Colour Rendering Properties of Light Sources*. Vienna: Bureau Central de la Commission Internationale de l'Éclairage.

Commission Internationale de l'Éclairage, 2001. *CIE 142-2001, Improvement to Industrial Colour-Difference Evaluation*. Vienna: Bureau Central de la Commission Internationale de l'Éclairage.

Connors, S., Sandra, A., Whitmore, P.M., Keyes, R. and Coombs, E.I., 2005. 'The Identification and light sensitivity of Japanese woodblock print colourants: impact on art history and preservation'. *Scientific research on the pictorial arts of Asia: proceedings of the second Forbes Symposium at the Freer Gallery of Art*. P. Jett, J. Winter, B. McCarthy, eds. Archetype Publications, London, pp.35-47

Crews, P.C. 1987. 'The fading rates of some natural dyes'. *Studies in Conservation* 32, pp.65-72

Cuttle. C., 1988. 'Lighting works of art for exhibition and conservation'. *Lighting Research and Technology*, 20, pp.128-132.

Dowling J. E., 1987. *The retina: An Approachable Part of the Brain*. Harvard University Press, Cambridge, Massachusetts, 1987.

Duff, D.G., Sinclair, R.S. and Stirling, D., 1977. 'Light-induced colour changes of natural dyes'. *Studies in Conservation* 22: pp.161-9

Dupont. A.L., Constanza. C., Loisel. C., Bacci. M. and Lavédrine. B., 2008. 'Development of Lightcheck® Ultra: A novel dosimeter for monitoring lighting conditions of highly photosensitive artefacts in museums'. *Studies in Conservation*, 53, pp.49-72

Eastaugh, N., Walsh, V., Chaplin. T. and Siddall. R., 2004. *Pigment Compendium: A Dictionary of Historical Pigments*. Elsevier Butterworth- Heinemann.

Eikema Hommes, M. van, 2004. 'Changing Pictures'. *Discolouration in 15<sup>th</sup> - 17<sup>th</sup> Century Oil Paintings*. Burlington Magazine Publications Ltd, London.

- Feller. R.L., 1963. *Standards of Exposure to Light*. Bull American Group, IIC, 4.
- Feller, R. L., 1975. 'Speeding up photochemical deterioration'. *Bulletin de l'Institute royal du Patrimoine artistique*, 15, pp.135–50.
- Feller, R.L 1994. 'Accelerated aging: Photochemical and Thermal Aspects'. *Research in Conservation* 4, Getty Conservation Institute, Marina del Rey, CA.
- Feller. R.L., Johnston-Feller. R.M., 1997, *Artists' Pigments. A handbook of their history and characteristics*. E.W Fitzhugh, ed. National Gallery of Art, Washington and Cambridge University Press. Cambridge, pp.157-190.
- Fiedler,. I., Bayard, M.A., 1986. *Artists' Pigments. A handbook of their history and characteristics*. R.L Feller, ed. National Gallery of Art, Washington and Cambridge University Press. Cambridge, pp.65-108.
- Fiedler,. I., Bayard, M.A., 1997. *Artists' Pigments. A handbook of their history and characteristics*. E.W. Fitzhugh, ed. National Gallery of Art, Washington and Cambridge University Press. Cambridge, pp.219-271.
- Fitzhugh. E. W, 1986. *Artists' Pigments. A handbook of their history and characteristics*. R.W. Feller, ed. National Gallery of Art, Washington and Cambridge University Press. Cambridge, pp.109-189.
- Fitzhugh. E.W., 1997. *Artists' Pigments. A handbook of their history and characteristics*. E.W. Fitzhugh, ed., National Gallery of Art, Washington and Cambridge University Press. Cambridge, pp.47-79.
- Ford. B.L., 1992. 'Monitoring Colour Change in Textiles on Display'. *Studies in Conservation*, Vol. 37, No. 1 pp.1-11.
- Gettens. R.J., Feller. R.L. and Chase. W.T., 1993. *Artists' Pigments. A handbook of their history and characteristics*. Ashok Roy, ed. National Gallery of Art, Washington and Cambridge University Press. Cambridge,

Geuskens, G., 1975. 'Photodegradation of polymers'. *Chemical Kinetics*, Vol. 14: 333–424. C. H. Bamford, ed. Amsterdam: Elsevier.

Giles C.H., Cumming J.W. and A. E McEachran., 1956. 'A Study of the Photochemistry of Dyes on Proteins and other Substrates'. *Journal of the Society of Dyers and Colourists*, 72, pp.373.

Giles, C.H., McKay, R.B., 1963. 'The lightfastness of dyes: a review'. *Textile Research Journal*, 33, pp.528–577.

Giles, C.H., Shah, C.D., and Watts, W.E., 1972. 'Oxidation and reduction in light fading of dyes'. *Journal of the Society of Dyers and Colourists*, 88, 12, pp.433–435.

Gordon Sobott, R.J., Heinze, T., Neumeister, K. and Hildenhagen, J., 2003. 'Laser interaction with polychromy: laboratory investigations and on-site observations'. *Journal of Cultural Heritage*, 4, pp.276–286.

Hackney, S., 2006. 'The development of an anoxic framing system for the display of works of art on paper'. in S. Bradley and P. Fletcher, *The Science of Galleries*, London: Icon.

Harley. R.D., 2001. *Artists' Pigments C.1600-1835: A Study in English Documentary Sources*. 2<sup>nd</sup> ed. Archetype Publications, London.

Harrison, L. S., 1953. *Report on the deteriorating effects of modern light sources*. New York: Metropolitan Museum of Art.

Harrison A.W.C., 1957. *The manufacture of lakes and precipitated pigments*. 2<sup>nd</sup> ed. L. Hill, London.

Hattar S., Liao H.-W., Takao M., Berson D. M., and Yau K.-W. 2002 'Melanopsin-containing retinal ganglion cells: Architecture, projections, and intrinsic photosensitivity'. *Science* 295, 1065.

Heller, H., 1986. 'New Fatigue-Resistant Organic Photochromic Materials'. *Fine Chemical for the Electronics industry*, P. Bamfield, ed. Special Publication No 60 The Royal Society of Chemistry, Burlington House London W1V0BN, pp.120-135.

Helwig, K., 2007. *'Artists' Pigments. A handbook of their history and characteristics'*. B.H. Berrie, ed. National Gallery of Art, Washington and Cambridge University Press. Cambridge, pp.39-109.

Hihara, T., Okada, Y. and Morita, Z., 2002. 'Photo-oxidation and reduction of vat dyes on water-swollen cellulose and their lightfastness on dry cellulose'. *Dyes and Pigments* 53, pp.153–77.

Hilbert G.S., 1987 *Sammlungsgut in Sicherheit. Teil 2: Lichtschutz, Klimatisierung*, Gebr. Mann Verlag, Berlin 76.

ISO CIE 10527, 1991. *CIE standard colorimetric observers*. International Organisation for Standardisation, Geneva.

Johnston-Feller, R. M., 1986. 'Reflections on the phenomenon of fading'. *Journal Coatings Technology*, 58, pp.33–50.

Kenjo, T., 1980. 'Effects of different concentrations of oxygen on pigments used for cultural properties'. *Studies on the long-term conservation of cultural properties* (part 1). 2, pp.103-107. [In Japanese]

Kenjo, T., 1986. 'Certain deterioration factors for works of art and simple devices to monitor them'. *International Journal of Museum Management and Curatorship*, 5, pp.295-300.

Kenjo, T., 1987 'Discolouration of some red colours irradiated with some monochromatic lights'. *Science for Conservation*, 26, pp.31-34. [In Japanese]

Kirby, J., 1993. 'Fading and colour change of Prussian blue: occurrences and early reports'. *National Gallery Technical Bulletin*, 14, pp.63–71.

Kirby, J., White, R., 1996. 'The identification of red lake pigments dyestuffs and a discussion of their use'. *National Gallery Technical Bulletin*, 17, pp.56-80.

Kirby, J., Saunders, D., 2004. 'Fading and colour change of Prussian blue: Methods of Manufacture and Influence of Extenders'. *National Gallery Technical Bulletin*, 25, pp.73–99.

Kollman, T. M., Wood, D. G. M., 1980. 'The effect of variations in light intensity on the photo-oxidation of polypropylene'. *Polymer Engineering and Science*, 20, pp.684–87.

Korenberg, C., 2008. 'The photo-ageing behaviour of selected watercolour paints under anoxic conditions'. *British Museum Technical Bulletin*, 2, pp.49-57.

Kühn, H., 1967. 'The effect of oxygen, relative humidity and temperature on the fading rate of watercolours. Reduced light-damage in a nitrogen atmosphere', in *London Conference on Museum Climatology*, G. Thomson ed., IIC, London, pp.79–85.

Kühn, H., Curran, M., 1986. *Artists Pigments. A handbook of their history and characteristics*. R.L. Feller, ed. National Gallery of Art, Washington and Cambridge University Press. Cambridge, pp.187-218.

Laidler, K.J., 1984. 'The Development of the Arrhenius Equation'. *Journal of Chemical Education*, Vol 61, No 6, pp.494-98.

Lasareff, P.Z., 1912. *Physical Chemistry*. 78, pp.657.

Lavédrine, B., 1998. 'The Blue Pink Scale: a new light dosimeter for the exhibition of photographs and sensitive artefacts'. In: *Care of photographic moving image & sound collections*, York, England, 20th-24th July 1998. United Kingdom: Institute of Paper Conservation. pp.124-128.

Lavédrine, B., Gillet, M. Viénot, F., Garnier, C. and Mahler, É., 2006. 'L'Exposition de Photographies Anciennes en Couleurs', *Couleur & Temps- La Couleur en conservation et restauration*, 12es journées d'études de la SFIIC, Paris, pp.272-279

Leaver, I.H., 1980, 'Photo-oxidation and photoreduction of dyes in polymers'. N.S. Allen and J.F. McKellar, eds. *Photochemistry of Dyes and Pigmented Polymers*. London: Applied Science Publishers, pp.161–239.

Leene, J.E., Demeny, L., Elema, R.J., de Graff, A.J and Surtel, J.J., 1975. Interim reports on 'Artificial ageing of yarns' to the ICOM Conservation Committee at the meetings final report.

Lerwill, A., Townsend, J.H., Liang, H., Thomas, J. and Hackney. S., 2008. 'A Portable Micro-fading Spectrometer for Versatile Lightfastness Testing'. *e-preservation science*, 5, pp.17-28.

Leona, M., Winter, J., 2003. 'The identification of indigo and Prussian blue on Japanese Edo-period paintings'. *Studies using Scientific Methods: Pigments in Later Japanese Paintings*, Smithsonian Institution Freer Gallery of Art, Washington, pp.53–81.

Levison. H.W., 1976. *Artists' pigments: Lightfastness Tests and Rating*. COLOURLAB, Hirshfeld, Hallandale, Florida.

Lightcheck, 2010. *How to use Lightcheck*. [www.Lightcheck.co.uk/howto.htm](http://www.Lightcheck.co.uk/howto.htm), accessed 13/April/2010.

Luo, M.R., Cui, G. and Rigg. B., 2001. 'The development of the CIE 2000 Colour-difference formula: CIE $\Delta E_{2000}$ '. *Colour Research and Application*, 26, pp.340-350.

Maekawa, S., 1998. *Oxygen-Free Museum Cases*. Getty Conservation Institute, Los Angeles.

McLaren, K., 1956. 'The Spectral Regions of Daylight which cause Fading'. *Journal of the Society of Dyers and Colourists*, 72, pp.86-99.

Michalski, S., 1987. 'Damage to Museum Objects by Visible Radiation (Light) and Ultraviolet radiation (UV)'. *Lighting*, United Kingdom Institute for Conservation, pp.3-16.

Michalski, S., 1997. 'The lighting decision' in *Fabric ofan Exhibition: An Interdisciplinary Approach*. Canadian Conservation Institute, Ottawa 97-104.

Mills, J.S., White, R., 1994. *The organic Chemistry of museum objects*. Butterworth-Heinemann, Oxford.

Mühlethaler, Thissen., M.A. 1993. '*Artists' Pigments. A handbook of their history and characteristics*'. R.L. Feller, ed. National Gallery of Art, Washington and Cambridge University Press. Cambridge, pp.113-130.

National Bureau of Standards, 1951. *Preservation of the Declaration of Independence and the Constitution of the United States A report by the National Bureau of Standards to the Library of Congress*. National Bureau of Standards Circular 505

Neevel, H., 28/06/2007. 'Optimization of the micro-destructive lightfastness tester, the  $\mu$ fado'. *Minutes of the ICN Picture meeting*.

Neeval. H., 2008. Personal Communication.

Nicholson, C., and Ritzenthaler, M.L., 2005. 'The Declaration of Independence, The United States Constitution and Bill of Rights: scientific basis and practice of encasement'. *Art on Paper: Mounting and Housing*, J. Rayner, J. Kosek and B. Christensen, eds. Archetype, London 75–80.

Norville-Day, H., Townsend, J.H., and Johnston, F., 1994. 'A study of the effects of bleaching treatments on C19 pigments, with special reference to Turner's watercolour palette'. *IPC Conference Papers*, London 1997, J. Eagan, ed. Institute of Paper Conservation, Leigh, UK, pp.137–149.

Padfield, T. Landi, S., 1966. 'The Light-Fastness of the Natural Dyes'. *Studies in Conservation*, Vol. 11, No. 4, pp.181-196.

Pascoe, M.W., Skinner, C., 1994. 'Studies with sodium borohydride and hydrogen peroxide acting on artists' colours and pigments'. *Conservation of Historic and Artistic Works of Art on Paper: Symposium 88*, H. Burgess, ed. Canadian Conservation Institute, Ottawa, pp.209–213.

Petushkova. J.P., Lyalikova. N., 1986. 'Microbiological Degradation of Lead-Containing Pigments in Mural Paintings'. *Studies in Conservation*, 31(2): pp.65-69.

Pey, I., 1998. 'The Hafkenschied Collection. The 'sample book' of the Amsterdam paintware trader, Michiel Hafkenschied (1772-1846) from A(sphaltum) to Z(innober green)'. *Looking through Paintings. The study of Painting Techniques and Materials of Art Historical Research*, E. Hermes, ed. Baarn/London, pp.465-500.

- Porck, H. J., 2000. 'Rate of paper degradation: The predictive value of artificial aging tests'. Amsterdam: European Commission on Preservation and Access.
- Pouli, P., Emmony, D.C., Madden, C.E. and Sutherland, I., 2003. 'Studies towards a thorough understanding of the laser-induced discolouration mechanism of medieval pigments'. *Journal of Cultural Heritage*, 4, pp.271–275.
- Pretzel, B. 2000. 'Determining the colour fastness of the Bullerswood carpet'. A. Roy and P. Smith, eds. *Tradition and innovation: advances in conservation*. London: IIC, 150–154.
- Pretzel, B., 2008, 'Now you see it, now you don't: lighting decisions for the Ardabil carpet based on the probability of visual perception and rates of fading'. Bridgland, J. ed. *Pre-prints of ICOM-CC: 15th Triennial Conference New Delhi*, 22-26 September 2008. New Delhi: Allied Publishers PVT. pp. 759- 765.
- Reiche, I., Vignaud, C. and Menu, M., 2002. 'The crystallinity of ancient bone and dentine: New insights by transmission electron microscopy'. *Archaeometry*, pp.447-459.
- Romich, H., Martin, G., 2003. 'LiDo: A light dosimeter for monitoring cultural heritage'. *V&A Conservation Journal*, 43, Spring 2-3.
- Rowe, S., 2004 'The effect of insect fumigation by anoxia on textiles dyed with Prussian blue'. *Studies in Conservation*, 49, pp.259–270.
- Russell, W., Abney, W. de., 1888. *Action of light on watercolours*. Report to the Science and Art Department of the Committee of Council on Education, HMSO, London.
- Salter, T.W., ed. 1869. *Field's Chromatography; or Treatise on colours and pigments as used by artists*. Winsor and Newton, London.
- Sandahl, M.D.F., 2009. *En undersøgelse af digitale tryks farvestabilitet med særligt fokus på Micro Fading-metodens anvendelsesmuligheder*. Masters thesis. School of Conservation, The Royal Danish Academy of Fine Art, Copenhagen.

Saunders, D., Kirby, J., 1994a. 'Wavelength-dependent fading of artists' pigments', *Preventive Conservation: Practice, Theory, and Research*. A. Roy and P. Smith, eds. London: IIC, London, pp.190–194.

Saunders, D., Kirby, J., 1994b. 'Light-induced colour changes in red and yellow lake pigments'. *National Gallery Technical Bulletin*, 15, pp.79–97.

Saunders, D., Kirby, J., 1996. 'Light-induced damage: investigating the reciprocity principle'. *Archaeological Conservation and its Consequences, Preprints of the ICOM-CC 11th Triennial Meeting*, Edinburgh, ICOM-CC, Paris, pp.87-90.

Saunders, D., Kirby, J., 2001. 'A comparison of light-accelerated ageing regimes in some galleries and museums'. *The Conservator*, 25, pp.95-104.

Saunders, D., Spring, M. and Higgitt, C., 2002. 'Colour change in red lead-containing paint films'. *ICOM-CC 13th Triennial Meeting*, Rio de Janeiro, R. Vontobel ed. James and James, London, pp.455–463.

Saunders, D., Kirby, J., 2009. 'A comparison of light-induced damage under common museum illuminants'. *ICOM-CC 15th Triennial Meeting Preprints*. J. Bridgland, ed. London: James and James, pp.766-774.

Schaeffer, T.T., 2001 *Effects of light on Materials in Collections: Data on Photoflash and Related sources*. Getty Conservation Institute, California.

Schweppe, H., and Rooosen-Runge, H., 1986. *Artists' Pigments. A handbook of their history and characteristics*. R.L Feller ed. National Gallery of Art, Washington and Cambridge University Press. Cambridge, pp.255-283.

Scott, T.J., 1887. *A Descriptive Handbook of Modern Water-Colour Pigments Illustrated with Seventy-two Colour Washes Skillfully (sic) Gradated by Hand on Whatman's Drawing Paper. With an Introductory Essay on the Recent Water-colour Controversy*. London: Winsor & Newton Limited.

Shaw, M., Fairchild, M., 2002. 'Evaluating the 1931 CIE Colour-Matching Functions'. *Colour Research and application*, 27, pp.316-329.

Smith, P.J., 1991. 'Photofading of pigments and photosensitiser materials'. *Journal of the Society of Dyers and Colourists*, 107, pp.282.

Tennent. N., Townsend. J.H., 1987. 'Light dosimeters for Museums Galleries and Historic houses'. *Lighting*, United Kingdom Institute for conservation, pp.31-35.

Thomas, J., Hackney, S., Townsend, J.H., 2009. '*Anoxic Frames at Tate*'. Showcases Inside Out, Porto 24-26 May.

Thomas, J., 2011. *Heritage Degradomics, High-Throughput GC-MS and Degradation Studies on Watercolours*. doctoral thesis in preparation, Department of Chemistry, University College London.

Thomson G., 1964. 'Impermanence – Some Chemical and Physical Aspects'. *Museums Journal*, Vol 64, No 1, pp.32.

Thomson, G., 1965. 'Topics in the conservation chemistry of surfaces, Application of Science in examination of works of art'. *Proceedings of the seminar*, Museum of fine arts, Boston, Mass, pp.78-85.

Thomson, G., 1967. 'Annual exposures within museums'. *Studies in Conservation* 12, pp.26–35.

Thomson, G., 1978. *The Museum Environment*.. The Butterworth series on conservation in the arts, archaeology and architecture, Butterworth & Co , London and Boston.

Townsend., J.H., 1993. 'The materials of J.M.W.Turner: Pigments', *Studies in Conservation* 38, pp.231-254.

Townsend, J., Thomas, J., Hackney, S. and Lerwill A., 2008. 'The benefits and risks of anoxic display for colourants'. *Conservation and Access*, D. Saunders, J.H. Townsend and S. Woodcock, eds. London: IIC, pp.76-81.

Townsend, J.H., Thomas, J., Caspers, C., Pis Marcos, M., Ormsby, B., Lerwill, and Hackney, S., A., 2009. '(De/Re) Constructing Turner for research projects at Tate'. *Sources and Serendipity*. E. Hermens and J.H. Townsend, eds. London: Archetype, 159-162.

Townsend, J.H., 2009. *Traditional watercolour pigments used for anoxic research*. unpublished analysis report, Tate Conservation Dept.

Ware, M., 1999a. 'Cyanotypes: their history, chemistry and conservation'. *Care of Photographic, Moving Image and Sound Collections Postprints*, S. Clark, ed. Institute of Paper Conservation, Leigh, UK, pp.115–123

Ware, M., 1999b. *Cyanotype : the History, Science and Art of Photographic Printing in Prussian blue*. Science Museum, London and National Museum of Photography, Film and Television, Bradford.

Ware, M., 2003. 'A blueprint for conserving Cyanotypes'. *Presented at the 30th AIC Annual Meeting, Topics in Photographic Preservation*, pp.10.

Watkins, P.W., 1978. *Physical Chemistry*. Oxford University Press, Walton Street, Oxford.

Watson, V., Clay, H.F., 1955. 'The lightfastness of lead chromate pigments'. *Journal of the Oil and Colour Chemists' Association*, Vol 38, (4), pp.167–177.

Weber, F.W., 1923. *Artists' pigments: their chemical and physical properties*. New York.: Van Nostrand. D

Whitmore, P.M., Pan, X. and Baillie, C., 1999. 'Predicting the fading of objects: Identification of fugitive colourants through direct nondestructive lightfastness measurements', *Journal of the American Institute of Conservation*, 38, pp.395-409.

Whitmore, P.M., Baillie, C. and Connors, S.A., 2001 'Micro-fading tests to predict the result of exhibition: progress and prospects'. *Tradition and Innovation: Advances in Conservation*. A. Roy and P. Smith, eds. International Institute for Conservation, London, pp.200-20.

Whitmore, P.M., 2002. 'Pursuing the Fugitive: Direct Measurement of Light Sensitivity with Micro-fading Tests'. *The Broad Spectrum: The Art and Science of Conserving Coloured Media on Paper*, H. K. Stratis and B. Salvesen, eds, Archetype Publications, London, pp.241-243.

Wilhelm, H., 1993. *The permanence and care of colour photographs: traditional and digital colour prints, colour negatives, slides, and motion picture*. Grinnell, Iowa: Preservation Publishing Company.

Winter, J. and FitzHugh, E.W., 2007. *Artists' Pigments. A handbook of their history and characteristic*. B. Berrie, ed. National Gallery of Art, Washington and Cambridge University Press. Cambridge, pp.1-37.

Wyszecki G. and Stiles W. S., 2000. *Color Science – Concepts and Methods, Quantitative Data and Formulae*. 2nd edition, John Wiley and Sons, New York.

# Appendix

## A Parts list

Item name / product	Code (if applicable)	Qty	Cost Total in 1999	Supplier address
Metric Single Axis Translation Stage	PT1/M	2	£336.15	www.thorlabs.com
PT-Series Angle Bracket	PT102/M	1	£44.55	www.newport.com
Translation stage mount	PT101	1	£10.13	www.thorlabs.com
Motorised single axis translation stage	PT1/M-Z6	1	£381.38	www.thorlabs.com
ASTD T-Cube DC Servo Controller	TDC001	1	£337.50	www.thorlabs.com
T-cube 15V Power supply	TPS001	1	£13.50	www.thorlabs.com
Matched Achromatic Pairs	MAP105075-A1	2	£270	www.thorlabs.com
SM1 to SMA Fiber adapter	SM1SMA	2	£39	www.newport.com
SM1 lens tube 3" long (one SMIRR included 1 inch diameter)	SMIL30	2	£39	www.thorlabs.com
Set of 4 swivel couplers	C2A	1	£208	www.thorlabs.com
30mm cage plate 1" threaded	CP02	2	£24.68	www.thorlabs.com
Cage assembly rod 3" 6mm	ER3	4	£26.12	www.thorlabs.com
Cage assembly rod 8" 6mm	ER8	4	£29.84	www.thorlabs.com
HPX2000 Lightsource	HPX2000	1	£3,112.00	www.thorlabs.com
Mounting cube with clearance holes	C6W	2	£88.50	www.thorlabs.com
Avantes Model AvaSpec-2048 Fiber Optic Spectrometer	AvaSpec-2048	1	£1,511	www.avantes.com
UV Detector Coating	DUV	1	£169	www.avantes.com
Order Sorting Coating	OSC	1	£104	www.avantes.com
Slit-50	Slit	1	£104	www.avantes.com
Detector Collection Lens	DCL-UV/VIS	1	£90.00	www.avantes.com
Solarization resistant optical fiber	P600-2-SR	2	£240.00	www.thorlabs.com
Extended Hot Mirror	EHR-1.00	1	£59	www.cvilaser.com
Optical Breadboards Performance Series I Breadboard - 600x300x60mm	PBH51502	1	£296.00	www.thorlabs.com
150 mm Travel, Light-Duty, Motorized Linear Stage (Metric)	NRT150/M	2	£2548.94	www.thorlabs.com
3 Unmounted Ø1" Absorptive ND Filters	NE10B, NE20B NE30B	3	£83.25	www.thorlabs.com
APT Benchtop 2-Ch Stepper Motor Controller	MST601	1	£1,249.20	www.thorlabs.com

## B. Accuracy measurements

This data set is summarised in table 1 in section 2.4. Note that the standard deviation provided is an equivalent standard deviation due to the data not displaying a normal distribution. This is calculated by dividing the maximum value of deviation by the cube root of 3.

Testing different locations on the same sample and refocusing at each location.

		Smooth							
		L*	a*	b*	$\Delta L$	$\Delta a$	$\Delta b$	$\Delta E_{ab}^*$	$\Delta E_{00}$
		99.95	0.03	-0.02	0	0	0	0	0
		99.98	0.18	-0.09	0.03	0.15	0.07	0.17	0.23
		99.9	0.18	-0.32	-0.05	0.15	0.3	0.34	0.37
		100.22	0.19	-0.11	0.27	0.16	0.09	0.33	0.3
		100.22	0.07	-0.09	0.27	0.04	0.07	0.28	0.18
		100.36	0.06	-0.04	0.41	0.03	0.02	0.41	0.24
		100.4	0.13	-0.08	0.45	0.1	0.06	0.46	0.3
		100.47	0.15	-0.11	0.52	0.12	0.09	0.54	0.36
		100.53	0.11	-0.1	0.58	0.08	0.08	0.59	0.36
		100.55	0.14	-0.08	0.6	0.11	0.06	0.61	0.38
Maximum		100.55	0.19	-0.02	0.6	0.16	0.3	0.61	0.38
Std dev					0.42	0.11	0.21	0.42	0.26
		Diffuse							
		L*	a*	b*	$\Delta L$	$\Delta a$	$\Delta b$	$\Delta E_{ab}^*$	$\Delta E_{00}$
		99.87	0.07	-0.31	0	0	0	0	0
		99.75	0.13	-0.27	-0.12	0.06	-0.04	0.14	0.12
		99.64	0.07	-0.65	-0.23	0	0.34	0.41	0.36
		99.3	-0.03	-0.22	-0.57	-0.1	-0.09	0.59	0.37
		100.01	0.01	-0.17	0.14	-0.06	-0.14	0.21	0.18
		100.19	0.09	-0.56	0.32	0.02	0.25	0.41	0.31
		99.09	0.01	-0.54	-0.78	-0.06	0.23	0.82	0.51
		100	-0.1	-0.25	0.13	-0.17	-0.06	0.22	0.27
		100.63	0.1	-0.46	0.76	0.03	0.15	0.78	0.46
		99.29	-0.11	-0.11	-0.58	-0.18	-0.2	0.64	0.47
Maximum		100.63	0.13	-0.11	0.78	-0.18	0.34	0.82	0.51
Std dev					0.54	0.12	0.24	0.57	0.35

Whatman Filter Paper

	L*	a*	b*	$\Delta L$	$\Delta a$	$\Delta b$	$\Delta E_{ab}^*$	$\Delta E_{00}$
	99.99	-0.02	0	0	0	0	0	0
	97.86	0.17	0.41	-2.13	0.19	-0.41	2.18	1.33
	98.13	0.15	0.09	-1.86	0.17	-0.09	1.87	1.1
	103.31	0.14	-0.89	3.32	0.16	0.89	3.44	2.08
	100.17	-0.04	0.62	0.18	-0.02	-0.62	0.65	0.62
	97.02	0.22	0.21	-2.97	0.24	-0.21	2.99	1.77
	95.7	0.5	-0.1	-4.29	0.52	0.1	4.32	2.62
	98.81	0.09	0.12	-1.18	0.11	-0.12	1.19	0.7
	92.1	0.34	-0.6	-7.89	0.36	0.6	7.92	4.74
	103.95	0.25	-0.38	3.96	0.27	0.38	3.99	2.29
Maximum	103.95	0.5	0.62	-7.89	0.52	0.89	7.92	4.74
Std dev				5.47	0.36	0.62	5.49	3.28

Stationary probe repeat measurements

Smooth

	L*	a*	b*	$\Delta L$	$\Delta a$	$\Delta b$	$\Delta E_{ab}^*$	$\Delta E_{00}$
	100.1	0	-0.08	0	0	0	0	0
	100.12	-0.01	-0.04	0.02	-0.01	-0.04	0.05	0.04
	100.14	-0.02	0.01	0.04	-0.02	-0.09	0.1	0.1
	100.14	-0.01	-0.03	0.04	-0.01	-0.05	0.06	0.06
	100.15	-0.02	-0.02	0.05	-0.02	-0.06	0.08	0.07
	100.16	0	-0.02	0.06	0	-0.06	0.08	0.07
	100.15	0	-0.04	0.05	0	-0.04	0.06	0.05
	100.17	0	-0.02	0.07	0	-0.06	0.09	0.07
	100.14	0.01	0	0.04	0.01	-0.08	0.09	0.08
	100.14	0.02	-0.06	0.04	0.02	-0.02	0.05	0.04
Maximum	100.17	0.02	0.01	0.07	0.02	-0.08	0.1	0.1
Std dev				0.04	0.01	0.05	0.06	0.07

Diffuse

	L*	a*	b*	$\Delta L$	$\Delta a$	$\Delta b$	$\Delta E_{ab}^*$	$\Delta E_{00}$
	98.19	0.02	0.54	0	0	0	0	0
	98.19	-0.02	0.6	0	-0.04	-0.06	0.07	0.08
	98.18	-0.02	0.6	-0.01	-0.04	-0.06	0.07	0.08
	98.17	0	0.6	-0.02	-0.02	-0.06	0.07	0.07
	98.17	0.02	0.58	-0.02	0	-0.04	0.04	0.04
	98.18	-0.03	0.58	-0.01	-0.05	-0.04	0.06	0.08
	98.18	0.03	0.55	-0.01	0.01	-0.01	0.02	0.2
	98.19	0.01	0.61	0	-0.01	-0.07	0.07	0.07
	98.17	0	0.6	-0.02	-0.02	-0.06	0.07	0.07
	98.18	0.06	0.56	-0.01	0.04	-0.02	0.05	0.06
Maximum	98.19	0.06	0.61	-0.02	-0.05	-0.07	0.07	0.2
Std dev				0.01	0.03	0.05	0.05	0.14

Whatman filter paper

	L*	a*	b*	$\Delta L$	$\Delta a$	$\Delta b$	$\Delta E^*_{ab}$	$\Delta E_{00}$
	100	0	0.01	-0.01	0.02	0	0.02	0
	100	0	0.04	-0.01	0.02	0.03	0.03	0.03
	100.01	-0.03	0.06	0	-0.01	0.05	0.05	0.07
	99.98	-0.04	0.02	-0.03	-0.02	0.01	0.03	0.06
	100	0	-0.05	-0.01	0.02	-0.06	0.06	0.06
	100	0	-0.05	-0.01	0.02	-0.06	0.06	0.06
	100	-0.01	0.03	-0.01	0.01	0.02	0.03	0.02
	99.98	0	-0.01	-0.03	0.02	-0.02	0.04	0.02
	99.98	0	-0.01	-0.03	0.02	-0.02	0.04	0.02
	100	-0.03	0	-0.01	-0.01	-0.01	0.02	0.05
Maximum	100.01	0	0.06	-0.03	0.02	0.05	0.06	0.07
Std dev				0.02	0.01	0.03	0.04	0.05

Remaining in a 6.67dE colour well and taking repeat readings

	L*	a*	b*	$\Delta L$	$\Delta a$	$\Delta b$	$\Delta E^*_{ab}$	$\Delta E_{00}$
	90.85	-5.18	36.43	0	0	0	0	0
	90.84	-5.16	36.39	0.01	-0.02	0.04	0.05	0.02
	90.85	-5.14	36.41	0	-0.04	0.02	0.04	0.03
	90.84	-5.14	36.38	0.01	-0.04	0.05	0.06	0.03
	90.83	-5.17	36.42	0.02	-0.01	0.01	0.02	0.01
	90.83	-5.17	36.45	0.02	-0.01	-0.02	0.03	0.02
	90.82	-5.13	36.38	0.03	-0.05	0.05	0.08	0.04
	90.84	-5.16	36.43	0.01	-0.02	0	0.02	0.02
	90.84	-5.17	36.41	0.01	-0.01	0.02	0.02	0.01
	90.83	-5.15	36.39	0.02	-0.03	0.04	0.05	0.03
Maximum	90.85	-5.13	36.45	0.03	-0.04	0.05	0.08	0.04
Std dev				0.02	0.03	0.03	0.06	0.03

Returning to the same spot many times using XYZ stage

	L*	a*	b*	$\Delta L$	$\Delta a$	$\Delta b$	$\Delta E^*_{ab}$	$\Delta E_{00}$
	100.02	-0.04	0.04	0	0	0	0	0
	100.04	-0.01	0.06	0.02	0.03	-0.02	0.04	0.05
	100.03	0.04	0.02	0.01	0.08	0.02	0.08	0.12
	100.04	0.02	0.02	0.02	0.06	0.02	0.07	0.09
	100.04	0	0.02	0.02	0.04	0.02	0.05	0.06
	100.05	0.03	0.06	0.03	0.07	-0.02	0.08	0.11
	100.05	0.04	0.06	0.03	0.08	-0.02	0.09	0.12
	100.03	0.04	0.04	0.01	0.08	0	0.08	0.12
	100.03	0.07	0.06	0.01	0.11	-0.02	0.11	0.17
	100.07	0.09	0.08	0.05	0.13	-0.04	0.14	0.2
Maximum	100.07	0.09	0.08	0.05	0.13	-0.04	0.14	0.2
Std dev				0.03	0.09	0.03	0.1	0.13



### C. Modeling of the fading of Prussian blue

The fading of Prussian blue pigment (TTB6) can be modeled as an exponential rise to maximum following the equation;

$$\Delta E_{ab}^* = \alpha(1 - e^{-\beta t})$$

Where;

$t$  is the time in hours since the reversion process began.

$\Delta E_{ab}^*$  is the colour difference of the pigment relative to original colour.

$\beta$  and  $\alpha$  are connected with the rate of fading obtained via a best fit of  $\Delta E_{ab}^*$  vs.  $t$ .

An example of a fit of the equation to a fading curve can be found in figure A below where the coloured lines are the fit to the data lines plotted in black:

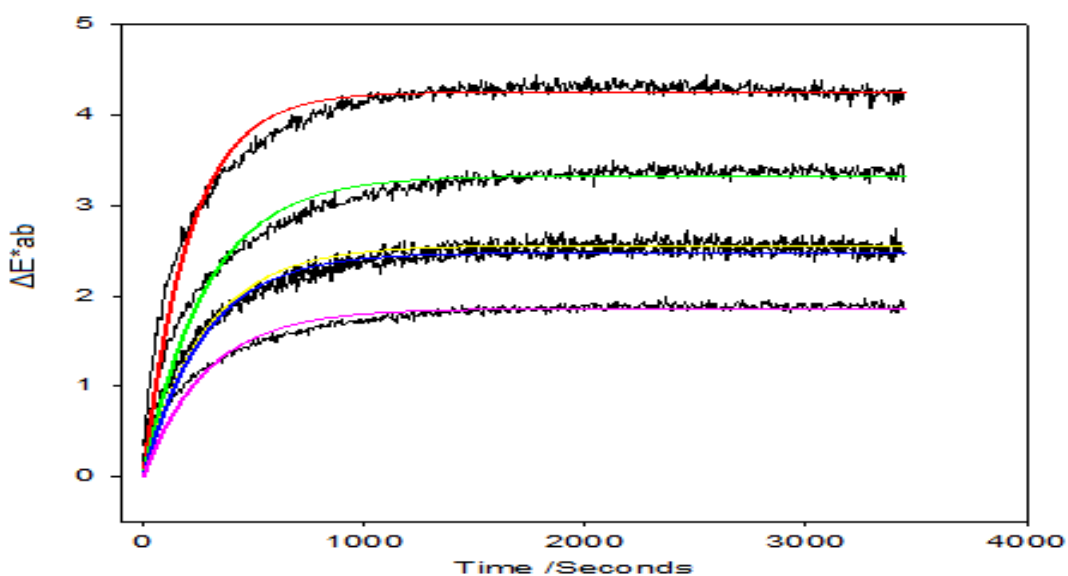


Figure A. The result of the application of the equation to 5 individual fading curves for Prussian blue (TTB6).

Data resulting from the application of the equation to the curve is shown below.

Plot	R <sup>2</sup>	$\alpha$	$\beta$
Red line	0.98 ± 0.95	4.250 ± 0.006	0.0048 ± 5.519E-005
Green line	0.98 ± 0.95	3.324 ± 0.006	0.0035 ± 4.113E-005
Yellow line	0.98 ± 0.97	2.557 ± 0.004	0.0036 ± 3.614E-005
Blue line	0.98 ± 0.96	2.475 ± 0.004	0.0036 ± 3.850E-005
Purple line	0.97 ± 0.94	1.858 ± 0.004	0.0035 ± 4.225E-005

Table A. R-Squared value indicated how well the line approximates to the data points. The standard errors associated with the corresponding values are also shown

#### D. Reversion plots of Prussian blue sample

Plots of the results as discussed in section 4.2.6. A large spread of results were obtained thought due to variation in the sample under test and the small sampling area of the instrument.

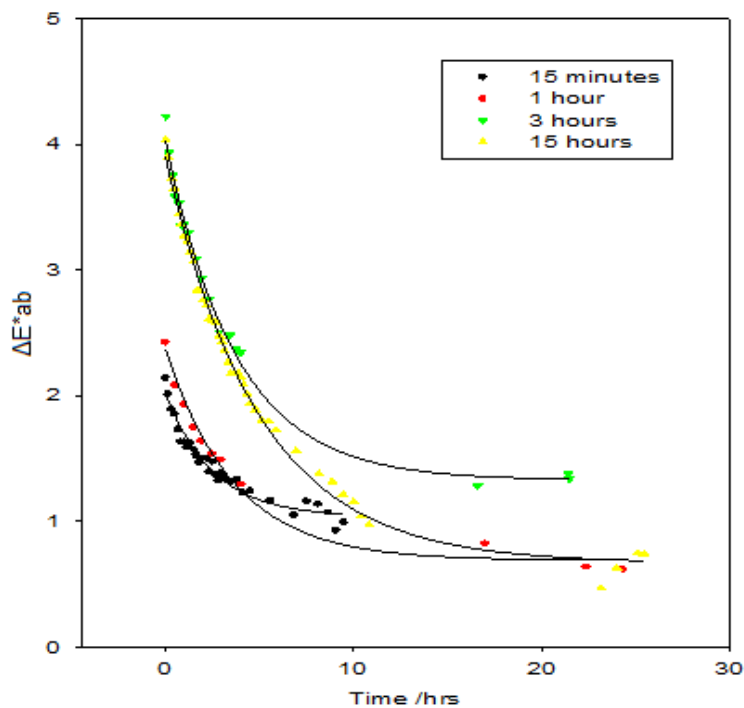


Figure B. The colour loss reversion characteristic of the Prussian blue (TTB6) sample in 21% oxygen.

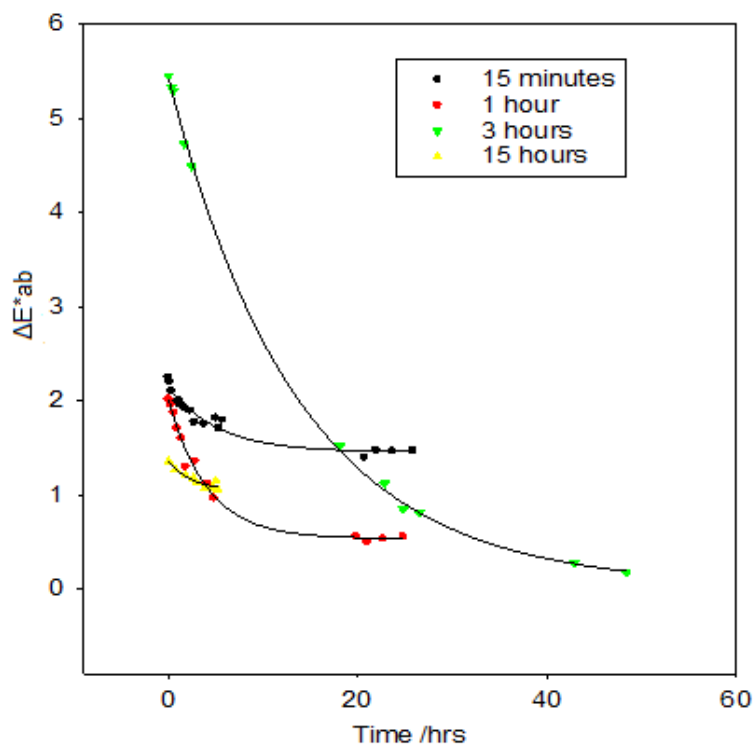


Figure C. The colour loss reversion characteristic of the Prussian blue (TTB6) sample in 10% oxygen.

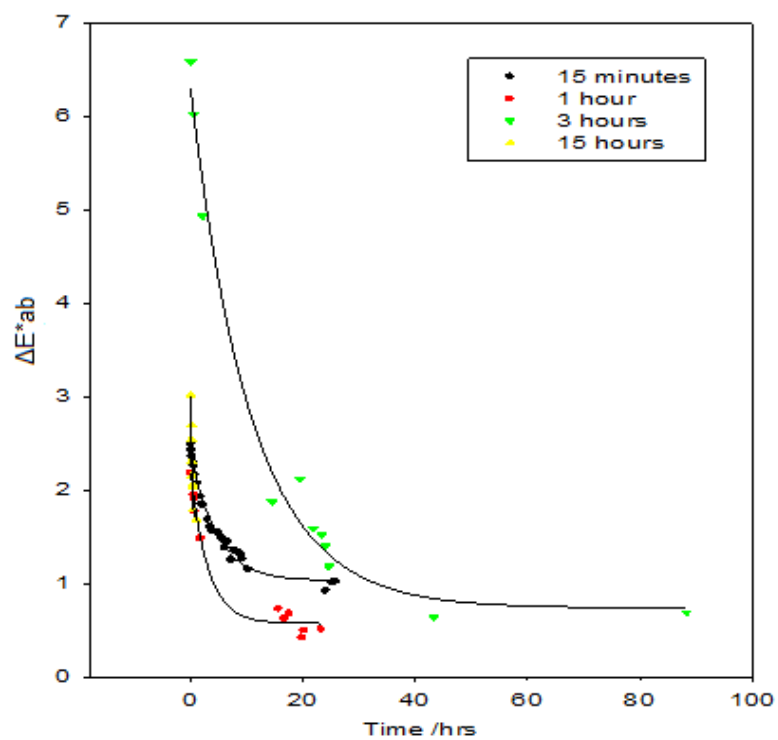


Figure D. The colour loss reversion characteristic of the Prussian blue (TTB6) sample in 5% oxygen.

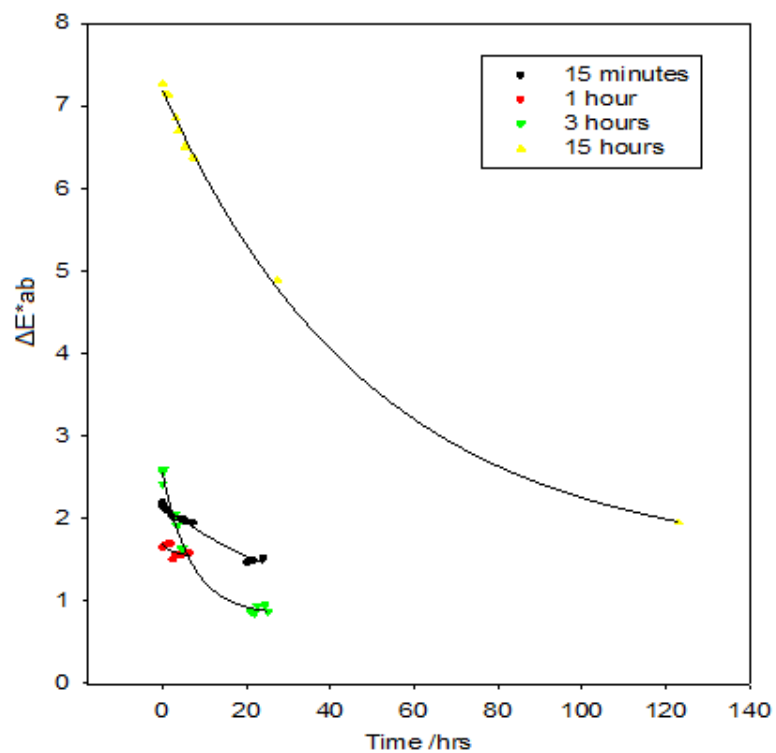


Figure E. The colour loss reversion characteristic of the Prussian blue (TTB6) sample in 3.5% oxygen.

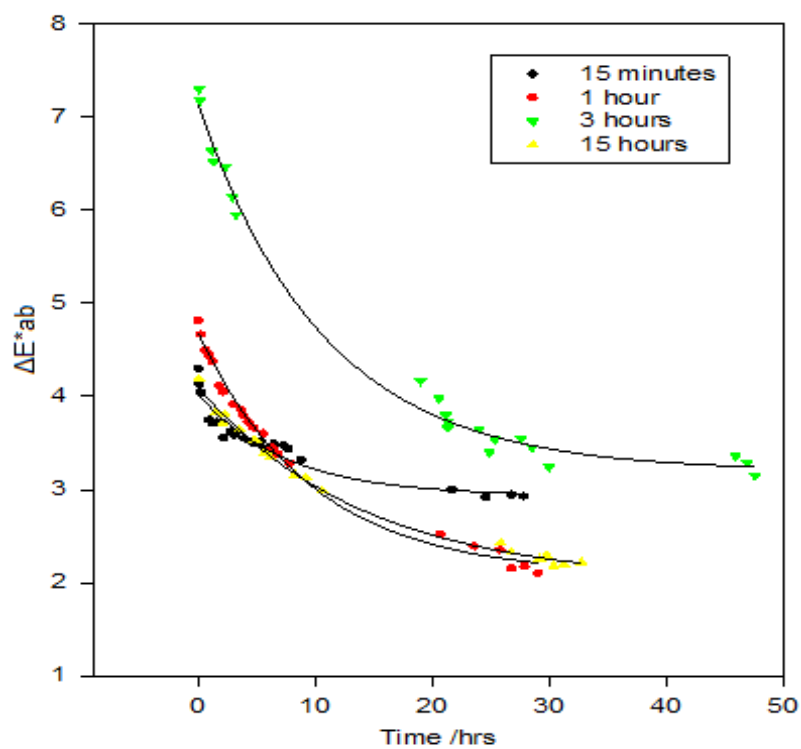


Figure F. The colour loss reversion characteristic of the Prussian blue (TTB6) sample in 2% oxygen.

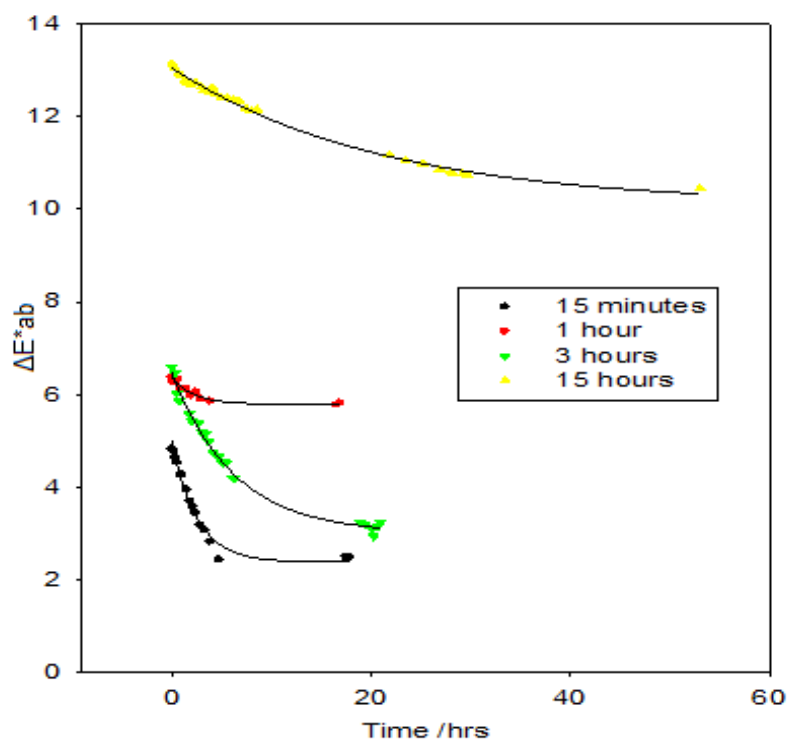


Figure G. The colour loss reversion characteristic of the Prussian blue (TTB6) sample in anoxic conditions.

## E. Pigment samples: sources and suppliers

Samples tested in this thesis were collected by Drs Charlotte Caspers, who researched surviving English watercolour recipes used by the colourmen Winsor & Newton and Roberson. Drs Caspers used the recipes to create historically accurate reconstructions of 19th-century watercolour paints. The pigments were provided from a variety of helpful sources: Martin Bijl (a private conservator in the Netherlands); Margriet van Eikema Hommes (a researcher at The University of Amsterdam (UvA), The Instituut Collectie Nederland (ICN), Amsterdam, Jeff Parkes (a private collector in the UK), The Museum of London, The National Gallery, London, Oud Holland Ltd, Zeist, the Netherlands, Tate, The Teylers Museum, Haarlem, the Netherlands, Renate Woudhuysen-Keller (specialist in producing lakes and conservator at the Hamilton Kerr Institute, University of Cambridge, UK (HKI)).

The pigments used in this research and the results of energy-dispersive X-ray analysis by Dr Joyce Townsend, senior conservation scientist, Tate, and in some case FTIR microscopy by Sarah Styler, Tate conservation science intern 2008-09, are summarised in the following tables. More pigments were supplied by many of the providers. For more information see Caspers (2008) and a Tate analysis report (Townsend 2009).

### Provided by Martin Bijl, the Netherlands

An Ackermann box dated around 1850.

Code	Pigment	Results of analysis
MB A1	Prussian blue	Prussian blue confirmed
MB A2	Prussian green	probably includes Prussian blue; yellow pigment has no ID
MB A3	Gamboge	gamboge was confirmed
MB A4	Brown pink	not a laked pigment
MB A5	Antwerp blue	neither Antwerp blue nor Prussian blue; not identified
MB A6	Indigo	synthetic indigo: later than 19th century onwards, not 1850
MB A7	Vermilion	vermilion confirmed

A Bourgeois Aîné box dated between 1876-79.

Code	Pigment	Results of analysis
MBBA1	Prussian blue	Prussian blue and gypsum
MBBA2	Prussian green	Prussian blue and zinc white and barium chromate
MBBA3	Vermilion	zinc white, calcium sulphate

Some small boxes, from *Huis weldijk* in Alkmaar. They cannot be dated with great certainty at around 1850.

Code	Pigment	Results of analysis
MB1	Prussian blue	Prussian blue and alumina
MB2	Blue	ultramarine
MB3	Smalt	not analysed

A dry pigment from the studio of M. Bijl dated before 1945.

Code	Pigment	Results of analysis
MB9	Prussian blue	Prussian blue confirmed

#### Provided by Margriet van Eikema Hommes, Amsterdam

Two modern indigo pigments used in research by van Eikema Hommes (2004) were sampled for the anoxic project (an indigo from Kremer and indigo from *Verfmolen de Kat*).

Code	Pigment	Results of analysis
MvEH1	Indigo 2	indigo plus kaolin or silica
MvEH2	Indigo 1	indigo

#### Provided by the Hamilton Kerr Institute (HKI), Cambridge

Dry pigments from the Roberson Archive, probably from the first half of the 20<sup>th</sup>-century were provided.

Code	Pigment	Results of analysis
HKI 1	Prussian blue	unusually K-rich Prussian blue
HKI 2	Prussian blue	Prussian blue with alumina extender
HKI 3	Antwerp blue	Prussian blue with large amounts of alumina extender
HKI 4	Prussian blue	Prussian blue
HKI 5	Prussian blue	Prussian blue
HKI 16	Zinc white	zinc white

#### Provided by the Instituut Collectie Nederland (ICN), Amsterdam

The ICN-reference collection of red lakes provided a number of dry pigments. The samples were prepared in an investigation of the materials and methods of Vincent van Gogh, see Burnstock *et al.* (2005).

Code	Pigment	Results of analysis
RC-ICN-M2	Kopp's purpurine	madder or alizarin on an Alum-based substrate
RC-ICN-B2	Brazil on potas	non-madder lake on Alum-based substrate
RC-ICN-BM	Brazilwood and madder	non-madder lake on Alum-based substrate
RC-ICN-C1	Cochineal on Alum	non-madder lake on Alum-based substrate

Pigments were also taken from the *Schoonman* collection, (dated between 1920 and 1970).

Code	Pigment	Results of analysis
RC-ICN-1	Prussian blue	Prussian blue confirmed
RC-ICN-2	Chinese blue	K-rich Prussian blue
RC-ICN-3	indigo	indigo confirmed
RC-ICN-7	English vermilion	not genuine, red iron oxide and calcium sulphate
RC-ICN-8	vermilion 4	vermilion confirmed
RC-ICN-9	gamboge	genuine gamboge

#### Provided by the Museum of London, London

Zinc white watercolour cakes were taken from a number of boxes of different dates. Analysis confirmed the pigments were zinc white.

Code	Pigment	Date	Source
MoL 1	Zinc white	Early 20th Century	Museum of London, Roberson vial
MoL 2	Chinese white	After 1845	Museum of London, Winsor and Newton cake
MoL 3	Chinese white	1841 to 1850	Museum of London, Newman cake

#### Provided by the National Gallery, London

The National Gallery donated a very large number of samples through Jo Kirby who prepared most of the lake pigments using traditional recipes. An Ackermann paint box, from the National Gallery's collection which was the former property of Queen Victoria, dated between 1796 and 1827 was supplied.

Code	Pigment	Results of analysis
NG WC1	Prussian blue	Prussian blue and alumina
NG WC2	Antwerp blue	Prussian blue with alumina extender
NG WC3	gamboge	genuine gamboge
NG WC4	Ackermann's yellow	quercitron on alumina
NG WC5	gallstone	may be genuine

NG WC6	Indian yellow	genuine Indian yellow
NG WC7	dragon's blood	genuine dragon's blood
NG WC8	Pale Neutral Tint	bone black, iron oxide and/or Prussian blue or indigo.
NG WC9	Bister	not analysed
NG WC10	Prussian green	Prussian blue and gamboge with extenders
NG WC11	vermilion	vermilion
NG WC12	red orpiment	orpiment
NG WC13	King's yellow	orpiment

Dry pigments were provided and generally these were prepared by National Gallery scientists, in the last quarter of the 20<sup>th</sup> century.

<b>Code</b>	<b>Pigment</b>	<b>Date</b>	<b>Results of analysis</b>
NG1	gamboges	1851	gamboge
NG2	weld on alum	July/93	weld on alum
NG3	weld lake	08/09/1989	weld on Ca with some alum present
NG4	Indian yellow	1965	not genuine, lead chromate
NG5	buckthorn lake alum/Ca	1993	buckthorn on Ca and less alum
NG6	buckthorn lake on alum	1993	buckthorn on alum sulfate
NG7	yellow lake/fustic lake	03/08/1972	fustic on alum based substrate
NG8	quercitron lake	24/07/1972	quercitron on alum
NG9	brazilwood	01/09/2005	probably brazilwood, with alumina
NG10	logwood	14/07/1972	brazilwood and alumina
NG11	sap green lake	24/10/1989	sap green on alum (KAlSO <sub>4</sub> )

Also supplied was a collection of Prussian blue and lake paint-outs for experimental purposes see Saunders and Kirby (1994a) (1994b) and Kirby and Saunders (2004). In this case the paper substrate of the National Gallery paint-outs were different from the substrate used for the historically accurate reconstructions made at Tate.

These samples were prepared on Whatman Silversafe paper, an unbuffered paper consisting of 100% cotton fibre sized with a neutral ketene dimer which results in the formation of a hydrophobic ester.

<b>Code</b>	<b>Pigment</b>	<b>Date</b>	<b>Results of analysis</b>
NG 12a	Prussian blue	1990s	hydrated alumina extender
NG 12b	Prussian blue	1990s	Prussian blue
NG AA	Ackermann ' Antwerp blue'	1796 to 1827	genuine with Al-based extender
NG ALP	Prussian blue	21 <sup>th</sup> century	Prussian blue
NG WC1	Ackermann ' Prussian blue'	1796 to 1827	Prussian blue
NG AR	Prussian blue	19 <sup>th</sup> century,	Prussian blue
NG B	buckthorn on alumina	1970 to 1990	no ID
NG BA	Good Berlin blue from Weimar'	11/04/1855	Prussian blue
NG BB	berlin blue	30/04/1842	Prussian blue
NG BCB	Prussian blue	19 <sup>th</sup> century,	Prussian blue
NG C8	cochineal lake	18/10/1973	no ID
NG CC3b	cochineal carmine	06/08/1973	no ID
NG CD 1b	cochineal lake	02/07/1991	no ID
NG GA	Prussian blue	early 1800s	Prussian blue
NG JSM	Prussian blue	1830 to 1840	Prussian blue
NG K7	Prussian blue	1990s	Prussian blue
NG L	litmus	24/04/1991	no ID
NG MA	Prussian blue	1805 to 1817	Prussian blue
NG MB	Prussian blue	18 <sup>th</sup> century	Indigo
NG MC	Prussian blue	1797	Indigo
NG NB	blue	mid 1800s	BaSO <sub>4</sub>
NG NC	celestial blue	mid 1800s	CaSO <sub>4</sub> extender
NG NP	Prussian blue	mid 1800s	Hydrated alumina extender
NG OZ	Prussian blue	1742 to 1810	Prussian blue
NG Q2	quercitron lake 2	27/07/1972	no ID
NG RA	Prussian blue, barytes, gypsum	1800 to 1830	PB & barium sulphate
NG RC	Prussian blue, gypsum	1800 to 1830	Prussian blue
NG RD	Prussian blue, kaolin, quartz	1800 to 1830	With kaolin
NG RE	Prussian blue, barytes	1800 to 1830	with barium sulphate
NG RF	Prussian blue, gypsum	1800 to 1830	Prussian blue
NG RG	Prussian blue, barytes	1800 to 1830	Prussian blue
NG SA	Prussian blue	21 <sup>st</sup> century	Prussian blue
NG SB	Prussian blue	21 <sup>st</sup> century	Prussian blue
NG SC	Prussian blue	21 <sup>st</sup> century	Prussian blue
NG SD	Prussian blue	21 <sup>st</sup> century	Prussian blue
NG SG	sap green	1991 or 1992	no ID
NG TB	'Turnbull's blue'	unknown	Prussian blue
NG VA	Prussian blue	1770 to 1831	lead white 'extender'
NG VB	Prussian blue	1770 to 1831	Al-based extender
NG W&N I	indigo	20 <sup>th</sup> century	no ID

### Provided by Oud Holland, Zeist

Pigments (mainly all 20<sup>th</sup>-century pigments) came from *Scheveningen*, Winsor and Newton and *Vettewinkel en Zonen*.

Code	Pigment	Date	Source	Results of analysis
OH1	sap green	20th century	Oud Holland, Winsor and Newton	possibly genuine
OH2	Prussian blue (Chinese blue)	20th century	Oud Holland, Winsor and Newton	Prussian blue
OH3	indigo	20th century	Oud Holland, Winsor and Newton	probably genuine
OH4	Prussian blue (Blue de Prusse)	20th century	Oud Holland	Prussian blue
OH5	Prussian blue (Mineraal blauw ijzercyanoür aluminium)	20th century, before OH8 and OH9	Oud Holland, Scheveningen	Prussian blue
OH6	Prussian blue (Parijs blauw)	20th century, before OH8 and OH9	Oud Holland, Scheveningen	Prussian blue
OH7	Prussian blue (Berlijns blauw)	1809 to 1821 or 1809 to 1921	Oud Holland, H. Vettewinkel en zonen	Prussian blue
OH8	Prussian blue (Mineraalblauw)	20th century	Oud Holland, Scheveningen	Prussian blue
OH9	Prussian blue (ijzercyaa Berlijns blauw)	20th century	Oud Holland, Scheveningen	Prussian blue
OH10	vermilion (Chem zuiver vermiljoen)	1809 to 1821 or 1809 to 1921	Oud Holland, H. Vettewinkel en zonen	vermilion
OH11	chrome red	1809 to 1821 or 1809 to 1921	Oud Holland, H. Vettewinkel en zonen	chrome red
OH12	chrome yellow (Chem. Zuiver chromaatgeel donker)	1809 to 1821 or 1809 to 1921	Oud Holland, H. Vettewinkel en zonen	chrome yellow
OH13	carmine	Unknown	Oud Holland, Koninklijke Fabriek van Geneesmiddelen	probably genuine
OH14	indigo	20th century	Oud Holland, Scheveningen	probably genuine
OH15	indigo (Plantaardig indigo op barium)	20th century	Oud Holland, Scheveningen	may not be genuine
OH16	vermiljoen (Engels vermiljoen)	1809 to 1821 or 1809 to 1921	Oud Holland, H. Vettewinkel en zonen	not vermilion

### Provided by Jeff Parkes

A Deforge and Carpentier paintbox, (the former property of Queen Viktoria of Sweden) was provided. It was dated before 1862.

Code	Pigment	Date	Results of analysis
D&C 08/01	Prussian blue	1862, or earlier	high-K Prussian blue (confirmed) and alumina
D&C 08/02	garance cerise [cherry madder]	1862, or earlier	madder (confirmed) on AlSO <sub>4</sub> substrate
D&C 08/03	vere jaune	1862, or earlier	natural yellow iron oxide with kaolin-type and other extenders
D&C 08/04	rouge de saturne [red lead]	1862, or earlier	red lead confirmed
D&C 08/05	chrome clair G	1862, or earlier	lead chromate (confirmed) with some extenders
D&C 08/06	vermilion	1862, or earlier	vermilion confirmed
D&C 08/07	jaune de Naples	1862, or earlier	not traditional Naples yellow, but massicot [same as other late 19th century British pigments labelled 'Naples yellow']
D&C 08/08	carmin extra	1862, or earlier	non-fl red lake on Al and/or Ca-based substrate, probably with extenders
D&C 08/09	jaune Indien	1862, or earlier	not genuine Indian yellow
D&C 08/10	vert de vessie i.e sap green	1862, or earlier	not genuine sap green, but Prussian blue and alumina extender

Also provided was a zinc white cake originating from H. M. Stationary Office, the dating of the pigment was mid-19<sup>th</sup> century.

Code	Pigment	Date	Results of analysis
SO11	Chinese white	Mid 19th century	zinc white, possibly from 2 sources

#### Provided by Tate, London

A Rowney watercolour box, dated around 1860, conservation archive Q04175, was purchased for the purpose of research.

Code	Pigment	Results of analysis
TR1	brown	synthetic iron oxide and chalk
TR2	scarlet over crimson	2 red lakes, not madder-based, and chalk

TR3	blue	synthetic ultramarine
TR4	dark blue black	bone black and non-madder red lake
TR5	green lake	Al-based lake of unknown type
TR6	blue	cobalt blue
TR7	yellow	unclear
TR8	blue	K-based Prussian blue for watercolour use
TR9	green	emerald green
TR10	brown/red	red lake on Sn-based substrate
TR11 lower layer	red	vermilion, zinc white

A Reeves Reward watercolour box, conservation archive Q04174, dated around 1890 was also purchased.

<b>Code</b>	<b>Pigment</b>	<b>Results of analysis</b>
TRR1	blue	Prussian blue
TRR2	crimson lake	Al and Sn substrate for lake
TRR3	Indian red	natural iron oxide
TRR4	vermilion	vermilion
TRR5	burnt sienna	synthetic iron oxide
TRR6	yellow ochre	natural iron oxide and kaolin
TRR7	burnt umber	natural umber, not ochre

A Reeves School watercolour box, conservation archive Q04176, dated 1910 was purchased.

<b>Code</b>	<b>Pigment</b>	<b>Results of analysis</b>
TRS1	burnt sienna	natural burnt sienna with extenders
TRS2	green	kaolin, with lead white and viridian, or but less likely, lead chromate and a non identified blue
TRS3	black	carbon black and extenders
TRS4	yellow ochre	natural yellow ochre with extenders
TRS5	cobalt blue	ultramarine and kaolin likely
TRS6	dark red	red lake on Al-based substrate, with extenders
TRS7	gamboge	gamboge, with extenders
TRS8	vermilion	red lake and extenders, not vermilion
TRS9	Van Dyke brown	Van Dyke brown likely, with extenders
TRS10	light red	(synthetic) iron oxide and extenders

A large source of pigments was the Tate conservation archive. Some of the pigments came from a printing firm active c. 1910-1950, which purchased materials from the colourman Cornelissen.

<b>Code</b>	<b>Pigment</b>	<b>Date</b>	<b>Results of analysis</b>
T CA1	Naples yellow	'Cornelissen, 1890s or later stock	Naples yellow
T CA3	cadmium dark 29	Cornelissen, 1890s or later stock	cadmium sulphide
T CA4	cadmium middle 30	Cornelissen, 1890s or later stock	cadmium sulphide
T CA5	cadmium red deep	Courtauld Technology Dept, 1988	cadmium sulphoselenide
T CA6	cadmium red no 36		cadmium sulphoselenide
T CA7	chinese blue 23	Cornelissen, 1890s or later stock	Fe, K in Prussian blue
T CA8	chrome yellow 2	Cornelissen 1890s or later stock	lead chromate
T CA9	lemon yellow		barium chromate
T CA10	lemon yellow 2	old stock	barium chromate
T CA11	massicot BLH		massicot
T CA12	Naples yellow	Winsor and Newton 1981	Naples yellow
T CA13	orange madder		madder or alizarin on Al-based substrate
T CA14	orpiment	Kremer 2000	orpiment
T CA15	permanent yellow 50 Schonfeld	Cornelissen, 1890s or later stock	barium chromate
T CA16	pinke, Dr Nathaniel Bacon's	8/1999, by Mary Bustin	unusual substrate
T CA17	Prussian blue	Cornelissen, 1890s or later stock	Prussian blue
T CA18	red lead	mid to late 20 <sup>th</sup> century	red lead
T CA19	rosso di saturno	mid to late 20 <sup>th</sup> century	red lead
T CA20	rutenia FFF barytes	mid to late 20 <sup>th</sup> century	barytes
T CA21	sepia 4	Cornelissen, 1890s or later stock	probably sepia
T CA22	Strontium yellow	Courtauld Technology Dept, 1988	strontium chromate
TCA23	zinc oxide, zincoli white seal	Morris Ashby Ltd 1977	zinc oxide
T CA24	zinc white 17	Cornelissen, 1890s or later stock	zinc oxide

T CA25	zinnober	Kremer, 2000	cinnabar or vermilion
--------	----------	--------------	--------------------------

Another source was the Tate paper conservation studio, whose pigment collection must date from after the formation of Tate's conservation department in 1955.

Code	Pigment	Source	Results of analysis
T PC5	indigo	R. Ackermann's	genuine indigo not clear from EDX
T PC6	madder carmine	Winsor&Newton	likely to be a lake on alumina and/or aluminium sulphate; is it genuine madder.
T PC10	sepia 12400	Kremer c2000	likely to be genuine sepia

An important selection was Turners studio pigments which were part of the Turner Bequest and are now in the Tate Gallery Archive (TGA 7315.7) with samples removed to the Tate Conservation Archive as Q04047. Analysis has been carried out earlier, Townsend (1993), wherein her sample s1 corresponds to TTB1 here, etc.

Code	Pigment	Results of 1993 analysis
TB1	scarlet madder	<i>R. tinct.</i> , on Al/Fe/Cu-containing substrate. Samples put in plastic bags before putting them in glass containers.
TB2	madder	<i>R. tinct.</i> , on Al-containing substrate. Samples put in plastic bags before putting them in glass containers.
TB3	gamboge	The jar was stuck in the case but it was possible to take some lumps out. Samples put in plastic bags before putting them in glass containers.
TB4	madder	<i>R. tinct.</i> on Al/Cu-containing substrate
TB5	brown madder	<i>R. tinct.</i> , on Fe/Ca/Si-containing substrate. Sample dropped on plastic covering table and picked up wearing gloves. Samples put in plastic bags before putting them in glass containers.
TB6	Prussian blue	Prussian blue with alumina
TB8	madder	<i>R. tinct.</i> , on Al/Cu-containing substrate, bluer than TTB2. TTB 4 and 8 are the same, 8 is finer grained than 4. The jar of TTB4 was stuck in the case, so this pigment has not been sampled, only TTB8. Samples put in plastic bags before putting them in glass containers.
TB11	madder	Similar to TTB2, but different shade of rose: Very electro static, when pigment enters plastic bag, little needles were formed and it 'jumped' of the spatula. Samples put in plastic bags before putting them in glass containers.
TB12	mid chrome yellow	Mid chrome yellow. Samples put in plastic bags before putting them in glass containers.

TB13	madder	Madder, not <i>R. tinct.</i> , on Cu/Si-containing substrate, dull yellow, reddens in alkali. Samples put in plastic bags before putting them in glass containers.
TB14	madder	Similar to T TB2, but different shade of rose, <i>R. tinct.</i> on Al-containing substrate: Electro static but not as much as T TB11. Samples put in plastic bags before putting them in glass containers.
TB15	brown madder	Similar to T TB5. brown madder, <i>R. tinct.</i> , on Al-containing substrate. Smelled like 'dried hay', or was it the smell of the cork in the lid..
TB16	brown madder	Similar to T TB5. brown madder, <i>R. tinct.</i> , on Si-containing substrate, or was it the smell of the cork in the lid..

### Provided by the Teylers Museum, Haarlem

The Teylers Museum in Haarlem provided samples of Prussian blue, indigo and vermilion. from *The Hafkenscheid Cabinet*. A collection of painting materials, turpentine and gums dated between 1800 and 1832, analysed by Pey (1998).

Code	Pigment	Date	Source	Results of analysis
T1	Prussian blue	1800-1832	Teylers Museum Haarlem, Hafkenscheid cabinet. Teylers nr: 239. Inventory: Berlijns blauw 236-240.	Prussian blue confirmed
T2	vermilion	1800-1832	Teylers Museum Haarlem, Hafkenscheid cabinet. Teylers nr. 227. Inventory: 224-227 Vermiljoen.	vermilion confirmed
T3	indigo	1800-1832	Teylers Museum Haarlem, Hafkenscheid cabinet. Teylers nr: 123. Inventory: Indigo 110-125.	genuine indigo

**Provided by Renate Woudhuysen-Keller, Hamilton Kerr Institute**

Renate Woudhuysen-Keller (a paintings conservator, specializing in old paint recipes and producing dyes and lakes) donated some lake pigments.

<b>Code</b>	<b>Pigment</b>	<b>Date</b>	<b>Results of analysis</b>
RK1	weld	prepared 31/08/2000	weld on Al, some chalk incorporated
RK2	weld with alum and chalk	Unknown	weld on aluminium sulphate with some chalk incorporated
RK3	buckthorn yellow	prepared 2001	not standard buckthorn, not ID
RK4	sap green and alum	prepared 15/11/2006	sap green on potassium aluminium sulphate
RK5	sap green berry juice	prepared 25/09/2003	also sap green on potassium aluminium sulphate
RK6	madder on alum + K <sub>2</sub> CO <sub>3</sub>	prepared 01/07/2002	madder on Al-based substrate, little takeup of elements other than Al
RK7	cochineal on alum + K <sub>2</sub> CO <sub>3</sub>	prepared 01/12/2004	non-fl red lake on Al-based substrate, little takeup of elements other than Al
RK8	brazilwood	prepared 01/06/2006	brazilwood laked on Al-based substrate
RK9	rose madder (W&N)	purchased before 1982	madder on Al-based substrate or aluminium sulphate base
RK10	cadmium orange (W&N)	purchased before 1982	CdS not CdSSe, with added titanium white
RK11	naples yellow (Schminke)	Unknown	not genuine, lead oxide and barium sulphate
RK12	cadmium yellow	purchased before 1982	CdS with added barium sulphate
RK13	Indian yellow (W&N)	purchased before 1982	not genuine Indian yellow, not ID
RK14	Prussian blue (W&N)	purchased before 1982	unusually K-rich Prussian blue
RK15	sepia (Verfmolen de Kat)	purchased before 2003	FTIR matches TCA21 sepia: probably genuine sepia

## F. List of publications arising from this research

Due to a patent application that has resulted from this research (WO 2010029314 “A Method for Preserving Objects Containing Pigment”), limitations were put on the dissemination of the projects findings until the application was completed.

Publications and posters of which I am first author are,

Andrew Lerwill, Joyce H Townsend, Haida Liang, Jacob Thomas and Stephen Hackney, A versatile micro-fadometer for lightfastness testing and pigment identification, in O3A: Optics for Arts, Architecture, and Archaeology, *Proc. SPIE* (2007), Vol. 6618, 66181G

Andrew Lerwill, Joyce H Townsend, Haida Liang, Jacob Thomas and Stephen Hackney. 2008. A portable micro-fadometer for versatile lightfastness testing, *ePreservation Science* 5:17-28.

Andrew Lerwill, Anna Brookes, Joyce H. Townsend, Haida Liang, Jacob Thomas, and Stephen Hackney. 2008 A versatile micro-fadometer for lightfastness testing and pigment identification. Poster presented *CREATE 2008*, Bristol.

Andrew Lerwill, Anna Brookes, Joyce H. Townsend, Haida Liang, Jacob Thomas, and Stephen Hackney. 2008. Micro-fading spectrometry: investigating the wavelength specificity of fading, poster presented at *OSAV 2008*, St Petersburg.

Others on which I am an author include,

Jacob Thomas, Andrew Lerwill, Matija Strlič, Joyce H. Townsend and Stephen Hackney. 2008. Evaluation of anoxic display and storage conditions on works of art on paper, poster presented at *Art 2008*, Jerusalem, 25-30 May 2008.

Joyce H. Townsend, Jacob Thomas, Charlotte Caspers, Monserrat Pis Marcos, Bronwyn Ormsby, Stephen Hackney and Andrew Lerwill,. 2009. ‘(De/Re) Constructing Turner for

research projects at 'Tate', *Sources and Serendipity* ed. E. Hermens and J.H. Townsend , London: Archetype,159-162..

Joyce H Townsend, Stephen Hackney, Jacob Thomas and Andrew Lerwill. 2008. 'The benefits and risks of anoxic display for colourants', *Conservation and Access*, ed. David Saunders, Joyce H. Townsend and Sally Woodcock, IIC, London, 76-81.